

MOLECULAR INTERACTIONS IN THE REPLICATION OF
MOUSE HEPATITIS VIRUS

1987

ROBBINS

Report Documentation Page

Form Approved
OMB No. 0704-0188

Public reporting burden for the collection of information is estimated to average 1 hour per response, including the time for reviewing instructions, searching existing data sources, gathering and maintaining the data needed, and completing and reviewing the collection of information. Send comments regarding this burden estimate or any other aspect of this collection of information, including suggestions for reducing this burden, to Washington Headquarters Services, Directorate for Information Operations and Reports, 1215 Jefferson Davis Highway, Suite 1204, Arlington VA 22202-4302. Respondents should be aware that notwithstanding any other provision of law, no person shall be subject to a penalty for failing to comply with a collection of information if it does not display a currently valid OMB control number.

1. REPORT DATE MAY 1987		2. REPORT TYPE N/A		3. DATES COVERED -	
4. TITLE AND SUBTITLE Molecular Interactions in the Replication of Mouse Hepatitis Virus				5a. CONTRACT NUMBER	
				5b. GRANT NUMBER	
				5c. PROGRAM ELEMENT NUMBER	
6. AUTHOR(S)				5d. PROJECT NUMBER	
				5e. TASK NUMBER	
				5f. WORK UNIT NUMBER	
7. PERFORMING ORGANIZATION NAME(S) AND ADDRESS(ES) Uniformed Services University Of The Health Sciences Bethesda, MD 20814				8. PERFORMING ORGANIZATION REPORT NUMBER	
9. SPONSORING/MONITORING AGENCY NAME(S) AND ADDRESS(ES)				10. SPONSOR/MONITOR'S ACRONYM(S)	
				11. SPONSOR/MONITOR'S REPORT NUMBER(S)	
12. DISTRIBUTION/AVAILABILITY STATEMENT Approved for public release, distribution unlimited					
13. SUPPLEMENTARY NOTES					
14. ABSTRACT					
15. SUBJECT TERMS					
16. SECURITY CLASSIFICATION OF:			17. LIMITATION OF ABSTRACT SAR	18. NUMBER OF PAGES 301	19a. NAME OF RESPONSIBLE PERSON
a. REPORT unclassified	b. ABSTRACT unclassified	c. THIS PAGE unclassified			



UNIFORMED SERVICES UNIVERSITY OF THE HEALTH SCIENCES
 F. EDWARD HÉBERT SCHOOL OF MEDICINE
 4301 JONES BRIDGE ROAD
 BETHESDA, MARYLAND 20814-4799



APPROVAL SHEET

GRADUATE AND
 CONTINUING EDUCATION

TEACHING HOSPITALS
 WALTER REED ARMY MEDICAL CENTER
 NAVAL HOSPITAL, BETHESDA
 MALCOLM GROW AIR FORCE MEDICAL CENTER
 WILFORD HALL AIR FORCE MEDICAL CENTER

Title of Thesis: Molecular Interactions in the Replication
 of Mouse Hepatitis Virus

Name of Candidate: Susan G. Robbins
 Doctor of Philosophy Degree
 May 8, 1987

Thesis and Abstract Approved:



 Committee Chairperson

5/12/87

 Date



 Committee Member

6/22/87

 Date



 Committee Member

6/29/87

 Date



 Committee Member

6/29/87

 Date



 Committee Member

6/29/87

 Date

The author hereby certifies that the use of any copyrighted material in the dissertation manuscript entitled:

"Molecular Interactions in the Replication of
Mouse Hepatitis Virus"

beyond brief excerpts is with the permission of the copyright owner, and will save and hold harmless the Uniformed Services University of the Health Sciences from any damage which may arise from such copyright violations.

Susan G. Robbins, Ph.D.

Susan G. Robbins
Department of Microbiology
Uniformed Services University
of the Health Sciences

ABSTRACT

Functions of two structural proteins of mouse hepatitis virus (MHV) have been studied to elucidate their biological significance. Others have shown that the 180K E2 glycoprotein of MHV is found on virions partially cleaved into 90K polypeptides, and further cleavage of E2 with trypsin activates cell fusion in vitro. The cellular site of E2 cleavage and the role of cleavage in virus infectivity were investigated. A method for isolating intracellular virus (ICV) particles was developed. Radiolabeled ICV carried less E2-90 than did released virions. Monensin treatment slowed virus budding, inhibited cleavage of E2, and reduced the yield of infectious virus by one hundred-fold. Trypsin treatment of ICV or virus grown in the presence of monensin did not enhance virus infectivity. These results suggest that E2 is cleaved on virions after they are transported from the medial region of the Golgi, and that only a portion of E2-180 must be cleaved to E2-90 to make virions infectious.

The RNA-binding proteins in MHV-infected cells and virions were identified using an RNA overlay-protein blot assay (ROPBA). In virions, the nucleocapsid protein N was the major RNA-binding protein. A minor RNA-binding protein of 140K was discovered, which appeared to be a disulfide-linked multimer of N protein. Two other N-related polypep-

tides (N' and N'') and numerous cellular proteins bound MHV RNA. In both the ROPBA and filter binding assays, N protein bound nonspecifically to a variety of nucleic acids.

Immunofluorescence analysis showed that N protein localized in the cytoplasm early in infection; late in infection, N concentrated within nuclei. Isolated nuclei contained the native form of the N protein and also N' and N''. Nuclear N protein was co-localized with the cell chromatin, shown by double labeling immunofluorescence experiments combining monoclonal antibody specific for the N protein and anti-DNA antibody or Hoechst dye 33258.

These results clarify the intracellular location and role of E2 cleavage in virus infectivity, and show that the nucleic acid-binding properties of the nucleocapsid protein may determine its intranuclear localization.

MOLECULAR INTERACTIONS IN THE REPLICATION
OF
MOUSE HEPATITIS VIRUS

by

SUSAN GALE ROBBINS

Dissertation submitted to the Faculty of the Department of Microbiology
Graduate Program of the Uniformed Services University of the Health
Sciences in partial fulfillment of the requirements for the
degree of Doctor of Philosophy, 1987

PREFACE

Mouse hepatitis virus (MHV) is the focus of this dissertation. Three research projects are presented, which concern molecular interactions of the E2 and N viral structural proteins with other viral and cellular macromolecules during virus assembly. Briefly, the questions addressed are: 1) Is proteolytic cleavage of the virus spike glycoprotein E2 essential for virus infectivity? 2) What are the RNA-binding proteins of MHV-infected cells and virions, and does N protein bind RNA in a sequence-specific manner? 3) Where is the N protein localized in cells at different times during infection, and how does it accumulate in nuclei? These studies are presented in three separate chapters, which are followed by a general discussion of conclusions.

DEDICATION

To Dagny and William Robbins, my parents, with much love. Their example, encouragement and support made this work possible.

ACKNOWLEDGMENTS

I am indebted to many people who helped in the planning, experimentation and writing of this dissertation. I am most grateful to Dr. Kathryn V. Holmes, my advisor, who guided me with intelligence, imagination and enthusiasm in every phase of the work. Her assistance with virology, cell biology and microscopy is cherished. I am also very grateful to Dr. John Hay, for his stimulating questions and rational advice on virology and molecular biology, and for the opportunity to work in his laboratory. Dr. William Ruyechan deserves many thanks for his assistance with both theory and experimentation on nucleic acid-binding proteins. These members of my committee and the two remaining members, Dr. Stefanie Vogel and Dr. Henry Wu, helped considerably in the interpretation of my results. Dr. Lawrence Sturman and Cynthia Ricard, of the New York State Department of Health, have magnanimously provided materials and information over the course of my research. Dr. John McGowan provided expertise on labeling and purifying coronavirus RNA. Drs. Robert Silverman and Carl Dieffenbach generously assisted with some of the RNA-binding studies. I must also thank Dr. Douglas Ward, who generated the computer predictions of secondary structure and hydropathy of the N protein.

I am extremely grateful for the support of all the people I have known in both the Microbiology and Pathology departments, especially everyone in Dr. Holmes' laboratory: Dr. Mark Frana, for collaborating on experiments on the N

protein and for many helpful discussions; Dr. John Boyle, for assisting with the RNA-overlay protein blot experiments; Susan Compton for providing RNA transcripts and expertise on coronavirus RNA; Dr. James Remenick for help with silver stains and RNA; and Eileen Bauer, Christine Cardellichio, Dr. Cynthia Duchala, Gary Goldberg, Mhorag Hay, Barbara O'Neill, Toni Scheiner, Dr. Stuart Snyder, Dr. Charles Stephensen, David Weismiller, and Dr. Richard Williams for countless times when their assistance made experiments possible, and for the pleasure of working with them. Everyone in Dr. Hay's lab has helped in some way, notably Michael Flora and Drs. Thomas Casey, Chester Roberts, Paul Kinchington and Michael Pensiero, who advised me on molecular biological techniques. I am especially grateful to Jace Houglund, whose assistance with word processing and computer graphics greatly facilitated my writing and editing. The Audio-Visual Department, especially Frances Langley (who drew Figure 4), Carlton Burr, and Cynthia Hodin, helped no end with the illustrations.

I would also like to thank all the graduate students and post-doctoral fellows in Microbiology, for what they have taught me and for their friendship. I am also very grateful to Drs. Randall Holmes and Robert Friedman for providing an excellent setting in which to learn and experiment, and to Dr. John Bullard for overseeing my graduate education.

Without the kindness and support of my family and

friends, this research could not have been completed. My mother, Dagny Gradin Robbins, has bolstered me with her strength and encouragement. My father, Dr. William Clinton Robbins, has inspired me on many occasions with his fundamental questions and comments, and has supported me all along. I am also grateful to my brother John Robbins for sharing his scientific thoughts, and for the companionship of my brother Wesley and my sister Elizabeth. The hospitality of my aunt and uncle, Alice and Frederick Robbins, was very enjoyable. Last but not least, I sincerely thank Mary P. Vinton for thoughtfully providing me with a good home.

TABLE OF CONTENTS

	<u>Page</u>
INTRODUCTION.....	1
History.....	1
Discovery and classification.....	1
Diseases.....	1
Epidemiology of MHV and human coronaviruses....	10
Genetic relationships among coronaviruses.....	11
Antigenic relationships.....	12
Structure of MHV.....	13
Morphology.....	13
Physical characteristics of virions.....	13
Chemical composition of virions.....	17
Replication of MHV.....	17
Growth cycle.....	17
RNA replication and transcription.....	19
Synthesis and processing of viral proteins.....	22
Viral assembly and release.....	23
Cytopathic effects and virus-induced structures.....	24
E2, the Spike Glycoprotein.....	25
Introduction.....	25
Structure.....	26
Synthesis and transport.....	29
Glycosylation.....	30
Cleavage.....	30
Functions of E2.....	31

N, the Nucleocapsid Protein.....	33
Structure.....	33
Synthesis.....	33
Phosphorylation.....	34
N-related polypeptides.....	35
Functions.....	35
GENERAL MATERIALS AND METHODS.....	40
Viruses and Cells.....	40
Virus Purification.....	40
Plaque Assay.....	41
Protein Determination.....	41
Gel Electrophoresis and Immunoblotting.....	41
Preparation of Antisera.....	42
Immunoblot Analysis.....	43
Radioisotope Counting.....	43
I. THE INTRACELLULAR MATURATION OF MHV AND ITS E2	
GLYCOPROTEIN.....	44
Introduction.....	44
Materials and Methods.....	46
Radiolabeling viral proteins.....	46
Preparation of intracellular (ICV) and cell-	
associated (CAV) virus.....	47
Cell fractionation.....	48
Transmission electron microscopy (TEM).....	48
Monensin experiments.....	49
Cytochalasin D experiments.....	50
Trypsin experiments.....	50

Results.....	52
Isolation of intracellular and cell-associated MHV.....	52
E2 cleavage on ICV and CAV.....	63
Morphology of ICV.....	63
Methods for increasing the concentration of ICVs.....	73
Monensin treatment.....	73
Effect of monensin on cleavage of E2.....	73
Effect of monensin on MHV infectivity.....	76
Effects of cytochalasin D on maturation and infectivity of MHV.....	81
Effects of trypsin on MHV infectivity.....	82
Discussion.....	85
II. NUCLEIC ACID-BINDING PROPERTIES OF N PROTEIN AND OTHER PROTEINS OF MHV-INFECTED CELLS AND VIRIONS....	98
Introduction.....	98
Materials and Methods.....	99
Viruses and cells.....	99
Preparation of endogenously labeled RNA for the RNA overlay-protein blot assay.....	100
Preparation of radiolabeled DNA and RNA probes.....	101
Preparation of cell extracts.....	102
Gel electrophoresis and electroblotting.....	103
RNA overlay-protein blot assay (ROPBA).....	103
Preparation of MHV [³ H]-uridine-RNA probe and	

unlabeled competitor nucleic acids.....	104
Preparation of an anti-N affinity column.....	105
Solubilization of N protein from nucleo-	
capsids.....	107
Isolation of the MHV-A59 N protein by affinity	
chromatography.....	107
Silver stain of affinity-purified N protein...	108
Filter binding assay.....	108
Results.....	110
Electrophoresis of MHV RNAs.....	110
Identification of RNA-binding proteins in	
virions.....	113
Characterization of the 140K protein.....	116
Detection of RNA-binding proteins in mock-	
infected and MHV-infected cells.....	121
RNA-binding by N-related proteins in ts-mutant	
infected cells.....	124
Interaction of MHV RNA-binding proteins with	
nucleic acids.....	124
Binding of N protein to RNA in a filter	
binding assay.....	136
Sequence-specificity of RNA binding by N	
protein.....	139
Discussion.....	147
III. CONCENTRATION OF THE N PROTEIN IN THE NUCLEI OF MHV-	
INFECTED CELLS.....	156
Introduction.....	156

Cellular and viral nuclear proteins.....	156
Mechanisms of nuclear transport.....	160
Materials and Methods.....	164
Antisera.....	164
Indirect immunofluorescence assay.....	165
Hoechst 33258 stain for DNA.....	165
Isolation of cell nuclei and preparation of nuclear and cytoplasmic extracts.....	166
Colchicine treatment.....	167
Results.....	167
Movement of N protein during the course of infection.....	167
Forms of nuclear N identified by cell fractionation.....	171
Mechanism of nuclear localization of N protein.....	174
Co-localization of N protein with chromatin...	177
Discussion.....	194
GENERAL DISCUSSION.....	199
Studies on the E2 Glycoprotein.....	199
Recent Developments in Research on E2.....	200
Studies on the N Protein.....	202
The 140K Protein.....	203
Nucleotide Sequence Specificity.....	205
Binding Domains of the Tobacco Mosaic Virus Coat Protein.....	207
Possible RNA-Binding Domains of the MHV N Protein..	209

Experimental Approaches.....	216
Summary.....	223
BIBLIOGRAPHY.....	226

LIST OF TABLES

<u>Table</u>		<u>Page</u>
1.	Diseases caused by coronaviruses.....	6
2.	Effects of monensin and trypsin on MHV infec- tivity and cleavage of E2.....	80
3.	Effect of ionic strength on RNA-binding by pro- teins in MHV-infected cells.....	131
4.	Regions of the MHV-A59 N protein with possible functional significance.....	214
5.	Forms and functions of the MHV N protein.....	225

LIST OF FIGURES

<u>Figure</u>	<u>Page</u>
1. Mouse hepatitis virus, strain A59.....	3
2. Models for the structure of mouse hepatitis virus (2A) and the replication of coronaviruses (2B).....	15
3. Model of the E2 glycoprotein.....	28
4. Model of N protein in the viral nucleocapsid.....	38
5. Removal of MHV virions from the cell surface by treatment with proteinase K.....	55
6. Distribution of infectivity across a discontinuous sucrose gradient.....	58
7. Cell-associated virions demonstrated by negative staining.....	60
8. Purification of intracellular and cell-associated virus particles by sucrose gradient ultracentrifugation.....	62
9. Proteins of partially purified cell-associated and intracellular virus preparations and cytoplasmic extracts, in the presence and absence of monensin..	65
10. Intracellular virus particles in thin section.....	68
11. Virus-induced tubules in MHV-infected cells in thin section.....	70
12. Virus-induced intracellular tubules demonstrated by negative staining.....	72
13. Arrest of MHV budding by monensin treatment.....	75
14. Inhibition of E2 cleavage by monensin, shown by immunoblotting.....	78

15.	Accumulation of intracellular MHV by cytochalasin D treatment.....	84
16.	Agarose gel electrophoresis of ³² P-labeled MHV RNAs.....	112
17.	RNA-binding proteins of purified MHV-A59 virions detected by the RNA overlay protein blot assay....	115
18.	Antigenic cross-reactivity between the 140K protein and the N protein.....	118
19.	The 140K protein is a disulfide-linked multimer of N protein.....	120
20.	Different species of N protein and cellular proteins are RNA-binding proteins in MHV-A59 and MHV-JHM-infected cells.....	123
21.	Temperature-sensitive mutants having N-related proteins with RNA-binding activity.....	126
22.	Effect of salt concentration on RNA-binding by proteins in MHV-infected cells.....	128
23.	Effect of pH on RNA-binding by proteins in MHV-infected and mock-infected cells.....	133
24.	Binding of cellular proteins by different nucleic acids.....	135
25.	Solubilization of N protein from nucleocapsids by RNase digestion.....	138
26.	N protein partially purified by affinity chromatography and analyzed by silver staining.....	141
27.	Binding of affinity-purified N protein to MHV RNAs in a filter binding assay.....	143

28.	Binding of N protein to MHV RNAs in a competitive filter binding assay.....	146
29.	Localization of N protein in MHV-infected cells by indirect immunofluorescence.....	170
30.	Nuclei purified from MHV-infected cells.....	173
31.	Forms of N protein in nuclear and cytoplasmic extracts from MHV-infected cells.....	176
32.	Nuclear localization of the N protein in MHV-infected cells treated with colchicine.....	179
33.	Induction of metaphase arrests in 17 Clone 1 cells treated with colchicine.....	182
34.	Localization of N protein on metaphase chromosomes shown by indirect immunofluorescence and orcein staining.....	184
35.	Identification of DNA in mock-infected cells using anti-DNA (SLE) serum.....	187
36.	Co-localization of N protein and DNA shown by double label immunofluorescence.....	189
37.	Double staining of interphase nuclei with Hoechst 33258 and anti-N immunofluorescence.....	191
38.	Mitotic cells with chromosomes staining positive or negative for N protein.....	193
39.	Hypothetical secondary structure and hydropathy of the N proteins of MHV strains A59 and JHM.....	213
40.	Amino acid sequence of the MHV-A59 N protein, showing the linear relationships of some regions of possible functional significance.....	218

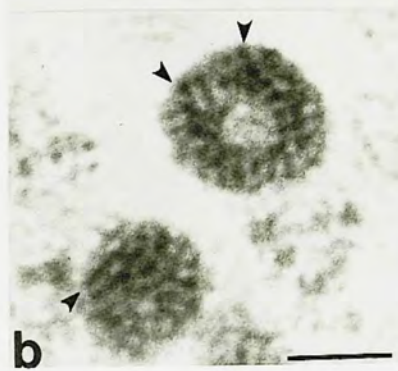
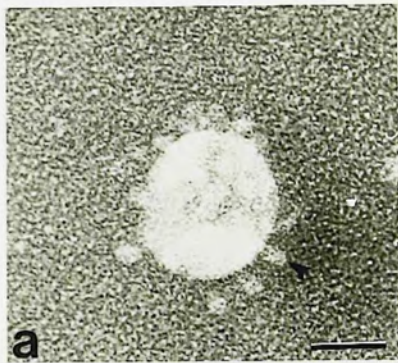
INTRODUCTION

History

Discovery and classification. Coronaviruses were declared a distinct virus group by Tyrrell and an international group of coronavirologists in 1968, on the basis of their appearance under the electron microscope after negative staining (Fig. 1a), ether lability and RNA content (Tyrrell et al., 1968). Their halo of glycoprotein spikes inspired the appellation "corona" (Tyrrell et al., 1968). Today, coronaviruses are round, often pleiomorphic particles of 60-220 nm diameter, enveloped by lipid and surrounded by characteristically large spikes. The virions contain three structural proteins and a single-stranded RNA of message sense, which is infectious and polyadenylated (Tyrrell et al., 1975, 1978). Coronavirus replication uniquely entails synthesis of a nested set of messages which share a common 3' end (Spaan et al., 1982). Infectious bronchitis virus (IBV) is used as the standard to which other coronaviruses are compared in terms of genome size, transcription and replication scheme (Schochetman et al., 1977; Lomniczi, 1977; Lomniczi and Kennedy, 1977), and serology (McIntosh, 1974; Robb and Bond, 1979b; Wege et al., 1982). Virions bud from the endoplasmic reticulum and Golgi membranes (reviewed by Siddell et al., 1982; Sturman and Holmes, 1983; Holmes, 1985).

Diseases. The family Coronaviridae contains eleven viruses of vertebrate species which cause a variety of acute

Figure 1. Mouse hepatitis virus, strain A59. (a) Negative stain of a virion purified from MHV-infected 17 Cl 1 cells. MHV-infected cells (labeled with [³H]leucine) were homogenized, and the cytoplasmic fraction was analyzed with discontinuous sucrose gradients. Virions were purified on continuous sucrose gradients and the virus band at 1.16 g/ml was detected at the peak of radiolabel. An aliquot from the peak fraction was stained with phosphotungstic acid. The prominent glycoprotein spikes (arrowhead) are characteristic of coronaviruses. Bar = 100 nm. (b) Thin section of two intracellular virions in a 17 Cl 1 cell infected with MHV-A59. The cells were processed for transmission electron microscopy as described in the Materials and Methods. The nucleocapsid can be seen as circular structures in cross section (arrowheads, larger virion) and as dark bands in longitudinal section (arrowhead, smaller virion). Bar = 75 nm.



and chronic diseases in man and domestic animals (Table 1). Many of these illnesses result in significant morbidity and economic losses. Coronaviruses cause respiratory and gastroenteric infections, hepatitis, wasting disease, infectious peritonitis, neurological diseases and chronic inapparent infections, to name some of the more common diseases (McIntosh, 1974; Wege et al., 1982). At least 15% of common colds of man have been linked to coronaviruses (McIntosh et al., 1970; Larson et al., 1980). Coronavirus biology and biochemistry have been reviewed in the past five years by Wege et al., 1982; Siddell et al., 1982; Sturman and Holmes, 1983; Holmes et al., 1984; Holmes, 1985; McIntosh, 1985).

Coronaviruses are classified into four major antigenic groups (Table 1). Avian infectious bronchitis virus (IBV) and mouse hepatitis virus (MHV) are the prototype coronaviruses, and the most extensively studied of the family. MHV causes a number of different diseases in mice, including neonatal diarrhea, hepatitis, acute and chronic demyelination, and persistent infection. MHV is unrelated to human hepatitis viruses. The type of organ involvement and severity of the disease depend on the age and strain of mouse, the route of inoculation, and the virus strain (Wege et al., 1982). MHV infection is nearly ubiquitous in laboratory colonies of mice (Rowe et al., 1963). Because MHV can cause persistent infections in vivo and in vitro, it is used as a model for studying persistent virus-cell

Table 1. Diseases caused by coronaviruses. Coronaviruses are presently classified into 4 major antigenic groups. Abbreviations: HCV, human coronavirus; TGEV, transmissible gastroenteritis virus; CCV, canine coronavirus; FIPV, feline infectious peritonitis virus; FECV, feline enteric coronavirus; MHV, mouse hepatitis virus; RCV, rat coronavirus; SDAV, sialodacryoadenitis virus; HEV, hemagglutinating encephalomyelitis virus; BCV, bovine coronavirus; IBV, infectious bronchitis virus; TCV, turkey coronavirus; HECV, human enteric coronavirus. This table was adapted from a table compiled by Holmes (1985).

Table 1

Antigenic Group	Host	Abbreviation	Respiratory Infection	Enteric Infection	Hepatitis	Neurological Infection	Other
I	Human	HCV-229E	X				
	Pig	TGEV	X	X			Nephritis
	Dog	CCV		X			
	Cat	FIPV	X	X	X	X	Eye infection
	Cat	FECV		X			
II	Human	HCV-OC43	X				
	Mouse	MHV	X	X	X	X	
	Rat	RCV	X				
	Rat	SDAV					Salivary adenitis
	Pig	HEV	X	X		X	Wasting
	Calf	BCV		X			
III	Chicken	IBV	X				Gonaditis
IV	Turkey	TCV	X	X			
Unclassified	Human	HECV		?			

interactions (Chaloner-Larsson and Johnson-Lussenburg, 1981; Holmes and Behnke., 1981; Sorensen et al., 1981). MHV-induced hepatitis has also served as a model for human hepatitis (Piazza, 1969; Levy et al., 1982). Furthermore, the ability of several MHV strains to induce acute or chronic demyelination has drawn attention to them as models for acute and chronic virus-induced demyelinating diseases (ter Meulen and Wege, 1978; Weiner and Stohlman, 1978). Thus, MHV is important as a model for studying the pathogenesis of some important diseases of humans as well as infection at the cellular level.

The first report of a disease caused by a coronavirus was in 1931, when Schalk and Hawn identified an acute upper respiratory infection of baby chicks which was distinct from other similar avian illnesses (Schalk and Hawn, 1931). The causative agent was later isolated, identified as a virus, and named infectious bronchitis virus (Beaudette and Hudson, 1937). IBV is a common infection of poultry, causing high mortality in chicks. When laying hens are infected, they produce fewer and poorer quality eggs. Pathology is strain-dependent, and can involve not only the respiratory tract but also kidneys and reproductive tracts of chickens (Cunningham, 1970). The virus may be shed in the feces for several months (Alexander and Gough, 1977).

Transmissible gastroenteritis of swine is an acute diarrheal illness involving vomiting, diarrhea and rapid dehydration in newborn pigs; it usually results in death

within 5 days. The virus causing this disease, transmissible gastroenteritis virus (TGEV), was first isolated in 1946 (Doyle and Hutchings, 1946).

Many strains of MHV have been isolated. Some cause only enteric infection, while others cause hepatitis and encephalitis to varying degrees (McIntosh, 1974; Wege et al., 1982). In 1949, the first murine coronavirus to be identified, MHV-JHM, was isolated from a spontaneously paralyzed Swiss mouse (Cheever et al., 1949). This strain was highly neurotropic and caused both acute and chronic demyelination, as well as focal hepatic necrosis (Cheever et al., 1949; Bailey et al., 1949). Soon after, Gledhill and Andrewes (1951) isolated viruses from mice with acute hepatic disease and later found them to be antigenically cross-reactive with MHV-JHM. MHV strain A59 (MHV-A59) was discovered serendipitously after mice which had received splenic implants during serial transmission of a mouse leukemia unexpectedly developed hepatitis (Nelson, 1952). MHV-A59 was isolated from the livers of these mice, and passed to mice of different strains and ages, where it produced hepatitis (Manaker et al., 1961). This strain can also cause mild encephalitis and chronic demyelination, but intracerebral inoculation is required (Lavi et al., 1984). MHV-A59 is one of the most well understood coronaviruses because it grows to relatively high titer when grown in cells such as the 17 Clone 1 line of transformed mouse fibroblasts (Sturman and Takemoto, 1972).

Feline infectious peritonitis was initially described and shown to be transmissible in 1963 (Holzworth, 1963). The disease is a chronic, debilitating, highly fatal illness of both wild and domestic cats. Normally, infection is inapparent, but can lead to fatal disease, basically involving either peritonitis or the central nervous system. The causative virus, feline infectious peritonitis virus (FIPV), was identified as a coronavirus on the basis of morphological and physiochemical data (Ward, 1970; Pedersen, 1976). Enteric coronaviruses of dogs, cows and turkeys were also identified in the early 1970s (reviewed by Wege et al., 1982).

Two groups of human coronaviruses have been identified, whose prototypes are strains 229E and OC43 (Hamre and Procknow, 1966; Bruckova et al., 1970). Human coronaviruses are extremely fastidious in their species and tissue specificity, preferring to grow in human organs. Thus, these viruses were not isolated until organ culture became available. They generally do not grow to high titer in tissue culture unless extensively adapted by passage (Schmidt et al., 1979). In 1965, Tyrrell and Bynoe obtained a virus (strain B814) from a young boy with a cold and passaged it in human embryonic trachea organ culture (Tyrrell and Bynoe, 1965). This isolate caused colds in volunteers given culture supernatants, and resembled IBV morphologically by electron microscopy (Almeida and Tyrrell, 1967). Later, common cold isolates were successively

passed in human embryonic kidney cells and shown to be morphologically similar to both IBV and the previously isolated respiratory virus, and distinct serologically from orthomyxoviruses and paramyxoviruses. One of these strains was named 229E (Hamre and Procknow, 1966). Like the murine coronaviruses, the human viruses assembled by budding into cytoplasmic vesicles (Becker et al., 1967; Hamre et al., 1967). McIntosh et al. (1967, 1969) adapted two human isolates to the brains of suckling mice and showed that these strains (OC38 and OC43) were serologically related to MHV, whereas strain 229E was not.

Whether human coronaviruses can cause gastroenteritis is not yet certain. Coronavirus-like particles have often been seen in negatively stained stool specimens from patients with diarrhea, however, often in association with rotaviruses (Curry and Paver, 1980). Children with acute gastroenteritis excrete coronaviruses with a significantly higher incidence than controls (Gerna et al., 1985). Also, coronaviruses from stools of infants with necrotizing enterocolitis have been propagated in human fetal intestinal organs (Resta et al., 1985).

Epidemiology of MHV and human coronaviruses. MHV is a highly contagious, widespread enteric infection of laboratory mice. The strain MHV-S causes high mortality in infant mice (Rowe et al., 1963). Other strains cause inapparent infection, or mild neurological disturbances (Woyciechowska et al., 1984). Patent MHV disease can be

induced in outwardly healthy animals which are stressed in some manner, e.g., by infection with murine leukemia viruses (Nelson, 1952), or injection of the normally harmless protozoan Eperythrozoon coccoides (Gledhill and Andrewes, 1951), or polyoma virus (Sturman and Takemoto, 1972).

Human exposure to coronaviruses is probably worldwide, since coronavirus-specific antibody has been found in sera in all geographic areas examined (McIntosh, 1974). Here in Bethesda, Maryland, an infection rate for 229E of 24% was discovered among 89 NIH employees with upper respiratory infections from December, 1966 to April, 1967 (Kapikian et al., 1969). In 1976, 100% of healthy adults in England who were tested had serum antibody to OC43, and 94% to 229E viruses, as determined by ELISA (Hasony and Macnaughton, 1982). In the United States, nationwide outbreaks of 229E have occurred at about two year intervals (Monto and Rhodes, 1974), usually in the winter or spring.

Genetic relationships among coronaviruses. Extensive sequence homology among MHV strains has been detected by hybridization of their mRNAs with a cDNA complementary to most of the MHV genome (Weiss and Leibowitz, 1982) or to the N gene (Cheley et al., 1981). RNase T₁ digests of MHV genomes (Lai and Stohlman, 1981) and peptide fingerprint analyses of the MHV proteins (Cheley et al., 1981) bear out this finding. However, in terms of oligonucleotide fingerprints, MHV-A59 is similar to MHV-3, but differs significantly from MHV-JHM (there are 14 oligonucleotides present

in A59 which are missing in JHM) (Wege et al., 1981a; Lai and Stohlman, 1981). Efforts have been made to correlate oligonucleotide differences with pathogenicity (Lai et al., 1981; Stohlman et al., 1982). There is no detectable RNA homology between murine coronaviruses and the human coronavirus 229E (Weiss and Leibowitz, 1981).

Antigenic relationships. Coronaviruses fall into two main groups, mammalian and avian, as outlined by Robb and Bond (1979b) (Table 1). The mammalian coronaviruses have been divided into two groups based on enzyme-linked immunoassay (Kraaijeveld et al., 1980; Macnaughton, 1981), immuno-fluorescence and immunoelectron microscopy reactivities (McIntosh et al., 1969; Pedersen et al., 1978; Pensaert et al., 1981), and neutralization and hemagglutination inhibition assays (McIntosh et al., 1969; Reynolds et al., 1980; Gerna et al., 1981). One group encompasses MHV, HCV-OC43, hemagglutinating encephalomyelitis virus (HEV) and bovine coronavirus; the other contains HCV-229E, TGEV, FIPV and canine coronavirus (McIntosh et al., 1969; Pedersen et al., 1978). These results were confirmed by studies with purified viral antigens (Reynolds et al., 1980; Gerna et al., 1981; Horzinek et al., 1982). However, some cross-reactivity between the N proteins of HCV-229E and MHV has been reported by Bradburne (1970) and Hasony and Macnaughton (1982) using immunoprecipitation and ELISA assays. Amino acid sequencing should resolve whether these N proteins share common epitopes.

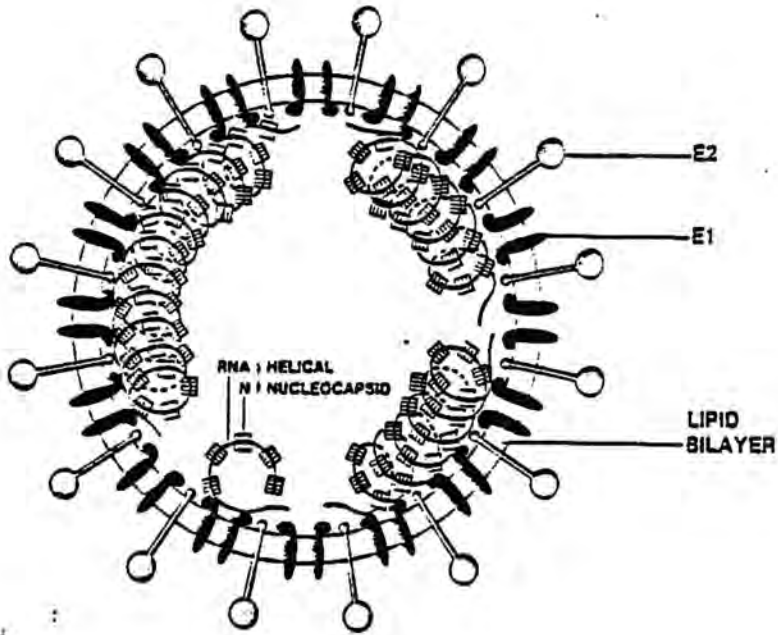
Structure of MHV

Morphology. When negatively stained, coronavirions appear as roughly spherical, pleiomorphic particles ranging from 60 to 220 nm diameter (McIntosh, 1974) (Figure 1a). When coronavirions are permeabilized to negative stains by treatment with antibody and complement, an internal tongue-like structure is apparent (Almeida and Tyrrell, 1967; Bingham and Almeida, 1977). Approximately 200 peplomers form the glycoprotein projections on the surface of each virion; these are large, 20 nm long and up to 7 nm wide (Sturman et al., 1980). Transmission electron microscopy of thin sections demonstrates a lipid bilayer surrounding an electron-dense, long, coiled, helical nucleocapsid (Apostolov et al., 1970; Bingham and Almeida, 1977) (Fig. 1b). A model of MHV structure, envisioned by Sturman et al. (1980), is shown in Fig. 2a.

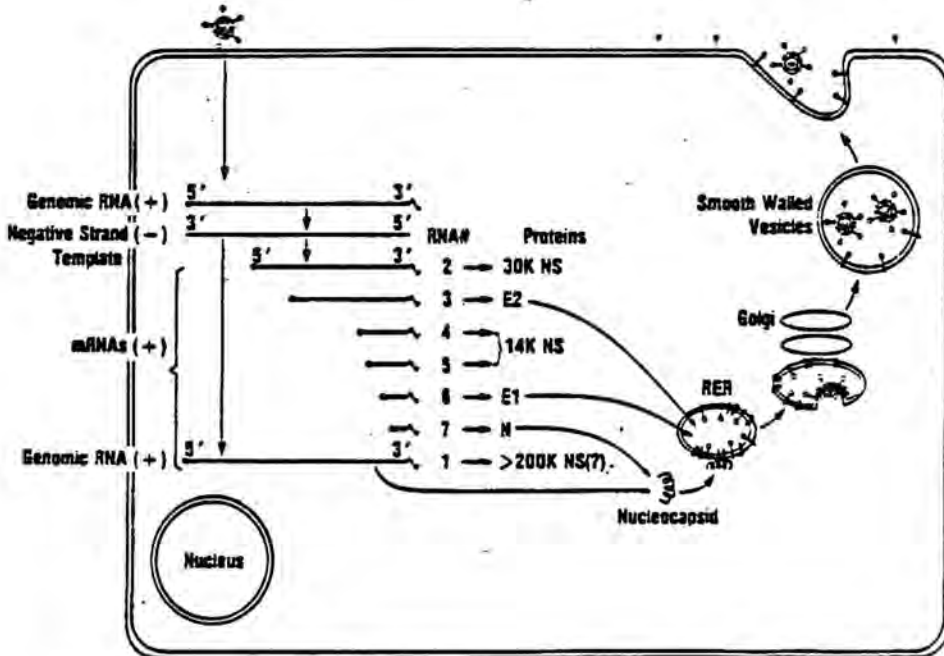
Physical characteristics of virions. Many coronaviruses can be readily purified for structural study, yielding titers of about 10^8 PFU/ml of tissue culture medium in the case of MHV-A59 grown in 17 Clone 1 or Sac(-) cells (Sturman et al., 1980; Spaan et al., 1981). Virions are usually concentrated by precipitation with polyethylene glycol or ammonium sulfate, followed by rate zonal and isopycnic centrifugation on density gradients. The density of coronaviruses in sucrose is 1.16 to 1.18 g/ml. Virions contain RNA, proteins, carbohydrates and lipids (Tyrrell et al., 1978; Robb and Bond, 1979b; Sturman et al., 1980). They are

Figure 2A. A model for the structure of mouse hepatitis virus. The viral nucleocapsid is helical and composed of a single strand of positively sensed RNA and the nucleocapsid protein N. The nucleocapsid is enveloped with a lipid bilayer containing the membrane glycoprotein E1 and the spike glycoprotein E2, which mediates virus attachment and cell fusion. Glycosaminoglycan is associated with the surface of the virion. (Figure from Sturman et al., 1980).

Figure 2B. Scheme for the replication of coronaviruses. Virions bind to the plasma membrane and enter the cell by fusion at the cell surface or in endocytic vesicles. In the cytoplasm, the viral RNA-dependent RNA polymerase is translated from the genome RNA and goes on to synthesize the subgenomic mRNAs (1-7). The mRNAs share the same 3' end, forming a nested set. A single protein is translated from each message. The N protein binds with newly synthesized genome RNAs to form nucleocapsids. Nucleocapsids are assembled into virions by budding into RER and Golgi membranes where the viral glycoproteins are localized. Virions are transported to post-Golgi vesicles, which fuse with the plasma membrane, allowing virus release. (Figure from Sturman and Holmes, 1983.)



A



B

thermolabile (Laude, 1981). Coronavirus stability is greatest between pH 6 and 6.5, with a half-life of infectivity of 24 hours in 10% fetal bovine serum (Alexander and Collins, 1975; Pocock and Garwes, 1975; Sturman, 1981). However, at pH 8, the half-life drops to less than one hour, possibly due to changes in the E2 glycoprotein (Sturman, 1981).

The coronavirus ribonucleoprotein (RNP) contains a genomic RNA strand of message sense. Its density in sucrose is higher than that of virions, 1.25-1.28 g/ml (Wege et al., 1979; Sturman et al., 1980). Thin sections of virions (Fig. 1b) or infected cells show that the RNP takes the form of a flexible helix (Apostolov et al., 1970). The nucleocapsid composition of coronaviruses has been elucidated by studying virions disrupted spontaneously or by non-ionic detergents, followed by fractionation on sucrose gradients (Sturman et al., 1980). RNPs from MHV-3 and HCV-229E were obtained by incubation at room temperature in phosphate-buffered saline for up to 24 hr (Macnaughton et al., 1978).

These appeared as flexible helical strands very similar to RNPs of myxo- and paramyxoviruses (Compans and Choppin, 1973), and contained nucleocapsid proteins of similar molecular weight (Lenard and Compans, 1974). The MHV and HCV nucleocapsids were helical, 14-16 nm in diameter, and up to 320 nm long. Globular capsomers of 5-7 nm, approximately 5 per turn of the helix, studded the nucleocapsids. From an estimate of their size it was concluded that each capsomer

corresponded to one monomer of the nucleocapsid protein N (Macnaughton et al., 1978).

Chemical composition of virions. The MHV genome is a single strand of RNA of about $5.5-5.9 \times 10^6$ daltons and 16-21 kilobases (Yogo et al., 1977; Macnaughton, 1978; Lai and Stohlman, 1978; Leibowitz et al., 1981; Spaan et al., 1981; Wege et al., 1981b; Weiss and Leibowitz, 1981). The virion RNA is infectious (Wege et al., 1978; Leibowitz and Weiss, 1981) and polyadenylated (Yogo et al., 1977; Lai and Stohlman, 1978; Wege et al., 1978). Associated with the genome in nucleocapsids is the phosphorylated nucleocapsid protein N (50-60K) (Sturman et al., 1980). Virions contain protein kinase activity, but which virion-associated protein has this enzyme activity is not known (Siddell et al., 1981a). Two glycoproteins, E1 and E2, are inserted into the lipid envelope (Sturman et al., 1980). E1 (20-35K) probably serves as a matrix protein and may be important in virus budding (Holmes et al., 1981a). E2 is the virus spike and neutralizing antigen, responsible for virus attachment to cells and cell fusion (reviewed by Sturman, 1981, and Sturman and Holmes, 1983). E2 is described in further detail below. Several nonstructural virus-encoded proteins have been identified in coronavirus-infected cells (Anderson et al., 1979; Bond et al., 1979).

Replication of MHV

Growth cycle. Most coronaviruses grow only in host

animals and tissue culture cells of their species of origin. Epithelial cells from respiratory and enteric tracts are usually preferred (Wege et al., 1982). Coronaviruses bind to cell surfaces at both 37° and 4°C (Richter, 1976). The cell receptor for MHV-A59 is destroyed by protease treatment of cells (Richter, 1976).

Electron microscopic evidence indicates that MHV enters cells by fusion of the viral envelope with the plasma membrane (Doughri et al., 1976). Blocking endocytosis with cytochalasin B does not prevent infection of cells by MHV-3 (Krystyniak and Dupuy, 1981). Virions may also be taken up via coated pits (Chasey and Alexander, 1976; Arnheiter et al., 1982) and have been observed in vesicles similar to endosomes (David-Ferreira and Manaker, 1965; Sabesin, 1971; Patterson and Bingham, 1976). Following entry, virions become associated with lysosomes (David-Ferreira and Manaker, 1965; Sabesin, 1971). MHV infection is inhibited by chloroquine (Mallucci, 1966), which elevates the intralysosomal pH and is known to prevent Semliki Forest virus and influenza virus penetration from endocytic vesicles into the cytoplasm (Helenius et al., 1980, 1982).

For MHV-A59 and -JHM in Sac- cells, infection follows "one-hit" kinetics. Infectious virus begins to be released by about 6-8 hours post-inoculation (p.i.), and the rate of release plateaus by 10-12 hours (Robb and Bond, 1979a; Spaan et al., 1981; Wege et al., 1981c).

Mammalian coronaviruses replicate exclusively in the

cytoplasm, having no absolute requirement for nuclear factors. Ultrastructural and immunofluorescence studies (McIntosh, 1974; Robb and Bond, 1979a) show that replication of MHV is cytoplasmic. By electron microscopy and immunofluorescence, MHV-A59 and MHV-JHM both replicated in enucleated cells; however, in one study (Wilhelmsen et al., 1981), virus yield was reduced by 2.1 logs (A59) and 0.84 log (JHM) (Wilhelmsen et al., 1981; Brayton et al., 1981). Actinomycin D does not inhibit MHV replication (Mallucci, 1965; Hirano et al., 1978; Brayton et al., 1981; Leibowitz et al., 1981; Spaan et al., 1981; Wege et al., 1981b). In contrast, IBV is prevented from growing in BHK-21 cells if the cells are enucleated, treated with alpha-amanitin, or UV-irradiated (Evans and Simpson, 1980), possibly indicating a requirement for host DNA-dependent RNA synthesis. These cells may produce a protein factor, necessary for coronavirus replication, which is encoded by a rapidly turning over RNA species.

RNA replication and transcription. The cycle of replication and assembly of MHV is diagrammed in Figure 2b. Coronavirus RNA-dependent RNA polymerase activity is not found in virions. The enzyme appears to be synthesized soon after virus entry (Brayton et al., 1982; Dennis and Brian, 1982; Mahy et al., 1983). MHV polymerase activity was detected at 4-6 hr in cells infected with TGEV or MHV, respectively (Dennis and Brian, 1981, 1982; Mahy et al., 1983), and found to be associated with cytoplasmic membrane

fractions, as in alphavirus and poliovirus replication (Grimley *et al.*, 1968, 1972; Caligiuri and Tamm, 1970). There has been one report of an early peak of virus-specific RNA synthesis detected at 2-3 hr p.i. in MHV-A59-infected cells, different in its requirement for pH and cations (Brayton *et al.*, 1982). The negative-stranded template codes for the synthesis of subgenomic and genomic RNAs (Brayton *et al.*, 1982), which serve as messages for the synthesis of structural and non-structural proteins. The viral mRNAs are transcribed at the same relative rates throughout infection (Leibowitz *et al.*, 1981; Spaan *et al.*, 1981; Wege *et al.*, 1981b). UV transcription mapping studies have shown that the UV target sizes of the mRNAs were nearly identical to their physical sizes, indicating that each transcript is initiated independently, and does not arise from a genome-length positive strand (Jacobs *et al.*, 1981; van der Zeijst *et al.*, 1981). These mRNAs become associated with polysomes, where they are translated (Spaan *et al.*, 1981; Lai *et al.*, 1982b).

The virus-specific RNAs in coronavirus-infected cells are of positive sense. The poly-A-containing RNAs isolated from MHV-infected cells which were labelled in the presence of actinomycin D consisted of multiple species of molecular weights $0.6-6 \times 10^6$ (Cheley *et al.*, 1981; Lai *et al.*, 1981; Leibowitz *et al.*, 1981; Spaan *et al.*, 1981; Wege *et al.*, 1981b) (Fig. 2b). The mRNAs of MHV are numbered from 1-7 in order of increasing molecular weight with the

largest of weight equal to that of genome RNA. Their total length is far greater than that of genome RNA. Oligonucleotide fingerprinting analysis has demonstrated that all of the mRNAs share the same 3' terminus, forming a "nested set" in which each mRNA possesses the same 3' genes as the next smaller mRNA but also bears a gene at the 5' end which is shared only with the next largest mRNA and genome RNA (Lai et al., 1981; Leibowitz et al., 1981; Spaan et al., 1982). RNA 7, which codes for the N protein, is synthesized in the greatest amount; RNA 6, coding for the glycoprotein E1, in the next greatest (Jacobs et al., 1981; Lai et al., 1981; Leibowitz et al., 1981). The relative amounts of messages are reflected in roughly similar ratios of polypeptides, but these relationships have not been quantitated.

MHV mRNAs and genome RNA share an identical leader sequence of about 70 nucleotides and are capped at the 5' end (Lai et al., 1982a). Several T₁ oligonucleotides are unique to certain of the mRNAs but not found in genome RNA (Lai et al., 1981; Leibowitz et al., 1981; Spaan et al., 1982). That these unusual sequences are probably junctions formed by joining the leader and the intergenic sequence at the start of the mRNA, was shown by sequence analysis and heteroduplex mapping (Spaan et al., 1983).

It is not yet clear how each mRNA obtains the same 5' end leader sequence as genome, since this 70 base leader sequence does not exist internally in the genome. Several different models have been proposed (Baric et al., 1983) to

explain how the leader sequence becomes joined to each message. Of these, the "leader-primed transcription" model is the most plausible, since leader is found on growing mRNAs in replicative intermediates (Baric et al., 1983). In this model, leader is transcribed, then freed from the template and re-associated at the initiation sites of different RNAs in order to prime transcription.

Synthesis and processing of viral proteins. In vitro translation studies have shown that coronavirus structural and nonstructural proteins are translated from individual messages (Siddell et al., 1980, 1981b,c; Rottier et al., 1981a; Leibowitz et al., 1982). This characteristic distinguishes the coronaviruses from picornaviruses and alphaviruses, where large polypeptide precursors are cleaved to form the polypeptides (Strauss and Strauss, 1983). The three major structural proteins (E2, E1 and N) of MHV were first identified by Sturman and Holmes (1977). Three non-structural proteins (200K, 30K and 14K) have been identified in MHV-infected cells (Bond et al., 1979; Siddell et al., 1981b; Leibowitz et al., 1982).

The N protein and the 14K, 30K and 200K nonstructural proteins are synthesized on free cytoplasmic polysomes, whereas the E1 and E2 glycoproteins are synthesized on ribosomes bound to the rough endoplasmic reticulum (RER). These glycoproteins are modified post-translationally in different ways. E2 of MHV-A59 is glycosylated in an N-linked manner similar to the VSV G glycoprotein (Holmes et

al., 1981a; Klenk and Rott, 1981). The oligosaccharide moiety of E1 is O-linked to serine residues (Holmes et al., 1981a; Niemann and Klenk, 1981a,b), since its glycosylation is not inhibited by tunicamycin, which specifically prevents N-linked glycosylation (Sturman, 1981; Holmes et al., 1981a; Rottier et al., 1981b). The synthesis and processing of E2 and the N protein will be presented in greater detail in their individual sections, below.

Viral assembly and release. Assembly of virions requires the interaction of genomic RNA with numerous molecules of N protein to form nucleocapsids. 90% of genomes become incorporated into EDTA-resistant nucleocapsids late during infection (Robb and Bond, 1979a; Spaan et al., 1981). Nucleocapsids then acquire a lipid and protein envelope by budding into the RER, Golgi complex and perinuclear smooth vesicles at areas containing E1 and E2 (David-Ferreira and Manaker, 1965; Oshiro, 1973; Massalski et al., 1981; Dubois-Dalcq et al., 1982; Tooze et al., 1984). Nucleocapsid helices have been observed by TEM to be on the cytoplasmic faces of membranes, forming arch-like structures during budding (Oshiro, 1973; Holmes et al., 1981a; Dubois-Dalcq et al., 1982; Massalski et al., 1982). Nucleocapsids bind E1 in vitro (Sturman et al., 1980). Taken together with evidence from tunicamycin experiments, this suggests that the nucleocapsid must recognize the cytoplasmic domain of E1 for budding to occur, as in rhabdo-, myxo-, and paramyxovirus assembly (Sturman et al., 1980; Holmes et al.,

1981a,b; Sturman and Holmes, 1983). E2 is not essential for assembly, since virions form in the presence of tunicamycin (Holmes et al., 1981a,b). At 6-7 hours p.i., spherical virions have been located in the lumens of the RER, Golgi apparatus and smooth-walled vesicles (David-Ferreira and Manaker, 1965; Massalski et al., 1981; Ducatelle et al., 1981; Dubois-Dalcq et al., 1982). Following budding, virions apparently migrate through the Golgi, where their glycoproteins are modified (Sturman and Holmes, 1984). These virions are then released from cells through the secretory apparatus (Sturman and Holmes, 1983, 1985). No polarity of secretion has been reported. Following release, many virions remain associated with the plasma membrane (for unknown reasons), and in doing so, may stimulate the host's immune response and cell fusion (Oshiro, 1973; Dubois-Dalcq et al., 1984a).

Cytopathic effects and virus-induced structures.

Coronavirus-infected cells characteristically become vacuolated and/or fused to form multinucleate syncytia; the time of onset depends on the virus and host cell (Oshiro, 1973; McIntosh, 1974). These syncytia die before nonfused cells do. MHV infection also induces several different structures in cells such as nucleocapsid inclusions (Watanabe, 1969; Caul and Egglestone, 1977; Dubois-Dalcq et al., 1982) and "myelin figures" (Dubois-Dalcq et al., 1982). "Reticular inclusions", consisting of electron-dense anastomosing filaments, have been detected in a mouse liver cell line

infected with MHV-A59 (David-Ferreira and Manaker, 1965; Watanabe, 1969). In addition, tubular inclusions of 16-25 nm diameter, have been found associated with the rough ER in MHV-infected cells (David-Ferreira and Manaker, 1965; Watanabe, 1969). Smooth walled vesicles sometimes contain virions connected to each other (Oshiro et al., 1971) and filaments of about 30 nm diameter (Takeuchi et al., 1976). Long 50 nm diameter tubules have been observed within both the RER and smooth vesicles (Dubois-Dalcq et al., 1982) and are enriched in tunicamycin-treated cells (Holmes et al., 1981a). Finally, membrane-bound structures containing fine filaments have been observed (Takeuchi et al., 1976) and these are now thought to be involved in viral RNA synthesis (Dubois-Dalcq et al., 1984a). The origins of these structures are not known.

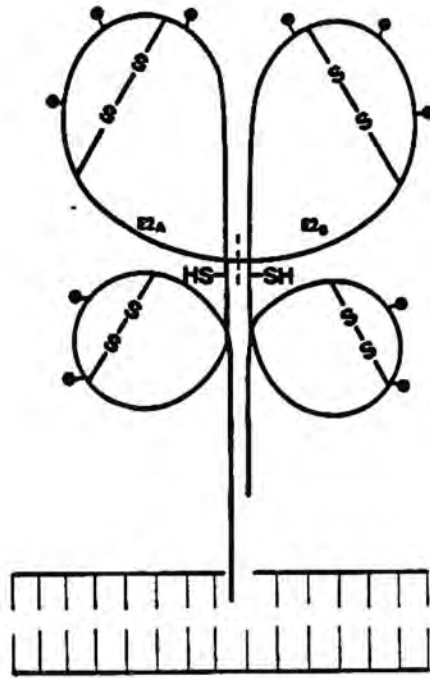
E2, the Spike Glycoprotein

Introduction. Prior to these studies, a model for the structure of E2 had been proposed, its modes of synthesis and glycosylation were understood, and it was known to be susceptible to proteolytic cleavage in vitro (discussed below). At that time, the roles of E2 in infectivity, cell fusion, pathogenicity, and immunogenicity were only beginning to be investigated. Of particular interest was whether E2 cleavage was required for viral infectivity, since cleavage of viral glycoproteins was already known to be essential for infectivity and cell fusion induced by

orthomyxo- and paramyxoviruses (see below). No source of coronavirus with uncleaved E2 had been discovered, to allow experiments on the effects of in vitro cleavage on infectivity.

Structure. The mature E2 molecule has an apparent M_r of 180,000 d, and is glycosylated with complex oligosaccharides (Holmes et al., 1981a; Niemann and Klenk, 1981a,b; Niemann et al., 1982). E2 was originally distinguished from E1 because the two glycoproteins were radiolabeled with fucose and glucosamine to different degrees. E2 is acylated by covalent addition of palmitic acid. In the virion, the ratio of E2 to E1 to N is estimated to be about 1:16:8 (Sturman et al., 1980). After it is separated from E1 and nucleocapsids, E2 forms regular rosette structures composed of peplomers similar in appearance to the virus spikes (Sturman et al., 1980). Growing virus in the presence of tunicamycin or treating purified virions with bromelain yielded virions without spikes or the E2 glycopolyptide, showing their identity (Sturman and Holmes, 1977; Holmes et al., 1981a,b). A model of E2 structure (Fig. 3) was proposed by Sturman (1981), in which E2 is inserted into the viral lipid envelope by a hydrophobic segment. The hydrophilic exterior portion of E2 is believed to bear the carbohydrate moieties. There are intramolecular disulfide bonds within 90A and 90B, but the two domains were held together by non-covalent bonds after proteolytic cleavage at the middle of the molecule.

Figure 3. Model of the E2 glycoprotein. The MHV-A59 spike glycoprotein E2 is 180K MW and is cleaved by a host cell protease (dotted line) into two polypeptides, E2_A and E2_B, each of ~90K MW. The external portion of E2 is glycosylated with N-linked complex oligosaccharides. The E2_A polypeptide is acylated with palmitic acid. Intrachain disulfide and sulfhydryl groups in E2 are important in determining its conformation, but the number and location of these cysteine residues and bridges was not known at the time this model was drawn. (Figure from Sturman, 1981.)



Synthesis and transport. The synthesis and transport of E2 has been reviewed by Sturman and Holmes (1984). During its synthesis on ribosomes of the RER, E2 is glycosylated coordinately with translation on asparagine residues by transfer of oligosaccharides from dolichol phosphate intermediates (Holmes et al., 1981a; Niemann and Klenk, 1981a,b; Siddell et al., 1983; Sturman and Holmes, 1983; Rottier et al., 1984). In the presence of tunicamycin, which prevents N-linked glycosylation of E2, or by translation in the absence of membranes, the unglycosylated precursor protein is detected as a 120K molecule (Niemann and Klenk, 1981a,b; Rottier et al., 1981a; Siddell et al., 1981c). The initial form of E2 detected by pulse-labeling MHV-infected cells was 150K in Sac(-) cells infected with A59 or JHM (Siddell et al., 1981b,c; Rottier et al., 1981b), and 180K when 17 Cl 1 and L cells were infected with A59 and MHV-3, respectively (Holmes et al., 1981a; Cheley and Anderson, 1981). In pulse-chase experiments, E2 (pulse-labeled at 6 hr p.i.) could be chased out of cells and became located in virions within two hours of its synthesis (Holmes et al., 1981a). The route of intracellular transport of E2 is similar to that of the glycoproteins of myxo-, paramyxo-, alpha- and rhabdoviruses (Sturman and Holmes, 1985). E2 transport within cells has been extensively studied by indirect immunofluorescence (Doller and Holmes, 1980). E2 was first detected in the perinuclear area by 3-4 hr p.i. By 8 hr, and through 24 hr, E2 was discovered

throughout the cytoplasmic membranes, in the Golgi and spread over the entire cell surface. Virions appear to bud only into the RER and Golgi (David-Ferreira and Manaker, 1965; Oshiro et al., 1971; Oshiro, 1973) and not from the plasma membrane, despite the presence of E2 on the plasma membrane

Glycosylation. E2 bears N-linked oligosaccharides (Sturman, 1981; Niemann and Klenk, 1981a,b). Tunicamycin, which prevents N-linked glycosylation by inhibiting the formation of the dolichol phosphate-linked oligosaccharide intermediate, inhibits E2 synthesis or allows its degradation. Tunicamycin treatment does not affect E1 glycosylation or synthesis. In the presence of the drug, virions are formed and released which lack E2 and, consequently, lack spikes (Holmes et al., 1981a,b; Sturman, 1981).

Cleavage. The 180K form of E2 can be cleaved into 90 K products. When this work was begun, all that was known about the proteolytic cleavage of E2 was the following: 1) it was followed by cell fusion (Yoshikura and Tejima, 1981), 2) the 180K and 90K forms yielded identical tryptic peptide patterns (Sturman and Holmes, 1977), and 3) some 90K was released from virions during inactivation at pH 8 (Sturman, 1977). If virions were treated with trypsin prior to inactivation, more 90K E2 was released. In pulse-chase studies, six hours after pulsing with [³H]leucine, only the 180 K form of E2 was present in infected cells (Anderson et al., 1979; Bond et al., 1979; Siddell et al., 1980; Holmes

et al., 1981a). Both the 180K and 90K forms of E2 were detected in virions (Sturman, 1977). IBV has a spike glycoprotein similar to that of MHV, composed of two polypeptides, S1 ($M_r \sim 90K$) and S2 ($M_r \sim 84K$), which are derived by cleavage of the precursor polypeptide S_0 (Stern and Sefton, 1982; Cavanagh, 1983a,b). Therefore, we wanted to learn where in its synthesis and transport cleavage of E2 occurs.

Depending on the virus strain and cell line, cleavage of E2 of MHV or other coronaviruses can enhance virus infectivity or cell fusion in tissue culture, depending on the system. The infectivity of purified MHV-A59 virions in cell culture was enhanced two-fold when incubated with trypsin at 100 ug/ml for 30 minutes, at 37°C (Sturman and Holmes, 1977). Trypsin stimulated plaque formation (i.e., cell fusion), but not replication of a mutant of MHV-S (Yoshikura and Tejima, 1981). Plaque formation of other coronaviruses in tissue culture is also enhanced by trypsin treatment, including various strains of IBV in chick embryo cells (Otsuki and Tsubokura, 1981), bovine coronavirus in fetal bovine brain or thyroid cells (Storz et al., 1981), and neonatal calf diarrhea virus in bovine embryonic lung cells (Toth, 1982).

Functions of E2. The importance of E2 for attachment of virions to cells was discovered by Holmes, Doller and Behnke (1981b) in studies with tunicamycin, in which released virions could not reattach to the cell surface in

untreated infected cells, apparently due to their lack of E2.

MHV infection induces cell fusion in vitro and in vivo (Sturman and Holmes, 1977; Sturman and Holmes, 1983), both mediated by E2. Trypsin cleavage of E2 on purified virions also causes cell fusion in vitro (Sturman and Holmes, 1977).

E2 is the dominant viral antigen, eliciting antibody which neutralizes the virus. Immunization of mice with denatured virus or surface projections, but not with viral envelopes or nucleocapsids, protected against challenge with MHV-3 (Hasony and Macnaughton, 1981), and antibody specific for E2 neutralized MHV-A59 infectivity in vitro (Holmes et al., 1981b). E2 is also the antigen expressed on the surface of infected cells which was recognized by spleen cells of uninfected mice in vitro (Welsh et al., 1986).

Thus, in terms of its structure and functions, E2 behaves similarly to the glycoproteins of orthomyxoviruses and paramyxoviruses which must be cleaved for both virus infectivity (Lazarowitz et al., 1973a; Klenk et al., 1975; Lazarowitz and Choppin, 1975; Nagai et al., 1976; Nagai and Klenk, 1977) and cell fusion (Lazarowitz and Choppin, 1975; Maeda et al., 1981; White et al., 1981). Since the role of E2 in MHV infectivity had not been well characterized, it was of interest to determine whether coronavirus infectivity also required proteolytic activation.

N, the Nucleocapsid Protein

The MHV N protein is fundamentally important in virus replication and assembly. However, little of its structure and function was understood in detail when the molecular biology of coronaviruses was reviewed by Siddell and colleagues in 1982, and again by Sturman and Holmes in 1983.

Structure. The nucleocapsid proteins of different MHV strains have molecular weights between 50 and 60K, and are phosphorylated but not glycosylated (Sturman, 1977; Sturman and Holmes, 1977; Stohlman and Lai, 1979; Siddell et al., 1981a; Rottier et al., 1981a). N protein is enriched for arginine and glutamic acid (Sturman, 1977; Anderson et al., 1979; Rottier et al., 1981a).

Synthesis. The MHV N protein is synthesized from mRNA 7, the viral message found in highest concentration in infected cells (Cheley et al., 1981; Rottier et al., 1981a; Armstrong et al., 1983a,b). It is the major viral polypeptide synthesized in MHV-infected cells (Anderson et al., 1979; Bond et al., 1981; Holmes et al., 1981b; Rottier et al., 1981b; Siddell et al., 1981b). Synthesis occurs on free ribosomes (Niemann et al., 1982) and the polypeptide can be specifically immunoprecipitated from infected cells (Bond et al., 1979; Gerdes et al., 1981; Siddell et al., 1981b). In radiolabeled MHV-A59-infected cells, N protein becomes detectable by 3 to 4 hours p.i. (Holmes et al., 1981a,b; Rottier et al., 1981b). Intracellular N protein is

very basic, shown by its behavior in non-equilibrium pH gel electrophoresis (Robb and Bond, 1979a; Siddell et al., 1981b). The intracellular polypeptide is nearly identical to the N protein found in virions by tryptic peptide fingerprinting and SDS-PAGE analysis of polypeptides translated in vitro (Siddell et al., 1980).

From the results of pulse-chase experiments, it is clear that only a small amount of the N protein which is made is incorporated into virions (Anderson et al., 1979; Bond et al., 1981; Holmes et al., 1981b; Rottier et al., 1981b; Siddell et al., 1981b). The large remaining pool of N protein is cell-associated, and could be either soluble or in the form of nucleocapsids or replicative intermediates.

Phosphorylation. From analysis of four different ^{32}P -labeled MHV strains, the N protein was found to be the only phosphorylated virion protein (Stohlman and Lai, 1979). The N proteins of strains A59 and JHM are phosphorylated at serine, but not threonine residues (Stohlman and Lai, 1979; Siddell et al., 1981a). Phosphorylation of N protein occurs within infected cells (Siddell et al., 1981a), where there is a heterogeneous population of N protein-related molecules of the same size but with different charges, shown by two-dimensional non-equilibrium isoelectric focusing (Bond et al., 1979). Protein kinase activity has been detected in MHV-JHM virions, but has not been traced to a particular protein. It has been suggested that the N protein itself may be a protein kinase (Siddell et al., 1981a). The role

of phosphorylation in the function of the N protein is unclear (Stohlman and Frelinger, 1978; Siddell *et al.*, 1981a; Stohlman *et al.*, 1983). In the case of Sendai virus, whose nucleocapsid protein is also phosphorylated, phosphorylation may be important in regulating uncoating of viral RNA or assembly of nucleocapsids (Lamb, 1975).

N-related polypeptides. Forms of N which migrate in SDS-PAGE slightly faster than virion N protein have been described in MHV-infected cells (Siddell *et al.*, 1980; Holmes *et al.*, 1981a). In one report, when polyadenylated RNAs from cells infected with MHV-JHM were fractionated on sucroseformamide gradients and translated *in vitro*, 4 to 5 bands appeared in addition to the 60 K form of N in SDS-PAGE (Siddell *et al.*, 1980). Since these products appeared regardless of whether the polypeptides had been immunoprecipitated, it was concluded that they were premature termination products. Others suggested that these polypeptides were cleavage artifacts of immunoprecipitation (Cheley and Anderson, 1981). They are never incorporated into virions. The significance of these polypeptides in virus replication is unclear.

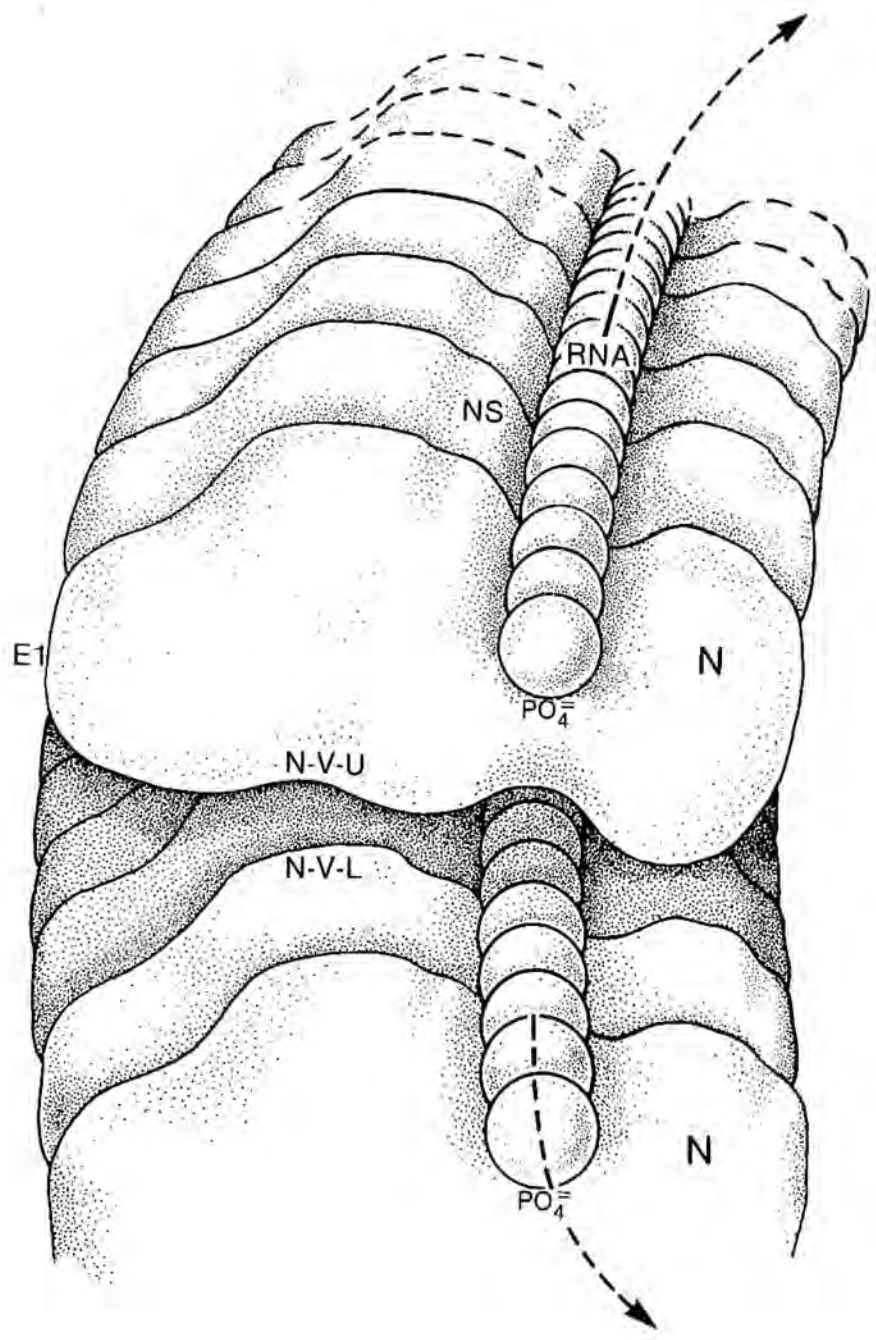
Functions. Transmission electron microscopy has demonstrated nucleocapsid structures in cells infected with MHV (Holmes and Behnke, 1981; Dubois-Dalcq *et al.*, 1982). These structures have been purified from virions solubilized with NP-40 by Sturman *et al.* (1980) and shown to contain both viral RNA and the 50K N protein, when solubilization

was performed at 4°C. After a 30 minute incubation of the detergent extract at 37°C, E1 became associated with nucleocapsids. Others have confirmed that the N protein and genome RNA comprise nucleocapsids isolated from virions (Stohlman and Lai, 1979; Siddell *et al.*, 1981). Numerous copies of N protein appear to encapsidate the genomic RNA to form helical nucleocapsids (Sturman and Holmes, 1977; Macnaughton *et al.*, 1978; Caul *et al.*, 1979; Stohlman and Lai, 1979). There is no evidence whether N protein also plays a role in virus RNA replication or transcription.

The structure of MHV virions, the interaction of nucleocapsids with E1 *in vitro*, and the possible involvement of N protein in RNA replication and/or transcription, all dictate that the N protein probably bears 6 or more important functional sites. A model of this protein as it might be assembled into a nucleocapsid is shown in Figure 4. This model shows regions of N protein which probably interact with other molecules during virus replication and assembly. Domains for binding RNA, E1, other N molecules (both horizontally and vertically), and possibly viral polymerase or other nonstructural proteins are hypothesized to exist.

By 1984, little was known about the nature of the interaction of the N protein with RNA. It was not known whether binding was nucleotide sequence-specific, as it is in the assembly of other viruses, and whether N was the sole viral RNA-binding protein. Thus, we sought to identify and characterize the RNA-binding proteins of MHV-infected cells

Figure 4. Model of N protein in the viral nucleocapsids. This model is derived from the current model of tobacco mosaic virus structure. The N protein is shown in association with portions of two consecutive turns of the viral RNA in the nucleocapsid helix. N protein probably interacts with the phosphate backbone of the RNA. Individual N molecules probably interact horizontally with other N monomers on each side. Each monomer of N may also interact vertically with an adjacent monomer above (N-V-U, N-vertical-upper binding site) and below it (N-V-L, N-vertical-lower binding site). N protein might bind nonstructural proteins (NS) during replication. It very likely binds E1 during virus budding. Arrows indicate the curvature of the nucleocapsid helix and are not intended to show the 5' and 3' ends of the RNA.



GENERAL MATERIALS AND METHODS

Viruses and Cells. The A59 and JHM strains of MHV (MHV-A59 and MHV-JHM) and the San Juan strain of vesicular stomatitis virus (VSV) were propagated and plaque assayed in the 17 Clone 1 (17 Cl 1) line of spontaneously transformed BALB/c 3T3 cells as described previously (Sturman et al., 1980).

Virus Purification. Released MHV-A59 was purified by ultracentrifugation on discontinuous and continuous sucrose gradients (Sturman et al., 1980). Late after inoculation of 17 Cl 1 cells with MHV-A59 (usually 24 hr p.i.), the infected cell supernatant was harvested and clarified at 4230 x g for 30 minutes. MHV was precipitated from the clarified supernatant by addition of polyethylene glycol and NaCl to final concentrations of 10% and 3.3% respectively, followed by incubation at 4°C for 1 hour. The precipitate was pelleted at 8000 x g in a Sorvall GS-3 rotor for 30 minutes at 4°C. Pellets were resuspended in TMS buffer (0.05 M Tris-maleate, pH 6, in 0.1 M NaCl) and layered onto discontinuous gradients consisting of 50% and 20% sucrose in TMS. Gradients were ultracentrifuged at 24,000 rpm in an SW 28 rotor (76,100 x g) for 5-6 hr at 4°C. The virus banding at the 20%/50% interface was collected with a bent needle, diluted in TMS and ultracentrifuged on continuous gradients of 20-50% sucrose at 24,000 rpm for 18 hr. The blue-white virus band of density 1.17-1.18 was collected and pelleted at 24,000 rpm for 2 hr at 4°C.

Pellets were resuspended in TMS, quick-frozen with dry-ice and stored at -70°C .

Plaque Assay. MHV was titered on confluent monolayers of L2 cells (mouse fibroblasts derived from the L929 cell line) by the method of Dulbecco (1952). Cells were inoculated with virus diluted ten-fold serially in DMEM with 10% fetal calf serum with penicillin (100 U/ml), amphotericin-B (25 ug/ml), and streptomycin (100 ug/ml), and virus was allowed to adsorb for one hour at 37°C . The inoculum was removed and the cells were overlaid with 0.95% Noble agar in minimal essential medium (GIBCO) with 5% fetal calf serum and 1% antibiotic/antimycotic. The plates were then incubated for approximately two days at 37°C , then stained with agar containing 0.02% neutral red to visualize all plaques.

Protein Determinations. Protein concentrations were determined by the methods of Bradford (1976) or Lowry *et al.* (1951).

Gel Electrophoresis and Immunoblotting. First, samples were incubated with sample treatment mix (STM; 0.06 M Tris-HCl, pH 6.7, 3 M urea, 2% sodium dodecyl sulfate) at 37°C for 20-30 minutes. Samples were then analyzed for protein by sodium dodecyl sulfate-polyacrylamide gel electrophoresis (SDS-PAGE) on 8, 10, 12%, or 5 to 15% gradient slab gels (Laemmli, 1970). Gels were electrophoresed at 150 V for 2 to 3 hr. Proteins were electroblotted using a Transblot apparatus (Bio-Rad) from gels onto

nitrocellulose paper (0.45 μ m pore size; Schleicher and Schuell) at 30 V for 16 to 20 hr or at 55 V for 4 hr, with cooling (Towbin et al., 1979; Bowen et al., 1980). The transfer buffer consisted of 25 mM Tris, 192 mM glycine, pH 8.3, and 20% methanol. Blots were stained for protein using amido black (Towbin et al., 1979).

Preparation of Antisera. The preparation of rabbit antisera to gradient purified NP40-disrupted MHV virions and to isolated E2 was previously described (Sturman et al., 1980). Monospecific anti-N antibody was prepared in rabbits similarly by Dr. John Boyle (USUHS), who immunized rabbits with N protein extracted from an SDS gel of purified virus. Antiserum to the E1 glycoprotein was prepared by immunization of rabbits with a synthetic peptide to the carboxy terminus of E1 from MHV-A59 (prepared by Dr. Chris Richardson, NIH), coupled to keyhole limpet hemocyanin.

Mouse antibody to the N protein was raised in female BALB/c mice (Jackson Laboratories) as described previously (Russell et al., 1970). Mice were inoculated intramuscularly and subcutaneously with N protein eluted from a band of an SDS gel and were inoculated intraperitoneally (i.p.) with complete Freund's adjuvant on day 3. Booster inoculations were administered i.p. on days 27 and 31. Ascites fluid was prepared by intraperitoneal inoculation of fresh sarcoma 180 cells (kindly provided by Dr. Walter Brandt, Walter Reed Army Institute for Research, Washington, D.C.) on day 31. The mice were tapped for ascites fluid on days 35 and 39.

Antibody specificities were determined by immunoblot analysis of proteins of MHV virions and MHV infected or control cell extracts.

Immunoblot analysis. Viral proteins on nitrocellulose blots were identified by immunoblotting (Towbin *et al.*, 1979). Antisera and [125 I]-staphylococcal protein A (SPA; Pharmacia) were diluted in 50 mM Tris, pH 7.4, 150 mM NaCl, 1 mM EDTA, 0.05% Tween 20, and 0.1% bovine serum albumin. Wash buffer was 150 mM NaCl with 0.05% Tween 20. Bound antibody was detected with 10^5 - 10^6 cpm/ml of [125 I]SPA. Radioiodinated SPA was prepared by the chloramine T method (Tsu and Herzenberg, 1980). Radiolabeled viral protein bands were detected by autoradiography with intensifying screens. Alternative development systems were horseradish peroxidase coupled anti-immunoglobulin (Kirkegaard and Perry Laboratories), followed by reaction with 3,3'-diaminobenzidine (DAB; Sigma), by the method of Partanen *et al.* (1983), except using 100 mM Tris-HCl, pH 7.4, or with 4-chloro-1-naphthol (Sigma) as described by Hawkes *et al.* (1982).

Radioisotope Counting. Samples (except gradient fractions) were TCA-precipitated on Millipore filters and counted in a Liquifluor-based scintillant. 3 H samples were counted in an LKB 1219 Rackbeta scintillation counter, and 32 P samples in a Beckman LS 9000 counter.

I. THE INTRACELLULAR MATURATION OF MHV AND ITS E2 GLYCOPROTEIN

Introduction

The E2 glycoprotein of MHV serves important functions, as described in the general introduction, such as binding to cell receptors, inducing neutralizing antibody and cell-mediated cytotoxicity, and causing cell fusion (Collins et al., 1982; Sturman and Holmes, 1983; Holmes et al., 1984).

At the time these studies began, we knew that the 180K and 90K polypeptides of MHV were both forms of E2, however, there was disagreement over whether the 180K form was a dimer of two identical 90K polypeptides derived from a 150K precursor (Siddell et al., 1981b,c) or was cleaved into two different products, both of 90K (Sturman et al., 1980). From pulse-labeling experiments (Sturman et al., 1980) and in vitro translation studies (van der Zeijst et al., 1981), it appeared that a large precursor was indeed cleaved. However, the intracellular site and time of cleavage were not known. Also, the functions of E2 were little understood at that time. It was not known whether proteolytic cleavage of E2 was necessary for virus infectivity, as it is for orthomyxo- and paramyxoviruses. Released virus from many different cell types bore 90K E2 (Frana et al., 1985), and therefore none of these virus preparations could serve as a source of virus with uncleaved E2. An additional problem was that MHV buds intracellularly, unlike other

enveloped RNA viruses which bud at the cell membrane; thus, the effects of protease inhibitors on virus infectivity could not be readily studied due to their limited penetration into cells.

We hypothesized that, because cleavage of E2 appeared to be a late event in virus maturation, just before virus release, most intracellular virions (ICV) would bear uncleaved E2. This was based on the assumption that E2 was cleaved after virus budding, probably as virions passed through the Golgi complex. If intracellular virions could be isolated, they could be characterized as to whether E2 was cleaved, and used to determine the effect of protease cleavage of E2 on infectivity. Therefore, we chose to isolate and characterize ICV particles by fractionating cells which had been enzymatically stripped of surface-associated virus. ICVs were compared to released virus (RV) and to total cell-associated virus (CAV, including intracellular and plasma-membrane associated virus) for a number of characteristics, including susceptibility to trypsin activation. Due to the lower yield of ICV compared to RV (especially after two purification steps), two different methods for increasing the intracellular concentration of virions were tested. First, virus was grown in the presence of the ionophore monensin, since monensin inhibits glycoprotein transport (Tartakoff and Vassalli, 1979; Griffiths et al., 1983), and thus possibly secretion of MHV. Second, virus was grown in the presence of cytochalasin D, which

inhibits the maturation and release of measles virus (Stallcup et al., 1983), and therefore might also increase the yield of intracellular MHV.

As shown below, we found that E2 was cleaved in ICV. In addition, trypsin treatment of RV, CAV and ICV failed to enhance virus infectivity. Monensin treatment of MHV-infected cells caused noninfectious virions to be released, and from the results of TEM, appeared to block virus release completely at a higher concentration. Monensin treatment also markedly inhibited cleavage of E2 and appeared to inhibit E2 glycosylation. These results indicate that in 17 Cl 1 cells, cleavage of only a small proportion of E2 molecules may be necessary for virus infectivity, and E2 is probably cleaved after transport from the medial region of the Golgi.

Materials and Methods

Radiolabeling. 17 Cl 1 cells were mock-infected or infected with MHV-A59 at an MOI of 3-10. When viral proteins were to be analyzed by SDS-PAGE and fluorography, the growth medium was replaced with leucine-deficient MEM with 5% dialyzed fetal calf serum. [³H]leucine (New England Nuclear) was added at the times and concentration (5, 10 or 20 uCi/ml) indicated in the figure legends. Unless otherwise indicated, actinomycin D (Sigma) was added to 5 ug/ml one hour before the [³H]leucine.

Preparation of intracellular and cell-associated virus. To obtain cells containing only ICV, virus particles adsorbed to the cell surface were removed by protease treatment. Cells were washed twice in ice-cold PBS and incubated with 0.5 mg/ml proteinase K in Dulbecco's-HEPES medium, pH 7-7.4 (Type XI, fungal, from Tritirachium album, Boehringer-Mannheim; 5x stock in Dulbecco's-HEPES medium) at 4°C for 45 minutes in an atmosphere of 5% CO₂ on a rocker platform. For CAV, cells were incubated with medium alone. The reaction was terminated by adding 3% BSA with 1 mM phenylmethylsulfonylfluoride (PMSF, Sigma). The cells were washed twice more with 0.2% BSA with 1 mM PMSF, pelleting at 200 x g for 3 minutes. At this point, an aliquot of cells was pelleted, fixed in 2% glutaraldehyde, and processed as described under the TEM section of this Methods. ICV and CAV virions were isolated as follows. The cells were scraped from the bottle with a rubber policeman. Cells were allowed to swell in reticulocyte standard buffer (RSB; 0.01 M Tris, pH 7.2-7.4, 0.01 M NaCl, 0.005 M MgCl₂) for 10 minutes on ice, and were then homogenized with a "Tissu-mizer" (Tekmar Instruments) at 40,000 rpm for 2, 20-30-second bursts. Cells resuspended in medium, rather than RSB, were very resistant to disruption by either tissumizer or dounce homogenization. Homogenates were freed of nuclei and large debris by centrifugation at 350 x g for 10 minutes.

Cell fractionation. Homogenates of mock-infected or MHV-infected cells were fractionated by the method of Caliguiri and Tamm (1970). Supernatants were layered onto discontinuous 25-60% sucrose gradients (consisting of layers of 25, 30, 40, 45 and 60% sucrose, or 15, 20, 30 and 50% sucrose) and centrifuged at $76,000 \times g$ for 3 hrs (19 hrs in the experiment shown in Fig. 7) at 4°C . The cell extract separated into 5 bands on this gradient. Bands were collected with a bent needle attached to a syringe. In certain experiments these bands were each layered onto continuous 20-50% sucrose gradients and centrifuged at $76,000 \times g$ for 14-16 hrs at 4°C . Fractions were collected from the top of each continuous gradient using a Densi-Flo gradient fractionator (Buchler). An aliquot of each fraction was counted for ^3H , and additional samples were taken for plaquing (1:10 dilution in medium), SDS-PAGE (1:2 in STM), and negative staining and embedding for transmission electron microscopy.

Transmission electron microscopy (TEM). For negative staining, gradient samples were diluted 1:3 in PBS to reduce the sucrose concentration, and stained with 2% phosphotungstic acid (Almeida and Tyrrell, 1967). For thin sections, whole cells were pelleted in a bench-top angle-head rotor, and gradient samples were diluted in TMS and pelleted at 44,000 rpm in an SW 50.1 rotor for 2.5 hr at 4°C . Fixation, dehydration and embedding were performed as by Holmes (1968). Pellets were carefully overlaid with 1% glutaraldehyde at 4°C (Sabatini *et al.*, 1962), washed, and

post-fixed in 1% osmium tetroxide in PBS (Palade, 1952). The fixed samples were then dehydrated in a series of increasing concentrations of ethanol and propylene oxide and embedded in Epon (Luft, 1961). Ultrathin sections were made with a diamond knife on an LKB ultramicrotome (model 8800 Ultratome III). Sections were stained with 2% uranyl acetate and 0.4% lead citrate (Reynolds, 1963), and examined with a JEOL JEM-100CX electron microscope operating at 80 kilovolts.

Monensin experiments. L2 cells maintained in spinner culture at 37°C at a concentration of $1-2 \times 10^8$ cells/ml in a volume of 100 ml were pelleted and resuspended with MHV-A59 (1.75×10^8 PFU) in 10 ml Dulbecco's HEPES medium with 5% fetal calf serum and antibiotic. Following adsorption for 1 hr, the cells were pelleted and resuspended in leucine-deficient MEM with 5% fetal calf serum and antibiotic. At 2 hr p.i., the cell suspension was divided in half, and monensin (Calbiochem-Behring) was added to one portion to a final concentration of 10^{-6} M. At 7.5 hr p.i., actinomycin D-mannitol (Sigma) was added to 3 ug/ml. At 8 hr, [3 H]leucine was added to both portions of cells to a final concentration of 10 uCi/ml. Monensin-treated cultures were then divided in two. At the time of harvest, one portion was treated with proteinase K and processed to obtain ICV, the other mock-treated and processed to obtain CAV. The cells were harvested at 12 hr p.i. and supernatant samples were taken for counting and plaque assay. To

harvest RV, supernatant medium over infected cells was pelleted through a 1 ml cushion of 20% sucrose in an SW 28 rotor at 76,000 x g for 3 hours. Pelleted material was resuspended in STM and incubated at 37°C for 30 min for analysis on SDS-PAGE, and aliquots were counted for ³H. ICV and CAV were prepared from infected cells as described above. Two major bands appeared on discontinuous gradients and samples from these bands were analyzed for density, radiolabel and proteins on SDS-PAGE. Bands collected from discontinuous gradients were centrifuged on continuous 20-50% sucrose gradients for 13.5 hr at 76,000 x g in an SW28 rotor. 0.5 ml fractions were collected and an aliquot of each fraction was counted. Peaks of [³H]leucine counts and/or fractions of virus density (1.17-1.18 g/ml) were pooled and analyzed by SDS-PAGE.

Cytochalasin D experiments. Cytochalasin D (Calbiochem-Behring) was added to cultures of 17 Cl 1 cells at a concentration of 0.2 uM at 6 hr p.i. Cells were harvested at 24 hr, and treated with acetylated trypsin (Sigma) at 100 ug/ml for 30' at 4°C, then processed for TEM. Infected cell supernatants were saved for plaquing.

Trypsin experiments. Cells were infected in the presence or absence of monensin (1 uM) and processed for RV, CAV or ICV as described above; samples were treated with trypsin or mock-trypsinized and titered for infectivity in plaque assays. Trypsin treatments were as follows:

Experiment #1. Samples of RV in DMEM with FCS were

diluted 1:50 with DMEM and pelleted through 0.5 ml cushions of 20% sucrose in TMS pH 6 with 1 mM PMSF at 44,000 rpm in an SW 50.1 rotor for 1 hr at 4°C. Pellets were resuspended in DMEM, and divided in two. Trypsin (Sigma) in DMEM (or DMEM alone) was added to a final concentration of 5 ug/ml. Mixtures were adjusted to neutral pH with 5% CO₂ and incubated at room temperature for 45 minutes, then diluted 1:10 (and further) in DMEM with 10% FCS for plaquing. Samples were plaqued in duplicate, with the exception of the lowest dilution of released virus grown in the presence of monensin, which was titered in quadruplicate.

Experiment #2. Samples of RV or CAV (CAV harvested at 12.5 hr and partially purified on discontinuous gradients) were diluted 1:3.3 with cold TMEN (0.05M Tris-maleate, pH 6, 0.001 M EDTA, 0.1 M NaCl) and layered upon 1 ml 50% sucrose and 1 ml 20% sucrose in SW 50.1 centrifuge tubes. The tubes were centrifuged at 40,000 rpm in an SW 50.1 rotor for 90 minutes at 4°C. The virus bands were collected with a bent needle and divided in half. Trypsin-diphenylcarbamyl chloride (trypsin-DPCC; Sigma; 150 ug/ml in TMEN) was added to one of the two samples, to a final concentration of 15 ug/ml, TMEN alone to the other. (The DPCC inhibits chymotrypsin activity.) The trypsin mixtures were incubated at 37°C for 30 min, with gentle shaking every 10 min. To stop the reaction, soybean trypsin inhibitor was added to all tubes to a final concentration of 50 ug/ml and the mixtures were incubated for 30 min on ice. The mixtures

were then resuspended in TMEN and pelleted through 0.5 ml of 20% sucrose at 40,000 rpm for 1.5 hr. Each pellet was resuspended in TMEN, then diluted in DMEM with FCS as usual for plaquing in triplicate.

Experiment #3. RV and ICV (harvested at 24 hr, partially purified on discontinuous gradients) in 1 mM PMSF, were pelleted at 44,000 rpm in an SW 50.1 rotor for 1 hr through a 0.5 ml cushion of 20% sucrose in TMS pH 6, and resuspended in TMEN. Trypsin (or TMEN) was added at 0.5 or 1 mg/ml and mixtures were incubated at 37°C for 1 hr with gentle shaking every 15 min. Samples were then diluted in DMEM and 5% FCS, 5% NCS, and titered in duplicate.

Results

Isolation of intracellular and cell-associated MHV.

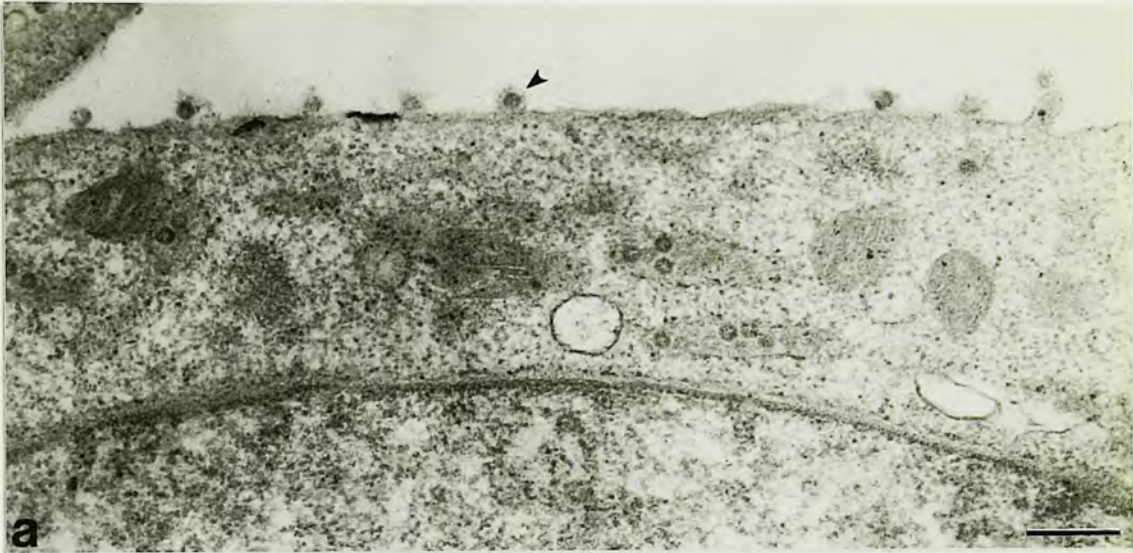
Virus maturation and its relation to the cleavage of E2 were studied. First, intracellular virus (ICV) was isolated and compared with released virus (RV) and cell-associated virus (CAV) to identify changes in E2 which occur between the site of budding and virus release at the cell membrane. Secondly, methods to increase the concentration of intracellular virus particles were investigated so that larger numbers could be isolated for characterization of their infectivity and susceptibility to trypsin activation.

To assess degrees of protease cleavage of E2 during virus maturation, a method of obtaining intracellular virus particles was required. For stripping virus from the cell

surface, four different enzymes were screened. Cells (17 Cl 1) infected for 24 hrs were treated with the following proteases in the cold (to prevent cell death) and processed for TEM: acetylated trypsin (100 ug/ml 30 min) (Fong et al., 1976), chymotrypsin (100 ug/ml 30 min), bromelain (1 mg/ml 30 min) (Compans et al., 1970), and proteinase K (100 ug/ml 45 min) (Ebeling et al., 1974). Cells were washed twice with PBS, then incubated at 4°C with enzyme on a rocker platform in an atmosphere of 5% CO₂. Proteolysis was terminated by incubation with 3% BSA and 1 mM PMSF for 10 minutes. The cells were then washed twice with 0.2% BSA in PBS and pelleted in round-bottomed tubes in an angle-head rotor. The cells were fixed in 1% glutaraldehyde before being embedded for thin sectioning. Of the proteases tested, only proteinase K caused the cells to detach as a single sheet, while treatment with the other enzymes caused the cells to detach and clump. More importantly, electron microscopy showed that proteinase K treatment removed all surface-bound virus particles from cells which were clearly infected, containing numerous virions in vesicles in the cytoplasm (Fig. 5), while the other enzymes left virus particles on the cell surface (data not shown).

Therefore, infected cells were labeled with [³H]leucine, treated with proteinase K, swollen in RSB and homogenized to release intracellular particles for purification and analysis. Nuclei were removed by centrifugation. Control experiments demonstrated that neither RSB treatment nor

Figure 5. Removal of MHV from the cell surface by enzymatic treatment with proteinase K. At 24.5 hr p.i., MHV-A59-infected 17 Cl 1 cells were incubated in Dulbecco's-HEPES medium at 4°C for 45 minutes in 5% CO₂ as a control (a). Other flasks of infected cells were incubated with proteinase K (0.5 mg/ml) under otherwise identical conditions (b). The cells were then incubated with 3% BSA with 1 mM PMSF to terminate the proteolysis. For electron microscopy, the cells were pelleted, fixed in 2% glutaraldehyde, dehydrated, embedded and thin sectioned as described in the Methods. The sections were stained with 2% uranyl acetate and 0.4% lead citrate and examined with a JEOL JEM-100 CX electron microscope. (a) Infected cell, showing virions in the RER and on the cell surface (arrowhead). Bar = 0.5 micron. (b) Infected cell after proteinase K treatment. Bar = 1 micron.



homogenization affected MHV-A59 virus infectivity in plaque assays. Homogenates were then fractionated on discontinuous gradients (Caligiuri and Tamm, 1970). Five bands and a pellet were obtained reproducibly. CAV or ICV were concentrated at the 30%/50% sucrose interface (band 4), as shown by negative stains (data not shown) and plaque assay (Fig. 6), as well as previous studies (Sturman et al., 1980). These virions were only partially purified, since virus-induced structures and nucleocapsids were also present in ICV preparations (see below). Cell fractions produced on these gradients have been characterized by TEM for HeLa cells (Caligiuri and Tamm, 1970). Enzymatic analyses of fractionated 17 Cl 1 cells (Niemann et al., 1982) have shown that in band 4, where MHV is localized (density 1.17-1.18 g/ml), rough and smooth ER and mitochondria would also be found. Figure 7 shows a negative stain of CAV from band 4 (i.e., fraction 4 from infected cells which were not treated with proteinase K). The virions had the diameter and peplomers characteristic of released virus. Some CAV were free, but most were associated with sheets of membranes. Intracellular virus particles isolated in this manner were less numerous, were usually not associated with membranes, and often associated with clumps of nucleocapsid, making analysis by negative stain difficult (not shown).

ICV and CAV were collected and purified further on continuous sucrose gradients. The profiles of radioactivity from these gradients are shown in Fig. 8. On continuous

Figure 6. Distribution of infectivity across a discontinuous sucrose gradient. MHV-A59-infected 17 Cl 1 cells were harvested at 24 hr. Cells were swollen in reticulocyte standard buffer, homogenized with a Tissumizer, and fractionated on discontinuous sucrose gradients. Gradient bands were collected with a bent needle and assayed for infectivity by plaque assay. Band 4 is the 30%/50% sucrose interface. Band 6 is the pellet. Bars indicate the titer of infectious virus in each fraction.

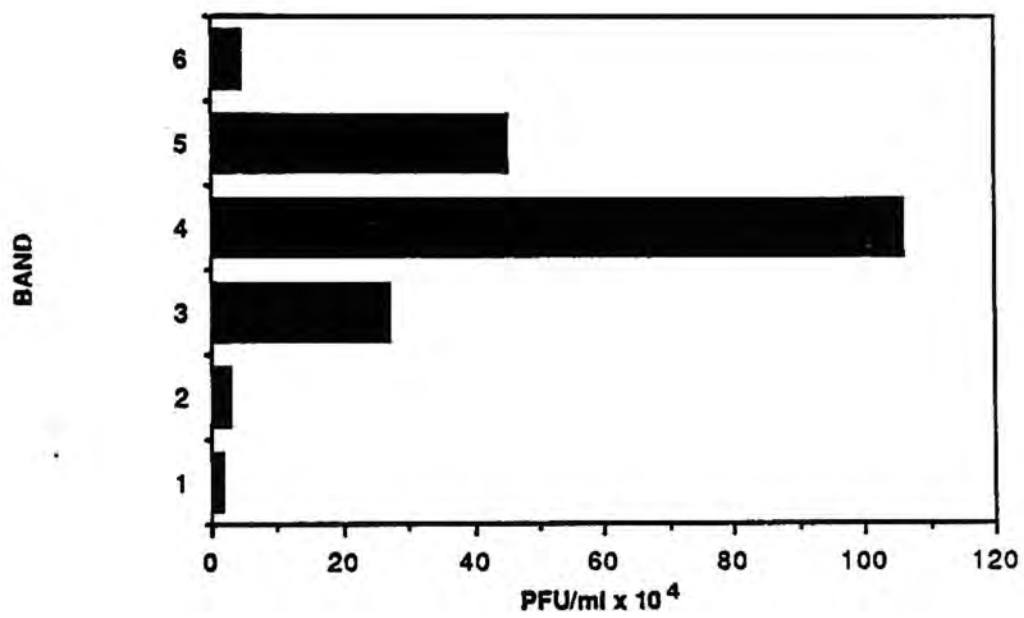


Figure 7. Cell-associated virions demonstrated by negative staining. Cell-associated virions were isolated by Dr. Mark Frana as follows: Cells (17 Cl 1) were infected with MHV-A59, and at 14 hr, actinomycin D was added to a final concentration of 5 ug/ml. At 17.75 hr, cycloheximide was added at 100 ug/ml, and the cells were harvested at 18 hr. At that time, the cells were washed, scraped, and allowed to swell in reticulocyte standard buffer. The cells were then homogenized and the cytoplasmic homogenate was ultracentrifuged on discontinuous sucrose gradients (consisting of layers of 25, 30, 40, 45 and 60% sucrose). The fourth band from the top of the gradient was diluted 1:3 with PBS and negatively stained with 2% phosphotungstic acid. This band contained the highest concentration of virus particles. Note the close relationship of virions to membranes (M). Glycoprotein spikes are visible on some virions (arrowhead). Bar = 200 nm.

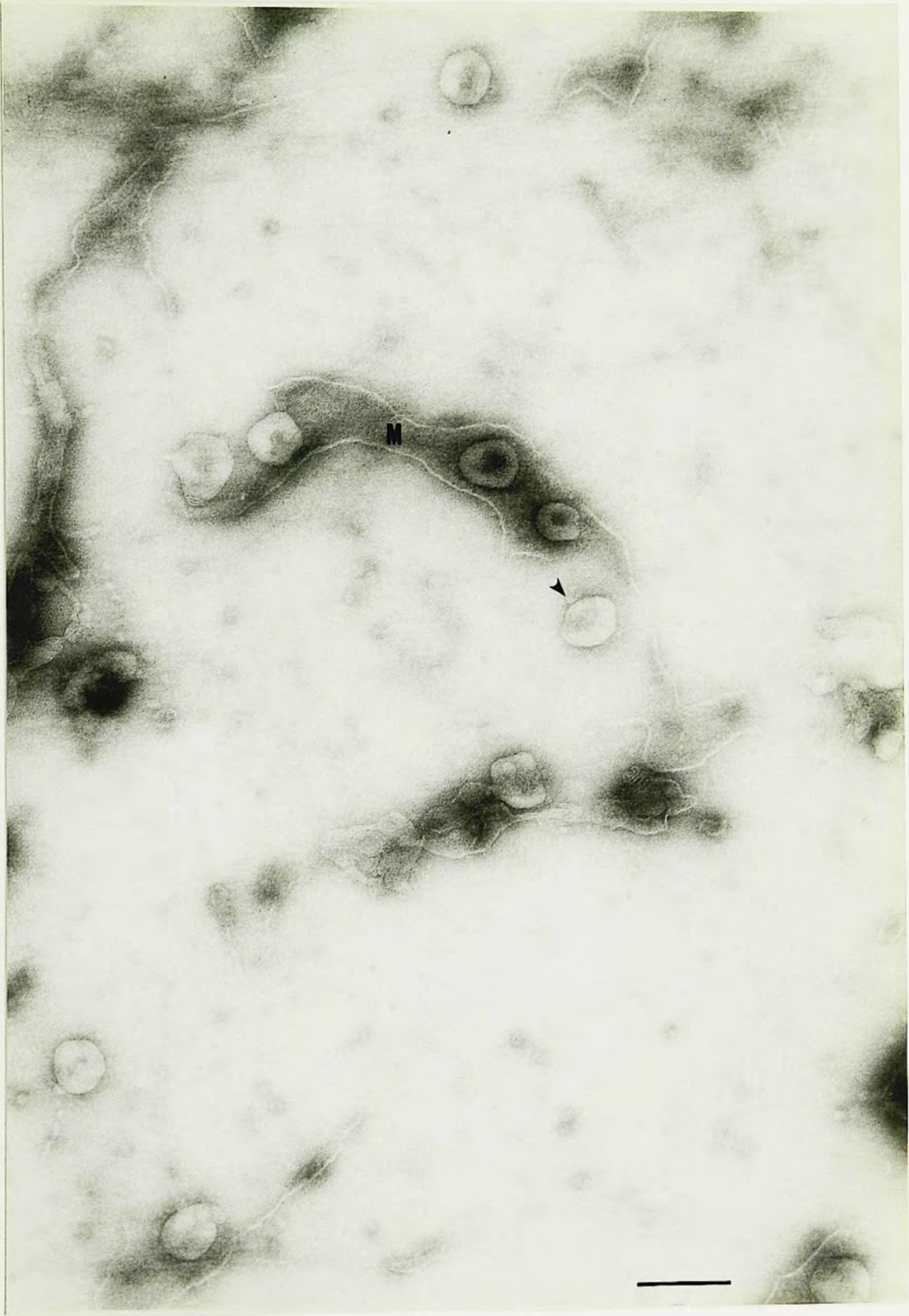
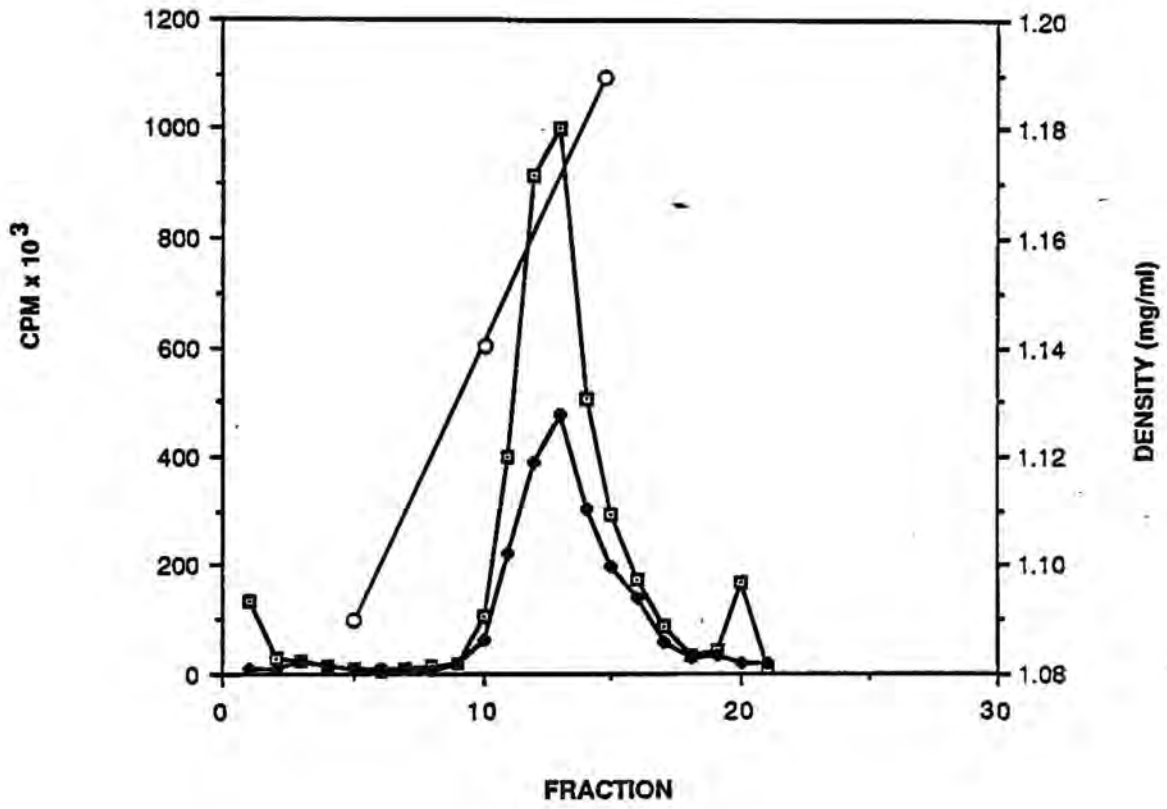


Figure 8. Purification of intracellular and cell-associated virus particles by sucrose gradient ultracentrifugation. MHV-A59-infected 17 Cl 1 cells were labeled with [³H]leucine from 21 to 25 hr (in the absence of actinomycin D) and fractionated on discontinuous sucrose gradients as described in the Materials and Methods. Bands at the 30%/50% interfaces of discontinuous gradients were collected, ultracentrifuged on continuous 20-50% sucrose gradients, and fractionated. (□-□) cell-associated virus (CAV); (◆-◆) intracellular virus (ICV); (O-O) density.

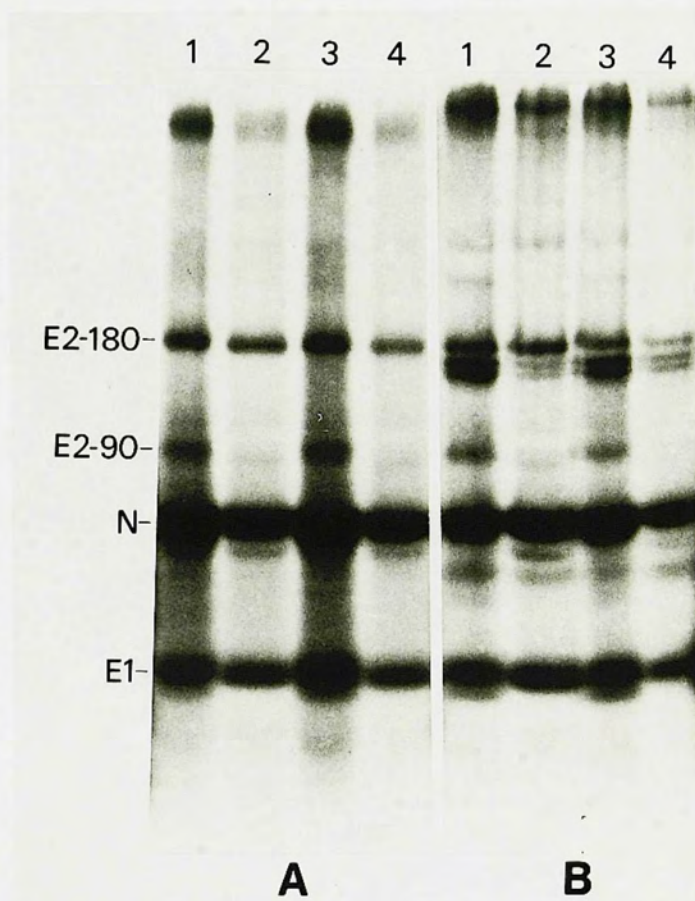


gradients of CAV, there appeared one major band of density ~ 1.17 g/ml, which contained viral proteins on SDS-polyacrylamide gels. This band was composed of well-separated virions, as seen by negative stain (not shown). These data indicate that ICV comprised $\sim 56\%$ of the total CAV and that ICV was of the same density as CAV.

E2 cleavage on ICV and CAV. The ratio of E2-90 to E2-180 in [3 H]leucine-labeled cell extracts and in ICV and CAV at 12 hr p.i. was compared by polyacrylamide gel electrophoresis of fractions from discontinuous gradients (Fig.9). L2 cells were infected with MHV-A59 and labeled from 8-12 hrs with [3 H]leucine. Cytoplasmic extracts of cells which had been treated with proteinase K (*i.e.*, intracellular viral proteins) showed the same relative amounts of the 180K and 90K forms of E2 as were seen in cells not treated with protease (Fig.9A). These preparations included both E2 on virions and on membranes. (The additional bands seen in panel B but not in panel A may have arisen from proteolysis during the purification procedure. This was the only experiment in which they were detected.) The gels showed that E2-90 was present in ICV as well as CAV, and in approximately the same amount relative to E2-180 (Fig. 9B). The ratio of E2-90 to E2-180 in ICV and CAV from 17 Cl 1 cells was less than in RV, where 90K and 180K are present in equal amounts.

Morphology of ICV. For morphological study, ICV from discontinuous gradients was pelleted, embedded,

Figure 9. Proteins of partially purified cell-associated and intracellular virus preparations and cytoplasmic extracts, in the presence and absence of monensin. L2 cells were infected and some were treated with monensin (1 μ M) at 2 hr p.i. as described in the Methods. Actinomycin D-mannitol was added at 7.5 hr, and 10 μ Ci/ml 3 H-labeled leucine at 8 hr. The cells were harvested at 12 hr p.i. Some samples were treated with proteinase K, homogenized, and the nuclei removed. These cytoplasmic extracts are shown in panel A. Proteins of virions partially purified on discontinuous sucrose gradients (harvested from the 30%/50% sucrose interface) are shown in panel B. Protein samples were electrophoresed on a 5-20% gradient SDS-polyacrylamide gel; the resulting fluorograph is shown. Panel A, Proteins of cytoplasmic extracts from MHV-infected cells. Lane 1, untreated cells; lane 2, cells incubated with monensin; lane 3, cells whose surface-bound virions were removed by proteinase K treatment; lane 4, cells incubated with monensin and treated with proteinase K. Panel B, Proteins of partially-purified virus from MHV-infected cells. Lane 1, cell-associated virus (CAV); lane 2, cell-associated virus from cells incubated with monensin; lane 3, intracellular virus (ICV); lane 4, intracellular virus from cells incubated with monensin.



sectioned and stained for TEM (Fig. 10). This band contained numerous virus particles, some circular in outline, others oval. The ratio of circular to oval ICV was ~5:1. The proportion of flattened virions may actually be higher, since some will appear circular. Eighty-five ICVs which appeared circular were measured manually for their smallest and largest diameters (magnification 74,000x), and found to range in diameter from 70 to 150 nm, with mean minimum and maximum diameters of 81 x 102 nm. In contrast, the average dimensions of 16 individual, apparently flattened virions were 48 x 110 nm. The electron-dense dots and rods lining the wall of these virus particles (Fig. 1b, arrowheads) correspond to the helical nucleocapsid seen in cross-section and longitudinal section in infected cells. MHV-A59 particles in 17 Cl 1 cells are transformed from spherical forms as virions pass from the RER and Golgi to flattened and disk-shaped particles in the Golgi and smooth-walled vesicles, possibly due to conformational changes in the nucleocapsid (Holmes and Behnke, 1981).

Virus-induced tubular structures were also apparent in the ICV preparation and not controls (Fig. 11 and 12). It has been suggested that they may be composed of E1, since they are especially prominent in tunicamycin-treated cells (Holmes et al., 1981a). Tubules ranged from ~32 to 58 nm in diameter and contained no nucleocapsid. Any proteins present in these tubules could be identified in immunoelectron microscopy experiments using antisera to viral

Figure 10. Intracellular virus particles in thin section. At 12 hr p.i., MHV-A59-infected 17 Cl 1 cells were incubated with proteinase K and homogenized as described in the Methods. The cytoplasmic homogenate was fractionated on a discontinuous sucrose gradient. The band of intracellular virus at the 25%/40% interface was diluted in TMS, pelleted, fixed, embedded and thin-sectioned for electron microscopy. Note both spherical and flattened virions. Bar = 0.5 micron.

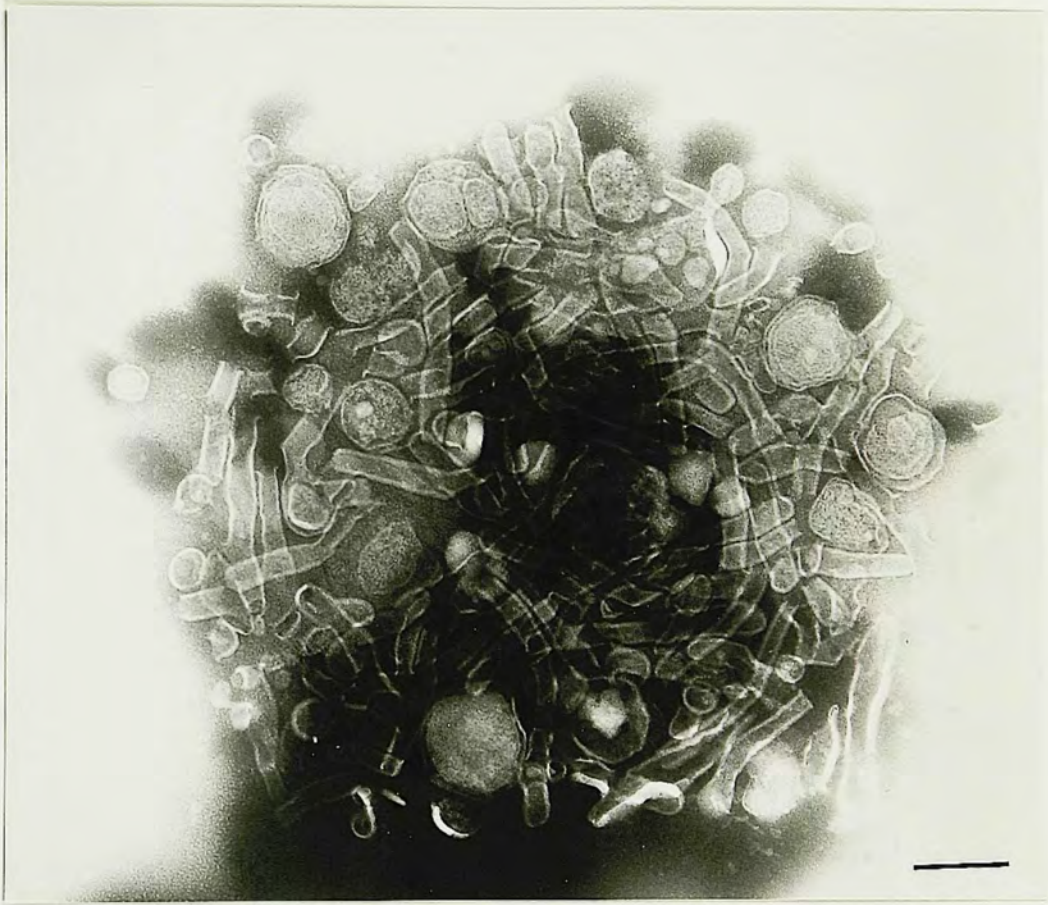


Figure 11. Virus-induced tubules in MHV-infected cells in thin section. MHV-A59-infected 17 Cl 1 cells were incubated with proteinase K at 24 hr p.i. to remove virions adsorbed to the plasma membrane. The cells were washed with 3% BSA with 1 mM PMSF, washed twice with 0.2% BSA with 1 mM PMSF, pelleted and fixed with glutaraldehyde and osmium tetroxide. The fixed cell pellet was processed for electron microscopy and stained as described in the Materials and Methods. Virus-induced tubules (arrows) are shown in the lumen of the RER, in both cross-section and longitudinal section. Intracellular virions (arrowhead) are also seen in the lumen of the RER. Bar = 200 nm.



Library of Science

Figure 12. Virus-induced intracellular tubules demonstrated by negative staining. MHV-A59-infected cells were labeled with [³H]leucine (in the absence of actinomycin D) from 21-25 hr p.i., then incubated with proteinase K and homogenized. The cytoplasmic homogenate was ultracentrifuged on discontinuous sucrose gradients. The intracellular virus band at the 30%/50% interface of that gradient was purified further on a continuous gradient of 20-50% sucrose. Fractions were collected and counted, and an aliquot of the peak of radiolabel (density 1.175 g/ml) was negatively stained with 2% phosphotungstic acid. This fraction contained both intracellular virus particles (ICV) and tubules. Bar = 200 nm.



structural proteins.

Methods for increasing the concentration of ICVs.

Because the yield of ICV was always significantly less than the yield of RV or CAV, two methods for enhancing the concentration of intracellular virus particles were tested: 1) monensin treatment, and 2) cytochalasin D treatment.

Monensin treatment. To test whether virus release would be inhibited by a drug known to block secretion of glycoproteins (and possibly of virions bearing glycoproteins), 17 Cl 1 cells were infected and treated with the ionophore monensin at 50 uM from 1-12 hr (Tartakoff and Vassalli, 1977, 1978, 1979; Griffiths *et al.*, 1983). L cells were chosen because they accumulate intracellular nucleocapsids, and are more readily lysed than other cell lines used to propagate MHV. Monensin appeared to prevent release of virus particles. Electron microscopy of monensin-treated MHV-A59-infected cells demonstrated virions budding into smooth vesicles and lining the walls of those vesicles (Fig. 13). No particles were seen attached to the cell surface. For MHV-A59 in 17 Cl 1 cells, formation of virions is normally so rapid that virions in the process of budding are only rarely observed. Monensin apparently slows or arrests the process of virus budding, yielding images like Fig. 13.

Effect of monensin on cleavage of E2. Fig. 9 shows a polyacrylamide gel of [³H]leucine-labeled samples from monensin treated cells at 12 hr p.i. In cytoplasmic

Figure 13. Arrest of MHV budding by monensin treatment. Cells (17 Cl 1) were infected with MHV-A59 in the presence of 50 μ M monensin and fixed with glutaraldehyde at 18 hr p.i. Budding is rarely seen in MHV-infected cells under normal conditions. Bar = 200 nm. Photograph courtesy of Dr. Kathryn V. Holmes.



extracts and CAV and ICV virus bands from discontinuous gradients from monensin-treated cells, little or no [³H]leucine-labeled E2-90 was detectable. Cytoplasmic extracts of monensin-treated cells showed little 90K E2 relative to 180K E2 when immunoblotted with antiserum to E2 (Fig. 14).

Similarly, monensin-treated cells yielded peaks of CAV from continuous gradients, and RV, which showed little detectable E2-90. The monensin CAV sample shown was derived from a peak with density ~ 1.21 g/ml. In addition, the small amount of E2-90 was in a tighter band, indicating a more homogeneous size than in E2-90 of control virus. These results show that monensin blocked the cleavage and probably some of the glycosylation of E2 as well.

Effect of monensin on MHV infectivity. The effect of monensin on virus infectivity was explored in two different experiments (Table 2). In experiment 1, RV from infected cells treated (or mock-treated) with monensin for 12 hr, were titered on L cells. The supernatants were tested either before or after ultracentrifugation through a cushion of 20% sucrose to insure that virus particles were being assayed. In experiment 2, CAV from mock-treated or monensin-treated cells was banded on discontinuous gradients and assayed for plaque formation. (Experiment 3 pertains only to trypsin treatment, and is described below.) The yield of infectious virus (RV and CAV) obtained from cells infected in the presence of monensin, was reduced by over 99% compared to controls. This reduction in infectivity was

Figure 14. Monensin inhibition of E2 cleavage, shown by immunoblotting. L2 cells were infected with MHV-A59 and incubated with monensin (1 μ M) from 1 to 12 hr p.i., when the cells were harvested. In the experiment shown in lanes 1-7, actinomycin D was added at 7.5 hr p.i., and 10 μ Ci/ml [3 H]leucine at 8 hr. In the experiment shown in lanes 8 and 9, the [3 H]leucine was added to a final concentration of 5 μ Ci/ml at 1 hr p.i. in the absence of actinomycin D.

Samples were electrophoresed on 10% SDS-polyacrylamide gels, and electroblotted onto nitrocellulose. The blots were reacted with goat anti-E2 antibody, followed by [125 I]staphylococcal protein A. Lanes 1-5 contain proteins from cells which were homogenized and the nuclei removed. Lane (1) mock-infected cell extract; (2) infected cells incubated without monensin, and not treated with proteinase K; (3) infected cells incubated with monensin, not treated with proteinase K; (4) infected cells incubated without monensin, then treated with proteinase K at 0.5 mg/ml for 45 minutes at 4°C; (5) infected cells incubated with monensin, then treated with proteinase K; (6) released virus (RV) purified from cells incubated without monensin; (7) released virus purified from cells incubated with monensin; (8) released virus from cells incubated without monensin; (9) released virus from cells incubated with monensin. E2-90 appears to be of slightly different molecular weight in lanes 6 and 8 due to the samples being run on different gels for different times.

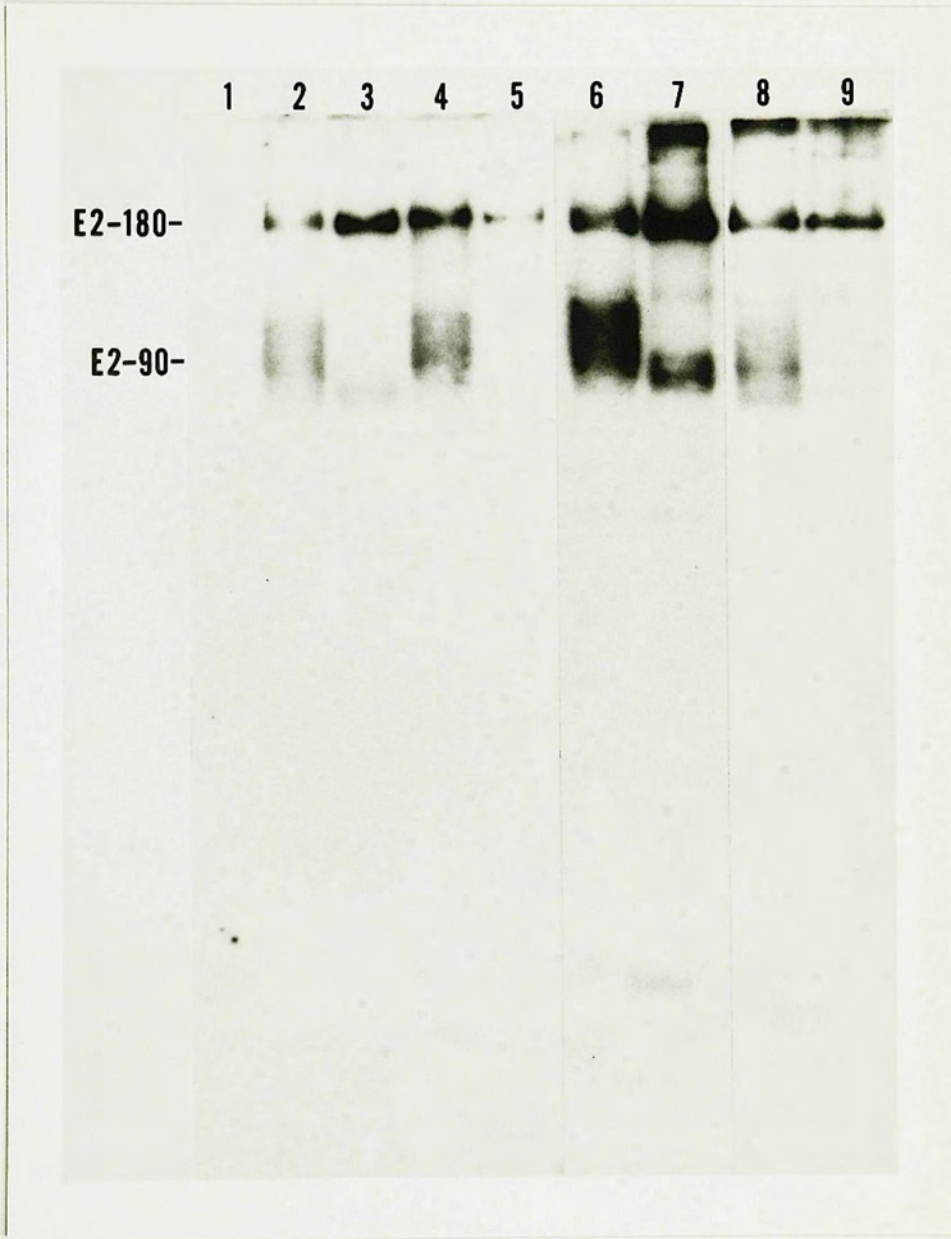


Table 2. Effects of monensin and trypsin on MHV-A59 infectivity and cleavage of E2. RV, CAV and ICV grown in the presence or absence of monensin (1 μ M), were tested for the effect of trypsin on virus infectivity. Samples were trypsinized as follows and titered in standard plaque assays. Exp. 1) Supernatant from MHV-infected cells (17 Cl 1), was either pelleted through a cushion of 20% sucrose at 44,000 rpm in an SW 50.1 rotor for 1 hour at 4°C, and resuspended in DMEM (RV^p), or not pelleted (RV). Trypsin in DMEM without serum (or DMEM alone) was added to 5 ug/ml and samples were incubated at room temperature for 45 minutes, then diluted in DMEM and FCS. Exp. 2) RV (grown in 17 Cl 1 cells) or CAV grown in L cells, was banded between 20% and 50% sucrose and incubated with trypsin-DPCC in TMEN (Tris-maleate EDTA buffer, pH 6) at 15 ug/ml, or TMEN alone, at 37°C for 30 minutes. Soybean trypsin inhibitor was added to 50 ug/ml and the mixtures were incubated on ice for 30 minutes, then pelleted through 20% sucrose and resuspended in FCS. Exp. 3) ICV grown in 17 Cl 1 cells was pelleted through 20% sucrose and incubated with trypsin at the final concentrations shown, or TMEN alone, at 37°C for one hour. The reaction was stopped by addition of DMEM with 5% FCS and 5% normal calf serum. RV, infected cell supernatant. RV^p, pelleted infected cell supernatant. CAV, cell-associated virus. ICV, intracellular virus.

Table 2

<u>Exp.</u>	<u>Virus sample</u>	<u>Monensin</u>	<u>Trypsin¹</u>	<u>PFU/ml</u>
1	RV	-	-	31 x 10 ⁶
		-	+	29 x 10 ⁶
	RV ^p	-	-	22 x 10 ⁵
		-	+	59 x 10 ⁴
		+	-	5 x 10 ²
		+	+	6-10 x 10 ²
2	RV	-	-	43 x 10 ⁵
		-	+	35 x 10 ⁵
	CAV	-	-	26 x 10 ³
		-	+	17 x 10 ³
		+	-	2 x 10 ²
		+	+	2 x 10 ²
3	ICV	-	-	17 x 10 ²
		-	0.5 mg/ml	19 x 10 ²
		-	1.0 mg/ml	17 x 10 ²

1. Trypsin conditions are described in the legend.

RV^p indicates released virus pelleted from infected cell supernatant, as described in the legend.

correlated with a large reduction in the ratio of cleaved E2-90 to uncleaved E2-180, and the extent of glycosylation of E2-90, as seen in gels and anti-E2 immunoblots. Therefore, monensin may affect release of infectious virus in several ways: by inhibiting virus transport, or the cleavage or glycosylation of E2.

Monensin caused about a 50% reduction in the incorporation of [³H]leucine into viral protein, based on the apparent amount of radiolabeled viral protein on fluorographs of polyacrylamide gels (Fig. 9). Therefore, the effect of monensin on overall cell and viral protein synthesis was not large enough by itself to account for the much greater decrease in output of released infectious virus. Since the results of electron microscopy showed that monensin (at a fifty-fold higher concentration) inhibited virus release from cells, some of the apparent decrease in infectivity of RV could be due to this effect. It may be significant that CAV infectivity was affected similarly to RV infectivity, since this suggests that an intracellular step in maturation, such as a defect in E2 processing, was perturbed by monensin and was the reason for decreased infectivity.

Effects of cytochalasin D treatment on maturation and infectivity of MHV. Cytochalasin D treatment (1 μ M) of MHV-infected cells reduced the total yield of released virus at 24 hrs by 75%, measured by plaque assay; at 0.2 μ M, the yield of infectious virus was not reduced at 24 hrs.

However, cytochalasin D treatment (0.2 μ M) appeared to increase the number of intracellular virus particles, apparently trapping many of them in the RER late in the infectious cycle (Fig. 15). In addition, the drug elicited an increase in the number of smooth-walled cytoplasmic vesicles, in which virions were located.

Effects of trypsin on MHV infectivity. The effect of trypsinization on virus infectivity was also tested (Table 2). Three different types of trypsin treatment were tested to evolve the optimal concentration and conditions. In each case, the infectivity of RV was decreased slightly. The infectivity of ICV and CAV, however, were unaffected by trypsin treatment. Because virus grown in the presence of monensin contained a very high ratio of 180K to 90K E2, and, from the results of plaque assays, this virus was possibly only one one-hundredth as infectious as control virus, we had expected that monensin virus infectivity might be readily activated by trypsin. This was not the case, however, since the infectivity of monensin RV and CAV was unaffected by trypsin treatment. Trypsin treatment of purified MHV-A59 at 10 μ g/ml trypsin at 37°C for 50 minutes caused only a two-fold increase in infectivity (Sturman and Holmes, 1977). Furthermore, the virus titer was not changed significantly by treatment of virions with 100 μ g/ml trypsin (Sturman et al., 1985).

Figure 15. Accumulation of intracellular MHV due to cytochalasin D treatment. Cells (17 Cl 1) were infected with MHV-A59 and treated with 0.2 uM cytochalasin D from 6 hr to 24 hr p.i., when the cells were harvested. The cells were processed for TEM as described in the Materials and Methods. Note that the RER is filled with an unusually large number of virions (see inset of the region indicated by the arrow), and that there is a profusion of smooth-walled vesicles. Bar = 1 micron. Inset bar = 50 nm.



Discussion

For several different virus groups, proteolytic cleavage of virus glycoproteins by host cell proteases is required for infectivity and fusion of the viral envelopes and for cell-to-cell fusion. For instance, the fusion protein, F₀, of paramyxoviruses, must be cleaved for the virus to exhibit infectivity, fusion or hemolysis (Scheid and Choppin, 1974; Nagai et al., 1976). In fact, for Newcastle disease virus, a paramyxovirus, the degree of virus virulence depends upon the protease activity of the host cell (Homma and Ohuchi, 1973; Scheid and Choppin, 1974). Cleavage of the influenza hemagglutinin HA₀ to HA₁ and HA₂, as well as a conformational change associated with a shift to pH 5.5 in endocytic vesicles, are required for fusion of the viral envelope with the endocytic membrane (Lazarowitz et al., 1973a,b). For retroviruses to be infectious, the env gene product must be cleaved correctly (Hardwick and Hunter, 1981). Cleavage of the influenza HA₀ is host-dependent, occurring at the plasma membrane (Klenk et al., 1975). Cleavage occurs in the lumen of the RER in the case of Newcastle disease virus, but at the plasma membrane or outside the cell for Sendai virus (Seto et al., 1981).

MHV differs from viruses which bud at plasma membranes in that its E2 glycoprotein is cleaved in every cell type examined so far (Frana et al., 1985). Thus it is unlike the fusion protein of Sendai virus, which is cleaved

in chick embryo cells, but uncleaved in MDBK cells (Scheid and Choppin, 1974), as well as the F₀ and the HA₀ glycoproteins of influenza virus, whose cleavage is also host dependent (Klenk et al., 1975; Lazarowitz and Choppin, 1975). For both MHV and Sendai virus, the extent of cleavage differs with the cell type (Scheid and Choppin, 1974; Frana et al., 1985). However, for MHV the degree of cleavage does not correlate with the degree of cell fusion as it does for Sendai virus (Klenk et al., 1975; Frana et al., 1985). Therefore, in order to better understand the molecular basis for virus infectivity, and the effects of proteolytic cleavage of E2, we sought to determine 1) the intracellular site of cleavage of E2, and 2) whether cleavage of E2 enhances virus infectivity.

Experimentally, MHV is a more difficult system for studying cleavage of virion glycoproteins than are orthomyxo- or paramyxoviruses, since MHV virions bud intracellularly and E2 appears to be cleaved at least partially within the cell. Nevertheless, we have investigated these questions in several ways. First, by analyzing the proteins of intracellular virus particles (ICVs) from 17 Cl 1 cells, we found that ICV particles contained slightly less E2-90K than did released virus (Fig. 9). This implies that some protease cleavage of E2 occurs within the cell, before virions reach the plasma membrane. Second, treating infected cells with monensin blocked most cleavage of E2 in both infected cells and virions, and appeared to block

elongation of oligosaccharide chains, but caused only a two-fold drop in protein synthesis (Figs. 9 and 14). This block in E2 processing was correlated with a block of over 99% in the yield of infectious virus (Table 2). Therefore, the block in transport, glycosylation and cleavage of E2 caused by monensin is probably accompanied by the production of non-infectious particles. The ratio of released particles to plaque forming units must be determined to resolve the issue of whether monensin directly affected virus infectivity or release or both. Also, the ratio of PFU to cpm should be determined for the same purpose.

In vitro trypsin treatment of RV, CAV, and ICV (grown in the presence or absence of monensin) did not activate infectivity, however (Table 2). Monensin blocks transport of glycoproteins from the cis to the trans region of the Golgi in certain cell types (Tartakoff and Vassalli, 1979; Griffiths et al., 1983). This strongly suggests that the E2 glycoprotein of MHV is normally cleaved in the trans Golgi or later. Cleavage may occur as virions are transported between the medial region of the Golgi complex and the plasma membrane.

From our gel analyses of ICV and CAV (Fig. 9) as well as pulse chase studies and immunoblot analysis of cell extracts, it is clear that a small number of E2 molecules are cleaved to 90K within one hour after synthesis (J.N. Behnke, unpublished; Frana et al., 1985). Analysis of released virions showed additional cleavage of E2 had

occurred, to ~50% in 17 Cl 1 cells and 100% in Sac- cells (Frana et al., 1985). This suggests that cleavage occurs prior to, and/or during, virus release. Our data extend these results, showing that by 12 hr p.i., a significant amount of E2 on ICV and CAV is cleaved (Fig. 9). To cleave all molecules of E2 on virions, purified MHV-A59 grown in 17 Cl 1 cells must be treated with trypsin (Sturman et al., 1985).

Using the ionophore monensin, we have produced a source of virus with predominantly uncleaved E2. The results of monensin studies indicate that MHV infectivity and cleavage of E2 to 90K may be correlated. Also, the studies utilizing proteinase K stripping of cells indicated that intracellular virus particles may be less infectious than those that reach the surface (data not shown). Thus, cleavage of E2 and possibly also complete glycosylation may be important in conferring infectivity upon MHV. However, the infectivity of virus grown in the presence of monensin was unaffected or slightly enhanced by trypsin treatment, whereas control virus infectivity was reduced under the conditions used (Table 2). It is not clear why trypsinization did not greatly enhance virus infectivity, as it enhances fusion-from-without using purified MHV (Sturman et al., 1985). One reason may be that underglycosylated E2 may be degraded more readily by trypsin treatment than normal E2. The mechanism of cellular cleavage of E2 was investigated by growing the A59 strain in 17 Cl 1 cells in the

presence of 10^{-4} M tosyl-L-lysyl-chloromethane (TLCK, a trypsin inhibitor) or tosyl-L-phenylalanyl-chloromethane (TPCK, which inhibits chymotrypsin), or in the absence of fetal bovine serum to prevent plasmin activity (Sturman and Holmes, 1977). None of these treatments affected the ratio of 180K/90K E2 in purified released virions. However, addition of either TPCK or leupeptin to the medium delayed the onset of cell fusion by 4-6 hr in L2 cells (Frana et al., 1985). These data suggest that infectivity and fusion may be mediated by different mechanisms.

It is not clear whether the trypsin conditions used for these experiments were ideal. Sturman et al. (1985) induced fusion-from-without using trypsin-TPCK at 100 ug/ml at 37°C for 30 min, and these particular conditions ought to be tested. In contrast, trypsin at only 2.5 ug/ml at 37°C for 8 minutes activated infectivity of NDV (Nagai et al., 1976). Future experiments, on a larger scale, with intracellular virus grown in the presence of monensin, using different concentrations and testing other proteases and conditions should confirm whether E2 cleavage is in fact necessary for MHV infectivity. Mutants in the E2 cleavage site, if they proved viable, could also shed light on this problem, as they have for the relation of glycoprotein cleavage to infectivity of murine leukemia and sarcoma viruses (Srinivas et al., 1982).

MHV virions may bud before E2 is cleaved or fully glycosylated. That monensin blocks glycosylation and

cleavage of E2, probably in the medial Golgi, suggests that virions are fully formed before being processed, since MHV can bud into both RER and perinuclear non-Golgi smooth vesicles prior to being transported to the Golgi (Holmes et al., 1981b; Dubois-Dalcq et al., 1984a; Tooze et al., 1984). These findings suggest that processing of E2 can occur even after virions have assembled.

The effect of cytochalasin D on MHV maturation which we observed is probably not specific to the virus maturation process, but instead, may be due to preventing transport to the plasma membrane of vesicles which contain virus. We did not examine virions grown in the presence of this drug for an effect on E2 cleavage or glycosylation. Cytochalasin D exerts its effect by inhibiting the polymerization of actin molecules, preventing elongation of microfilaments (Tannenbaum, 1978; Lin et al., 1980).

By TEM examination, we have found that isolated intracellular virus particles are pleiomorphic and sometimes flattened (Fig. 10). Studies of virus morphogenesis have usually relied on transmission EM of thin sections of whole cells and biochemical analyses of cell fractions, rather than isolation of intracellular virus particles. Thus, a technique for isolating intracellular virions, as described here, may be useful for the study of virus maturation in many other systems in which virions bud from intracellular membranes.

Earlier studies of thin sections of infected cells

have shown that during transport of MHV particles through smooth-walled, Golgi-associated vesicles in certain cell types, virions become flattened and more electron-dense (Holmes et al., 1981b; Dubois-Dalcq et al. 1984a). Interestingly, these flattened virions become attached to the cell surface on the narrow end when lined up in tight rows (K.V. Holmes et al., unpublished). Our results using partially purified intracellular particles confirm that flattening occurs within the cell, not after release into the extracellular medium. This transformation may be due to either 1) a change in pH or ionic strength in a particular region of the cell, or 2) processing of E2, such as cleavage, during transport through the Golgi (Holmes et al., 1981b).

Flattening has also been observed in BCV-infected cells (D.A. Brian, personal communication), but only spherical virions have been reported in TEM studies of coronaviruses from other species of animals (Doughri et al., 1976; Caul and Egglestone, 1977; Ducatelle et al., 1981). In addition to coronaviruses, retro-, paramyxo-, and possibly orthomyxoviruses may undergo morphological changes very late in their maturation, all apparently involving separation of the nucleocapsid from the underside of the lipid bilayer of the virus envelope (Kim et al., 1979; Bachi, 1980).

The coronavirus-induced tubules which we have partially purified from infected cells (Figs. 11 and 12) were seen previously in TEM studies of MHV-A59-infected cells late in infection and in tunicamycin-treated cells

(Holmes et al., 1981a; Dubois-Dalcq et al., 1982). These tubules were reported to be about 50 nm in diameter, similar to our observations, accumulating within the lumen of the RER late during infection. It was then hypothesized that they are membranes bound with E1. Similar structures were formed in vitro using the paramyxovirus matrix protein M (Heggeness et al., 1982), and comparable tubules have been observed in influenza-infected HeLa cells; they were suggested to be empty viral envelopes (Caliguiri and Holmes, 1979). Coronavirus and influenza virus-induced tubules are distinct from togavirus-induced tubules (Grimley et al., 1972) in that they appear to be somewhat flexible. Reticular inclusions (David-Ferreira and Manaker, 1965) observed in cells infected with certain coronaviruses did not copurify with ICVs and tubules. The whorled membranes seen in negative stains of ICV (Fig. 12) may be related to the anastomosing SER membranes reported by Tooze et al. (1984). Virus-induced tubules may be the result of increased membrane synthesis as a homeostatic response to the loss of RER and Golgi membranes which occurs during virus budding (Tooze et al., 1984). The viral protein composition of these virus-induced structures could be determined by immunoelectron microscopy and immunoprecipitation or immunoblotting of further-purified samples, using monoclonal antibodies raised against each of the MHV structural proteins.

Monensin is a Na⁺ ionophore which destroys proton

gradients by intercalating into membranes and causing an equilibrium of Na^+ and K^+ across them (Pressman, 1976; Tartakoff and Vassalli, 1977, 1978). Monensin acts primarily on membranes of the Golgi complex, blocking transport of not only sodium ions but also glycoproteins (Tartakoff and Vassali, 1978; Johnson and Schlesinger, 1980). More specifically, monensin has been shown to block transport of glycoproteins from the cis to the trans compartments of the Golgi in certain cell lines (Tartakoff and Vassalli, 1978, 1979). Therefore, it may be by blocking transport of E2 or virions that monensin prevents cleavage and glycosylation of E2. Because E2 cleavage is sensitive to monensin, it probably takes place during or after passage of the glycoprotein through the trans region of the Golgi.

Our results from PAGE analysis of virus grown in the presence of monensin showed that E2-90 was lower and less heterogeneous in molecular weight than the E2-90 of control virus (Figs. 9 and 14). This result can be interpreted through a finding of Niemann et al. (1982), that co-translational glycosylation of E2 with high mannose oligosaccharides was not inhibited by 5 μM monensin, but addition of neuraminic acid and fucose was prevented. This result suggested that these terminal sugars are added in the trans Golgi.

We found that in the presence of only 1 μM monensin, not only were 100-fold fewer infectious virions released, but also cell-associated virus was 100-fold less infectious than control virus (Table 2). The effect of monensin on the

number of infectious virions released may be due not only to effects on cleavage and glycosylation, but also to blocks in the budding process and release of virions from the cell. On the basis of electron microscopic analysis of thin sections in this study, budding appeared to be inhibited in the presence of 50 μ M monensin (Fig. 13). At 18 hr p.i., virus particles had also accumulated within smooth vesicles and the RER, as if those that succeeded in budding could not be transported. Niemann and colleagues (1982), using 5 μ M monensin, found that budding was not inhibited. In their studies, the RER was filled with virus particles and the Golgi stacks were replaced with large vacuoles. Washing away the monensin did not allow virus release. The differences in EM results between the two laboratories may be due to the ten-fold difference in monensin concentration. In both studies, no virus particles were found on the surface of cells. We detected only fully glycosylated E1 at 1 μ M monensin (Fig. 9), whereas Niemann detected only nonglycosylated E1 at 5 μ M monensin. It may be that the budding defect seen at 50 μ M monensin was due to an E1 defect, since it has been suggested that E1 links the nucleocapsid with the viral envelope during budding (Holmes *et al.*, 1984).

Numerous difficulties are encountered in interpreting experiments using monensin, discussed by Griffiths *et al.* (1983). The ionophore affects more than glycoprotein transport and has cell-dependent effects. Also, its effects

differ with the glycoprotein and cell type being studied. Any lysosomotropic effects of monensin which would raise the intralysosomal pH, are unlikely to affect MHV penetration, since MHV fusion has a pH optimum between 7.2 and 7.8 (Sturman and Holmes, 1984). However, the processing of glycoproteins of several different viruses is affected by monensin in similar ways, including the VSV G protein (Johnson and Schlessinger, 1980), the SFV glycoproteins (Kaariainen et al., 1980), Sindbis virus glycoproteins (Strous and Lodish, 1980), and env gene products of retroviruses (Chatterjee et al., 1982; Srinivas et al., 1982). In particular, the susceptibility of MHV E2 cleavage and virus infectivity to monensin treatment is strikingly similar to that of the env gene product of Mason-Pfizer virus (MPV) (Chatterjee et al., 1982) and murine leukemia virus (Srinivas et al., 1982). Monensin inhibited cleavage of the MPV Pr86^{env} precursor into gp20 and gp70. Unlike MHV E2, this occurred without inhibiting glycoprotein transport to the cell surface. At 0.1 μ M monensin, released MPV was 1000-fold less infectious and of lower buoyant density (1.15 g/ml) than control virus not grown in the presence of monensin. The authors suggested that this change in density reflected the altered carbohydrate content of the virus, since a similar change in density occurred in Rous sarcoma virus made glycoprotein-free by tunicamycin or proteases (Rifkin and Compans, 1971). Apparently due to their lack of gp70, MLV particles could not bud at the plasma membrane

(Srinivas et al., 1982). With 10 μ M monensin, there was over a 50-fold drop in virus infectivity, but only a two-fold drop in particle production, similar to our results with MHV, also suggesting that the effect of monensin on virus infectivity was not caused indirectly by decreased viral protein synthesis. Similar results have been shown for the glycoproteins of Semliki Forest virus (SFV) (Pesonen and Kaariainen, 1982). The SFV glycoprotein E3, like E2 of MHV, was not fully glycosylated due to the action of monensin. Pulse-labeling studies showed that p62 was cleaved to form E1, E2 and E3. Cytochemical studies with lectins and immunoelectron microscopic studies showed that the block in transport occurred in the medial region of the Golgi, where nucleocapsids accumulated. Similar studies would be useful to identify where in the Golgi the transport of MHV E2 is blocked.

Monensin also inhibits the release of herpes virions, but not their budding at the nuclear envelope, and causes infectious particles to accumulate within the cell (Johnson and Spear, 1982). Glycosylation of the surface glycoproteins gB, gC and gD is inhibited and virus-induced cell fusion is prevented (Kousoulas et al., 1983).

We have shown that the MHV E2 glycoprotein is cleaved intracellularly. This procedure has allowed us to characterize the morphology of intracellular virus particles, confirming the results of earlier TEM studies of thin sections, which showed that MHV particles become

flattened once they appear in smooth vesicles as they exit the cell. From the results of studies with the ionophore monensin, we conclude that cleavage probably occurs during transport of virions from the medial Golgi apparatus to the cell membrane. The precise location of the monensin block must be determined for MHV-A59 grown in 17 Cl 1 cells, since the effects of monensin are cell dependent. These data, integrated with those reported by Niemann and co-workers in the same system, strongly suggest that processing of E2 can occur on virions themselves during their maturation and transport through the Golgi. Since monensin also appears to have allowed production of mainly noninfectious particles, we have hypothesized that cleavage of E2 may be essential for virus infectivity. Further studies using virus grown in the presence of relatively low concentrations of monensin (e.g., 1 uM) and lacking cleaved E2 and infectivity, should help to answer this fundamental question in coronavirus biology.

II. NUCLEIC ACID-BINDING PROPERTIES OF N PROTEIN AND OTHER PROTEINS OF MHV-INFECTED CELLS AND VIRIONS

Introduction

The N protein of MHV, a phosphoprotein of 50-60 K molecular weight, has been identified as the core protein which interacts with the genome RNA to form nucleocapsids during virus assembly (Stohlman and Lai, 1979; Sturman et al., 1980). The RNA-binding properties of the N protein, however, have not been characterized in detail. In addition, no other RNA-binding proteins in MHV-infected cells, including the viral nonstructural proteins (Anderson et al., 1979; Bond et al., 1979) have been examined for RNA-binding activity. Therefore, we chose to identify the RNA-binding proteins in MHV virions and MHV-infected cells.

During the assembly of other enveloped RNA viruses, such as VSV (Blumberg et al., 1983) and TMV (Butler, 1984), the nucleocapsid proteins initially interact with specific nucleotide signal sequences near the 5' and 3' ends of the genomes, respectively. Subsequently, monomers of coat protein appear to bind to the RNA in a nonspecific manner. We hypothesized that MHV might assemble by a similar mechanism, and therefore chose to determine whether N would bind MHV RNA preferentially over other viral and cellular nucleic acids.

A sensitive nucleic acid overlay-protein blotting method (Bowen et al., 1980) has been useful for the initial identification of both DNA-binding proteins (Blair and

Honess, 1983; Braun *et al.*, 1984; Ichihashi *et al.*, 1984; Petit and Pillot, 1985; Roberts *et al.*, 1985) and RNA-binding proteins of Rous sarcoma virus (Bowen *et al.*, 1980; Meric *et al.*, 1984), adenovirus-infected cells (van Eekelen *et al.*, 1982) and ribosomes of yeast and plants (El-Boradi *et al.*, 1984; Rozier and Mache, 1984). We have adapted the RNA overlay-protein blot assay (ROPBA) to detect the virus-specific RNA-binding proteins in coronavirus infected cells and virions. Our results indicated that in virions, N was the major RNA-binding protein. This molecule was not highly specific for binding MHV nucleotide sequences, and also bound cellular RNA and DNA as well as nucleic acids of various viruses. A minor protein of molecular weight 140K was discovered, and this protein also bound RNA. The 140K protein appears to be a multimer of N molecules linked by disulfide bonds.

To better identify a nucleotide sequence-specific binding component for the binding of MHV RNA to the N protein, we affinity-purified the N protein and studied its interaction with viral RNA in filter binding assays. In solution, the N protein was found to bind viral RNA purified from MHV-infected cells. Most of this binding could be competed with cellular RNAs and was not virus-specific.

Materials and Methods

Viruses and cells. MHV and vesicular stomatitis virus (VSV) were propagated in 17 Cl 1 cells and purified as

described previously (Sturman *et al.*, 1980). The purified MHV-A59 used in RNA overlay-protein blots and immunoblots was prepared by Dr. Cynthia Duchala. Bovine rotavirus (BRV, Lincoln strain), kindly provided by Dr. Albert Kapikian (NIH), was grown in MA104 cells obtained from Monroe Vincent (USUHS), which were cultured in Medium 199 with Hank's balanced salts (Whittaker MA Bioproducts) with 10% fetal bovine serum, penicillin (100 U/ml), and streptomycin (100 ug/ml). Temperature-sensitive mutants (Alb4, 5 and 7) generated by nitrous acid treatment, were kindly provided by Dr. Lawrence Sturman (New York State Dept. of Laboratories and Research, Albany, New York).

Preparation of endogenously labeled RNA for the ROPBA. Cytoplasmic RNA from MHV-infected cells was labeled endogenously with inorganic phosphate as described previously (Baric *et al.*, 1983), with the following modifications. Confluent 17 Cl 1 cell monolayers were inoculated with MHV-A59 at a multiplicity of infection (MOI) of 5-10 PFU per cell. At 1.5 hr post-inoculation (p.i.) the inoculum was replaced with phosphate-free minimum essential medium with Earle's salts (Eagle, 1959), 12% Dulbecco's medium (Grand Island Biological Co., GIBCO), and 5 ug/ml actinomycin D-mannitol (Sigma Chemicals). At 2.75 hr p.i., [³²P]orthophosphate (ICN Pharmaceuticals) was added to a final concentration of 130-180 uCi/ml. At 9 hr p.i., each flask was washed with ice-cold PBS, and cells were detached with disposable plastic scrapers and pelleted.

Cytoplasmic RNA was purified using SDS (1%), proteinase K (200 ug/ml) and diethylpyrocarbonate (DEPC, 0.05%) as described by Maniatis (1982), but omitting the RNase inhibitor, RNasin. The precipitated RNA was pelleted at 16,300 x g for 15 minutes, air- and vacuum-dried, and resuspended in double-distilled water. RNA was stored in aliquots at -70°C and its concentration and purity were determined by spectrophotometric analysis at 260 and 280 nm. Specific activities ranged from about 4×10^3 to 4×10^4 cpm/ug. RNA samples were analyzed by electrophoresis for approximately 22 hr in 1% Seakem LE agarose (FMC Corp.) horizontal slab gels (Zeevi et al., 1981), using 6 M formaldehyde in both gel and sample buffers and 0.1% DEPC in the running buffer. Nick-translated, denatured [32 P]dCTP-labeled lambda phage DNA digested with HindIII (Bethesda Research Laboratories) was used as a molecular weight standard. Intracellular virus-specific RNA was prepared similarly from VSV-infected cells harvested at 8.5 hr p.i. and BRV-infected cells at 8-9 hr p.i.

Preparation of radiolabeled DNA and RNA probes.

HSV-1 and calf thymus DNAs, and a 22-nucleotide cDNA probe complementary to a portion of the MHV leader (5'-AATGTTTG-GATTAGATTTAAAC-3') were generously provided by Drs. John Hay and John McGowan, respectively (USUHS). These DNAs were labeled at the 5' end with [32 P]ATP with T4 polynucleotide kinase (Bethesda Research Laboratories; Maxam and Gilbert, 1980). [3 H]labeled HSV-2 DNA was kindly donated by Dr.

William Ruyechan (USUHS). Double-stranded RNA genome segments purified from bovine rotavirus were labeled at the 3' end with ^{32}P using T4 polynucleotide ligase as described previously (England and Uhlenbeck, 1978). Poly A oligonucleotide RNA was obtained from Sigma.

Preparation of cell extracts. Cytoplasmic extracts of 17 Cl 1 cells were prepared by washing mock-inoculated or MHV-A59 infected flasks with ice-cold PBS containing 0.01% phenylmethylsulfonylfluoride (PMSF, Sigma), and then incubating for 10 minutes on wet ice with RIPA buffer (1% deoxycholate, 0.1% sodium dodecyl sulfate, 0.01 M Tris, pH 7.4., 1 mM disodium EDTA) (Okuno *et al.*, 1983), and containing the following protease inhibitors: 0.01% PMSF, 0.1 mg/ml soybean trypsin inhibitor (GIBCO), and 1% (v/v) aprotinin (Sigma). Floating cells were washed twice in PBS, pelleted, and added to the rest of the cell extract. After 15 minutes on ice, cell extracts were vortexed and insoluble material was removed by centrifugation. Cell extracts were stored at -70°C .

RIPA buffer was chosen after testing two other extraction buffers on MHV-JHM-infected cells. One buffer was identical to RIPA, except with high salt (1.5 M NaCl). The other buffer contained 1% NP-40, 0.5% deoxycholate, 0.01 M Tris, pH 7.4, 0.1 M NaCl, 1 mM disodium EDTA, and 0.15 M NaCl. Cell extracts were run on an 8% gel and immunoblotted with convalescent anti-JHM antiserum and ^{125}I SPA. The results (not shown) indicated that RIPA buffer extracted the

greatest quantity of viral proteins, especially those of higher molecular weight.

Gel electrophoresis and electroblotting. Cell extracts were analyzed by sodium dodecyl sulfate polyacrylamide gel electrophoresis (SDS-PAGE) and protein electroblotting as described in the General Materials and Methods. Blots were stained for protein using amido black (Towbin *et al.*, 1979). Blots which had been immunoblotted, dried, and stored at room temperature, could be rehydrated in transfer buffer and used for ROPBAs. Blots could be stored for as long as three weeks in transfer buffer at 4 C prior to reaction with probes. In certain experiments, gels, immunoblots and ROPBAs were scanned with a transmittance/reflectance densitometer (model GS-300, Hoefer Scientific Instruments) interfaced with a Shimadzu C-R1B Chromatopac integrator/printer.

RNA overlay-protein blot assay (ROPBA). For reaction with labeled nucleic acid probes, blots were treated as described by Bowen *et al.* (1980) except that they were not soaked in urea, and reactions and washes were done on a rocker platform in small polystyrene trays (reservoir inserts; Dynatech Labs, Inc.). Briefly, blots were rinsed with standard binding buffer (SBB; 0.05 M NaCl, 1 mM disodium EDTA, 10 mM Tris-HCl, pH 7, 0.02% BSA, 0.02% Ficoll, 0.02% polyvinyl pyrrolidone (PVP-40) for 30 minutes, incubated with 10^4 to 1.5×10^5 cpm/ml [32 P]RNA (or DNA) probe for 1 hr at room temperature, washed 3 times with SBB

for 15 min each, then air-dried and autoradiographed against intensifying screens. Conditions were varied as described in the text.

The bands which appeared after probing with [^{32}P]RNA were entirely due to binding by RNA and not by free label, since reaction with 10^4 cpm/ml of free [^{32}P]orthophosphate yielded no detectable bands (data not shown).

Only certain molecular weight markers bound MHV RNA, including RNase T1 (Calbiochem), RNase A, chymotrypsinogen (Pharmacia), and phosphorylase B (Bio-Rad). Proteins which did not bind detectable amounts of RNA included BSA, ovalbumin, aldolase, myosin, β -galactosidase, soybean trypsin inhibitor, and lysozyme.

Preparation of MHV [^3H]uridine-RNA probe and unlabeled competitor nucleic acids. For use in the filter binding assay, MHV RNAs in infected cells were labeled by a modification of the method of Rottier *et al.* (1981a). 17 Cl 1 cells were inoculated with MHV-A59 at an MOI of 1-10 PFU/cell and virus was adsorbed for 1 hour, after which the inoculum was replaced by fresh medium. At 1.5 hr p.i. the medium was changed to DMEM with 5% fetal calf serum and 1% antibiotic-antimycotic with 5 ug/ml actinomycin D. At 2.5 hr p.i., [^3H]uridine (ICN; specific activity 47 Ci/mM, 1 mCi/ml) was added to a final concentration of 30 uCi/ml. The cells were harvested at ~8 hr p.i., when about 30% of the cells were fused. Cytoplasmic RNA was purified by the method described for [^{32}P]RNA above. Its specific activity

was 1.48×10^4 cpm/ug. By agarose gel electrophoresis, only the viral RNAs were labeled. Unlabelled cytoplasmic RNA from infected and mock-infected cells, for use in competitive binding assays, was prepared similarly, with one flask of cells labeled for analysis of RNA on agarose gels.

MHV-A59-specific probes were kindly prepared by Susan Compton (USUHS). A cDNA mapping from about 200 bp in gene 4 to 200 bp in gene 7 of the genome RNA, containing 1800 base pairs, named "g344" (Budzilowicz et al., 1985), was donated by Dr. Susan Weiss (University of Pennsylvania). This clone had been inserted into a plasmid by Dr. John McGowan. It was amplified in HB101 cells, and transcribed in the Gemini system (Promega) by Dr. John McGowan. In vitro transcription with the SP6 polymerase yielded a plus stranded RNA, whereas the T7 polymerase generated a minus stranded transcript. Agarose gel electrophoresis showed these transcripts to be largely homogeneous, with the SP6 transcripts migrating at 6.3 kb and the T7 transcripts at 6.15 kb (data not shown). There were two small molecular weight bands (1.62 and 1.75 kb) in trace amounts in the SP6 transcript preparation, which probably arose from premature termination of transcription.

Preparation of an anti-N affinity column. Rabbit polyclonal antiserum raised against MHV N protein eluted from a polyacrylamide gel, was clarified and precipitated twice with saturated ammonium sulfate, as described by Campbell et al. (1970). The precipitate was de-salted on G-

25 columns (PD-10, Pharmacia), eluting with affinity column coupling buffer (0.2 M citrate, pH 6.5, 0.5 M NaCl). Protein determination by the Bradford method (1976) indicated that approximately 98 mg of immunoglobulin was isolated from 19 ml of immune rabbit serum. Using this immunoglobulin, an anti-N affinity column was prepared (Cuatrecasas and Anfinsen, 1971; Pharmacia pamphlet "Affinity Chromatography Principles and Methods"). Cyanogen bromide-activated Sepharose 4B (Sigma) was swollen and washed 4 times in 1 mM HCl. The slurry was packed into an empty PD-10 column and washed once with suction. After the sepharose was drained of HCl and coupling buffer, the anti-N immunoglobulin precipitate was added. The mixture was rotated end-over-end on a tissue culture roller drum (New Brunswick Scientific Co.) for 3.5 hr at room temperature, after which the column was washed with coupling buffer. Protein determination of the eluate and wash showed indirectly that 99.3% of the initial immunoglobulin preparation was bound to the activated sepharose. The beads were transferred to a 50 ml plastic tube containing 0.1 M lysine to block remaining active groups, and rotated again for 2.75 hr. The beads were washed extensively with 0.1 M acetate, pH 4, 0.5 M NaCl, then with 0.1 M borate, pH 8, 0.5 M NaCl. The sepharose was transferred to a glass column (Rainin "omni", 10 cm internal diameter, 150 mm in length) for affinity chromatography. For storage, the column was washed with PBS with 0.02% azide and stored at 4°C.

Solubilization of N protein from nucleocapsids. N protein was released from nucleocapsids in cytoplasmic extracts of A59-infected cells by treatment with RNase. RNase A (Sigma) was dissolved in water to 50 mg/ml and boiled for 10 minutes to destroy DNase activity. RNase (or water, for the control) was added to a RIPA cell extract of MHV-A59-infected 17 Cl 1 cells, to a final concentration of 1.24 mg/ml, and the mixture incubated at 37°C for 1 hour. Insoluble N protein in RNPs and virions was removed by pelleting the samples at 100,000 x g for 2 hours in a Beckman TL-100 tabletop ultracentrifuge. Samples of supernatants and pellets were analyzed qualitatively for viral proteins by application to nitrocellulose paper using a filtration manifold (Minifold; Schleicher and Schuell) and reacting with polyclonal antisera raised against each MHV protein.

Isolation of the MHV-A59 N protein by affinity chromatography. A peristaltic pump (P-1, Pharmacia) was used to pump buffer into the column from top to bottom. The outlet tubing of the column passed through a UV detector unit (LKB model 8300, Pharmacia) controlled by a Uvicord II unit (LKB model 8300, Pharmacia) and a chart recorder (LKB model 2550, Pharmacia). The affinity column, detector, fraction collector and buffers were stored and used at 4°C. All buffers were filtered and de-gassed for 5 minutes.

Before each run, the column was equilibrated with wash buffer (50 mM borate, pH 8.5, 0.1 M NaCl, 0.1% Triton

X-100). The column was pre-stripped with one volume of 1 M NaSCN and washed again. RNase-treated cell extract supernatant (containing ~0.01% PMSF to minimize proteolysis) was applied and adsorbed for 2 hours at 4°C. The column was then washed slowly with 10 volumes of wash buffer containing 0.01% PMSF, overnight. The column was eluted with 1 M NaSCN in wash buffer, and thirty 0.5 ml fractions were collected. Every four fractions were pooled and de-salted on PD-10 G-25 columns, eluting with NT buffer (0.01 M NaCl, 0.01 M Tris-HCl, pH 7.4). A sample of each PD-10 fraction was saved and analyzed for N protein in a dot immunoblot. Fractions containing the most N protein by dot-blot were pooled and analyzed for purity by silver stain, and for viral proteins by polyacrylamide gel electrophoresis and immunoblot assay.

Silver stain of affinity-purified N protein. The affinity-purified N protein samples and RNase-treated starting cell extract were first concentrated by acetone precipitation (Hay, 1979) by addition of 4 volumes of ice cold acetone, precipitation overnight at 0°C, and centrifugation at 3,000 x g for 45 min. Pellets were resuspended in STM and boiled 2 minutes. Samples of RNase-treated starting material and affinity-purified N protein were electrophoresed on unreduced and reduced polyacrylamide gels and silver stained by the method of Wray *et al.* (1981).

Filter binding assay. Binding of N protein to viral RNA in solution was studied using a method modified from the filter binding assay of Riggs *et al.* (1970). Eppendorf

tubes and pipets were autoclaved and baked to destroy RNase activity. Nitrocellulose filters (Schleicher and Schuell, 0.45 micron pore size, 25 mm diameter) were soaked in Riggs' standard binding buffer (RSBB) (0.01 M Tris-HCl, pH 7.4, 0.01 M magnesium acetate, 0.01 M potassium chloride, 0.1 mM disodium EDTA, 50 ug/ml BSA) for at least 30 minutes before use. A single well filtration apparatus was assembled from a Millipore filtration manifold and a vacuum flask hooked up to a vacuum. Filtration speed was adjusted to about 1 drop per second.

For the experiments shown in Figure 27, the N protein was first concentrated in a Centricon-30 tube (Amicon). The final protein concentration was estimated from the reduction in volume. For competition experiments, binding mixtures were set up in duplicate, each with a total volume of 25 ul in 400 ul eppendorf tubes. Binding mixtures contained RSBB with 5 mM dithiothreitol and 4 units/ul of the placental RNase inhibitor RNasin (Biotec, Madison, WI) to inhibit RNase activity. In control experiments, when used at ~1 U/ul, RNasin enhanced binding of RNA by 2.7 to 6.5-fold, apparently preventing degradation of the labeled RNA probe. To a 3.6x concentrate of this mixture were added different amounts of competitor RNAs, then approximately 14,500 cpm of MHV [³H]RNA from MHV-infected cells. The mixtures were resuspended and ~0.2 ug of affinity-purified N protein was added at 2.5 minute intervals (the time needed to filter one sample). Tubes were incubated on ice 45-60

minutes and were then filtered at 2.5 minute intervals. For collecting protein-RNA complexes, the filters were first rinsed with 1 ml ice-cold RSBB. Immediately, 20 ul of the binding mixture was applied directly to the filter, followed by 2 ml of ice-cold buffer to wash through unbound RNA. For drying, filters were placed on aluminum foil under a heat lamp or held overnight at room temperature. The filters were counted repeatedly for [³H]uridine for 5 minutes in plastic minivials (Research Products International Corp.) containing scintillation fluid (57.8% toluene, 28.9% Triton X-100, 4.6% Liquifluor), using an LKB 1219 Rackbeta counter. Counting was repeated until the counts stabilized. Different dilutions of [³H]RNA were counted in the presence and absence of filters to establish a quenching curve. Graphs show cpm bound after correction for background and quenching.

Results

Electrophoresis of MHV RNAs. ³²P-labeled RNA from coronavirus-infected cells was used as a probe to detect RNA-binding proteins in purified virions. The probe was a mixture of genomic RNA and six subgenomic mRNAs which form a nested set with common 3' ends (Fig. 16; Robb and Bond, 1979a; Spaan et al., 1981; Wege et al., 1981b). By densitometric scan, 52% of the labeled RNA was found to be of genome size (band 1; 5.5×10^6). The molecular masses, in megadaltons, of the mRNAs were as follows, and were similar

Figure 16. Agarose gel electrophoresis of ^{32}P -labeled MHV-A59 cytoplasmic RNAs. MHV-A59 was used to infect 17 Cl 1 cells at a MOI of 10. The cells were radiolabeled with inorganic phosphate at 150 $\mu\text{Ci/ml}$ in the presence of 5 $\mu\text{g/ml}$ actinomycin D. Cytoplasmic extracts were made at 8.75 hr p.i., from which RNA was purified as described in the Materials and Methods. The RNA sample loaded onto the gel contained 7.25×10^3 cpm.



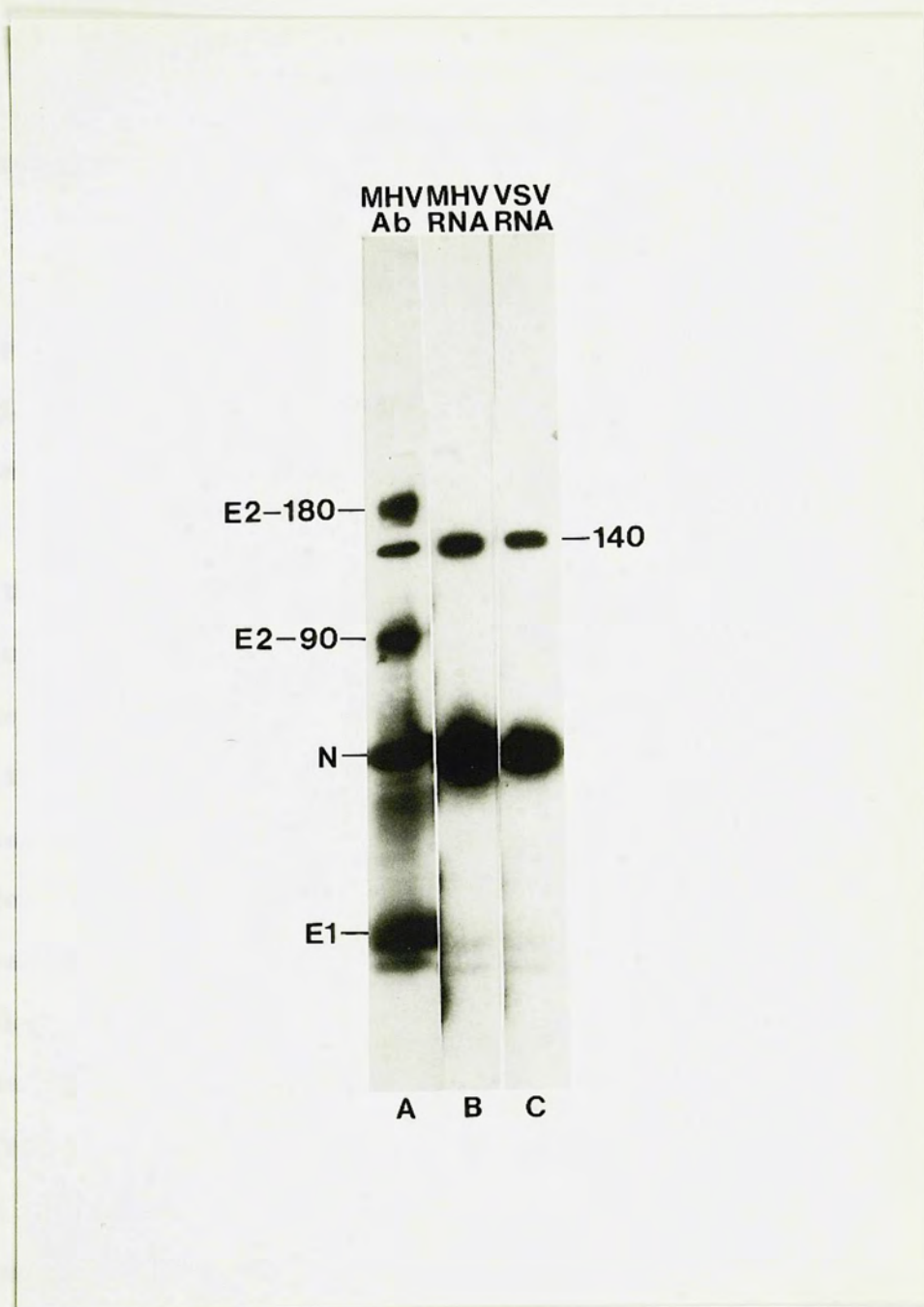
112

to those reported previously by Leibowitz *et al.*, 1981; Spaan *et al.*, 1981): band 2, 3.41; band 3, 2.71; band 4, 1.16; band 5, 1.03; band 6, 0.79; band 7, 0.65. The band at the top of the gel was at the origin and probably consisted of RNA aggregates. ^{32}P -labeled MHV-A59 RNA and cytoplasmic RNA from uninfected cells were totally degraded by RNase and were therefore free of radiolabeled DNA and protein (data not shown).

Identification of RNA-binding proteins in virions.

RNA-binding proteins from purified virions were identified with the RNA overlay-protein blot assay using cytoplasmic MHV [^{32}P]RNA as the probe (Fig. 17). The major RNA-binding protein in MHV virions was the 50K nucleocapsid protein, N (lane B). A previously undetected 140K viral protein was also identified as an RNA-binding protein. It comprised approximately 3.4% of the total virion protein as estimated by densitometric scans of an immunoblot (lane A) and a Coomassie blue-stained gel. Preliminary studies suggest that the 140K protein bound RNA as effectively as did the N protein on a weight-by-weight basis. Not surprisingly, there was no detectable binding of RNA by either the 180K or 90K forms of the E2 glycoprotein, which forms the viral spikes. Glycosylated and unglycosylated forms of E1, the membrane glycoprotein, bound only trace amounts of RNA. [^{32}P]RNA from VSV-infected cells also bound to the N and 140K proteins of MHV with high efficiency (lane C), indicating that the observed RNA-binding was not specific for MHV

Figure 17. RNA-binding proteins of purified MHV-A59 virions detected by the RNA overlay protein blot assay. Gradient-purified virions (35 ug protein) were resolved on a 5-15% SDS polyacrylamide gel and electroblotted to nitrocellulose. The protein blot was cut into strips and individual strips were reacted with the following probes: lane A, virus-specific rabbit antiserum followed by ^{125}I -labeled-staphylococcal protein A; lane B, ^{32}P -labeled MHV-A59 cytoplasmic RNA (1.5×10^5 cpm/ml); lane C, ^{32}P -labeled VSV cytoplasmic RNA (1.3×10^5 cpm/ml).



RNA.

Characterization of the 140K protein. The 140K protein was detected by immunoblotting proteins of purified virions isolated from 17 Cl 1 cells, with monospecific antiserum against the N protein, but not with monospecific antisera against the other viral proteins E1 and E2 (Fig. 18). A faint broad band with an average molecular weight of 73K occasionally seen in heavily loaded gels reacted specifically with antiserum to N (lane C) but did not associate significantly with RNA (data not shown). Anti-E1 detected both monomeric and dimeric E1 (lane D). Antiserum raised against NP-40-disrupted virions also detected the 140K protein in virions grown in other cell types, including DBT, Sac-, and L2 cells (M.F. Frana, unpublished observation). The 140K protein was also detected in 17 Cl 1 and DBT cell extracts 18 to 24 hr p.i. (data not shown).

To determine whether the 140K protein was a multimer of N, total virion proteins and the 140K band excised from a gel were boiled and treated with 5% 2-mercaptoethanol before electrophoresis (Fig. 19). The purification of the 140K protein from a polyacrylamide gel, and the gel electrophoresis were performed by Dr. Mark Frana. Reduction of the 140K protein yielded only N (panel B, lane 2). When purified virus was analyzed in unreduced or reduced form in the ROPBA assay, the same result was obtained (panel C). Thus, the 140K protein is a trimer composed of three N

Figure 18. Antigenic cross-reactivity between the 140K protein and the N protein. Proteins of purified MHV-A59 virions were electrophoresed (10 ug virus protein per lane) on an 8% SDS-polyacrylamide gel in each of the five lanes shown and electroblotted to nitrocellulose. Viral proteins stained with amido black are shown in lane A. Other lanes were probed with monospecific rabbit antisera to purified virion proteins (1:50 dilution), and developed with horseradish peroxidase-coupled anti-immunoglobulin and 3,3'-diaminobenzidine as substrate. Lane B, anti-E2; lane C, anti-N; lane D, anti-E1; lane E, normal rabbit serum.

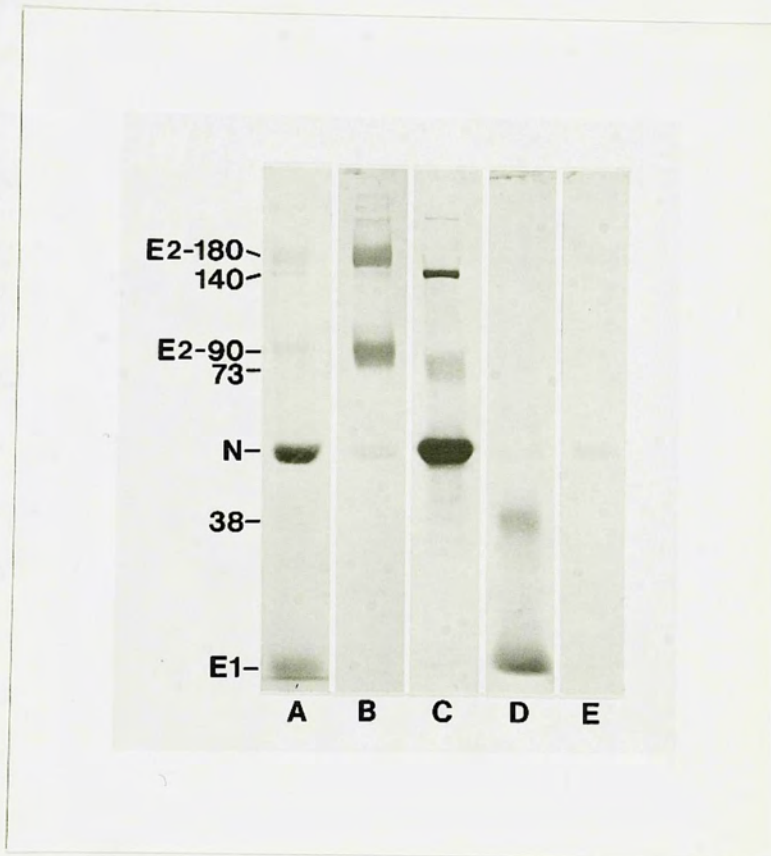
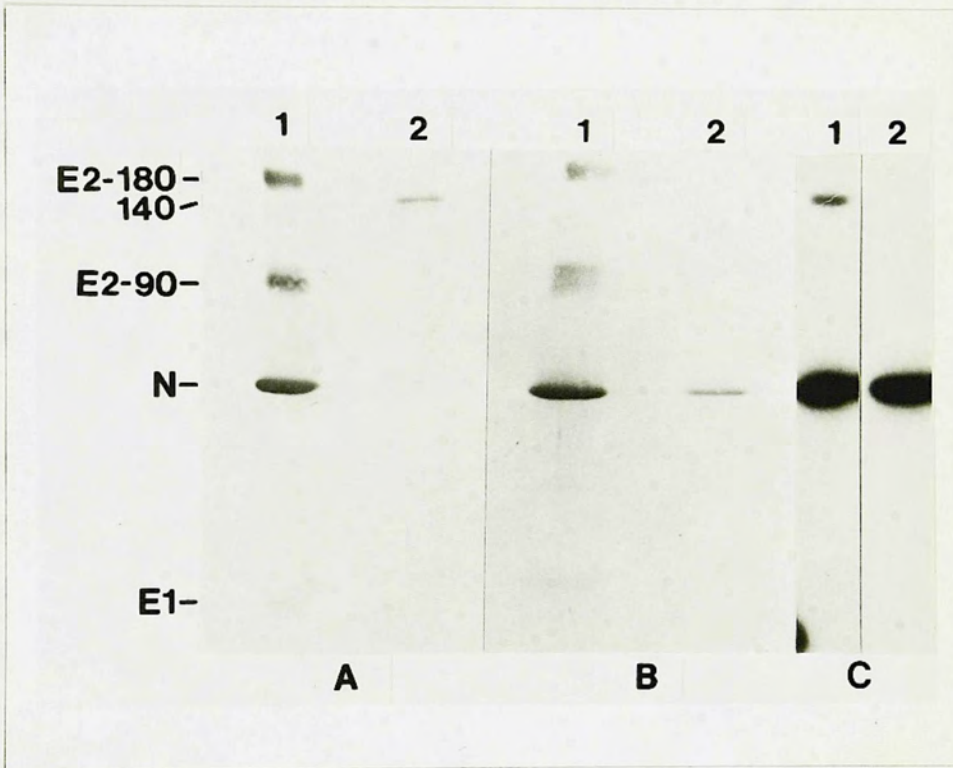


Figure 19. The 140K protein is a disulfide-linked multimer of N protein. Protein samples were run on a 5-15% SDS-polyacrylamide gradient gel after 37°C treatment for 30 min (A, C1) or after boiling for 5 min, followed by reduction with 5% 2-mercaptoethanol (B, C2). After electroblotting, the blots shown in panels A and B were reacted with virion-specific antiserum (1:100 dilution), and developed with horseradish peroxidase and 4-chloro-1-naphthol. The blot in panel C was reacted with ³²P-labeled MHV cytoplasmic RNA at 10⁵ cpm/ml in an RNA overlay-protein blot assay (ROPBA). Lanes 1, purified MHV-A59 virus (2.8 ug protein); lanes 2, gel-purified 140K protein (except C2, which contains purified MHV virions), boiled and reduced. The 140K protein was purified from a band in an SDS-polyacrylamide gel, and the samples in panels A and B were electrophoresed and electroblotted by Dr. Mark F. Frana.



monomers held together by intermolecular sulfhydryl bonds.

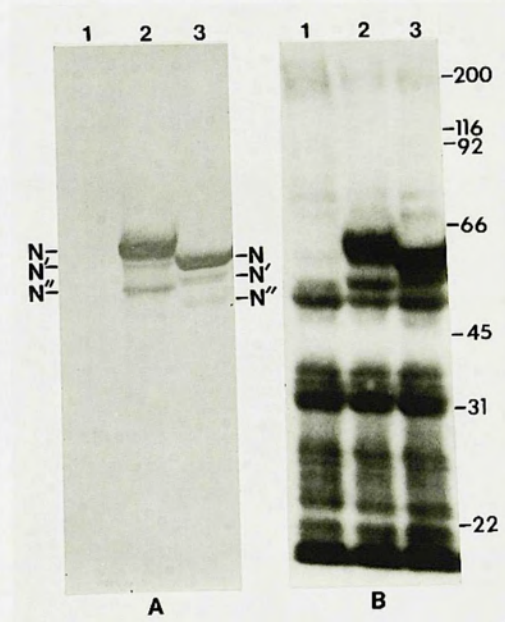
Detection of RNA-binding proteins in mock-infected and MHV-infected cells. The RNA-binding proteins of mock-infected and MHV-infected 17 Cl 1 cells were identified using the ROPBA (Fig. 20). N protein was readily detectable as an RNA-binding protein at 8 hr p.i. in MHV-A59- and MHV-JHM-infected cell extracts (data not shown). The electrophoretic mobility of N protein from MHV-A59 and MHV-JHM cell extracts differed by 3 K. In cell extracts prepared at 15 hr (MHV-A59) and 13 hr (MHV-JHM) p.i., the ROPBA detected two additional virus-specific RNA-binding proteins which migrated slightly ahead of N (panel B, lanes 2 and 3). These proteins are designated N' and N'' because they reacted with monospecific anti-N antibody (panel A, lanes 2 and 3). They are not present in virions, and may be either cleavage products of N, different phosphorylated forms of N, or translation products of prematurely terminated transcripts. It is now known from immunoblotting with antibody to a synthetic peptide, that the N' of the Alb4 mutant lacks a portion of its carboxy-terminal region (Holmes et al., 1987). That N' and N'' have RNA-binding activity suggests that their RNA-binding domains are intact.

There were many cellular proteins in the protein blots of uninfected 17 Cl 1 cell extracts. Of these, at least 12 bound MHV-A59 RNA in the ROPBA (Fig. 20B). Cellular RNA-binding proteins, including ribosomal proteins and proteins involved in translation, have been studied by the

Figure 20. Different species of N protein and cellular proteins are RNA-binding proteins in MHV-A59- and MHV-JHM-infected cells. Samples of cell extracts (75 ug protein) prepared with RIPA buffer, were electrophoresed on a 10% SDS-polyacrylamide gel and electroblotted to nitrocellulose. (A) Immunoblot after probing with N-specific mouse ascites fluid and reacting with horseradish peroxidase and diaminobenzidine. (B) ROPBA using ^{32}P -labeled MHV-A59 cytoplasmic RNA (2.5×10^4 cpm/ml). Lanes 1, mock-infected cell extract; lanes 2, MHV-JHM-infected cell extract prepared at 13 hr p.i.; lanes 3, MHV-A59-infected cell extract prepared at 15 hr p.i. The molecular weights of marker proteins, in kilodalton units, are shown on the right.

SDS-PAGE and other methods (Kumar et al., 1981; Shetty et al., 1982; Varier and Varma, 1984).

SDS-PAGE ANALYSIS OF ISOLATED PROTEIN



ROPBA and other methods (Gourse *et al.*, 1981; Shatkin *et al.*, 1982; Rozier and Mache, 1984).

RNA-binding by N-related proteins in ts-mutant infected cells. Certain RNA-positive temperature sensitive mutants of MHV-A59 were examined for their N protein composition by polyacrylamide gel electrophoresis and immunoblotting with anti-N ascites fluid. The results shown (Fig. 21A) indicate that at the nonpermissive temperature, the ts mutants synthesized less native N protein than did wild type virus. Also, both wild type- and mutant-infected cells contained smaller molecular weight forms of the N protein, which were present at 39°C but not at 32°C. Furthermore, cells infected with ts mutants Alb 4, 5 and 7 contained different amounts of N' and N'' compared to wild type virus cell extracts. All three mutants contained an even smaller species of N (not seen in wild type-infected cells) which we call N'''. These mutant cell extracts were tested for RNA-binding in a ROPBA assay (Fig. 21B). Their smaller forms of N bound the labeled probe. However, these results should be considered highly preliminary since panel B was not also stained for protein.

Interaction of MHV RNA-binding proteins with nucleic acids. The affinity of viral RNA for proteins in infected cell extracts was studied by reacting separate strips of a protein blot with RNA in buffers containing different sodium chloride concentrations and washing in the corresponding buffer (Fig. 22). Increasing the salt concentration above

Figure 21. Temperature-sensitive mutants having N-related proteins with RNA-binding activity. Cytoplasmic extracts of 17 Cl 1 cells infected with MHV-A59 wild-type virus or ts mutants were electrophoresed on SDS-polyacrylamide gels and analyzed as follows: (A) Immunoblot of a 12% gel, using anti-N ascites fluid. (B) ROPBA of a 10% gel, using ^{32}P -labeled MHV-A59 cytoplasmic RNA at 2.5×10^4 cpm/ml. (V) Purified MHV-A59; (M) mock-infected cell extract; (WT) wild-type MHV-A59; (ts 4, 5 and 7) temperature-sensitive mutants Alb 4, 5 and 7. The sample in the left lane of each pair was from cells infected at 32°C , and the sample in the right lane was from cells infected at 39°C . In panel B, WT denotes cells which were infected with MHV-A59 wild-type virus at 32°C . The cell extracts used in panel B were prepared by Dr. Mark Frana.

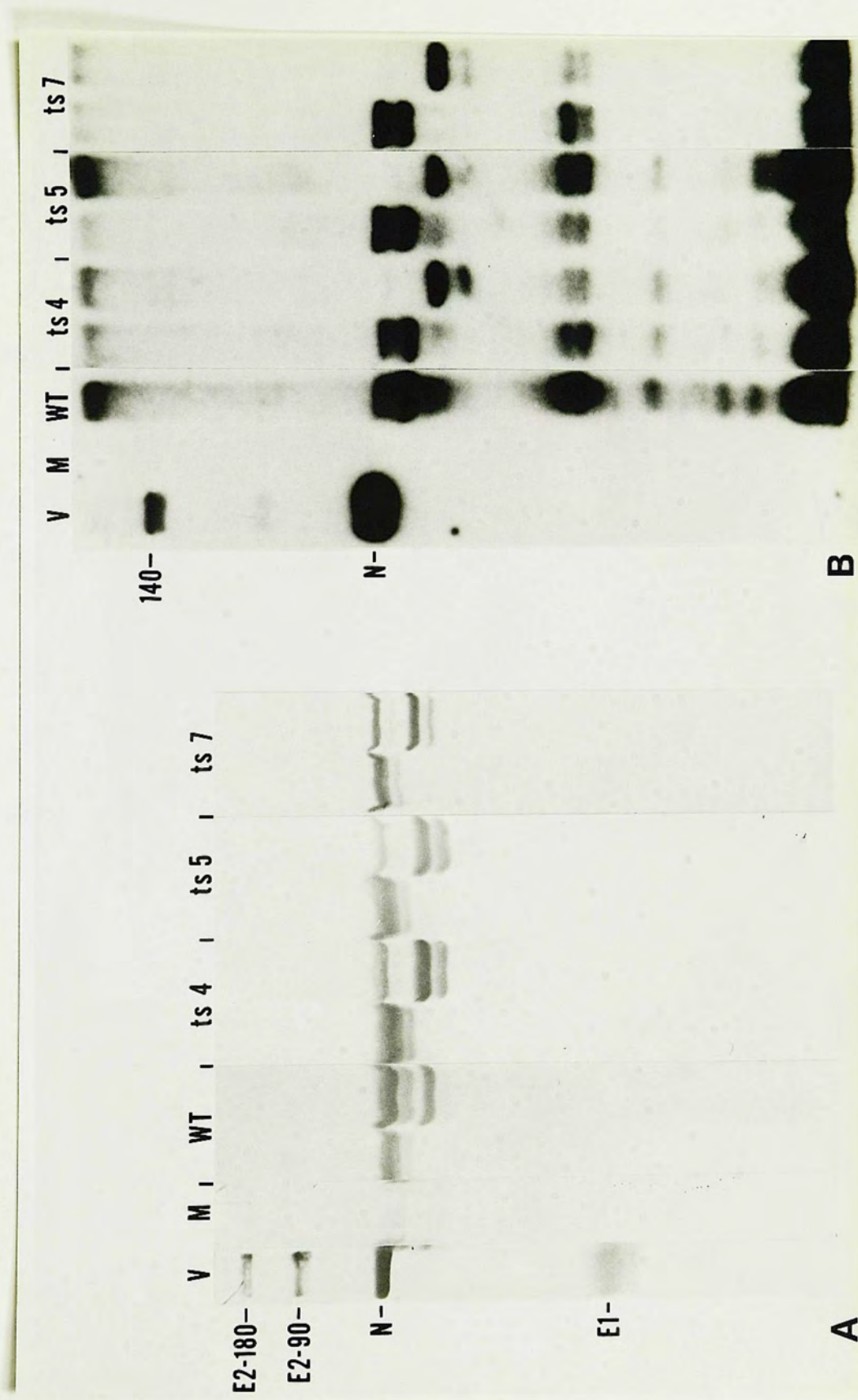
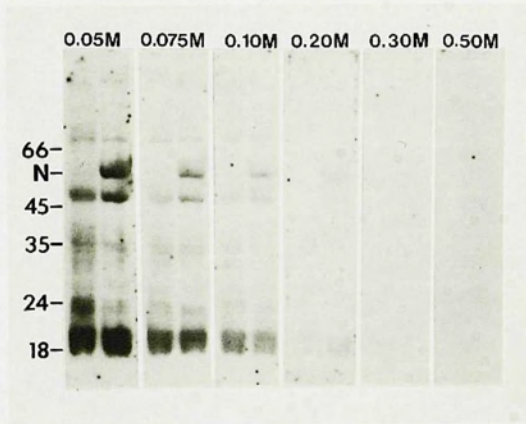


Figure 22. Effect of salt concentration on RNA-binding by proteins in mock-infected and MHV-A59-infected 17 Cl 1 cells. Proteins from cell extracts prepared with RIPA buffer were electrophoresed on a 10% SDS-polyacrylamide gel and electroblotted. The blot was cut into strips and each strip was washed and reacted in a ROPBA with ^{32}P -labeled MHV-A59 cytoplasmic RNA (4.4×10^3 cpm/ml) in buffers of the different NaCl concentrations indicated in the figure. Mock-infected cell extract (130 ug protein) was run in the left lane of each panel; MHV-A59-infected cell extract (140 ug protein), harvested at 16 hr p.i., was run in the right lane. Molecular weight markers are indicated at the left.



0.075 M reduced RNA binding and very little binding was detected above 0.1 M NaCl. Subsequent amido black staining of the same blot showed that proteins were not dissociated from the paper at this ionic strength.

The results of scanning the ROPBA shown in Fig. 22 are shown in Table 3. The N protein bound about 23% of the total bound RNA at the lowest salt concentration. A little more than half of the RNA was bound by proteins of infected cells, mainly low molecular weight polypeptides. The relative resistance of various proteins to elution of RNA by 0.075 M NaCl differed in infected cells compared to mock-infected cells.

RNA binding was also pH dependent. It diminished above pH 8, where RNA is unstable, and background increased below pH 7 (Fig. 23). Protonation of the nitrocellulose at low pH may have prevented the BSA/Ficoll/PVP in the buffer from coating the paper and thereby resulted in nonspecific binding of the RNA at low pHs. All other ROPBAs were performed at pH 7.

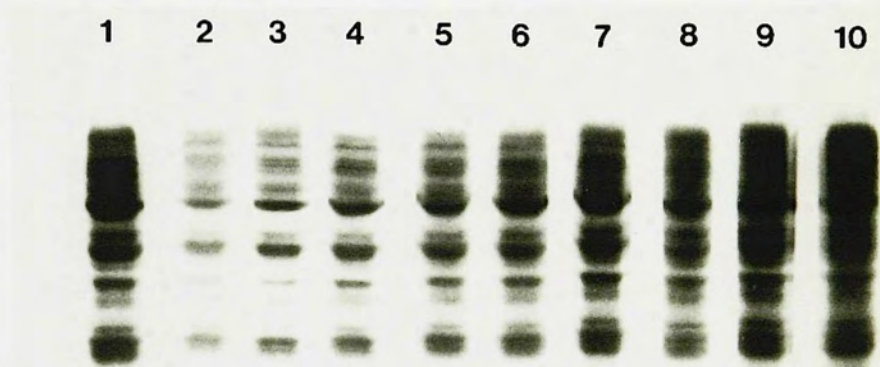
To examine the nucleotide sequence specificity of the RNA-protein interaction, mock-infected and MHV-A59-infected 17 Cl 1 cell extracts were electroblotted from SDS gels and probed with several different ^{32}P -labeled nucleic acids (Fig. 24). Probes were equalized with respect to counts per minute per milliliter. In 15-hr MHV-A59 infected cell extracts, similar bands of RNA-binding proteins were detected using as probes MHV-A59 RNA (panel A), cellular RNA

Table 3. Relative RNA binding affinities of proteins in mock- and MHV-infected cells. The lanes of the ROPBA shown in Figure 22 were scanned with a densitometer. The percent of total area represents the proportion of the total bound RNA which was bound by each protein band. The 48K cellular protein and N" overlap.

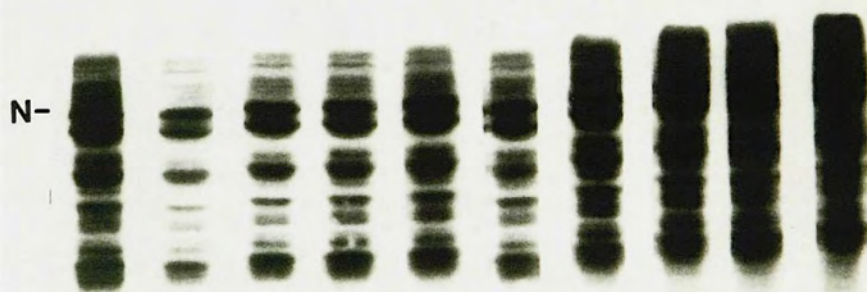
Table 3

Cell extract	NaCl (mM)	RNA Bound (% of Total Area)				
		Protein Molecular Weight (Kd)				
		74	56(N)	48+N"	36	<20
Mock- infected	50	5	—	12	16	67
	75	—	—	10	15	75
	100	—	—	—	—	100
	200	—	—	—	—	—
A59- infected	50	—	23	15	7	55
	75	—	18	9	10	63
	100	—	21	—	—	79
	200	—	—	—	—	—

Figure 23. Effect of pH on RNA-binding by proteins in MHV-infected and mock-infected cells. Mock-infected (A) and MHV-A59-infected (B) 17 Cl 1 cell extracts prepared with RIPA buffer, were electrophoresed on 15% SDS-polyacrylamide gels and electroblotted onto nitrocellulose. Lanes were cut out and reacted in a ROPBA in 10 mM Tris buffers of different pH, using ^{32}P -labeled MHV-A59 cytoplasmic RNA at 2.4×10^4 cpm/ml. The same buffer was used for the pre-wash, RNA incubation, and final wash steps. The pHs were as follows: 1) pH 7.00; 2) pH 9.19; 3) pH 8.83; 4) pH 8.41; 5) pH 7.98; 6) pH 7.59; 7) pH 7.18; 8) pH 6.79; 9) pH 6.41; 10) pH 5.96.

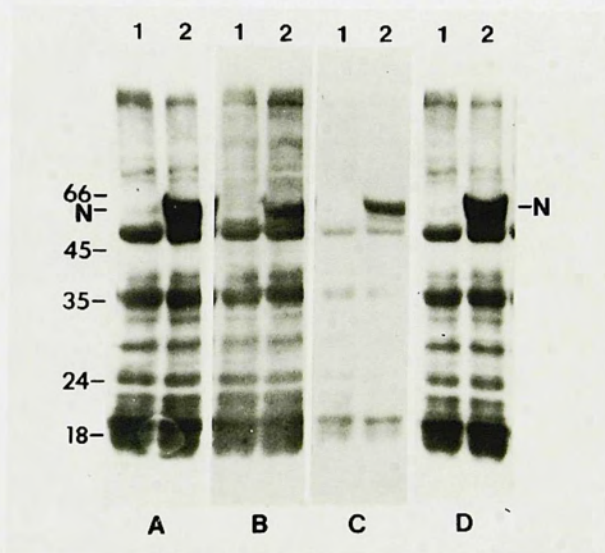


A



B

Figure 24. Binding of cellular proteins by different nucleic acids. Proteins from 17 Cl 1 cell extracts prepared with RIPA buffer (75 ug protein) were electrophoresed on a 12% SDS-polyacrylamide gel and electroblotted. Blot strips were reacted in RNA or DNA overlay-protein blot assays with the following ^{32}P -labeled probes, all at 10^4 cpm/ml: (A) MHV-A59 cytoplasmic RNA (specific activity 1.15×10^4 cpm/ug); (B) 17 Cl 1 cellular cytoplasmic RNA (specific activity 1.85×10^4 cpm/ug); (C) 22-nucleotide cDNA from the MHV leader, 5'-end labeled with ^{32}P ; (D) double-stranded genome RNA isolated from purified bovine rotavirus, 3'-end labeled with ^{32}P pCp. Lanes 1, mock-infected cell extract; lanes 2, A59-infected cell extract, 15 hr p.i.



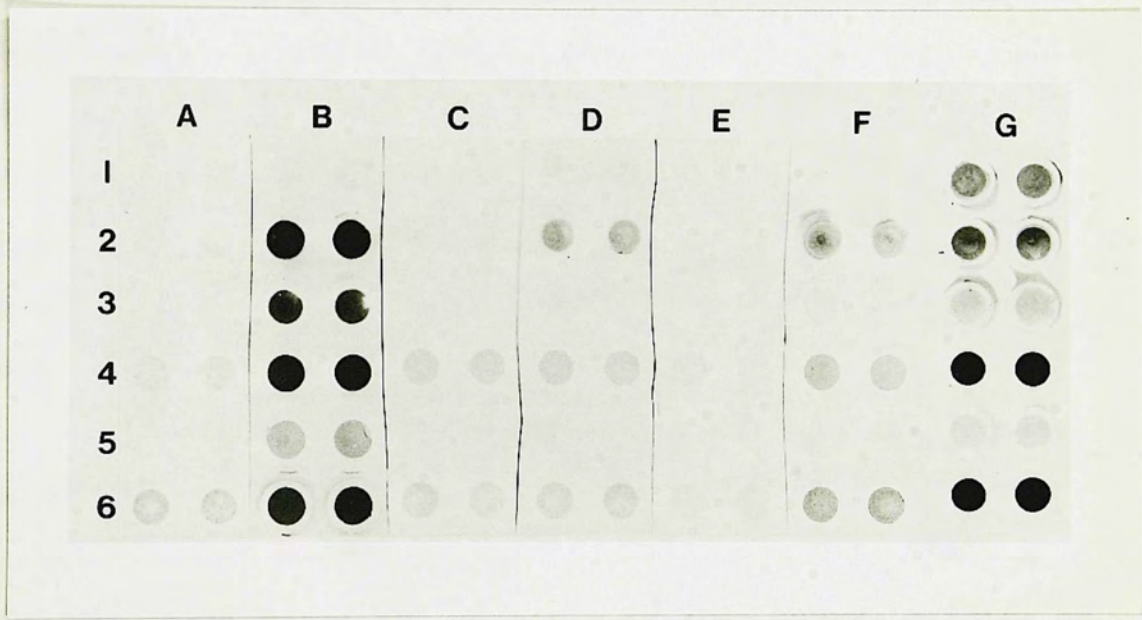
(panel B), MHV leader cDNA (panel C), and ds BRV RNA (panel D). N bound all of the probes tested. Longer exposure (not shown) of panel C yielded the same pattern of viral and cellular RNA-binding proteins seen with the other probes. Less of this cDNA was bound than the other probes, likely because the probe was of lower specific activity. N also bound HSV-1 and calf thymus DNAs which had been labeled at the 5' end with ^{32}P (data not shown). These results showed that, in the ROPBA, radiolabeled nucleic acids bound to N in a manner which was not specific for nucleotide sequence.

Binding of N protein to RNA in a filter binding assay. To demonstrate the interaction of the N protein with RNA in solution and detect virus-specific binding, N protein was affinity-purified from MHV-infected cell extracts and reacted with [^3H]uridine-labeled cytoplasmic MHV RNA in filter-binding assays. To maximize the concentration of soluble N protein in cell extracts, the extracts were treated with a high concentration of RNase (over 1 mg/ml) and soluble N protein was separated from nucleocapsids by ultracentrifugation. This treatment freed significant amounts of N protein from nucleocapsids, as shown in the immuno-dot blot in Fig. 25. In addition, most of the cellular proteins and membranes containing E1 and E2 glycoproteins were removed by pelleting. E1 and E2 are found only associated with membranes in infected cells. Thus, this procedure served to greatly enrich cell extracts for N protein but not the other viral structural proteins

Figure 25. Solubilization of N protein from nucleocapsids by RNase digestion. An A59-infected 17 Cl 1 cell extract prepared with RIPA buffer was extensively digested with RNase A (or water, as control) and centrifuged as described in Materials and Methods. Aliquots of supernatants and pellets were applied to nitrocellulose paper using a filtration manifold. Panels A-F were reacted with polyclonal antibodies to each of the three virus structural proteins and developed with staphylococcal protein A peroxidase, with diaminobenzidine as substrate. Panel G was stained for protein with amido black. Row 1, mock-infected cell extract; 2, MHV-A59-infected cell extract; 3, supernatant of RNase-treated cell extract; 4, pellet of RNase-treated cell extract; 5, supernatant of control cell extract; 6, pellet of control cell extract. Panel A, rabbit pre-(immunization with N) serum; B, rabbit anti-N serum; C, rabbit pre-(immunization with E1) serum; D, rabbit anti-E1 peptide serum; E, goat pre-(immunization with E2) serum; F, goat anti-E2 serum; G, amido black stain for protein.

(Fig. 25, 82).

The H-enriched preparation described in the preceding section was then subjected to a series of experiments designed to test the effect of various factors on the rate of H₂ evolution. The results are shown in Table I. The rate of H₂ evolution was measured by the volume of gas evolved in a fixed time interval. The results show that the rate of H₂ evolution is affected by the concentration of the H₂ gas, the concentration of the H₂ gas, and the concentration of the H₂ gas. The rate of H₂ evolution is also affected by the concentration of the H₂ gas, the concentration of the H₂ gas, and the concentration of the H₂ gas.



The extent of H₂ evolution was measured by the volume of gas evolved in a fixed time interval. The results show that the rate of H₂ evolution is affected by the concentration of the H₂ gas, the concentration of the H₂ gas, and the concentration of the H₂ gas. The rate of H₂ evolution is also affected by the concentration of the H₂ gas, the concentration of the H₂ gas, and the concentration of the H₂ gas.

(Fig. 25, B3).

The N-enriched preparation derived from RNase treatment was then affinity-purified on a column of rabbit polyclonal anti-N antibody. Fractions eluted from the affinity column were analyzed by silver stain (Fig. 26) and immunoblotting (not shown). These results show that the major protein band had a molecular weight of about 50K, co-migrating with virion N protein. Some N' was also present. The affinity fractions contained a contaminant of molecular weight 180 K (Fig. 26, lane 3), which remained the same molecular weight upon reduction with 2-ME and reacted with anti-E2 in immunoblots (data not shown), and therefore was E2. From results using the ROPBA, this protein does not bind to RNA. Small amounts of several lower molecular weight bands consisting of degradation products of N itself were also seen in immunoblots (data not shown).

N bound MHV RNA in solution in the filter binding assay (Fig. 27). In one experiment (Fig. 27A), the amount of input N protein was varied; in another (Fig. 27B), it was the RNA probe which was varied. In both cases, binding of the N protein to MHV RNAs did not reach saturation. MHV nucleocapsids, purified by extraction of virions with Triton X-114, also bound N in solution in a linear manner (not shown). These data show that the filter binding assay can be used to study interactions between the N protein and RNA.

Sequence specificity of RNA binding by the N protein. The extent of MHV-specific RNA binding was examined

Figure 26. N protein partially purified by affinity chromatography. A crude preparation of the MHV-A59 N protein was prepared by RNase treatment of MHV-A59-infected 17 Cl 1 cell extracts (see Fig. 25). This preparation was further purified on an affinity column consisting of rabbit antiserum raised against polyacrylamide gel-purified N protein, coupled to cyanogen bromide-activated Sepharose 4B. N protein was eluted from the column using 1 M sodium isothiocyanate, and fractions of the eluate were pooled and de-salted by passage over Sephadex G-25 columns. Affinity-purified N protein samples were precipitated with ice-cold acetone overnight. Precipitates were resuspended in sample treatment mix, boiled for two minutes (without reducing agent) and electrophoresed on a 10% SDS-polyacrylamide gel. The gel was silver stained by the method of Wray et al. (1981). Lane 1, purified MHV-A59 virions; 2, RNase-treated cell extract which was placed on the affinity column; 3, affinity-purified N protein, pool A; 4, affinity-purified N protein, pool D.

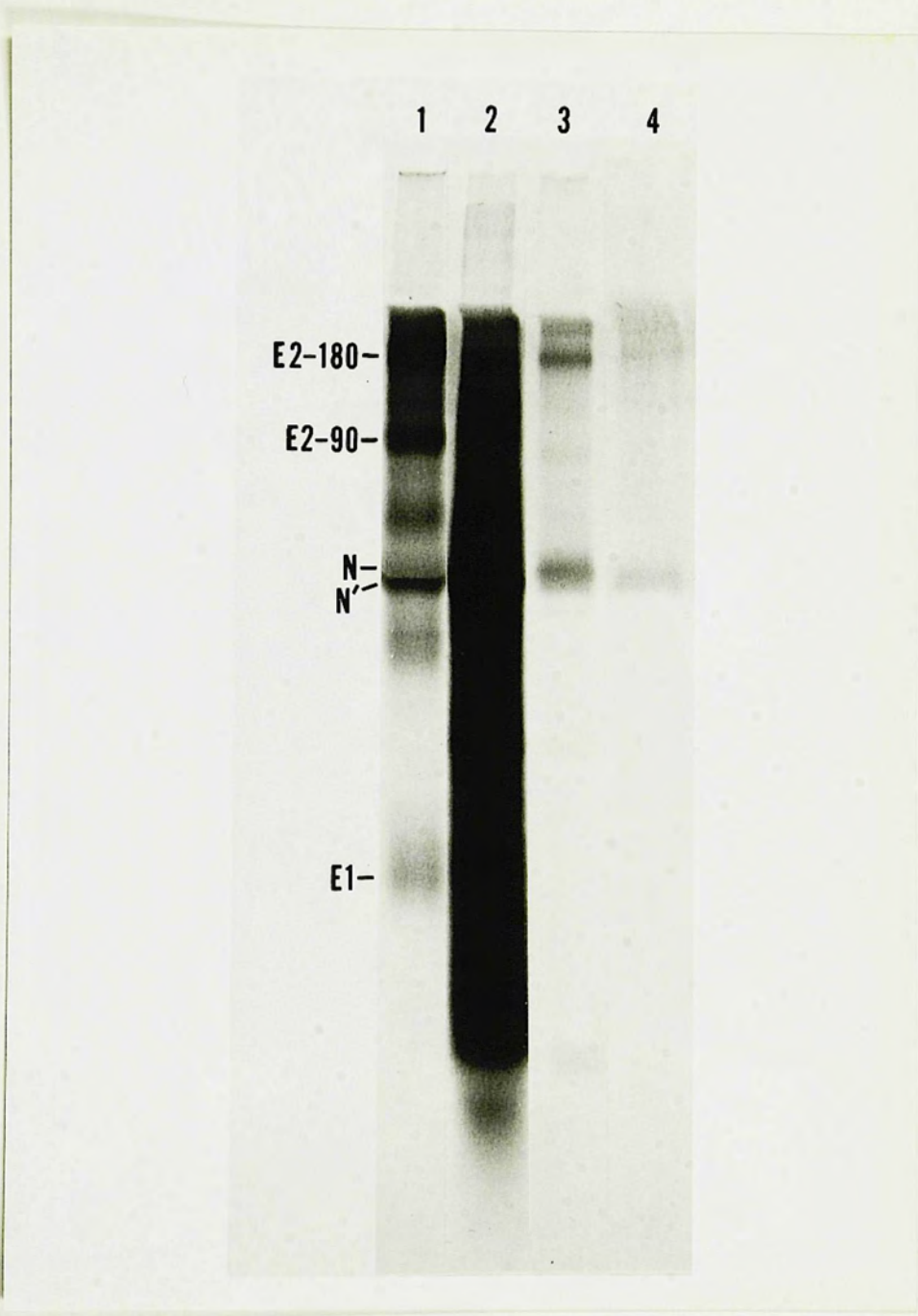
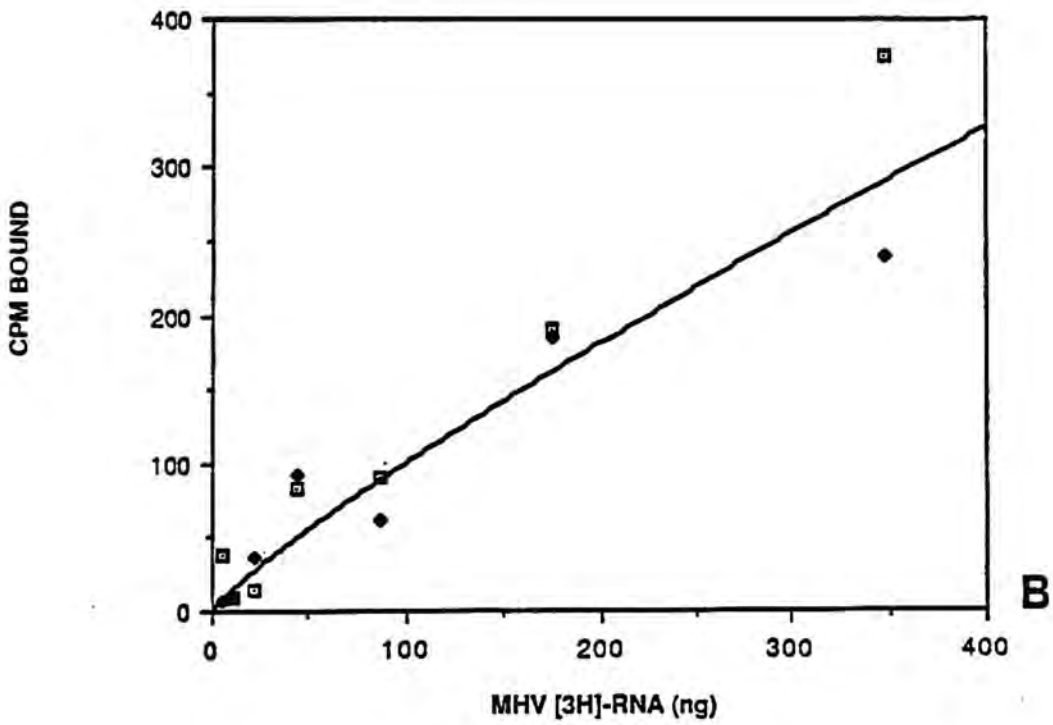
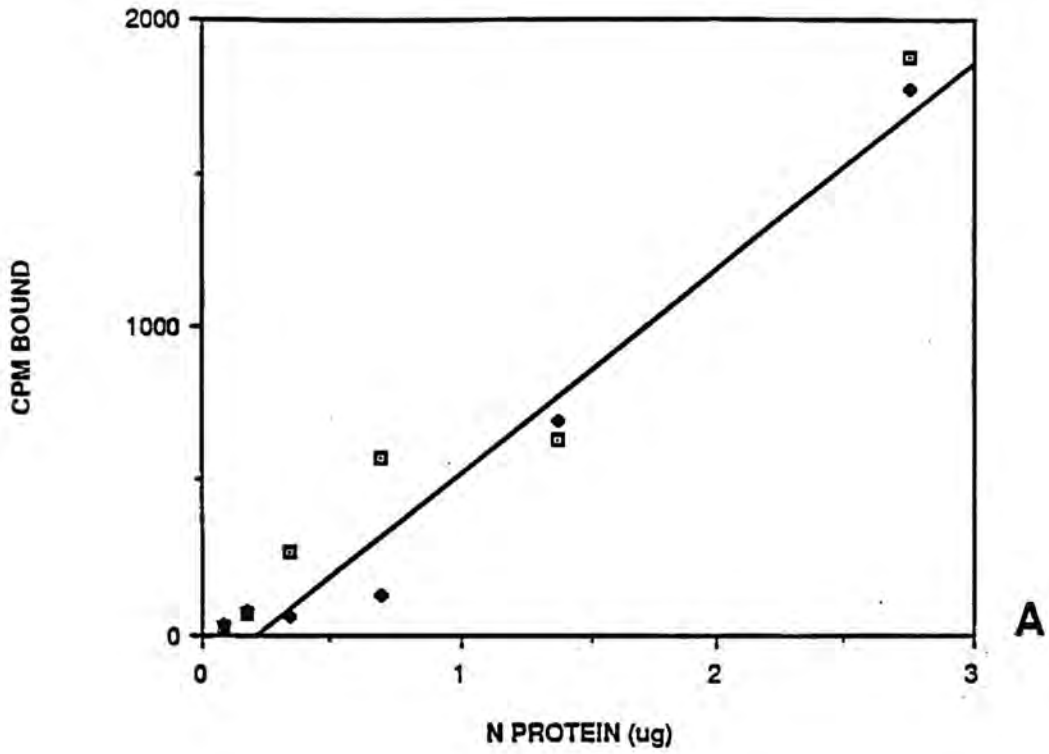


Figure 27. Binding of affinity-purified N protein to MHV RNAs in a filter binding assay. (A) N protein was diluted serially in half with Riggs buffer with RNAsin (1 U/ul) and dithiothreitol (5 mM). Twenty-five ul of each dilution were added to an equal volume containing a constant amount of ^3H -labeled MHV-A59 cytoplasmic RNA (~7800 cpm). The mixtures were incubated for 30 minutes on ice, and two 22.5 ul samples of each mixture were filtered. (B) N protein (2.75 ug) was diluted in Riggs buffer with RNAsin and DTT. Five ul of ^3H -labeled MHV-A59 cytoplasmic RNA at different dilutions was added to 45 ul of N protein. Binding mixtures were incubated as described above, and two 20 ul samples were filtered. Replicate samples are shown with different symbols (\square and \blacklozenge).

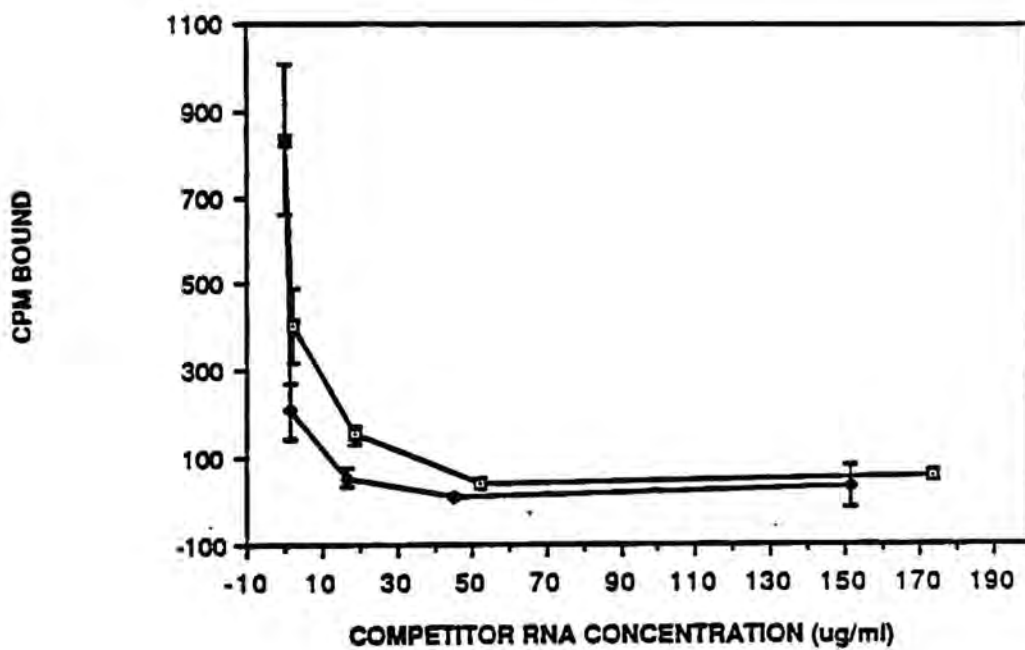


in competitive filter binding assays. In these experiments, unlabeled RNA isolated from uninfected or MHV-infected cells was added at different concentrations to the binding reaction mixtures immediately before labeled RNA and N protein were added. Figure 28 shows a representative of three experiments. A small difference in the curves (about 200 cpm) was apparent at ~ 1 ug/ml of competitor RNA. However, no significant difference was detected at the highest concentration of competitors, where the amount of labeled RNA bound was very low. Thus, binding of viral RNA by N protein, which was measured in this assay, was apparently not MHV-specific nor of high affinity, and was outweighed by nonspecific binding of cellular RNAs to N protein. One would expect that, in an improved protocol, viral genome RNA purified from MHV virions would compete more efficiently than cellular RNAs or infected cell RNAs, giving a better indication of the proportion of binding which is specific for genome strands.

It is not known to what extent N protein bound genome RNA over messenger RNAs 1-7. This question should be examined comparing purified genome RNA and poly A-selected messages as probes, and N protein derived from cDNA clones.

To identify possible strand-specific binding by N protein, a preliminary study comparing competition by positively-stranded and negatively stranded transcripts of MHV clone g344 was performed. The results indicated that the positive strand competed more efficiently than the

Figure 28. Binding of N protein to MHV RNAs in a competitive filter binding assay. ^3H -labeled MHV cytoplasmic RNA was added to unlabeled RNAs isolated from mock-infected or MHV-A59-infected 17 Cl 1 cells. The final concentrations of competitors are shown on the x-axis. The probe RNA was added to a final concentration of 23 ug/ml. N protein (pool D, 0.21 ug in 5 ul) was added to yield a total volume of 25 ul. The mixture was incubated for 30 minutes at 4°C, and 20 ul duplicate samples were filtered through nitrocellulose. RNA bound to protein was detected by counting the tritium retained on the filters. The averages of duplicate samples were graphed. Vertical error bars indicate standard deviations. Competitor RNAs are indicated as follows: (□-□) RNA from mock-infected cells; (◆-◆) RNA from MHV-A59-infected cells. These results were reproduced on three separate occasions, using the same preparations of N protein and RNAs.



negative strand. However, these results are difficult to interpret in light of the fact that the plasmid DNA used for cloning the MHV cDNA competed as well as the positive strand. All three nucleic acids competed less well than cellular RNA.

In preliminary experiments, N protein also bound various nucleic acids other than MHV RNA in solution, paralleling its binding behavior in the ROPBA. In these experiments, the N protein appeared to bind significant amounts of poly A RNA and both double-stranded and single-stranded HSV-2 DNAs in the filter binding assay.

Discussion

We have identified RNA-binding proteins of a coronavirus using a sensitive and direct method, the RNA overlay-protein blot assay (Bowen *et al.*, 1980). This assay is very useful for identifying RNA-binding proteins in low concentration or that cannot be isolated easily. In MHV virions, the N protein was found to be the major viral RNA-binding protein (Fig. 17), as expected since the helical viral nucleocapsid is composed of N protein and genomic RNA (Stohlman and Lai, 1979; Sturman *et al.*, 1980). In purified MHV-A59 virions we detected a new 140K Mr RNA-binding protein which is apparently a trimer of N protein held together by intermolecular disulfide bonds. The 140K protein was not detected previously because reduction of SDS-PAGE samples dissociated its intermolecular disulfide

bonds (Fig. 19). Formation of intermolecular disulfide bonds does not prevent the N subunits of 140K from binding to RNA.

Our results help to elucidate the mechanism of coronavirus nucleocapsid assembly, about which little has been known. In the filter binding assay, as in the ROPBA, the RNA-binding by N protein was not nucleotide sequence specific. N bound HSV DNA and cellular RNA in both assays, as well as poly A RNA in the filter binding assay. The biological significance of weak, nonsequence specific RNA-binding is unclear. Partial denaturation of N during SDS-PAGE and electroblotting may have favored non-sequence-specific binding in the ROPBA, and the denaturing effects of sodium isothiocyanate, or dephosphorylation of N protein by cellular phosphatases during affinity chromatography may have influenced the specificity of binding in the filter binding assay. Alternatively, lack of nucleotide sequence specificity in N binding may reflect a property intrinsic to proteins which form helical nucleocapsids encasing the entire genome. That is to say, binding may in fact occur randomly either at initiation or subsequent binding of nucleoprotein monomers, or both.

However, since only the genome-length RNA of MHV is assembled into virions, it is likely that a specific signal directs this process, which is probably missing from sub-genomic RNAs. This signal may be in the form of an RNA sequence or secondary structure, e.g., in tobacco and papaya

mosaic virus nucleation (Butler et al., 1977; Lok and Abouhaider, 1986). It may involve proteins and/or cell structures which are absent on purified RNA or N protein. During assembly of some other viruses with helical nucleocapsids, such as VSV (Blumberg et al., 1983) and TMV (Butler, 1984), a specific nucleation site on the viral RNA is required to bind the first few protein molecules, but binding of all subsequent protein monomers to the remainder of the genomic RNA is not nucleotide sequence specific. For TMV, the nucleation site is 55-65 nucleotides out of a 6395-6398 nucleotide genome (Butler, 1984). Thus, less than 1% of the viral genome is bound by coat protein in a sequence-specific manner, and would likely be difficult to detect with all but the most sensitive assays.

Specific binding of N protein to MHV genome RNA should be studied in a more sensitive filter binding assay in the future by using purified genome RNA labeled to higher specificity than in these studies. Competitive filter binding assays using these reagents would indicate more accurately the extent of MHV-specific binding. RNase protection studies could also be done to identify any nucleotide signal sequence.

Although initially we were concerned about the non-sequence specificity of nucleic acid binding by the MHV N protein, recent studies show that this may be a general property of many nucleic acid binding proteins of viruses with helical nucleocapsids. Recently, RNPs of influenza A

virus have been assembled in vitro from recombinant fusion NP protein and transcripts of the NP gene (Kingsbury et al., 1987). Binding of NP was found to be nonspecific, interacting with a number of different ssRNAs, ssDNA and dextran sulfate. This binding did not require a nucleotide sequence specific to the 3' end of influenza complementary RNAs and lacking in mRNAs, which are nonencapsidated. Similar studies could be done with MHV N protein prepared from cloned cDNA, SP6 viral transcripts, and MHV genome RNA isolated from purified virions. It would not be surprising if, in such in vitro assembly studies, the MHV N protein interacted nonspecifically with nucleic acids (as it did in the ROPBA and filter binding assays) and polyanions. TMV coat protein also bound polyribonucleotides in vitro to form structures identical to natural virus (Fraenkel-Conrat and Singer, 1964; Butler and Durham, 1977) and Sindbis virus core protein also formed complexes with nonviral ssRNA or DNA in vitro (Wengler et al., 1982).

Binding of RNA to N protein in the ROPBA was weak since RNA was dissociated at a salt concentration of 0.1 M (Fig. 22, Table 3). The interaction of the rotavirus core protein VP2 with rotavirus RNA in the ROPBA is affected similarly by ionic strength (Boyle and Holmes, 1986). Biologically significant interactions of RNA with viral proteins can occur at low ionic strength. For example, in vitro assembly of TMV RNA and protein is routinely done at 0.1 M ionic strength and pH 7 (Butler, 1984). Increasing

the ionic strength causes the nucleocapsids of Sendai virus and VSV to become more tightly coiled (Heggeness et al., 1982). Similar experiments with MHV nucleocapsid assembly in vitro can be done once a reproducible means of isolating the delicate nucleocapsids becomes available.

It is interesting that N' and N'' bound viral RNA in the ROPBA, yet are not present in virions. These polypeptides must lack a region or regions for binding to RNA, E1 or themselves. In fact, N' appears to lack the carboxy-terminus, shown by immunoblotting with an antibody raised against a synthetic peptide near the C-terminus (Holmes et al., 1987). Comparison of tryptic peptide digests of proteins in A59 and JHM-infected DBT cells (Bond et al., 1984) and cell-free translation products (Leibowitz et al., 1982), showed that these polypeptides are nearly identical within each strain and between strains. Leibowitz and colleagues have suggested that N' and N'' may arise from post-translational processing of N, premature termination of transcription, or proteolysis after cell lysis (Leibowitz et al., 1982).

The affinity-purified N protein preparation used in these studies was contaminated by some E2 glycoprotein. However, it is unlikely that this affected the filter binding assay results significantly, since E2 bound no RNA in the sensitive ROPBA. For future experiments, it would be wise to try to remove this E2, perhaps by passage over columns of RNA-cellulose.

Once all the available and appropriate viral RNAs are encapsidated, excess N protein might be expected to bind to ribosomal or other cellular RNAs. Such binding might affect cell functions such as protein synthesis and thereby cause cytopathic effects. The identity of the cellular RNA-binding proteins seen in the ROPBA is not known, however, reasonable candidates include ribosomal proteins (Blobel, 1971), poly-A-binding proteins (Blobel, 1973), cap-binding proteins (Sonnenberg et al., 1980), and translation initiation factors (Grifo et al., 1982). The mammalian ribosomal 5S RNA-protein complex contains a 37K MW protein (Blobel, 1971), and a 48K protein is a component of RNA storage particle complexes in Xenopus laevis oocytes (Johnson et al., 1984); these could be identical to RNA-binding proteins in 17 Cl 1 cells.

A trimeric assembly of N protein may be a general feature of coronaviruses. In bovine coronavirus a 160K disulfide-linked protein which reacts with antiserum to the nucleocapsid protein has recently been detected (Hogue et al., 1984). Oligomerization of some molecules of N protein might be associated with nucleocapsid or virion assembly, perhaps stabilizing the helical structure of the nucleocapsid by linking N protein monomers on successive turns of the helix. Considerable evidence already exists for the idea that oligomeric nucleic acid-binding proteins are common virus structural components and may be important in stabilizing virion structures. The nucleoprotein of Newcastle

disease virions exists as both a monomer (92%) and a trimer (8%) in the native unreduced form (Markwell and Fox, 1980). The nucleocapsid of HSV-2 contains a 350K protein which consists of two disulfide-linked proteins (Zweig et al., 1979), and disulfide-bonded, highly multimeric forms of vaccinia virus DNA-binding proteins have been detected (Ichihashi et al., 1984). As an elegant example, by systematic disruption of vaccinia virus and correlation of EM findings with protein composition, Ichihashi et al. (1984) have shown that disulfide-linked capsid protein complexes make up several subunits of vaccinia virus cores.

The nucleotide sequences of the N genes of MHV-A59 and -JHM have been determined (Armstrong et al., 1983a,b; Skinner and Siddell, 1983). The amino acid sequence of the N protein is considered in detail in the General Discussion. The RNA-binding domains of N and the 140K trimer of N are probably in one or more of the five basic regions of the N protein, and those which are phosphorylated may be most critical. In other viral and non-viral nucleic acid-binding proteins, phosphorylation regulates nucleic acid-binding (Wilcox et al., 1980; DeBenedetti and Baglioni, 1984; Leis and Johnson, 1984). Phosphorylation of viral proteins may regulate transcription and genome replication (Clinton et al., 1978), and control assembly of Sendai virus (Hsu and Kingsbury, 1982). In MHV N protein, a serine-rich region (ser 194-ser 220), which could be a site for phosphorylation, may also be involved in RNA-binding. Using a solid

phase binding assay with synthetic peptides of N protein domains, it should soon be possible to identify the RNA-binding domain(s) of the N protein.

The ROPBA has proved to be a useful approach for initial identification of the major RNA-binding proteins of coronavirus MHV. Following reports of this work (Robbins et al., 1984, 1986), the ROPBA method was used to identify the RNA-binding nucleocapsid proteins of Berne virus, a member of the Toroviridae (Horzinek et al., 1985), RNA-binding proteins in flavivirus-infected cells (Brinton and Grun, 1987), and to detect structural and nonstructural RNA-binding proteins in extracts of rotavirus-infected cells (Boyle and Holmes, 1986). DNA-binding proteins in varicella-zoster virus infected cells (Roberts et al., 1985) and hepatitis B virus cores (Petit and Pillot, 1985) were also identified using the same assay. Coronavirus nonstructural proteins (200K, 35K, 14K, 11K and 9K MWs) were not detected with the ROPBA, possibly because they are present in very small amounts in infected cells or they co-migrate with cellular RNA-binding proteins. Two-dimensional electrophoresis might help to detect RNA-binding activity of coronavirus nonstructural proteins.

To summarize, the N protein binds a variety of nucleic acids in a nonspecific manner. We have not succeeded in demonstrating nucleotide sequence specific binding of the N protein to MHV RNA in the ROPBA or filter binding assay. Proteins such as the 140K trimer of N and N', N" and

N''', as well as numerous cellular proteins also bound MHV RNA. Any nucleotide sequence specific binding of N protein to genome RNA, if it exists, might be detected using more specific probes in more sensitive quantitative assays.

III. CONCENTRATION OF THE N PROTEIN IN THE NUCLEI OF MHV-INFECTED CELLS

Introduction

The MHV N protein has been shown by indirect immunofluorescence to accumulate in the nuclei of infected cells late in the infectious cycle (Duchala et al., 1986). However, the nucleus is apparently not necessary for the replication of MHV, since the virus can replicate in enucleated cells (Brayton et al., 1981; Wilhelmson et al., 1981). The mechanism of transport of the N protein is unknown. Therefore, the studies described below were undertaken to understand when and how N protein enters cell nuclei.

Cellular and viral nuclear proteins. Proteins may be classified into four groups on the basis of their location within cells. Certain cellular proteins migrate rapidly into the nucleus immediately after synthesis and remain there exclusively, some are located in both the nucleus and cytoplasm, others are restricted to the cytoplasm, and still others are inserted into the plasma membrane. Little is known about the mechanisms and signals involved in the localization of most nuclear proteins. Migration into nuclei by cellular proteins has been studied primarily by microinjection, e.g., of iodinated histones into the cytoplasm of Xenopus laevis oocytes (Yamaizumi et al., 1978; Rechsteiner and Kuehl, 1979) nuclear transplantation, e.g., of proteins of amoebae (Jelinek and Goldstein,

1973), gene fusions (Silver et al., 1984; Hall et al., 1984) and virus protein mutants (Kauffman and Ginsberg 1976).

Proteins and nucleocapsids of a number of different virus groups, including some which do not assemble in nuclei, enter nuclei during the course of infection. For DNA viruses in general, except poxvirus, proteins required for DNA synthesis and virus capsid proteins required for virus assembly must migrate to the nucleus where these processes occur (Olshevsky et al., 1967; Fujiwara and Kaplan, 1967; Spear and Roizman, 1968; Ben-Porat et al., 1969). For example, following uncoating, herpesvirus nucleocapsids migrate into the nucleus (Smith and de Harven, 1974), where virus DNA replication, transcription and assembly occurs (Fenwick et al., 1978; Bibor-Hardy et al., 1982a; Fenwick et al., 1978). The migration to the nucleus of ICPs (infected cell proteins) 5 and 8 has been studied in detail (Ben Ze'ev et al., 1983; Quinlan and Knipe, 1983; Quinlan et al., 1984). ICP5 is transported to the nucleus in association with the cytoskeleton (Ben Ze'ev et al., 1983; Quinlan and Knipe, 1983). Migration of herpesvirus proteins is thought to require the amino acid arginine (Mark and Kaplan, 1971). Additionally, three EBV antigens have been found to be associated with cellular chromatin: two structural proteins of 12K and 38K MW, and a nonstructural protein of 65K MW (Habel, 1965; Reedman and Klein, 1973; Knopf and Kaerner, 1980; Spelsberg et al., 1982).

SV-40 structural proteins localize in the nucleus

where virion assembly occurs (Kasamatsu and Nehorayan, 1979; Tegtmeyer et al., 1974). Large T antigen of SV-40 is located predominantly in the nuclei of infected and transformed cells (Tegtmeyer et al., 1975; Ito et al., 1977). T antigen is detected in the nucleus within the first 10 hours of infection, preceding viral DNA synthesis (Lewis and Rowe, 1971). It is required for the initiation of each round of viral DNA replication (Myers et al., 1981) and causes cell transformation (Clayton et al., 1982). Polyoma virus replication also involves viral proteins which are localized within cell nuclei (Habel, 1965; Reedman and Klein, 1973). During replication of hepatitis B virus, the core antigen accumulates in nuclei (Ray et al., 1976; Yamada and Nakane, 1977) where it assembles with viral nucleic acid and polymerases to form viral cores (Yamada et al., 1978).

Most RNA viruses replicate solely in the cytoplasm; influenza virus is the classic exception. Certain proteins of orthomyxoviruses, measles virus and retroviruses have been identified within nuclei of infected cells. Nuclei from influenza virus-infected cells have long been known from immunofluorescence studies to contain the viral nucleocapsid protein NP, which begins to accumulate in nuclei within three hours post-inoculation (Watson and Coons, 1954; Liu, 1955; Breitenfeld and Schafer, 1957). These studies were confirmed by pulse-label and cell fractionation experiments (Briedis et al., 1981), and introduction of cloned NP DNA into cells in an SV-40 vector

(Lin and Lai, 1983). NP probably functions in protecting and transporting the viral genomic RNA from the nucleus in RNPs after it is capped and synthesized there. A nonstructural influenza protein, NS1, migrates to the nucleolus preferentially (Breitenfeld and Schafer, 1957; Briedis et al., 1981; Lamb and Choppin, 1983; Lamb, 1983).

In contrast to the proteins of myxoviruses, the proteins of most paramyxoviruses accumulate exclusively in the cytoplasm, as these viruses have a wholly cytoplasmic replicative cycle. Morbilliviruses and parainfluenza 3 (Norrby, 1972) are exceptions, whose proteins can be identified in nuclei very late in the infectious cycle. Measles virus-infected cells also accumulate viral nucleocapsids within nuclei (Nakai et al., 1969). The measles virus nucleocapsid protein NP (a phosphoprotein of ~60K MW) is the only virus-specific protein which becomes localized in the nucleus (as well as cytoplasm), shown by immunofluorescence staining of lytically and persistently infected cells, using monoclonal antibodies (Norrby et al., 1982). NP forms tubules relatively late in infection in either nucleus or cytoplasm (but not both), and cytoplasmic inclusions of varying size (Nakai et al., 1969; Norrby et al., 1982). The intranuclear inclusions appear rather late during infection, and only appear with the LEC strain of measles (Nakai et al., 1969; Norrby, 1972). Whether they play a role in virus replication is unknown. Some virus replication occurs in enucleated cells (Follett et al., 1976) and is not inhibited

by actinomycin D (Hall and ter Meulen, 1977). Lastly, the p30 gag protein of certain murine leukemia viruses has been detected in the nuclei of mouse oocytes and early embryos (Piko, 1977).

Mechanisms of nuclear transport. Two basic mechanisms of protein accumulation in interphase nuclei can be envisioned: selective retention or selective entry (Laskey *et al.*, 1985). The former mechanism involves diffusion of the protein through pores in the nuclear envelope (or possibly diffusion to the vicinity of the chromosomes during mitosis, when the nuclear envelope disassembles), and binding to a nuclear component; the latter requires that the protein have a specific amino acid sequence and/or conformation to move through the pores, and the protein may or may not subsequently interact with molecules in the nucleus.

Nuclear envelope permeability is similar in all the cells which have been tested with microinjected tracers. In general, this envelope acts as a sieve through which molecules diffuse (reviewed by Feldherr and Ogburn, 1982; Feldherr, 1985; Laskey *et al.*, 1985; Paine, 1985). The channel through which the nucleus and cytoplasm communicate is known as the nuclear pore complex. This complex spans the two nuclear membranes and the perinuclear space and consists of an octagonal structure whose central annulus has a functional radius of 45 Å (Bonner, 1975; Feldherr, 1975; DeRobertis *et al.*, 1978; Yamaizumi *et al.*, 1978). Fluorescence photo-bleaching studies of dextran transport indicate

that the radius of the nuclear pore annulus is regulated by changes in ATPase activity (Jiang and Schindler, 1986). Both passive diffusion and facilitated transport of proteins into and out of nuclei are believed to involve passage of molecules through nuclear pores (Feldherr, 1985).

Nuclear pores have an exclusion size limit of ~70K for globular proteins (Paine and Feldherr, 1972; Paine et al., 1975; Feldherr, 1985). Polypeptides from the cytoplasm which are smaller than this can diffuse through these pores at a rate inversely related to their size. Larger nuclear proteins are transported at a rate too fast to be explained by simple diffusion. Intracellular reference phase analysis, in which protein diffusion into microinjected gelatin is measured, has demonstrated that most nuclear proteins are non-diffusive, i.e., do not readily diffuse into a gelatin matrix (Paine, 1985). Such non-diffusive, facilitated transport may involve the nuclear envelope and/or the cytoskeleton or nuclear matrix (Agutter, 1984; Fulton, 1984). Nuclear proteins which are diffusive require a mechanism for being retained within nuclei (Paine, 1985). Thus, for a protein to reside in the nucleus it must bear a specific transport or binding sequence or conformation for that purpose. The isoelectric points of proteins which are most concentrated in the nucleus are 5.3 or less, suggesting that an overall negative charge is also required (Paine, 1982).

Specific amino acid sequences may be essential for

either selective transport or binding of some nuclear proteins. Structural studies of nucleoplasmin and the SV-40 large T antigen have elucidated the mechanism of entry of these large molecules (94K or greater) into nuclei. Nucleoplasmin enters nuclei at a 50-fold faster rate than small molecules such as dextrans. Microinjection studies on the effects of protease treatment on nucleoplasmin have shown that this protein requires its carboxyterminal "tail" to enter nuclei. Nucleoplasmin can form pentamers, and the rate of accumulation, but not its concentration in nuclei, is related to the number of tails present (Laskey et al., 1985).

A particular amino acid sequence has been identified which is necessary for entrance of the SV-40 large T antigen (MW 94K) into nuclei of infected cells. Gene fusion of T antigen sequences with the amino terminus of E. coli -galactosidase and pyruvate kinase defined the shortest required sequence as pro-lys-lys-lys-arg-lys-val (Kalderon et al., 1984a,b). By mixed oligonucleotide mutagenesis, mutants at each amino acid in the region of ¹²⁷Lys-Lys-Lys-Arg-Lys¹³¹ were generated and cloned in a plasmid. A mutant in which lys 128 was replaced by threonine was still able to transform cells, but no longer preferentially accumulated in nuclei as did wild type T antigen. When the signal sequence of the influenza hemagglutinin was fused with the SV-40 large T antigen sequence, the T antigen did not localize within nuclei, showing that the influenza

hemagglutinin protein signal sequence was cis-dominant over the T antigen signal sequence (Sharma et al., 1985). Also, the perinuclear-nuclear localization of VP1, the major SV-40 capsid protein, depends on the synthesis of a 61-amino acid virion structural protein, the agnoprotein, since such localization occurs more slowly in cells infected with agnoprotein-minus mutants (Carswell and Alwine, 1986).

Studies of hybrid proteins in yeast have shown that specific amino-terminal sequences from the MAT alpha 2 nuclear protein and GAL 4 regulatory protein are required for selective accumulation of these proteins in nuclei (Hall et al., 1984; Silver et al., 1984). The 13 N-terminal amino acids of the MAT alpha 2 protein contain the sequence lys-ile-pro-ile-lys, a consensus sequence which is found (slightly altered) in certain histone proteins: H2B (Wallis et al., 1980); H2A (Choe et al., 1982), H4, but not H3 (Smith and Andresson, 1983). These histones have two basic amino acids flanking three hydrophobic amino acids including one proline (Hall et al., 1984). Ribosomal proteins have similar sequences (reviewed by Feldherr, 1985). It is intriguing that this sequence is also found in two yeast mitochondrial proteins, cytochrome c peroxidase and cytochrome b mRNA maturase (Hall et al., 1984), suggesting that another level of specificity for entering nuclei, rather than mitochondria, is required.

Thus, knowledge of the mechanism of nuclear localization of viral proteins is limited at present. Little is

known about the interactions which take place between these proteins and components of the nucleus, and how these may affect cell function. These points are addressed in the studies of the MHV N protein which follow. The results indicate that the N protein not only selectively accumulates within nuclei, but may also interact with the cell chromatin.

Materials and Methods

Antisera. A monoclonal antibody raised against the N protein of MHV-JHM was kindly provided by Dr. Julian Leibowitz (University of Texas, Houston). This was a chromatographic fraction of an ammonium sulfate precipitate of a hybridoma supernatant. This monoclonal antibody reacted well with the N protein by radioimmunoprecipitation and immunoblotting. Serum from a patient with systemic lupus erythematosus was generously donated by Dr. Olivia Preble (USUHS). This serum was tested by Doris Gracey at the Clinical Pathology Laboratory at NIH and shown to have elevated anti-dsDNA antibody activity (57%) in a Farr radioimmunoassay (Swaak et al., 1979), strong reactivity against trypanosome kinetoplasts (a more sensitive measure of anti-dsDNA activity than the Farr assay) (Aarden et al., 1975), and reactivity in an Ouchterlony assay against Ro, but not La nuclear antigen (Immuno Concepts, Inc.). Antiserum against the MHV glycoprotein E2 was raised in a goat against E2 purified from MHV-A59 virions disrupted with

1% NP-40 (Sturman et al., 1980). When used at a dilution of 1:50, this antiserum delayed fusion at least past 16 hr, that normally begins among MHV-infected 17 Cl 1 cells at 8-10 hr p.i.

Indirect immunofluorescence assay. For fluorescent antibody staining, 17 Cl 1 cells were grown on glass coverslips and inoculated at an MOI of 3-7 PFU/cell. Virus was allowed to adsorb for one hour, then the inoculum was replaced with medium. At harvest, cells were washed in PBS (or RSB where indicated), fixed in ice cold acetone for 10 minutes, and stored at -20°C until being stained. The immunofluorescence procedure used was that of Dubois-Dalcq et al. (1982). N protein was localized by first reacting cells with the murine N-specific monoclonal antibody (or normal mouse serum as a control), then with either rhodamine-conjugated goat anti-mouse immunoglobulin or fluorescein isothiocyanate (FITC) coupled to rabbit anti-mouse immunoglobulin (Accurate Chemicals, Westbury, NY). Slides which had been reacted with SLE serum or control human serum were stained with FITC-conjugated goat anti-human immunoglobulin (IgG fraction, H and L chain specific; Cappel). Slides were examined with the Zeiss IIIRS fluorescence photomicroscope using an oil immersion objective (63x). A 487714 exciter filter was employed for rhodamine and a 487705 exciter filter for fluorescein.

Hoechst 33258 stain for DNA. DNA was detected along with N protein in double-labeling experiments by first

immunolabeling coverslips with anti-N, then staining in the dark with Hoechst 33258 (American Hoechst, ICD Division) at 1 ug/ml in Hanks' Balanced Salt Solution (HBSS, GIBCO) for 10 minutes, followed by 3 washes in HBSS (Hilwig and Gropp, 1972). Slips were mounted in 40% glycerol in HBSS and examined with the same Zeiss fluorescence photomicroscope with a 487702 exciter filter.

Isolation of cell nuclei and preparation of nuclear and cytoplasmic extracts. Nuclei were isolated by a modification of the method of Blobel and Potter (1966). 17 Cl 1 cells were inoculated (or mock-inoculated) at an MOI of ~100 PFU/cell. At harvest, plates were washed with 1x EDTA (0.54 mM disodium EDTA, 0.14 M NaCl, 1.5 mM KH₂PO₄, 2.7 mM KCl, 8.1 mM Na₂HPO₄), and trypsinized. After the cells had detached, an equal volume of medium containing 10% fetal calf serum was added and the cells pelleted. The cells were resuspended to a concentration of 2 x 10⁴/ml in RSB and left to swell for 30 minutes. The cells were then homogenized in a Tissumizer (Tekmar) at 60K rpm for 20 seconds on ice. Nuclei were pelleted at 1200 x g for 10 minutes, resuspended in TKM buffer (0.05 M Tris-HCl, pH 7.5., 0.025 M KCl, 0.005 M MgCl₂), and transferred to SW41 centrifuge tubes. Two volumes of 2.3 M sucrose in TKM were added to the nuclei and the tubes inverted several times to yield a final concentration of 1.5 M. The suspension was underlaid with a cushion of 2.3 M sucrose in TKM and centrifuged at 124 x g in an SW 41 rotor. The white band of nuclei at the interface was

collected with a syringe with a bent needle. To remove the outer nuclear envelope and attached RER, the nuclei were washed once in TEMT (0.01 M Tris, pH 7.6, 0.1 mM disodium EDTA, 5 mM MgCl₂-6H₂O, 4% Triton X-100 [Sigma] 0.01% PMSF) and resuspended in TE with MgCl₂. PMSF was added to 0.02% and DNase I (Sigma) to 100 ug/ml. Cytoplasmic extracts were made by washing cells twice with PBS and extracting with RIPA buffer, all in the presence of 0.1% PMSF. Nuclei were removed by centrifugation at 1200 x g. Samples were diluted two-fold in sample treatment mix and incubated at 37°C for 30 minutes prior to running on SDS gels. Nuclei were disrupted and incubated in STM in the presence of DNase prior to electrophoresis.

Colchicine treatment. Colchicine (Sigma) was added to cells at the times indicated, by dilution from a 10⁻³ M stock in ethanol. An equal volume of ethanol was added to control cell cultures.

Results

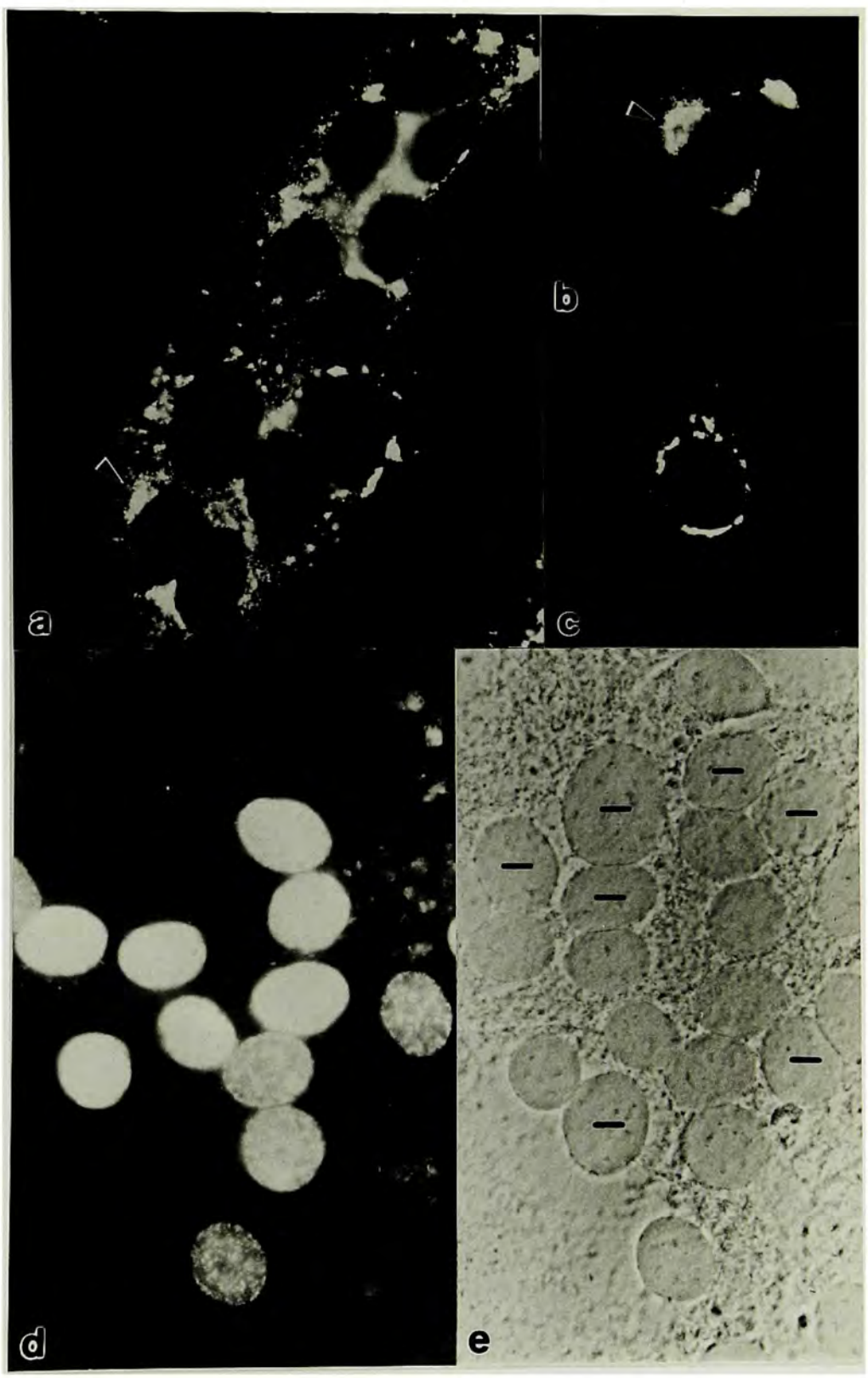
Movement of the N protein during the course of infection. The localization of the nucleocapsid protein in 17 Cl 1 cells at different times after inoculation was studied by indirect immunofluorescence analysis. Cells grown on glass coverslips were infected with MHV-A59, fixed at different times p.i. with cold acetone, stained indirectly using a mouse monoclonal antibody specific for the MHV-A59 N protein and a goat-anti-mouse fluorescent conju-

gate (Fig. 29). Cells harvested at 7 hours p.i. exhibited only cytoplasmic fluorescence (Fig. 29a), and N protein was often seen in patches near the nucleus in the region of the Golgi complex (Fig. 29b) (possibly associating with E1) as well as in the perinuclear region alone (Fig. 29c). N was usually first detected within some nuclei at late times; the pictures shown in Figures 29(d) and (e) were of cells harvested at 17 hours p.i. Nuclear N protein first appeared as a pattern of small dots and larger patches of fluorescence, and was not located in nucleoli. This nuclear pattern is remarkably similar to that of the SV-40 large T antigen (Sharma et al., 1985) and the influenza NP nucleoprotein (Breitenfeld and Schafer, 1957). Fluorescent nuclei were seen in single cells or in giant cells of various sizes. Giant cells containing fluorescent nuclei usually contained some nuclei which were completely negative for N protein (Fig. 29e).

The time at which N protein could first be detected varied from as early as 8 hr, to as late as 16 hr. The reason for this variability is not clear, however, it may be related to the fact that N always began to accumulate within nuclei after most of the cells had fused, and that the time of cell fusion was variable.

The intensity of nuclear fluorescence varied among different nuclei (Fig. 29d), although the general pattern was the same. When present at high concentrations in nuclei, especially late in infection, N protein tended to be

Figure 29. Localization of the N protein in MHV-infected cells by indirect immunofluorescence. Cells (17 Cl 1) were fixed with acetone at -20°C , and then stained with an anti-N monoclonal antibody followed by a goat anti-mouse IgG antibody conjugated to fluorescein or rhodamine. (a-c) Cells were inoculated with MHV-A59 and fixed at 7 hr p.i. The conjugate was rhodamine goat anti-mouse immunoglobulin. (d) Cells were inoculated at an MOI of 7 and fixed at 17 hrs p.i. The conjugate was fluoresceinated goat anti-mouse immunoglobulin. (e) Phase contrast image of the same field as in (d). Nuclei which are negative for N are indicated by bars. Note that nuclei in (a), (d) and (e) are in multinucleate syncytia. Single infected cells are shown in (b) and (c). Magnification 888x.



of correspondingly lower concentration in the cytoplasm. The intensity of nuclear fluorescence was reduced in cells incubated at 32°C compared to 37°C (not shown), as was the overall rate of viral protein synthesis (J.N. Behnke, personal communication),

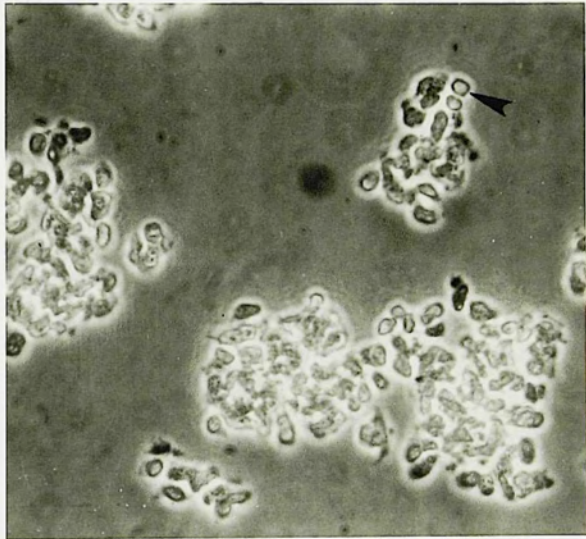
Immunofluorescence experiments showed that nuclear accumulation was a property of N only, and not E1 or E2. In double-labeling experiments using antibody to a synthetic peptide of E1 followed by goat-anti-rabbit rhodamine, E1 was never seen in nuclei, but was localized mainly in the perinuclear Golgi region (not shown). Earlier immunofluorescence experiments localized the E2 glycoprotein only to the cytoplasmic and plasma membranes (Holmes et al., 1981a,b). This was expected, as membrane proteins usually do not go to the nucleus.

Forms of nuclear N identified by cell fractionation.

In order to determine which forms of N protein were in nuclei, a method of purifying nuclei from 17 Cl 1 cells was developed, based on a technique described by Blobel and Potter (1966). This technique, which is described in detail in the Methods section, involves ultracentrifugation of nuclei from homogenized cells through sucrose onto a cushion of higher density sucrose, and washing in buffer containing MgCl₂ and 4% Triton X-100. A preparation of purified nuclei is shown in Fig. 30. The nuclei formed large clumps in both MHV- and mock-infected preparations. Most of the membranes were removed from nuclei by this technique.

Figure 30. Nuclei purified from MHV-A59-infected cells. Cells (17 Cl 1) were inoculated at an MOI of ~100 PFU/cell, to ensure that every cell was infected, and thus, the highest yield of viral protein. Cells were harvested at 13.5 hr p.i., and the nuclei were purified by centrifugation through sucrose step gradients, and washed with 4% Triton X-100 to remove RER, as described in the Materials and Methods. The arrowhead points to a nucleus which is apparently free of any cytoplasmic attachments. Magnification 320x.

Nuclei purified from *HeLa* cells were analyzed for viral proteins by immunofluorescence. The cytoplasmic products of the virus were also detected by immunofluorescence. The results are shown in Figure 1.



The results of the immunofluorescence analysis are shown in Figure 1. The cells were stained with a rabbit anti-viral protein serum. The results show that the viral protein is present in the cytoplasm of the cells. The arrow points to a cell in which the viral protein is present in the cytoplasm. The results of the immunofluorescence analysis are shown in Figure 1.

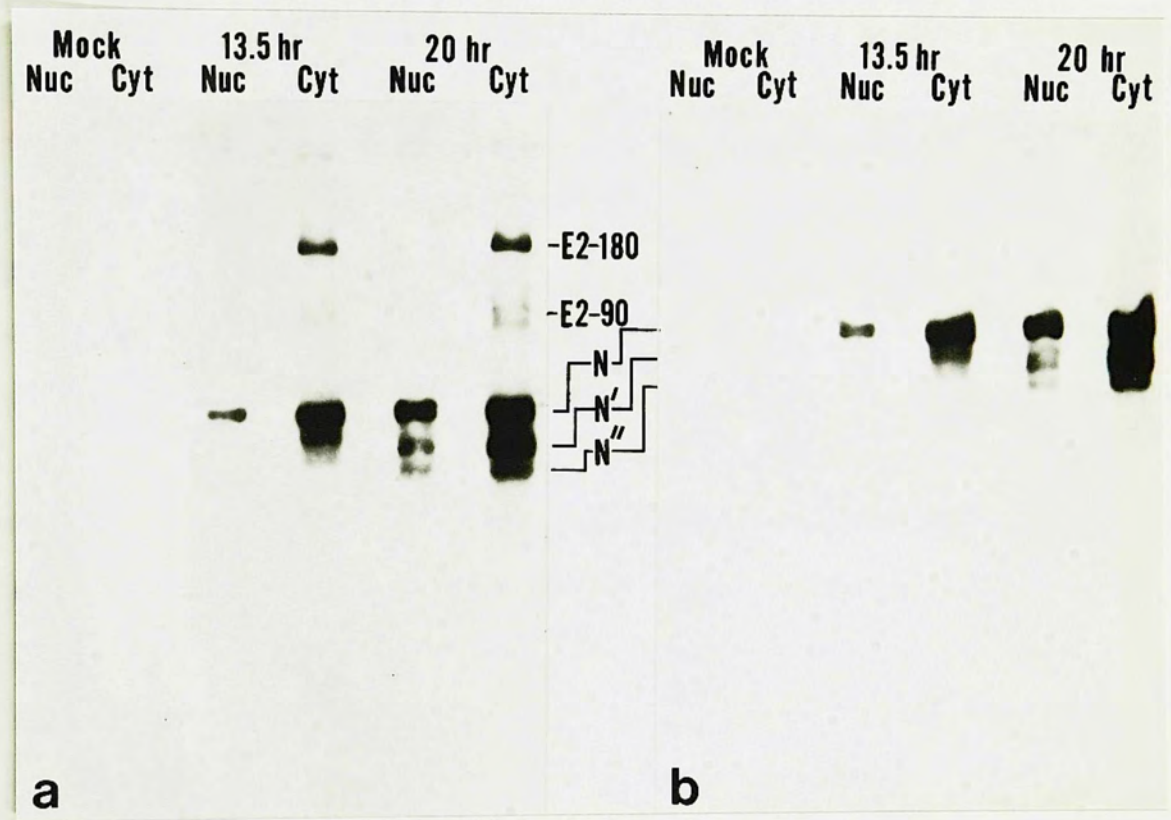
Nuclei purified from MHV-A59-infected cells were analyzed for viral proteins by SDS-PAGE. Nuclear and RIPA-extracted cytoplasmic preparations were analyzed on 10% SDS-polyacrylamide gels and immunoblotted with either polyclonal antiserum prepared by immunization with disrupted whole virions, with specificity predominantly for E2 and N (Fig. 31a), or polyclonal antiserum specific for the N protein (Fig. 31b). The results of these blots indicate that significant amounts of N protein were localized in nuclei at both 13.5 and 20 hours p.i., whereas most of the available cytoplasmic E2 protein was excluded from nuclei. In addition, whereas largely the native form of N (50K MW) was present in nuclei at both 13.5 and 20 hr p.i., by 20 hr p.i. the faster migrating species N' and N'' became clearly apparent. These results indicate that all three forms of the N protein can be transported to the nucleus, and the 50K form of the N protein may be better transported or retained in nuclei than N' or N''. In contrast, only the 50K form of N protein can be incorporated into virions.

Mechanism of nuclear localization of N protein.

The mechanism by which N accumulates within nuclei was studied. It was hypothesized that this might occur during mitosis due to disassembly of the nuclear envelope, allowing a DNA-binding protein like N protein to bind to chromatin and then become trapped in the nucleus when new nuclei were formed in the daughter cells (discussed by Maul, 1982, and Goldstein, 1985). Attempts to film infected cells during

Figure 31. Forms of N protein in nuclear and cytoplasmic extracts from MHV-infected cells. Cells (17 Cl 1) were inoculated at an MOI of ~ 100 PFU/cell, harvested at 13.5 hr p.i., and the nuclei were purified as described in the Materials and Methods (see Fig. 30). Cytoplasmic extracts were prepared by lysing cells in RIPA buffer and removing the nuclei by centrifugation. Samples were run on 10% SDS-polyacrylamide gels and electroblotted onto nitrocellulose. Panel a, immunoblot using antibody to NP-40-disrupted whole virions. Panel b, immunoblot using antibody to gel-purified N protein. Lane 1, Nuclear extract from 5×10^3 mock-inoculated cells. Lane 2, Cytoplasmic extract from 2×10^3 mock-inoculated cells. Lane 3, 13.5 hr nuclear extract from 5×10^3 cells. Lane 4, 13.5 hr cytoplasmic extract from 2×10^3 cells. Lane 5, 20 hr nuclear extract from 3×10^3 cells. Lane 6, 20 hr cytoplasmic extract from 1×10^3 cells.

...for studying the ...
...protein within ...
...difficult ...
...
...



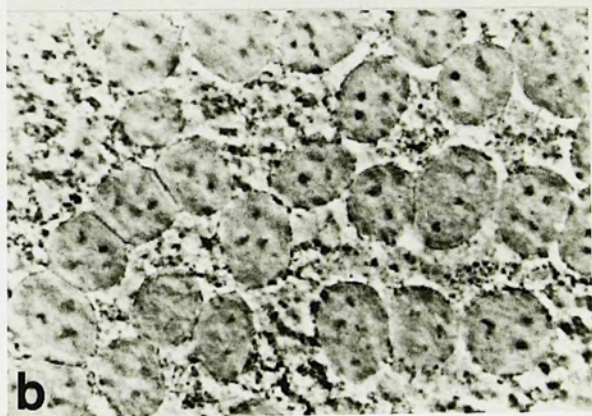
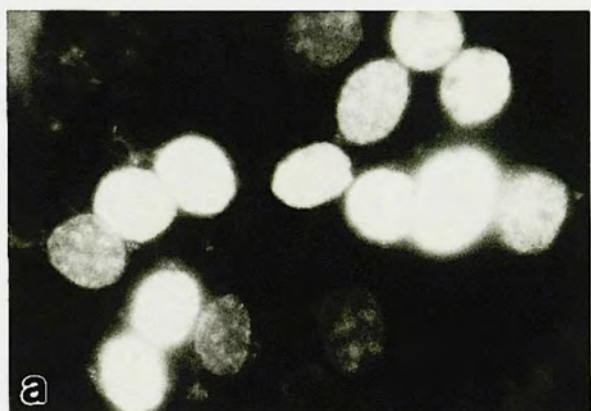
Co-localization of E2-180 and E2-90

mitosis, for studying the effect of mitosis on accumulation of N protein within nuclei, were unsuccessful due to technical difficulties. If the above hypothesis were true, then inhibition of mitosis by colchicine would be expected to prevent the appearance of N in interphase nuclei. Colchicine apparently has no effect on infection of macrophages by MHV-3 (Mallucci and Edwards, 1982), but its effect on MHV-A59 infection of mouse fibroblasts has not been reported. In an experiment in which colchicine was added at 6 hrs p.i. (to avoid any possible effects on synthesis of the N protein), no effect on entry of N into interphase nuclei was observed (Fig. 32). These results indicate that a mechanism other than mitosis is required for N to localize in nuclei.

The effect of inhibiting cell fusion on accumulation of N in the nucleus was studied, since cell fusion always preceded localization of N protein within nuclei. In two experiments cell fusion was completely inhibited by addition of goat anti-E2 antiserum at a 1:50 dilution at 2 hrs after adsorption (1 hour after the medium was changed). The cells were examined for fusion at 16 hr p.i. and harvested. Comparable numbers of nuclei were positive for N in both untreated and treated cultures (not shown). It had also been observed that single cells could acquire nuclear N. Therefore, cell fusion is not required for N to accumulate within nuclei.

Co-localization of N protein with chromatin. The

Figure 32. Nuclear localization of the N protein in MHV-infected cells treated with colchicine. Cells (17 Cl 1) were inoculated with MHV-A59 at an MOI of 3 and incubated with 10^{-4} M colchicine from 6 hr p.i. until harvest. At 17 hr p.i., the cells were swollen in RSB (which allowed better visualization of mitotic chromosomes, useful in the experiments shown in Figures 33-36) and fixed. (a) The coverslip was reacted with an anti-N monoclonal antibody, then fluoresceinated goat anti-mouse immunoglobulin. (b) Same field examined with phase contrast. Note that the nuclei all lie within one giant cell. Magnification 916x.



localization of N protein within nuclei was examined in more detail to determine whether N was associated with cellular chromatin. Studies described earlier utilizing the ROPBA and filter binding assays showed that MHV N protein readily binds to DNAs. To better visualize chromatin, metaphase arrests were induced by colchicine treatment. Colchicine was added at 6 hours p.i., and at 17 hrs cells were resuspended in RSB and fixed. The cells were then stained with orcein, a dye which stains chromosomes purple. Cells were arrested in metaphase and the greatest number of metaphase arrests in attached cells was seen at a concentration of 10^{-5} M colchicine (Fig. 33). Mitotic arrests were present in a significant number of cells which remained attached to the dish (Fig. 34a); many cells had detached as cells rounded up due to colchicine treatment. This occurred because, in binding tubulin and causing disassembly of microtubules, colchicine causes destruction of the cytoskeleton (Richardson and Vance, 1978; reviewed by Brachet, 1985).

Cells were treated at this concentration and stained for N protein by indirect immunofluorescence as before, with the result that many chromosomes stained brightly for N protein (Fig. 34c and d). These metaphase chromosomes were best appreciated by focussing the microscope at different levels. Occasionally a dispersed pattern of metaphase chromosomes was detected using anti-N (Fig. 34d). Therefore, single labeling showed that N protein was localized

Figure 33. Induction of metaphase arrests in MHV-A59-infected 17 Cl 1 cells treated with colchicine. Cells were inoculated with MHV-A59 at an MOI of 7 and treated with varying concentrations of colchicine from 6 hr p.i., then swollen in RSB and fixed at ~17 hr p.i. Metaphase arrests were counted and expressed as percent of total cells.

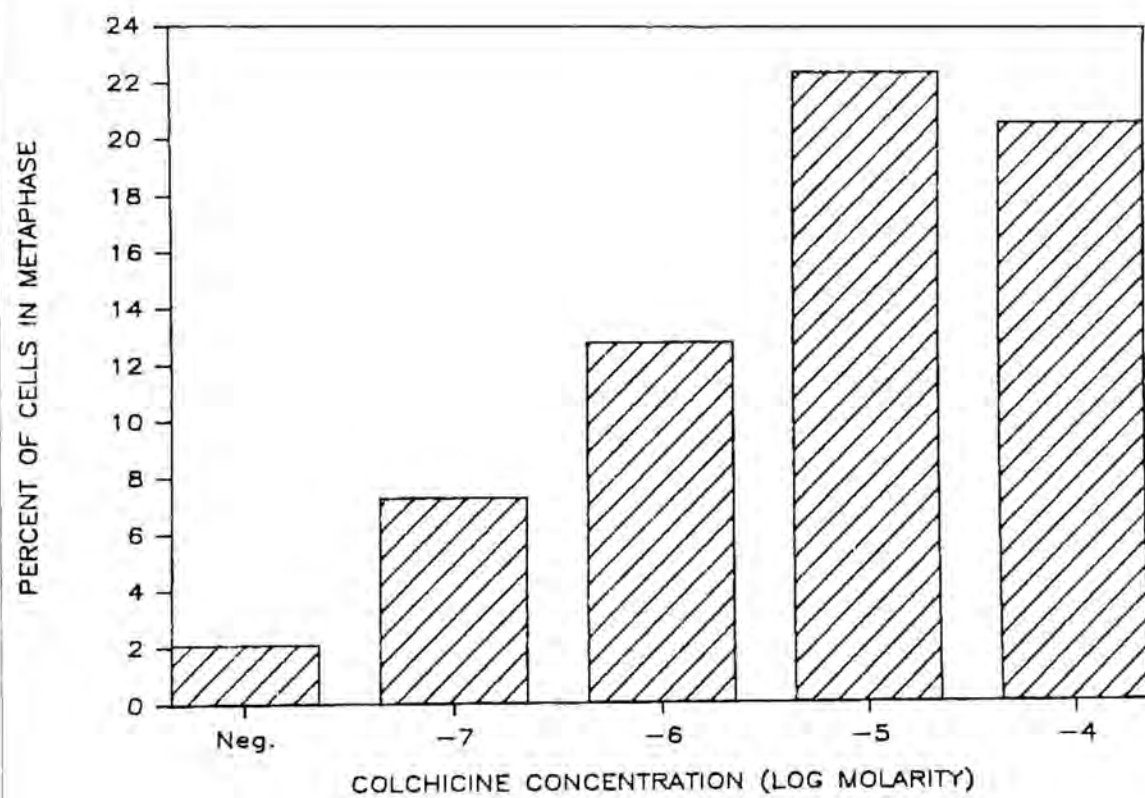
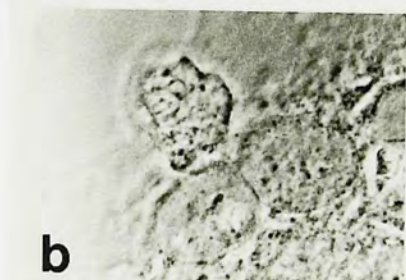
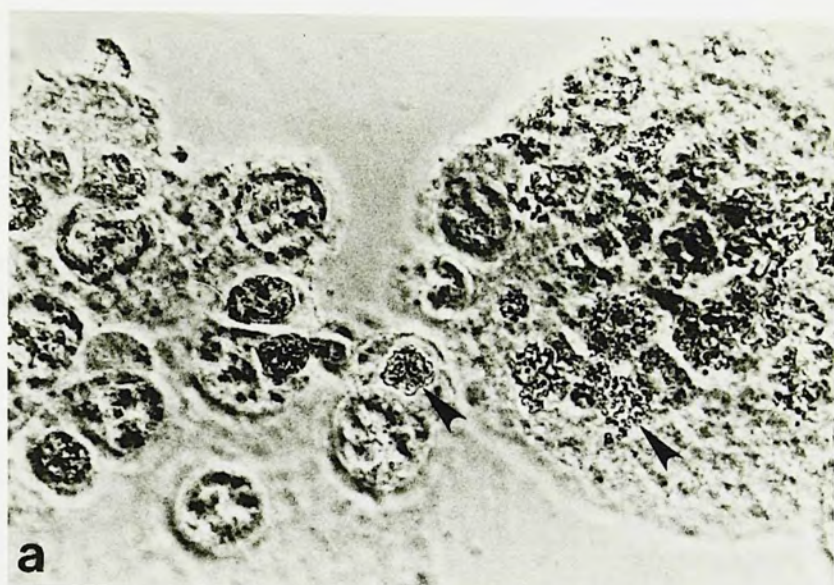


Figure 34. Localization of N protein on metaphase chromosomes shown by indirect immunofluorescence and orcein staining. Cells (17 Cl 1) were inoculated with MHV-A59 at an MOI of 7, incubated with colchicine at 10^{-5} M at 6 hr. p.i., then swollen in RSB and fixed at ~17 hr p.i. (a) Cells were stained with 1% orcein. The arrowheads point to metaphase chromosomes. Magnification 448x. (b) Infected cell (unstained) in metaphase. (c) Same cell as in (b), reacted with anti-N monoclonal antibody and fluoresceinated goat anti-mouse immunoglobulin. (d) One cell in late prophase or early metaphase, with chromatin dispersed. Cells were stained as in (c). Magnification 882x.



with chromosomes, made readily apparent due to the condensation of chromosomes during metaphase.

This finding was corroborated when MHV-infected cells were doubly stained with anti-N monoclonal antiserum and serum from a patient with systemic lupus erythematosus (SLE), which stained both metaphase and interphase nuclei (Figs. 35 and 36). The pattern of the anti-DNA stain was homogeneous across interphase nuclei, but was globular and far brighter for some metaphase cells (Fig. 35a). This serum was known to be specific for anti-dsDNA and Ro antigen but not La antigen. The results in Figure 36 show that N protein was colocalized with metaphase chromatin. Staining of interphase nuclei by the anti-N monoclonal antibody was reduced when added simultaneously with anti-DNA serum, perhaps due to competition for the antigenic sites on the DNA by anti-DNA antibodies.

An additional study was performed in which cells (not treated with colchicine) were stained with the DNA-specific dye Hoechst 33258, a bisbenzimidazole derivative. This dye has a high affinity for adenine-thymine pairs, and less affinity for guanine-cytosine pairs (Bontemps *et al.*, 1975). It is thought not to intercalate between bases (Comings, 1975). Figures 37 and 38 show that this dye specifically stained both interphase nuclei and metaphase chromosomes. The Hoechst dye stained large clumps of chromatin very intensely in interphase nuclei. These structures have been termed "chromocentres", and are

Figure 35. Identification of DNA in mock-infected cells using anti-DNA (SLE) serum. Cells (17 Cl 1) were incubated with 10^{-5} M colchicine at 6 hr after mock-inoculation, then swollen in RSB and fixed in acetone at -20°C , at ~17 hr p.i. (a) Cells were reacted with SLE serum, then fluoresceinated goat anti-human immunoglobulin. (b) Same field examined by phase contrast. Magnification 1260x.

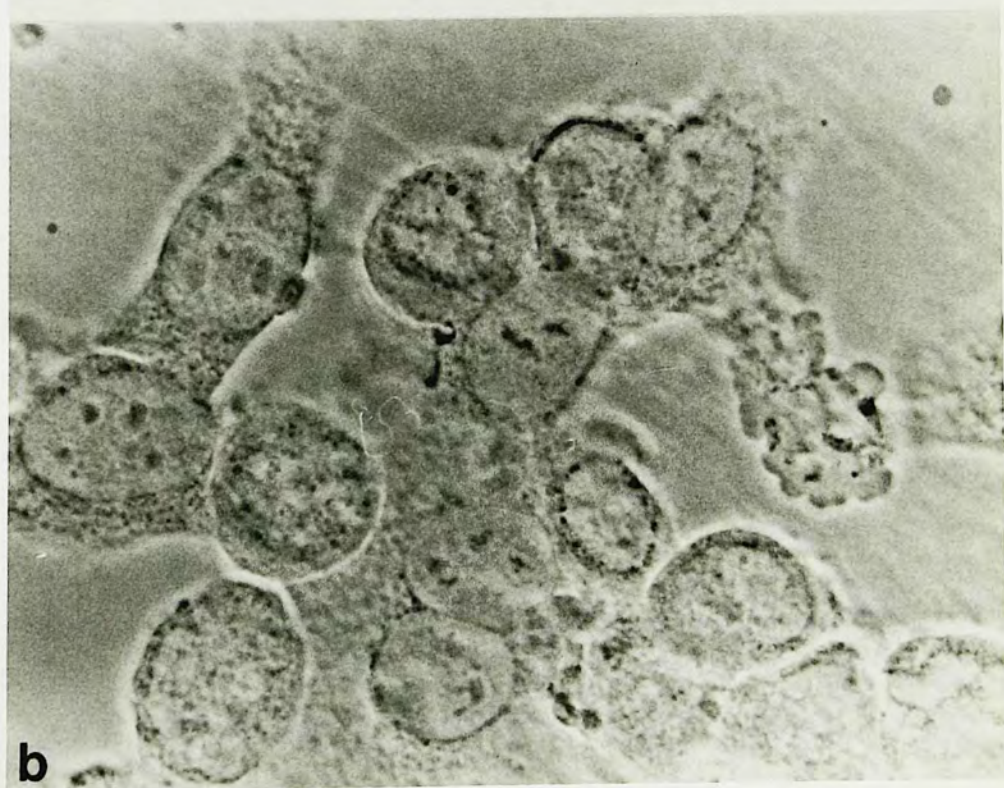
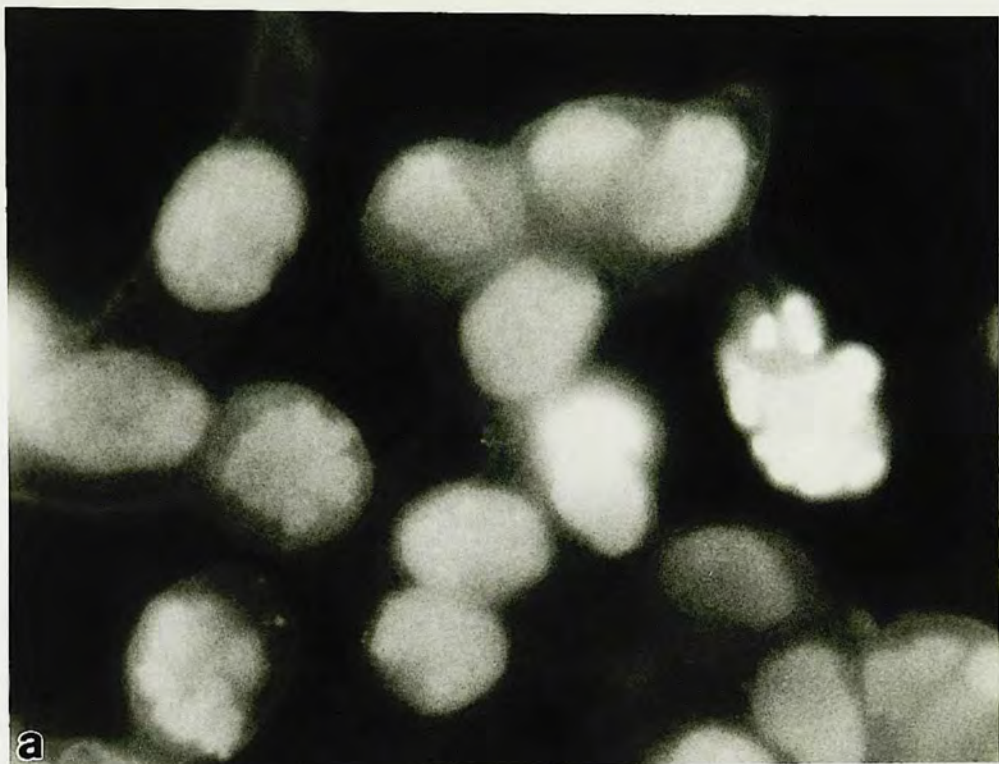


Figure 36. Co-localization of N protein and DNA shown by double label immunofluorescence. Cells (17 Cl 1) were inoculated with MHV-A59 at an MOI of 3, and incubated with colchicine at 10^{-4} M at 6 hr until harvest, swollen in RSB and fixed at ~17 hr p.i. Cells were then reacted with human anti-DNA serum and fluoresceinated goat anti-human immunoglobulin, as well as mouse anti-N monoclonal antibody and rhodamine goat anti-mouse immunoglobulin. (a) Fluorescein-labeled DNA, photographed with a Zeiss 487705 exciter filter. (b) Rhodamine-labeled N protein, photographed with a 487714 exciter filter. Magnification 1260x.



Figure 37. Double staining of interphase nuclei with the dye Hoechst 33258 and anti-N monoclonal antibody. MHV-A59 infected 17 Cl 1 cells (not incubated with colchicine) were washed in PBS and fixed at 14 hr p.i. Coverslips were reacted with anti-N monoclonal antibody and rhodamine conjugated goat anti-mouse immunoglobulin, followed by Hoechst 33258. (A) Anti-N stain, photographed with a Zeiss 487714 exciter filter. (B) Hoechst stain specific for DNA, photographed with a Zeiss 487702 exciter filter. The brightly staining areas in (B) correspond to adenine-thymine-rich regions near centromeres, known as "chromocentres". Note that the loci of N protein (A) do not overlap with the DNA chromocentres (B). Magnification 1600x.

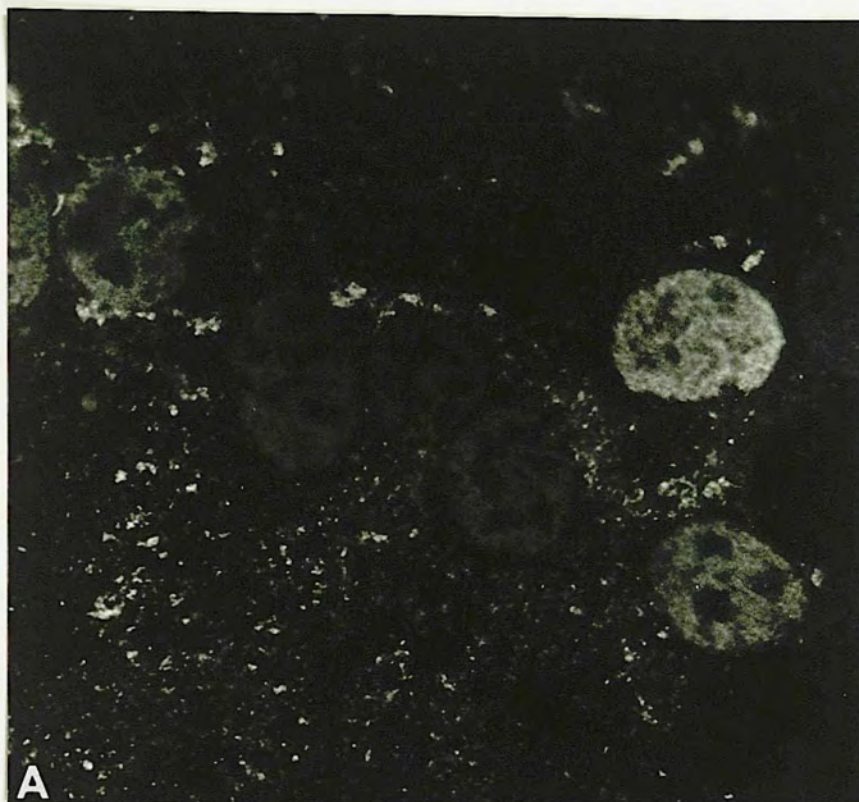
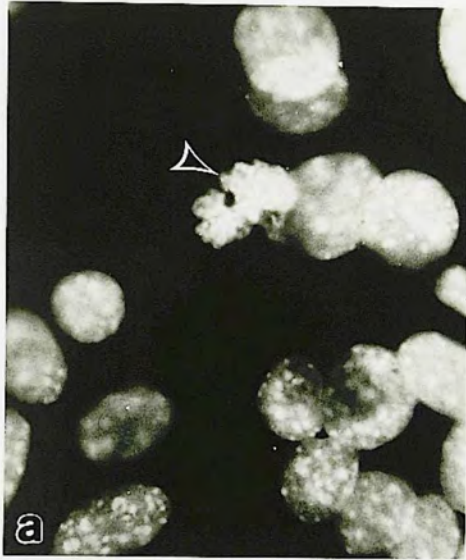


Figure 38. Mitotic cells with chromosomes staining positive or negative for N protein. MHV-A59 infected 17 Cl 1 cells were washed in PBS and fixed at 14 hr p.i. The coverslips were reacted with anti-N monoclonal antibody and rhodamine-labeled goat anti-mouse immunoglobulin, then Hoechst 33258. (a) Cells examined for Hoechst stain, photographed with a Zeiss 487702 exciter filter. The arrowhead points to a cell in metaphase. (b) Same field, examined for N antigen location (photographed with Zeiss exciter filter 487714), showing a cell whose metaphase chromosomes are positive for N. Note several interphase nuclei positive for N antigen. Cytoplasmic N antigen appears as bright flecks. (c) Hoechst DNA stain, showing a metaphase cell. (d) Same field, rhodamine-labeled N protein. Note that the N protein is restricted to the cytoplasm and is not co-localized with chromosomes. Magnification 1040x.



heterochromatic blocks of DNA at centromeres which have become aggregated (Natarajan and Gropp, 1972). They are often adjacent to nucleoli. The anti-N stain did not overlap the chromocentres in interphase nuclei (Fig. 37), showing that it was not localized at these structures. N protein was sometimes seen co-localized with metaphase chromatin (Fig. 38b), made visible apparently due to the condensation of the DNA. However, metaphase chromosomes did not always show N-specific fluorescence, even though N protein was present in the cytoplasm (Fig. 38c and d).

Discussion

The results presented show that the MHV-A59 N protein behaves like the Sendai virus nucleocapsid protein in that both proteins are localized in the perinuclear area 7-8 hrs after inoculation (Orvell and Grandien, 1982). However, unlike the Sendai NP protein, later in infection the MHV N protein is transported to some but not all nuclei. In this respect the MHV N protein behaves similarly to the measles virus NP (Norrby et al., 1982). It is also similar to the influenza virus NP, although migration of NP into nuclei has been detected by 3 hrs after inoculation, suggesting a different mechanism of transport (Watson and Coons, 1954; Liu, 1955; Breitenfeld and Schafer, 1957). The immunofluorescence pattern of N within nuclei is remarkably similar to that of the influenza NP (Breitenfeld and Schafer, 1957) and the SV-40 large T antigen (Sharma et al.,

1985), being rather diffuse but sparing the nucleoli. The significance of this similarity is unknown, but could mean that these proteins are interacting with the same nuclear structures. The nuclear pattern of the measles NP is quite different from that of MHV, exhibiting small dot-like inclusions associated with inclusions of formed nucleocapsids (Norrby et al., 1982). In a previous study involving immunofluorescence analysis of MHV-infected cells (Robb and Bond, 1979a), convalescent mouse ascites antibody detected viral protein(s) within the nucleus at early times after inoculation. However, this result has not proved reproducible by other laboratories.

The results from three different staining approaches showed that N protein clearly associated with structures in interphase nuclei and sometimes associated with metaphase chromatin. It is not surprising that N appears to bind cellular DNA since results presented in the preceding chapter on N as a nucleic acid-binding protein suggest that N protein can bind to cellular DNA and RNA in vitro. The N protein might also be bound to RNA (possibly forming nucleocapsids) or proteins, interactions which cannot be discerned by the techniques used. Purified nuclei could be disrupted and examined for nucleocapsids.

The mechanism for N accumulation within nuclei has been studied. Although cell fusion always precedes the appearance of N protein in nuclei, fusion is not required for transport of N protein to nuclei, because N is found in

the nuclei of single cells, cells with two nuclei, and giant cells, and nuclear N was seen in cells treated early in infection with anti-E2, which inhibited cell fusion completely. Studies with colchicine indicated that N protein does not require mitosis to become associated with nuclear components. If mitosis had been required, at least a 21% drop in the number of N-positive nuclei would have been observed.

The relatively small size of N argues against a need for an entry sequence, since transport consensus sequences have only been reported so far for proteins with MWs of 95K and above (Dingwall *et al.*, 1982; Dingwall and Allan, 1984; Kalderon *et al.*, 1984a,b). Computer scanning (IBI Subsequence Homology Search Program) of the amino acid sequence of the MHV-A59 N protein (translated from the nucleotide sequence stored in GenBank 40.0) indicated that it does not bear a sequence exactly like those of other nuclear proteins, but has several sequences that are very similar. The sequences most similar to that of T antigen (pro-lys-lys-lys-arg-lys-val) began at amino acid 390: pro-lys-pro-gln-arg-lys-gly. The yeast sequence lys-ile-pro-ile-lys was not represented, but six similar sequences of five amino acids with lysine at each end and containing at least one neutral amino acid were present within the amino acid region 253-405.

There is a lag period of at least two hours between detection of the N protein in the cytoplasm and its detec-

tion within nuclei. This suggests that it probably does not enter nuclei by facilitated transport, which would occur within minutes (Laskey et al., 1985). That the N protein appears to associate with chromatin suggests that it may be selectively retained there due to its nucleic acid-binding properties. Direct isolation and biochemical analysis of chromatin from infected cells would confirm that N becomes associated with chromatin.

It is clear from immunofluorescence studies, including one in which infection was synchronized, that MHV-infected cells express different amounts of N at any given time after inoculation. There are a number of possible reasons for this. The amount of N protein detected in nuclei by immunofluorescence may reflect the amount of N already available in the cytoplasm at any given time. Cells differ in their phase of the cell cycle, and therefore might be expected to synthesize and transport N protein at different rates unless they are synchronized prior to inoculation.

Whether the cell was originally uninfected and fused with an infected cell could also be a factor determining the amount of N protein it contains. Syncytia arise when MHV-infected cells fuse with the uninfected or infected cells which surround them. Fusion is followed by migration of nuclei towards the center of the syncytium (Holmes and Choppin, 1966; Holmes et al., 1968; Norrby et al., 1982). This may explain why some nuclei in MHV-induced syncytia

contain more N protein than others. The cytoplasmic N protein of the infected cell becomes diluted upon fusion with uninfected cells, and so, by the law of mass action, less N can equilibrate between the cytoplasm and the nuclei of originally uninfected cells. Also, less time has elapsed for diffusion to take place, the more recently a cell has fused with a giant cell.

Concentration of the N protein in infected cell nuclei may have significant implications for the survival of both the cell and the virus. By binding to the cell's DNA, this protein might interfere with host macromolecular synthesis and cause cytopathology. Also, if N protein enters nuclei in association with viral RNA in nucleocapsids (as do measles nucleocapsids), this could be a mechanism for persistence of the genome.

GENERAL DISCUSSION

The purpose of this work has been to study the molecular interactions of two of the three MHV structural proteins, the E2 glycoprotein and the nucleocapsid protein N. During virus replication and assembly, both proteins interact with other proteins, and the N protein also interacts with nucleic acids.

Studies of the E2 Glycoprotein. E2 undergoes glycosylation and cleavage, and the results of my studies show that cleavage probably occurs after transport of the glycoprotein from the medial region of the Golgi complex. Virions bearing uncleaved E2 were obtained by treating infected cells with the ionophore monensin. Lack of E2 cleavage following treatment with monensin was correlated with a significant reduction in the overall infectivity released from infected cells, probably due more to an effect on the infectivity of virions rather than their release from the cell. Trypsin treatment of virus grown in the presence of monensin, however, did not enhance virus infectivity. Therefore, additional experiments which assess alternative cleavage proteases and different mechanisms for E2 function in virus infectivity must be done. Virions with different ratios of E2-90K to E2-180K (purified from different cell lines) should be tested for whether they possess corresponding differences in infectivity, *i.e.*, particle/PFU ratios. Also, the importance of glycosylation on infectivity should be considered, because monensin prevented addition of the

terminal sugars fucose and N-acetyl-neuraminic acid to E2.

Recent Developments in Research on E2. Additional information on the structure of E2 became available after the majority of these experiments were completed. E2-90 from trypsin-treated virions was purified by Triton X-114 solubilization and phase fractionation (Ricard and Sturman, 1985). Two distinct 90K species of E2 were then separated by size exclusion HPLC followed by SDS-hydroxyapatite HPLC (Sturman et al., 1985). One, termed "90A", was acylated with palmitic acid, whereas "90B" was not. Limited digestion with thermolysin or staphylococcal V8 protease yielded two different patterns of peptides from 90A and 90B, indicating that these polypeptides are distinct.

The susceptibility of E2 to cleavage into two 90K polypeptides by proteases other than trypsin was studied as well (Sturman et al., 1985). E2 was cleaved into two 90K species by chymotrypsin, elastase, and thermolysin. In this respect, the glycoprotein is similar to the paramyxovirus HN glycoprotein, and different from the F glycoprotein (Sturman et al., 1985). These enzymes may now be tested for their effects on infectivity of virus grown in the presence of monensin. Proteases which reside in the Golgi complex should also be tested for their effects on virus infectivity, since cleavage probably occurs in the trans Golgi or in post-Golgi vesicles. While the E2 cleavage products on virions have always been observed to be of roughly 90K M_r , there are in fact small differences in the molecular weights of these

polypeptides in virions grown in different cell lines (Frana et al., 1985). For example, E2 on virus grown in Sac- and L2 cells has cleavage products of slightly higher molecular weight than virion E2 from 17 Cl 1 and DBT cells. This implies that different cellular proteases cleave E2 at different sites, or that there are host-specific differences in glycosylation.

The gene for E2 has been cloned (Luytjes et al., 1987; Schmidt et al., 1987), and the trypsin cleavage site has been identified by amino terminal sequencing of 90A and comparison with the predicted amino acid sequence (Luytjes et al., 1987). It should be possible to localize the functions of E2 to different regions of the molecule.

The role of E2 in the host's immune response to MHV-infected cells is now better understood. The natural cytotoxicity of mouse spleen cells ("virus killer" activity) against MHV-infected target cells has been correlated with binding of MHV to leukocytes of B cell origin (Holmes et al., 1986). This binding is mediated by E2, since antibody to E2 inhibits cytotoxic killing in vitro.

E2 also appears to determine the neurovirulence of MHV-JHM. Variants selected by neutralization with monoclonal antibodies to E2 demonstrate altered tissue tropisms and pathogenicity (Dalziel et al., 1986; Fleming et al., 1986).

A receptor for MHV-A59 on the membranes of intestinal epithelial cells and hepatic cells has recently been identified using a virus overlay protein blot assay and a

solid phase binding assay (Boyle et al., 1987). This receptor is found on cells of mice susceptible to MHV (Balb/c and C3H), but not resistant mice (SJL) (Boyle et al., 1987). It is now being characterized biochemically and for virus strain and species specificity in the laboratory of Dr. Kathryn V. Holmes. Understanding of virus-receptor interactions should yield important information on the molecular level regarding E2 as a virus attachment protein.

Studies of the N Protein. In two in vitro assays, N protein readily bound a variety of different nucleic acids in a nonspecific manner. Late in the infectious cycle of MHV, N protein accumulated in nuclei. A small percentage of the protein formed disulfide-linked trimers, which were also found as components of released virions. N protein was first detected in the cytoplasm, was often found adjacent to the nucleus early in infection, and accumulated within interphase nuclei at relatively late times during infection. This accumulation occurred by means other than mitosis, since it was not affected by colchicine, which arrests cells in metaphase, so that new interphase nuclei cannot be formed. If dissolution of the nuclear envelope were the only mechanism by which N accumulated in nuclei, reduced numbers of N-positive interphase nuclei would have been seen in colchicine-treated cells. In addition, cell fusion was not required for transport of N to nuclei. Evidence from fluorescence dual labeling studies showed that N protein associated with the cell chromatin in vivo. Thus, the

nonspecific binding activity of N protein observed in vitro was also observed in vivo. These properties are similar in some respects to those of the nucleocapsids of other enveloped viruses such as TMV, VSV, and influenza virus, and suggest that the ability to form multimers and to bind nucleic acids nonspecifically may be universal properties of nucleocapsid proteins of RNA viruses with helical nucleocapsids.

The 140K protein. The 140K protein (N trimer) of MHV-A59 may be of functional significance because it apparently forms in infected cells, and binds RNA as well as does native N protein. An analogous disulfide-bonded multimer of nucleocapsid protein, a 160K protein, has been observed in bovine coronavirus (Hogue et al., 1984). Core proteins of several DNA viruses have been identified which are disulfide-linked oligomers. Some DNA-binding proteins must oligomerize in order to be active (not necessarily by disulfide-bonding). Examples include the lac repressor, lambda C1 gene product, the T4 gene 41 protein, the E. coli DNA gyrase, and the SV-40 T antigen (discussed by Bradley et al., 1982). Indeed, in contrast to the MHV N protein, the SV-40 T antigen monomer lacks DNA-binding activity (Bradley et al., 1982). The VSV N protein is difficult to purify from virions, due to its tendency to aggregate (Blumberg et al., 1984), and the TMV coat protein readily forms "disks" and "lock-washer" multimeric structures depending on ionic strength and pH (Butler, 1984). A tendency to aggregate

with itself might be predicted of a protein which binds other monomers during assembly.

The 140K protein formed in four different cell lines (17 Cl 1, Sac-, DBT and L2), showing lack of host-dependence. It has not been detected in pulse-chase experiments due to its low concentration relative to monomeric N protein in infected cells. To determine the time at which the 140K protein appears, one would have to immunoprecipitate cell extract using N-specific monoclonal antibody. The 140K trimer probably forms by oxidation and exchange of sulfhydryl groups which normally form intrachain disulfide bonds, and this may be facilitated by the large accumulation of N protein within the cytoplasm late during infection. A sulfhydryl isomerase might be involved in such a process (Freedman, 1984). The 140K protein is assembled into, or forms within, MHV virions.

The 140K protein possibly plays a role in assembly, transcription, or replication. MHV nucleocapsids are difficult to isolate from infected cells. However, once a reproducible technique for their isolation is developed, it should be determined whether they contain the 140K protein. Nucleocapsids could be isolated in an alkylating environment at different salt concentrations and fixed (Heggeness et al., 1980), then analyzed for protein content. If progressive reduction caused more and more loosely coiled nucleocapsids, then this might suggest that the 140 K protein is important in turn-to-turn bonding within nucleocapsids.

Also, in vitro, nucleocapsid assembly might be sensitive to reduction.

Nucleotide Sequence Specific Binding. Our data suggest that N protein participates in nucleocapsid assembly by binding nonspecifically to the RNA genome. In vitro assembly studies would be worthwhile, as for TMV (Fraenkel-Conrat and Williams, 1955), VSV (Blumberg et al., 1984) and influenza virus (Kingsbury, 1987). In pioneering studies on virus assembly, Fraenkel-Conrat and Williams (1955) showed that infectious TMV can be reconstituted from viral RNA and protein in vitro. TMV has become the model system for studying protein-nucleic acid interactions and assembly processes. Virus assembly is initiated by interaction of the RNA with a short protein helix (containing coat protein monomers) of about two turns, the nucleating "disk". In the absence of RNA, disks do not polymerize due to the presence of a disordered loop structure in the disk caused by electrostatic repulsion of two neighboring carboxyl groups. Binding of RNA to an initiating helix induces an ordered structure and is followed by elongation of the NP complex by addition of more disks (reviewed by Kamba and Stubbs, 1986). The initial event of nucleation is nucleotide sequence-specific, occurring at an internal RNA hairpin loop of unique structure near the 3' end of the genome, containing two critical contiguous AAGs (Zimmern, 1977; Steckert and Schuster, 1982). After initiation, the free 3' and 5' tails both extrude from the same end of the central core of the

disk, shown by EM (Butler et al., 1977; Lebeurier et al., 1977). During elongation of the rod, protein disks are added in both the 3' and 5' direction and in a manner independent of nucleotide sequence. The RNA is progressively "pulled" up through the center of the helix (Butler et al., 1977; Lebeurier et al., 1977). In coronavirus assembly also, it appears likely that nonspecific binding of the N protein may account for most of the encapsidation of viral RNA.

In several plant virus systems, the RNA nucleation sequences (and hypothetical secondary structures) required for nucleocapsid assembly have been identified. In tobacco mosaic and alfalfa mosaic virus assembly, specific sequences have been localized near the 3' ends of the RNAs (Butler, 1974; Zuidema et al., 1984), and at the 5' end of papaya mosaic virus RNA (Lok and Abouhaidar, 1986).

The role of the VSV N protein in virus assembly was recently discussed in a review of rhabdovirus replication (Banerjee, 1987). VSV N protein has a high affinity for an 18 base pair sequence rich in adenosine in the 5' region of VSV leader RNA (Blumberg et al., 1981). Beginning at the leader, the N protein assembles with the genome RNA in a highly cooperative manner (Blumberg et al., 1983). The domain(s) of N which bind leader is not known. N protein freed from virion nucleocapsids rapidly aggregates into disk-like structures identical to rings isolated from VSV nucleocapsids and very reminiscent of disks made of purified

TMV coat protein (Blumberg et al., 1984).

Binding Domains of the TMV Coat Protein. The precise sites of interaction between the MHV N protein and the RNA remain to be identified. A molecular model of TMV structure has been proposed in exquisite detail using data from X-ray fiber diffraction analysis at 3.6 Å resolution (Stubbs et al., 1977; Kamba and Stubbs, 1986). This model describes the sites of interaction of one monomer of the TMV coat protein with the RNA and with other coat protein monomers. The central region of the coat protein molecule contains 4 alpha-helices, two "slewed" and two "radial" helices. One of the alpha helices (the left radial helix) probably interacts most with the RNA. In each protein subunit there are three arginines which interact with three phosphate groups of the RNA (not all by simple ion pairs) and one threonine, in the hairpin loop of a slewed helix, which forms a hydrogen bond with a phosphate group. These are non-RNA sequence-specific interactions. The true three-dimensional structure of the crystallized MHV N protein and MHV nucleocapsids could be determined in a similar manner to TMV, by X-ray crystallography or X-ray fiber diffraction analysis. The MHV-A59 N protein has been cloned and sequenced (Armstrong et al., 1983a,b). Expression of N protein in a eukaryotic vector should permit such studies.

The regions of contact between the MHV N protein and other N protein monomers during nucleocapsid assembly are not known (Fig. 4). In TMV assembly, there are predicted to

be basically two classes of protein-protein interaction in TMV assembly: top-to-bottom contacts and side-to-side contacts (Kamba and Stubbs, 1986). There is a closer side-to-side packing of coat protein monomers with each other in the TMV rod than in the disk, due to large side-chain conformational changes, but mainly the same residues interact in both structures (Kamba and Stubbs, 1986). One side-to-side binding region, at a low radius from the axis, involves charge-charge interactions in a "carboxyl cage", with glu106 of one subunit associating with glu95, asp109 and asn 101 of the neighboring subunit. In this model of the MHV nucleocapsid (Fig. 4), there may be similar types of interactions. Each monomer of the N protein is hypothesized to interact with the genome RNA, with two adjacent molecules of N protein, as well as with neighboring monomers above and below it in adjacent turns of the helix. In addition, N protein probably binds E1 during budding, and possibly nonstructural proteins such as polymerase during replication of the RNA.

By analogy with DNA-binding proteins, the RNA-binding regions of N protein might be areas of high concentration of basic and possibly hydrophobic amino acid residues (reviewed by von Hippel, 1979). The basic amino acids are likely to interact with the negatively charged phosphate backbone of RNA, and the hydrophobic amino acids with phosphates and/or bases. Sequence specific nucleotide binding is usually mediated by hydrogen bonds, for which

there is potential in almost all amino acids. In the nucleation region of the TMV RNA, a guanine residue is repeated at every third base. Since one coat protein molecule binds for every three nucleotides, it has been suggested that the protein binds to the repeating Gs (Zimmern and Wilson, 1976; Butler, 1984). Most of the RNA-protein interactions which occur within nucleocapsids of RNA viruses, holding together the nucleocapsid protein and the RNA, are probably not nucleotide sequence specific, but may involve ionic bonding between basic residues on the protein and acidic phosphate residues on the backbone of the RNA molecule. Therefore, it is reasonable to propose that one or more of the basic regions of the N protein which are predicted from its nucleic acid sequence should be its nonspecific RNA-binding regions, or fold together to form those regions.

Possible RNA-Binding Domains of the MHV N Protein.

From the nucleotide sequence of the MHV-A59 N protein, one can calculate that it contains 14.98% basic and 9.91% acidic residues, giving it a net charge of +25 (Armstrong *et al.*, 1983a,b; 1984). This amino acid composition is different from that of the Sendai virus (Morgan *et al.*, 1984) and parainfluenza virus-3 (Sanchez *et al.*, 1986) NP proteins, which have a significantly higher proportion (45%) of hydrophobic residues. The nucleocapsid genes from two strains of avian infectious bronchitis virus have been sequenced and compared with the MHV-JHM N sequence, using a

matrix comparison computer program (Bournsnell et al., 1985). Basic and serine-rich regions of the predicted amino acid sequences were conserved between these two coronaviruses from distinct subgroups, suggesting that they are important in coronavirus replication. In particular, there exists a long region (glu85-leu185) which is highly homologous with part of the IBV N molecule and is probably of fundamental importance to nucleocapsid structure.

The secondary structure of a protein may be critical in the binding of proteins to nucleic acids, as for example, in the binding of the phage 434 protein (Wharton and Ptashne, 1986) and lambda repressor protein (Sauer and Pabo, 1983) proteins to their respective DNA operons (reviewed by Pabo and Sauer, 1984). Binding of these proteins to DNA probably involves an alpha-helix/beta-turn/alpha-helix structure. A sequence conserved among the lambda CRO and repressor proteins and the E. coli CAP protein appears to be important in the formation of these structural signals (Sauer et al., 1982; Pabo and Sauer, 1984). As already mentioned, the TMV coat protein also probably interacts with RNA via alpha-helical structures (Kamba and Stubbs, 1986).

To determine hypothetical secondary structures of the MHV N protein, the nucleotide sequences of the MHV-A59 and -JHM N proteins were obtained using GenBank (40.0), accessed by the Cyborg program (International Biotechnologies Inc., IBI) and translated using an IBI DNA program. The secondary structures of different regions of the N

protein were then analyzed by the Protlyze Predictor program developed by Dr. Douglas Ward. These programs are based on the models for protein structure developed by Chou and Fasman (1978) and Kyte and Doolittle (1982). The MHV-A59 N protein was estimated to be about 32.8% alpha-helix and 21.1% beta-sheet; the composition of JHM was slightly different, with 35.2% alpha-helix and 19.6% beta-sheet. A plot of predicted secondary structure and hydropathy for the A59 N protein is compared with that of MHV-JHM N protein in Fig. 39.

The secondary structure and hydropathy patterns of these two MHV N proteins are nearly identical, which was expected, since they differ in only 28 of 454 residues (Armstrong et al., 1983a,b, 1984; Skinner and Siddell, 1983). However, there are four regions which appear to differ structurally between these strains: aa95-101 (A59 has an alpha-helix, JHM does not); aa142-146 (A59 has beta-turns, JHM alpha-helical and beta-turns); aa157-164 (A59 has beta-turns and some alpha-helical structure, while JHM has alpha-helix only); and aa319-327 (A59 is beta-sheet, JHM alpha-helix). None of these differences lies in regions which are shown in Table 4, and therefore they may be of minor significance to the function of N protein (or of unknown function). At this point, the relationship of structural differences to pathogenicity are not known.

I have selected several regions of N protein which may be of great interest and listed them in Table 4. The

Figure 39. The N proteins of MHV strains A59 and JHM compared for hypothetical secondary structure and hydrophathy. The probability of different amino acid regions of the N protein being alpha-helices, beta-sheets, or beta-turns, and their degrees of hydrophobicity were predicted by Dr. Douglas Ward, using his Protylze Predictor computer program, based on the theories of Chou and Fasman (1978) and Kyte and Doolittle (1982), respectively. The profile of the MHV-A59 N protein lies above that of the MHV-JHM N protein for each comparative analysis. The amino acid sequences were translated by computer from the MHV N protein nucleotide sequences stored in GenBank (Armstrong *et al.*, 1983b). For secondary structure predictions, average probabilities were taken at consecutive groups of 4 amino acids. The probability scale is based on empirical observations of the frequency with which a given amino acid is located within each of the three structures. The baseline value is 1, indicating no preference for secondary structure, with 1.5 the highest probability, and 0.5 the lowest value. Horizontal bars indicate regions with high probability of a given secondary structure, bounded by amino acids which break that structure. For hydrophathy predictions, consecutive groups of 5 amino acids were averaged. The scale is normalized to show relative degrees of hydrophobicity, with the baseline set at 0 and the vertical axis extending from -4 to +4. Hydrophobic regions lie above the line, hydrophilic regions below it.

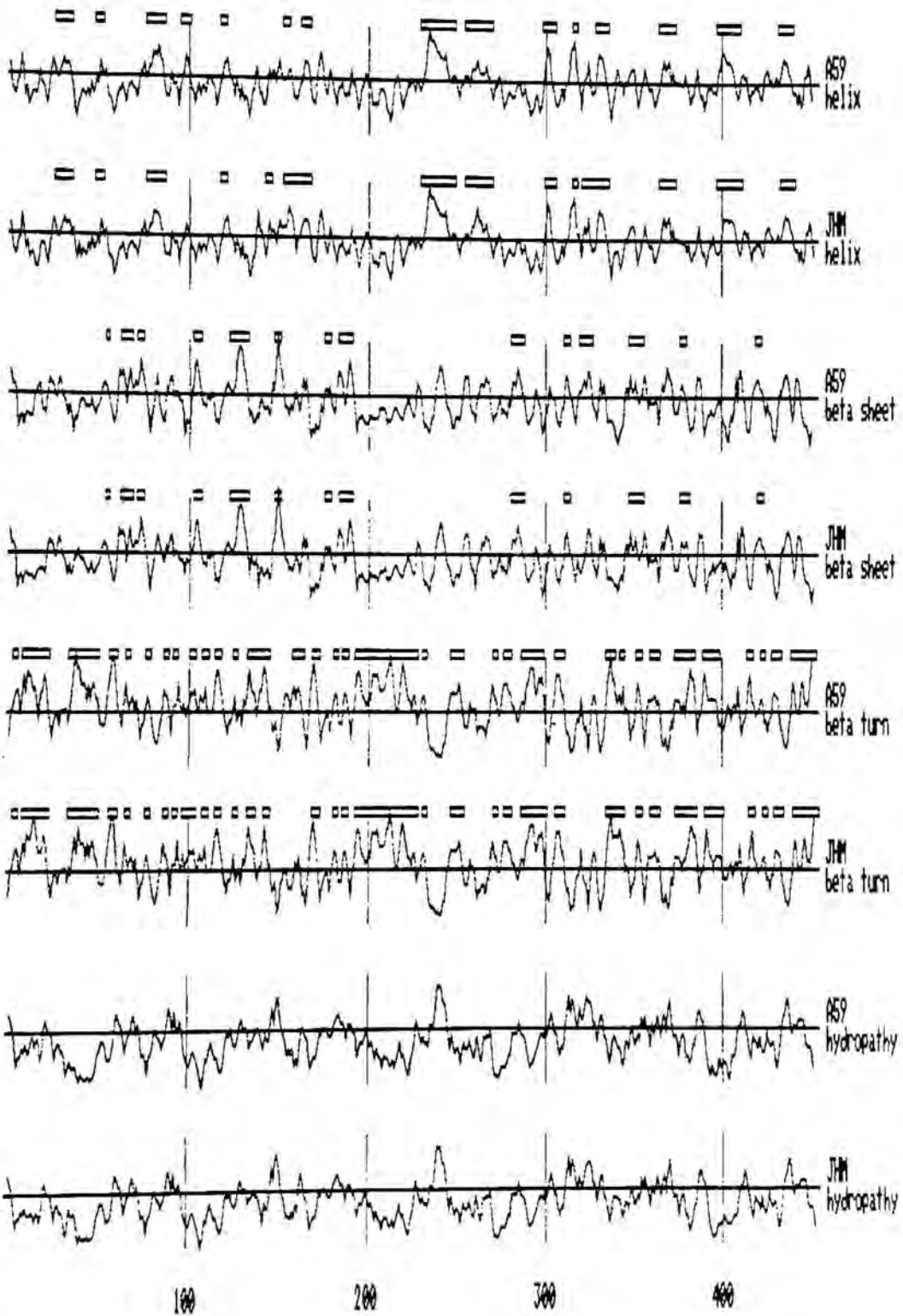


Table 4

Regions of the MHV-A59 N Protein with Possible Functional Significance

Amino acid region	Charge at neutral pH	Predicted secondary structure	Hydropathy	Possible functions
ser14-ser16	?	beta-turn	-philic	phosphorylation (3 serines)
arg43-lys50	+4	beta-turn	-philic	nucleic acid binding
gly86-ser154*	+5	mixed	-philic	nucleic acid binding; phosphorylation (5 serines)
ser194-lys230*	+9	beta-turn	-philic	nucleic acid binding; phosphorylation (11 serines)
ile237-lys244	+1	alpha-helix	-phobic	nucleic acid binding; budding
lys244-lys279*	+12	alpha-helix, beta-turn, alpha-helix, beta-turn	-philic	major nucleic acid binding
cys281-cys286	0	beta-sheet	-philic	oligomerization by disulfide-bonding (2 cysteines)
lys391-arg404	+6	beta-turn,	-philic	nucleic acid binding
ser411-ser433	?+2	beta-turn, beta sheet, beta turn, alpha helix	-philic, -phobic	phosphorylation (5 serines)
asp440-asp451	-5	alpha-helix, beta-turn	-phobic, -philic	binding E1 or N

* Nucleotide sequences highly conserved among coronaviruses.

region aa86-aal54 (MHV) is greater than 90% homologous with IBV, TGEV and BCoV (Lapps et al., 1987; Boursnell et al., 1985; Kapke et al., 1986). The regions arg196-lys230 and lys244-lys279 are not only extremely basic but also contain sequences conserved between MHV-A59 and IBV (Boursnell et al., 1985). Therefore, these regions are possibly important in binding the protein to the genome RNA in the nucleocapsid. In addition, the serine-rich regions (ser14-ser16, ser194-lys230, ser411-ser433) are conserved between MHV and IBV. The major serine cluster of MHV-A59 lies in the same region of the molecule as that of BCoV N protein. Regions of hydrophobicity, e.g., ile237-lys244, may be important for specific binding of N to RNA, or for association with hydrophobic regions of E1 or the lipid envelope.

The amino acid region lys244-lys279 is the most basic of the five basic regions, with a net charge of +12 at neutral pH, and also carries the potential for an alpha-helix/beta-turn/alpha-helix structure, seen in the TMV coat protein (Kamba and Stubbs, 1986) and the lambda repressor and cro proteins (Sauer and Pabo, 1983; Pabo and Sauer, 1984). This region is ~80% homologous between MHV and BCoV (Lapps et al., 1987), strongly indicating that this structure is conserved within the coronavirus group, is probably essential to virus replication, and may be important for RNA binding.

The carboxy-terminus asp440-asp451 carries a large negative charge, as is the case in MHV-JHM (Skinner and

Siddell, 1983), IBV (Bournsnell et al., 1985), BCV (Lapps et al., 1987), Sendai virus (Morgan et al., 1984) and parainfluenza-3 virus (PIV-3) (Sanchez et al., 1986). Morgan et al. (1984) and Sanchez et al. (1986) have suggested that the negatively charged carboxy-terminus of the NP protein of Sendai virus interacts electrostatically with the matrix protein M, which is positively charged. In Sendai virus nucleocapsids, the amino-terminal domain of the NP in nucleocapsids is trypsin-resistant and bears a higher proportion of basic and hydrophobic residues than the trypsin-sensitive carboxy-terminal domain (Morgan et al., 1984). It is possible that the MHV N protein interacts with the E1 protein by a similar mechanism. This can now be tested by blocking the association of nucleocapsids with E1 in vitro (Sturman et al., 1980) using an antibody already raised against a synthetic peptide of a portion of the carboxy-terminus of the MHV-A59 N protein (Holmes et al., 1987).

Experimental Approaches. Several experiments could be performed to determine whether a particular secondary structural region is important in the binding of the N protein with RNA or other N molecules or E1. First, to test whether particular regions are important in RNA-binding, one could use cleavage fragments of N protein in the ROPBA or filter binding assays. A cyanogen bromide and trypsin cleavage map was generated from the MHV-A59 amino acid sequence using the IBI peptide analysis program (Fig. 41).

Figure 40. Amino acid sequence of the MHV-A59 N protein, showing the linear relationships of some regions of possible functional significance (see Table 4). Cyanogen bromide (C) and trypsin (T) cleavage sites were predicted from the nucleotide sequence using the Peptide Analysis program of International Biotechnologies, Inc.

10 20 30 40 50 60
 * * * * * *
 MSFVPGQENAGGRSSSVNRAGNGILKKTWADQTERGPNNQNRRGRRNQPKQTATTQPNSG
 ^ ^ ^^ ^ ^^ ^
 C T T TT T T TT T

70 80 90 100 110 120
 * * * * * *
 SVVPHYSWFSGITQFQKGFQFAEGQGVPIANGIPASEQKGYWYRHNRRSFKTPDGQQK
 ^ ^ ^ ^ ^ ^
 T T T T TT T T

130 140 150 160 170 180
 * * * * * *
QLLPRWYFYLLGTGPHAGASYGDSIEGVFWVANSQADTNTRSDIVERDPSSSHEAIPTRFA
 ^ ^ ^ ^ ^ ^
 T T T T

190 200 210 220 230 240
 * * * * * *
 PGTVLPQGFYVEGSGRSAPASRSRSRSGPNNRARSSSNQRQPASTVKPDMAEEIAAL
 ^ ^ ^ ^ ^ ^
 T T T T T T T T T C

250 260 270 280 290 300
 * * * * * *
VLAKLGKDAGQPKQVTKQSAKVRQKILNKPRQKRTPNKQCPVQQCFGKRGPNQNFGGSE
 ^ ^ ^ ^ ^ ^
 T T T T TT T T T T TT T TT

310 320 330 340 350 360
 * * * * * *
 MLKLGTSDPQFPILAELAPTVGAFFFGSKLELVKKNSSGGADEPTKDVYELQYSGAVRFDS
 ^ ^ ^ ^ ^ ^
 C T T TT T T

370 380 390 400 410 420
 * * * * * *
 TLPGFETIMKVLNENLNAYQKDGADVVSPKPQRKGRQAQEKDEVDNVSVAKPKSSVQ
 ^^ ^ ^ ^^ ^^ ^^
 CT T T TT TT TT T T

430 440 450
 * * *
RNVSRELTPEDRSLLAQILDDGVVPDGLEDDSNV
 ^ ^ ^
 T T T

Of the three CNBr fragments, I would predict that the amino-terminal and central fragments would bind RNA, since these fragments contain highly basic regions. Secondly, site-specific mutagenesis would be useful for generating mutants in the N protein in the regions outlined in Table 4. The binding properties of these mutants could then be studied in filter binding assays. RNA-cellulose columns could be used for RNA-binding studies (Stark et al., 1981). One could also construct a recombinant which lacks a putative RNA-binding region or has an unrelated sequence inserted in its place in a "helix swap" experiment (Wharton and Ptashne, 1986) and test its RNA-binding activity. It would also be advisable to make a synthetic peptide of this region and show that it can bind the RNA with high affinity and compete for binding more efficiently than unrelated sequences. Altered N proteins could also be crystallized for determination of their tertiary structure by x-ray procedures.

It is interesting that a possible phosphorylation region may lie in an RNA-binding region. In the SV-40 T antigen, there is a DNA-binding domain which also contains a cluster of serine and threonine phosphorylation sites (Kalderon et al., 1984a). With phosphatase-treated N protein or N protein mutagenized at serine residues, the importance of phosphorylation to N functions could be determined.

Soon after MHV enters cells, the N protein is believed to disassemble from the genome so that the viral

polymerase can be translated. Filamentous plant viruses such as TMV, tobacco vein mottling virus (a Potyvirus) and potato virus X (a Potexvirus), and tobacco rattle virus (a Tobravirus) were observed electron microscopically to be undergoing uncoating during in vitro translation, where they formed "striposome" structures (Wilson and Shaw, 1987). Uncoating of the genome probably began at the 5' end, allowing translation of early genes. Possibly MHV undergoes a similar process after entry of virions, to allow translation of gene 1, thought to code for the viral RNA polymerase (Leibowitz and Weiss, 1981; Siddell et al., 1980, 1981c; Leibowitz et al., 1982).

A number of RNA-positive mutants have been induced by nitrous acid mutagenesis (Sturman et al., 1987), and are defective in the viral structural proteins. Of these, at least three have mutations affecting N protein structure and function. A small plaque mutant, Albany 4 (Alb 4), is of great interest and potential because it has a constitutive defect in the N protein: the majority of this protein exists as a 47K molecule at both 32° and 39°C in infected cells and virions, suggesting that there is a defect in the N gene. Amino acid sequencing of the N gene of Alb 4 would identify precisely the missing residues. Alb 4 virions are 100 times more thermolabile than wild type virus at 45°C, pH 6. A possible explanation for their thermolability is that at the elevated temperature, nucleocapsids are less stable due to impaired ability of N to bind RNA. Some RNA-binding

activity of its truncated N protein was evident, however, in the ROPBA (Fig. 21). It would be interesting to compare the affinity of binding to RNA of Alb 4 N with wild type N, using ^{32}P -labeled genomic RNA in a filter binding assay.

Studying the Alb 4 and Alb 8 mutants should also uncover the mechanism by which N localizes in nuclei, because each is defective in this function, showing different immunofluorescence patterns from wild type at both 32° and 39°C , and thermolabile transport of N protein to the nucleus (Duchala *et al.*, 1986). N protein appears in large specks (differing from the wild type pattern) in nuclei of Alb 4-infected cells late in infection. Alb 8 appears to lack nuclear N protein altogether. Tryptic peptide digests of these mutant proteins could be compared and any aberrant peptides could be sequenced, to identify the amino acid changes associated with any change in function. Also, cloning the N gene for each mutant, followed by microinjection of the protein or introduction of the cDNA into cells by other means, could show true differences in the abilities of these molecules to enter nuclei in the absence of any other viral proteins or any pathologic effects on the cell. The different immunofluorescence nuclear patterns observed should be followed up by immunoelectron microscopic analysis of cells infected with the viral mutants, where the precise localization of N protein could be identified using the ferritin-bridge technique (Willingham *et al.*, 1971) or immunogold labeling (De Mey *et al.*, 1982). Also, any

critical portion(s) of N needed for transport into nuclei might be identified by genetically fusing different parts of the N protein (e.g., those with possible nuclear signal sequences or RNA and DNA-binding activity) with β -galactosidase and determining whether enzyme activity localized within the nucleus (Hall et al., 1984).

N protein may be involved in functions other than virus assembly. Compton et al. (1987) have found that a polyclonal antibody specific for the N protein (but not anti-E1 or E2) significantly inhibited in vitro replication of the MHV genome RNA. In their in vitro replication system, viral genome RNA was encapsidated to form nucleocapsids, and it was suggested that association of RNA with N protein protected newly synthesized genomes from degradation by RNase. Elongation of nascent polypeptides was required for replication in vitro. Therefore, it is possible that synthesis of the N protein is critical for MHV RNA replication, as is synthesis of the nucleocapsid proteins in VSV and Sendai virus replication (Davis and Wertz, 1982; Peluso and Moyer, 1983; Carlsen et al., 1985). The VSV N protein interacts with the L and NS proteins during VSV transcription, but the domains involved have not been identified (Thornton et al., 1984). Possibly the MHV N protein also interacts with the polymerase during replication.

Similarly, one monoclonal antibody to influenza A nucleoprotein was found to be particularly effective at inhibiting transcription of RNA in vitro (van Wyke et al.,

1981). Kinetic studies showed that this antibody was inhibiting elongation of transcripts, not initiation. Antibodies to VSV nucleocapsids behaved similarly in VSV transcription (Carroll and Wagner, 1978). VSV transcription and translation were inhibited by microinjecting N-specific monoclonal antibodies into VSV mutant-infected cells in the presence or absence of cycloheximide (Arnheiter *et al.*, 1985). One antibody may have been specific for an epitope of the N protein in nucleocapsids, and this antibody inhibited *in vitro* transcription and translation, whereas another antibody, specific for soluble N protein, inhibited only translation. For MHV, it would be illuminating to study the effects of microinjecting well-characterized anti-N monoclonal antibodies and antibodies raised against synthetic peptides of interesting regions of the MHV N protein. Such experiments could be coupled with electron microscopy and nucleocapsid isolation to identify assembly defects. The same antibodies could be tested in *in vitro* transcription and translation assays to assess the role of N protein in these processes.

Summary. In conclusion, my colleagues and I have obtained some basic information on the interactions of the E2 glycoprotein and N protein with other molecules within the infected cell. Our electron microscopic studies on intracellular virus particles confirmed that these particles change shape during maturation, becoming flattened and disk-shaped. By characterizing both ICV and virus grown in the

presence of monensin, we found that the E2 glycoprotein is probably cleaved after virions and/or E2 are transported from the medial Golgi region. The MHV N protein exists in multiple forms within infected cells (N, N', N" and the 140K protein) and virions (only N and the 140K protein), and has several different functions (Table 5). We have shown that the N protein binds a variety of nucleic acids in vitro and that it also binds to nuclear DNA. It is hoped that by pursuing the lines of investigation suggested here that more will be learned of the structure and function of the E2 and N proteins.

Table 5Forms and Functions of the MHV N ProteinNative N Protein

- in infected cells and virions
- virus strain specific differences in molecular weight
- necessary for replication
- binds genome RNA for nucleocapsid assembly
- probably binds E1 during budding
- nonspecifically binds viral and cellular RNAs and DNAs
- localizes in the nucleus and binds cell chromatin
- phosphorylated; may be a protein kinase
- can form trimers

140 K Trimer of N Protein

- in infected cells and virions
- nonspecifically binds viral RNAs
- possibly plays a role in nucleocapsid assembly, e.g., nucleation or stabilization

N' and N''

- only in infected cells; not in virions
- nonspecifically bind viral and cellular RNAs and DNAs
- localize within both cytoplasm and nuclei

Mutant N Proteins

- Albany 4 mutant
 - truncated N in both infected cells and virions
 - speckled nuclear N pattern
- Albany 8 mutant
 - N of native molecular weight
 - N does not go to nucleus

BIBLIOGRAPHY

- Aarden, L.A., de Groot, E.R. and Feltkamp, T.E.W. 1975. Immunology of DNA. III. Crithidia luciliae, a simple substrate for the determination of anti-dsDNA with the immunofluorescence technique. Ann.N.Y. Acad. Sci. 254: 505-515.
- Abrams, H.D., Rohrschneider, L.R. and Eisenman, R.N. 1982. Nuclear location of the putative transforming protein of avian myelocytomatosis virus. Cell 29: 427-439.
- Agutter, P.S. 1984. Nucleocytoplasmic transport. In: Subcellular Biochemistry (Roodyn, D.B., ed.). Plenum Press, New York. Vol. 10, pp. 281-357.
- Agutter, P.S. and Suckling, K.E. 1982. Effect of colchicine on mammalian liver nuclear envelope and on nucleocytoplasmic RNA transport. Biochim. Biophys. Acta 698: 223-229.
- Alexander, D.J. and Collins, M.S. 1975. Effect of pH on the growth and cytopathogenicity of avian infectious bronchitis virus in chick kidney cells. Arch. Virol. 49: 339-348.
- Alexander, D.J. and Gough, R.E. 1977. Isolation of avian infectious bronchitis virus from experimentally infected chickens. Res. Vet. Sci. 23: 344-347.
- Almeida, J.D. and Tyrrell, D.A.J. 1967. The morphology of three previously uncharacterized human respiratory viruses that grow in organ culture. J. Gen. Virol. 1: 175-178.
- Anderson, R., Cheley, S. and Haworth-Hatherell, E. 1979. Comparison of polypeptides of two strains of murine

- hepatitis virus. Virology 97: 492-494.
- Apostolov, K., Flewett, T.H. and Kendal, A.P. 1970. Morphology of influenza ABC and infectious bronchitis virus (IBV) virions and their replication. In: The Biology of Large RNA Viruses (Barry, R.D. and Mahy, B.W.J., eds.). Academic Press, New York. pp. 3-26.
- Armstrong, J., Smeekens, S. and Rottier, P. 1983a. Sequence of the nucleocapsid gene from murine coronavirus MHV-A59. Nuc. Acids Res. 11: 883-891.
- Armstrong, J., Smeekens, S., Spaan, W., Rottier, P. and van der Zeijst, B. 1983b. Cloning and sequencing the nucleocapsid and E1 genes of coronavirus. In: Biochemistry and Biology of Coronaviruses (ter Meulen, V., Siddell, S. and Wege, H., eds.). Plenum Press, New York. pp. 155-162.
- Arnheiter, H., Baechi, T. and Haller, O. 1982. Adult mouse hepatocytes in primary monolayer culture express genetic resistance to mouse hepatitis virus type 3. J. Immunol. 129: 1275-1281.
- Arnheiter, H., Davis, N.L., Wertz, G., Schubert, M. and Lazzarini, R.A. 1985. Role of the nucleocapsid protein in regulating vesicular stomatitis virus RNA synthesis. Cell 41: 259-267.
- Auperin, D.D., Galinski, M and Bishop, D.H.L. 1984. The sequences of the N protein gene and intergenic region of the S RNA of Pichinde arenavirus. Virology 134: 208-219.
- Bachi, T. 1980. Intramembrane structural differentiation in Sendai virus maturation. Virology 106: 41-49.

- Bailey, O.T., Pappenheimer, A.M., Cheever, F.S. and Daniels, J.B. 1949. A murine virus (JHM) causing disseminated encephalomyelitis with extensive destruction of myelin. II. Pathology. J. Exp. Med. 90: 195-212.
- Banerjee, A.K. 1987. Transcription and replication of rhabdoviruses. Microbiol. Rev. 51: 66-87.
- Baric, R.S., Stohlman, S.A. and Lai, M.M.C. 1983. Characterization of replicative intermediate RNA of mouse hepatitis virus: Presence of leader RNA sequences on nascent chains. J. Virol. 48: 633-640.
- Basu, S.K., Goldstein, J.L., Anderson, R.G.W. and Brown, M.S. 1981. Monensin interrupts the recycling of low density lipoprotein receptors in human fibroblasts. Cell 24: 493-502.
- Beaudette, F.R. and Hudson, C.B. 1937. Cultivation of the virus of infectious bronchitis. J. Amer. Vet. Med. Assoc. 90: 51-60.
- Becker, W.B., McIntosh, K., Dees, J.H. and Chanock, R.M. 1967. Morphogenesis of avian infectious bronchitis virus and a related human virus (strain 229E). J. Virol. 1: 1019-1027.
- Ben-Porat, T., Shimono, H. and Kaplan, A.S. 1969. Synthesis of proteins in cells infected with herpesvirus. II. Flow of structural viral proteins from cytoplasm to nucleus. Virology 37: 56-61.
- Ben Ze'ev, A., Abulafia, R. and Bratosin, S. 1983. Herpes simplex virus assembly and protein transport are as-

- sociated with the cytoskeletal framework and the nuclear matrix in infected BSC-1 cells. Virology 129: 501-507.
- Bibor-Hardy, V., Pouchelet, M., St. Pierre, E., Herzberg, M. and Simard, R. 1982a. The nuclear matrix is involved in herpes simplex virogenesis. Virology 121: 296-306.
- Bibor-Hardy, V., Suh, M., Pouchelet, M. and Simard, R. 1982b. Modifications of the nuclear envelope of BHK cells after infection with herpes simplex virus type 1. J. Gen. Virol. 63: 81-94.
- Bingham, R.W. and Almeida, J.D. 1977. Studies on the structure of a coronavirus-Avian infectious bronchitis virus. J. Gen. Virol. 36: 495-502.
- Blair, E.D. and Honess, R.W. 1983. DNA-binding proteins specified by herpesvirus saimiri. J. Gen. Virol. 64: 2697-2715.
- Blobel, G. 1971. Isolation of a 5S RNA-protein complex from mammalian ribosomes. Proc. Natl. Acad. Sci. USA 68: 1881-1885.
- Blobel, G. 1973. A protein of molecular weight 78,000 bound to the polyadenylate region of eukaryotic messenger RNAs. Proc. Natl. Acad. Sci. USA 70: 924-928.
- Blobel, G. and Potter, V.R. 1966. Nuclei from rat liver: Isolation method that combines purity with high yield. Science 154: 1662-1665.
- Blumberg, B.M., Leppert, M. and Kolakofsky, D. 1981. Interaction of VSV leader RNA and nucleocapsid protein may control VSV genome replication. Cell 23: 837-845.

- Blumberg, B.M., Giorgi, C. and Kolakofsky, D. 1983. N protein of vesicular stomatitis virus selectively encapsidates leader RNA in vitro. Cell 32: 559-567.
- Blumberg, B.M., Giorgi, C., Rose, K. and Kolakofsky, D. 1984. Preparation and analysis of the nucleocapsid proteins of vesicular stomatitis virus and Sendai virus, and analysis of the Sendai virus leader-NP gene region. J. Gen. Virol. 65: 769-779.
- Bond, C.W., Leibowitz, J.L. and Robb, J.A. 1979. Pathogenic murine coronaviruses. II. Characterization of virus-specific proteins of murine coronavirus JHMV and A59V. Virology 94: 371-384.
- Bond, C.W., Anderson, K., Goss, S. and Sardinia, L. 1981. Relatedness of virion and intracellular proteins of the murine coronaviruses JHM and A59. In: Biochemistry and Biology of Coronaviruses (ter Meulen, V., Siddell, S., and Wege, H., eds.). Plenum Press, New York. pp. 103-110.
- Bond, C.W., Anderson, K. and Leibowitz, J.L. 1984. Protein synthesis in cells infected by murine hepatitis viruses JHM and A59: Tryptic peptide analysis. Arch. Virol. 80: 333-347.
- Bonner, W.M. 1975. Protein migration into nuclei. I. Frog oocyte nuclei in vivo accumulate microinjected histones, allow entry to small proteins, and exclude large proteins. J. Cell Biol. 64: 421-430.
- Bontemps, C., Houssier, C. and Fredericq, E. 1975. Physico-chemical study of the complexes of 33258 Hoechst with DNA

- and nucleohistone. Nucl. Acids Res. 2: 971.
- Bournsnell, M.E., Binns, M.M., Foulds, I.J. and Brown, T.D. 1985. Sequences of the nucleocapsid genes from two strains of avian infectious bronchitis virus. J. Gen. Virol. 66: 573-580.
- Bowen, B., Steinberg, J., Laemmli, U.K., and Weintraub, H. 1980. The detection of DNA-binding proteins by protein blotting. Nuc. Acids Res. 8: 1-21.
- Boyle, J.F. and Holmes, K.V. 1986. RNA-binding proteins of bovine rotavirus. J. Virol. 58: 561-568.
- Boyle, J.F., Weismiller, D.G. and Holmes, K.V. 1987. Genetic resistance to mouse hepatitis virus correlates with absence of virus-binding activity on target tissue. J. Virol. 61: 185-189.
- Brachet, J. 1985. Molecular Cytology. Vol. 1. The Cell Cycle. Academic Press, Inc. pp. 73, 341, 345, 352-353.
- Bradburne, A.F. 1970. Antigenic relationships amongst coronaviruses. Archiv. ges. Virusforsch 31: 352-364.
- Bradford, M.M. 1976. A rapid and sensitive method for the quantitation of microgram quantities of protein utilizing the principle of protein-dye binding. Anal. Biochem. 72: 248-254.
- Bradley, M.K., Griffin, J.D. and Livingston, D.M. 1982. Relationship of oligomerization to enzymatic and DNA-binding properties of the SV40 large T antigen. Cell 28: 125-134.
- Braun, D.K., Batterson, W. and Roizman, B. 1984. Iden-

- tification and genetic mapping of a herpes simplex capsid protein that binds DNA. J. Virol. 50: 645-648.
- Brayton, P.R., Ganges, R.G. and Stohlman, S.A. 1981. Host cell nuclear function and murine hepatitis virus replication. J. Gen. Virol. 56: 457-460.
- Brayton, P.R., Lai, M.M.C., Patton, C.D. and Stohlman, S.A. 1982. Characterization of two RNA polymerase activities induced by mouse hepatitis virus. J. Virol. 42: 847-853.
- Breitenfeld, P.M. and Schafer, W. 1957. The formation of fowl plague virus antigens in infected cells, as studied with fluorescent antibodies. Virology 4: 328-345.
- Briedis, D.J., Conti, G., Munn, E.A., and Mahy, B.W.J. 1981. Migration of influenza virus-specific polypeptides from cytoplasm to nucleus of infected cells. Virology 111: 154-164.
- Brinton, M.A. and Grun, J.B. 1987. Replication of flaviviruses. In: Positive Strand RNA Viruses. (Brinton, M.A. and Rueckert, R.R., eds.). Alan R. Liss, Inc. New York. pp. 261-272.
- Bruckova, M., McIntosh, K., Kapikian, A.Z. and Chanock, R.M. 1970. The adaptation of two human coronavirus strains (OC38 and OC43) to growth in cell monolayers (35068). Proc. Soc. Exp. Biol. Med. 135: 431-435.
- Budzilowicz, C.J., Wilczynski, S.P. and Weiss, S.R. 1985. Three intergenic regions of coronavirus mouse hepatitis virus strain A59 genome RNA contain a common nucleotide sequence that is homologous to the 3' end of the viral

- mRNA leader sequence. J. Virol. 53: 834-840.
- Butler, P.J.G. 1974. Structures and roles of the polymorphic forms of tobacco mosaic virus protein. 8. Initial stages of assembly of nucleoprotein rods from virus RNA and the protein disks. J. Mol. Biol. 82: 343-353.
- Butler, P.J.G. 1984. The current picture of the structure and assembly of tobacco mosaic virus. J. Gen Virol. 65: 253-279.
- Butler, P.J.G. and Durham, A.C.H. 1977. Tobacco mosaic virus aggregation and the virus assembly. Adv. Prot. Chem. 31: 187-251.
- Butler, P.J.G., Finch, J.T. and Zimmern, D. 1977. Configuration of tobacco mosaic virus RNA during virus assembly. Nature 265: 217.
- Caliguiri, L.A. and Holmes, K.V. 1979. Host-dependent restriction of influenza virus maturation. Virology 92: 15-30.
- Caliguiri, L.A. and Tamm, I. 1970. Characterization of poliovirus-specific structures associated with cytoplasmic membranes. Virology 42: 112-122.
- Campbell, D.H., Garvey, J.S., Cremer, N.E. and Susssdorf, D.H. 1970. Methods in Immunology. 2nd edition. W.A. Benjamin, Inc., Reading, MA. p. 190.
- Carlsen, S.R., Peluso, R.W. and Moyer, S.A. 1985. In vitro replication of Sendai virus wild-type and defective interfering particle genome RNAs. J. Virol. 54: 493-500.
- Carroll, A.R. and Wagner, R.A. 1978. Inhibition of trans-

- cription by immunoglobulins directed against the ribonucleoprotein of homotypic and heterotypic vesicular stomatitis viruses. J. Virol. 25: 675-684.
- Carswell, S. and Alwine, J.C. 1986. Simian virus 40 agnoprotein facilitates perinuclear-nuclear localization of VP1, the major capsid protein. J. Virol. 60: 1055-1061.
- Caul, E.O. and Egglestone, S.I. 1977. Further studies on human enteric coronaviruses. Arch. Virol. 54: 107-117.
- Caul, E.O., Ashley, C.R., Ferguson, M. and Egglestone, S.I. 1979. Preliminary studies on the isolation of coronavirus-229E nucleocapsids. FEMS Microbiol. Lett. 5: 101-105.
- Cavanagh, D. 1983a. Coronavirus IBV glycopolypeptides. Size of their polypeptide moieties and nature of their oligosaccharides. J. Gen. Virol. 64: 1187-1191.
- Cavanagh, D. 1983b. Coronavirus IBV. Further evidence that the surface projections are associated with two glycopolypeptides. J. Gen. Virol. 64: 1787-1791.
- Chaloner-Larsson, G. and Johnson-Lussenburg, C.M. 1981. Characteristics of a long term in vitro persistent infection with human coronavirus 229E. In: Biochemistry and Biology of Coronaviruses. (ter Meulen, V., Siddell, S. and Wege, H., eds.). Plenum Press, New York. pp. 309-322.
- Chasey, D. and Alexander, D.J. 1976. Morphogenesis of avian infectious bronchitis virus in primary chick kidney cells. Arch. Virol. 52: 101-111.
- Chatterjee, S., Bradac, J.A. and Hunter, E. 1982. Effect of monensin on Mason-Pfizer monkey virus glycoprotein syn-

- thesis. J. Virol. 44: 1003-1012.
- Cheever, F.S., Daniels, J.B., Pappenheimer, A.M. and Bailey, O.T. 1949. A murine virus (JHM) causing disseminated encephalomyelitis with extensive destruction of myelin. I. Isolation and biologic properties of the virus. J. Exp. Med. 90: 181-194.
- Cheley, S. and Anderson, R. 1981. Cellular synthesis and modification of murine hepatitis virus polypeptides. J. Gen. Virol. 54: 301-311.
- Cheley, S., Morris, V.L., Cupples, M. and Anderson, R. 1981. RNA and polypeptide homology among murine coronaviruses. Virology 115: 310-321.
- Choe, J., Kolodrubetz, D. and Grunstein, M. 1982. The two yeast histone H2A genes encode similar protein subtypes. Proc. Natl. Acad. Sci. USA 79: 1484-1487.
- Chou, P. and Fasman, G.D. 1978. Prediction of the secondary structure of proteins from their amino acid sequence. Adv. Enzymol. 47: 45-148.
- Clayton, C.E., Murphy, D., Lovett, M. and Rigby, P.W.J. 1982. A fragment of the SV40 large-T antigen transforms. Nature (Lond.) 299: 59-61.
- Clinton, G.M., Burge, B.W. and Huang, A.S. 1978. Effects of phosphorylation and pH on the association of NS protein with vesicular stomatitis virus cores. J. Virol. 27: 340-346.
- Clayton, C.E., Murphy, D., Lovett, M. and Rigby, P.W.J. 1982. A fragment of the SV40 large-T antigen transforms.

- Nature (Lond.) 299: 59-61.
- Clinton, G.M., Burge, B.W. and Huang, A.S. 1978. Effects of phosphorylation and pH on the association of NS protein with vesicular stomatitis virus cores. J. Virol. 27: 340-346.
- Collins, A.R., Knobler, R.L., Powell, H. and Buchmeier, M.J. 1982. Monoclonal antibodies to murine hepatitis virus 4 (strain JHM) define the viral glycoprotein responsible for attachment and cell-cell fusion. Virology 119: 358-371.
- Comings, D.E. 1975. Mechanisms of chromosome banding. VIII. Hoechst 33258-DNA interaction. Chromosoma (Berl.) 52: 229-243.
- Compans, R.W. and Choppin, P.W. 1973. Orthomyxoviruses and paramyxoviruses. In: Ultrastructure of Animal Viruses and Bacteriophages: an Atlas (Dalton, A.J. and Haguenu, F., eds.). Academic Press, New York. pp. 213-237.
- Compans, R.W., Klenk, H.-D., Caliguiri, L.A. and Choppin, P.W. 1970. Influenza virus proteins. I. Analysis of polypeptides of the virion and identification of spike glycoproteins. Virology 42: 880-889.
- Compton, S.R., Rogers, D.B., Holmes, K.V., Fertsch, D., Remenick, J. and McGowan, J.J. 1987. In vitro replication of mouse hepatitis virus strain A59. J. Virol. 61: 1814-1820.
- Cuatrecasas, P. and Anfinsen, C.B. 1971. Affinity chromatography. Ann. Rev. Biochem. 40: 259-278.
- Cunningham, C.H. 1970. Avian infectious bronchitis. Adv.

- Vet. Sci. Comp. Med. 14: 105-148.
- Curry, A. and Paver, W.K. 1980. Coronavirus-like particles in diarrhoea stools. The Lancet December 20/27: 1370.
- Dalziel, R.G., Lampert, P.W., Talbot, P.J. and Buchmeier, M.J. 1986. Site-specific alteration of mouse hepatitis type 4 peplomer glycoprotein E2 results in reduced neurovirulence. J. Virol. 59: 463-471.
- David-Ferreira, J.F. and Manaker, R.A. 1965. An electron microscope study of the development of a mouse hepatitis virus in tissue culture cells. J. Cell Biol. 24: 57-78.
- Davis, N.L. and Wertz, G.W. 1982. Synthesis of vesicular stomatitis virus negative-strand RNA in vitro: dependence on viral protein synthesis. J. Virol. 41: 821-832.
- DeBenedetti, A. and Baglioni, C. 1984. Inhibition of mRNA binding to ribosomes by localized activation of ds RNA-dependent protein kinase. Nature (London) 311: 79-81.
- De Mey, J., Lambert, A.M., Bajer, A.S., Moeremans, M. and De Brabander, M. 1982. Visualization of microtubules in interphase and mitotic plant cells of *Haemanthus endosperm* with the immuno-gold staining method. Proc. Natl. Acad. Sci. USA 79: 1898-1902.
- Dennis, D.E. and Brian, D.A. 1981. Coronavirus cell-associated RNA-dependent RNA polymerase activity. In: Biochemistry and Biology of Coronaviruses (ter Meulen, V., Siddell, S. and Wege, H., eds.), Plenum Press, New York. pp. 155-170.
- Dennis, D.E. and Brian, D.A. 1982. RNA-dependent RNA

- polymerase activity in coronavirus-infected cells. J. Virol. 42: 153-164.
- DeRobertis, E.M., Longthorne, R.F. and Gurdon, J.B. 1978. Intracellular migration of nuclear proteins in Xenopus oocytes. Nature 272: 254-256.
- Dingwall, C., Sharnick, S.V., and Laskey, R.A. 1982. A polypeptide domain that specifies migration of nucleoplasm into the nucleus. Cell 30: 449-458.
- Dingwall, C. and Allan, J. 1984. Accumulation of the isolated carboxyterminal domain of histone H1 in the Xenopus oocyte nucleus. EMBO J. 3: 1933-1937.
- Doller, E.W. and Holmes, K.V. 1980. Different intracellular transportation of the envelope glycoproteins E1 and E2 of the coronavirus MHV. Annual Meeting of the American Society for Microbiology.
- Doughri, A.M., Storz, J., Hajer, I. and Fernando, H.S. 1976. Morphology and morphogenesis of a coronavirus infecting intestinal epithelial cells of newborn calves. Exp. Mol. Pathol. 25: 355-370.
- Doyle, L.P. and Hutchings, L.M. 1946. A transmissible gastroenteritis in pigs. J. Amer. Vet. Assoc. 108: 257-259.
- Dubois-Dalcq, M.E., Doller, E.W., Haspel, M.V. and Holmes, K.V. 1982. Cell tropism and expression of mouse hepatitis viruses (MHV) in mouse spinal cord cultures. Virology 119: 317-331.
- Dubois-Dalcq, M., Holmes, K.V. and Rentier, B. 1984a.

- Assembly of Coronaviridae. In: Assembly of Enveloped RNA Viruses. (D.W. Kingsbury, ed. assist.). Springer-Verlag, New York. pp. 100-119.
- Dubois-Dalcq, M., Holmes, K.V. and Rentier, B. 1984b. Assembly of Orthomyxoviridae. In: Assembly of Enveloped RNA Viruses. (D.W. Kingsbury, ed. assist.). Springer-Verlag, New York. pp. 66-82.
- Ducatelle, R., Coussement, W., Pensaert, M.B., DeBouck, P. and Hoorens, J. 1981. In vivo morphogenesis of a new porcine enteric coronavirus CV 777. Arch. Virol. 68: 35-44.
- Duchala, C.S., Bauer, E.C., Leibowitz, J., Sturman, L.S. and Holmes, K.V. 1986. Transport of coronavirus nucleocapsid protein to the nucleus. Abstract. Annual Meeting of the American Society for Microbiology, Washington, D.C.
- Dulbecco, R. 1952. Plaques produced on a monolayer tissue culture by single particles of an animal virus. Science 115: 481-482.
- Eagle, H. 1959. Amino acid metabolism in mammalian cell cultures. Science (Washington, D.C.) 130: 432-437.
- Ebeling, W., Hennrich, N., Klockow, M., Metz, H., Orth, H.D. and Lang, H. 1974. Proteinase K from Tritirachium album Limber. Eur. J. Biochem. 47: 91-97.
- El-Boradi, T.T.A.L., Raue, H.A., Regt, V.C.H.F. and Planta, R.J. 1984. Stepwise dissociation of yeast 60S ribosomal subunits by LiCl and identification of L25 as a primary 26S rRNA binding protein. Eur. J. Biochem. 144: 393-400.

- England, T.E. and Uhlenbeck, O.C. 1978. 3'-terminal labelling of RNA with T4 RNA ligase. Nature (Lond.) 275: 560-561.
- Evans, M.R. and Simpson, R.W. 1980. The coronavirus avian infectious bronchitis virus requires the cell nucleus and host transcriptional factors. Virology 105: 582-591.
- Feldherr, C.M. 1975. The uptake of endogenous proteins by oocyte nuclei. Exp. Cell Res. 93: 411-419.
- Feldherr, C.M. 1985. The facilitated transport of proteins across the nuclear envelope. In: Nuclear Envelope Structure and RNA Maturation (Smuckler, E.A. and Clawson, G.A., eds). Alan R. Liss, Inc., New York. pp. 207-214.
- Feldherr, C.M. and Ogburn, J.A. 1982. The uptake of nuclear proteins in oocytes. In: The Nuclear Envelope and the Nuclear Matrix (Maul, G.G., ed.). Alan R. Liss, Inc. New York. pp. 63-74.
- Fenwick, M.L., Walker, M.J. and Petkevich, J.M. 1978. Association of virus proteins with nuclei of cells infected with herpes simplex virus. J. Gen. Virol. 39: 519-529.
- Fleming, J.O., Stohlman, S.A., Harmon, R.C., Lai, M.C., Frelinger, J.A. and Weiner, L.P. 1983. Antigenic relationships of murine coronaviruses: Analysis using monoclonal antibodies to JHM (MHV-4) virus. Virology 131: 296-307.
- Fleming, J.O., Trousdale, M.D., El-Zaatari, F.A.K., Stohlman, S.A. and Weiner, L.P. 1986. Pathogenicity of antigenic

- variants of murine coronavirus JHM selected with monoclonal antibodies. J. Virol. 58: 869-875.
- Follett, E.A.C., Pringle, C.R., Pennington, T.H. and Shirodaria, P. 1976. Events following the infection of enucleate cells with measles virus. J. Gen. Virol. 32: 163-175.
- Fong, B.S., Hunt, R.C. and Brown, J.C. 1976. Asymmetric distribution of phosphatidylethanolamine in the membrane of vesicular stomatitis virus. J. Virol. 20: 658-663.
- Fraenkel-Conrat, H. and Singer, B. 1964. Reconstitution of tobacco mosaic virus. IV. Inhibition by enzymes and other proteins, and use of polynucleotides. Virology 23: 354-362.
- Fraenkel-Conrat, H. and Williams, R.C. 1955. Reconstitution of active tobacco mosaic virus from its inactive protein and nucleic acid components. Proc. Natl. Acad. Sci. USA 41: 690-698.
- Frana, M.F., Behnke, J.N., Sturman, L.S. and Holmes, K.V. 1985. Proteolytic cleavage of the E2 glycoprotein of murine coronavirus: Host-dependent differences in proteolytic cleavage and cell fusion. J. Virol. 56: 912-920.
- Freedman, R.B. 1984. Native disulfide bond formation in protein biosynthesis: evidence for the role of protein disulphide isomerase. Trends Biochem. Sci. 9: 438-441.
- Fulton, A.B. 1984. Assembly associated with the cytomatrix. J. Cell Biol. 99: 209s.
- Fujiwara, S. and Kaplan, A.S. 1967. Site of protein syn-

- thesis in cells infected with pseudorabies virus. Virology 32: 60-68.
- Gerdes, J.C., Jankovsky, L.D., DeVald, B.L., Klein, I. and Burks, J.S. 1981. Antigenic relationships of coronaviruses detectable by plaque neutralization, competitive enzyme-linked immunoabsorbent assay and immunoprecipitation. In: Biochemistry and Biology of Coronaviruses (ter Meulen, V., Siddell, S. and Wege, H., eds.). Plenum Press, New York. pp. 29-42.
- Gerna, G., Cereda, P.M., Grazia-Revello, M., Cattaneo, E., Battaglia, M. and Torsellini-Gerna, M. 1981. Antigenic and biological relationships between human coronavirus OC43 and neonatal calf diarrhoea coronavirus. J. Gen. Virol. 54: 91-102.
- Gerna, G., Passarani, N., Battaglia, M. and Rondanelli, E.G. 1985. Human enteric coronaviruses: Antigenic relatedness to human coronavirus OC43 and possible etiologic role in viral gastroenteritis. J. Infect. Dis. 151: 796-803.
- Gharakhanian, E., Takahashi, J. and Kasamatsu, H. 1987. The carboxyl 35 amino acids of SV40 Vp3 are essential for its nuclear accumulation. Virology 157: 440-448.
- Gledhill, A.W. and Andrewes, C.A. 1951. A hepatitis of mice. Brit. J. Exp. Path. 32: 559-568.
- Goldstein, L. 1985. A survey of how proteins are segregated between nucleus and cytoplasm. In: Nuclear Envelope Structure and RNA Maturation. (Smuckler, E.A. and Clawson, G.A., eds.). Alan R. Liss, Inc., New York. pp. 167-191.

- Gourse, R.L., Thurlow, D.L., Gerbi, S.A. and Zimmerman, R.A. 1981. Specific binding of a prokaryotic ribosomal protein to a eukaryotic ribosomal RNA: Implications for evolution and autoregulation. Proc. Natl. Acad. Sci. USA 78: 2722-2726.
- Griffiths, G., Quinn, P. and Warren, G. 1983. Dissection of the Golgi complex. I. Monensin inhibits the transport of viral membrane proteins from medial to trans Golgi cisternae in baby hamster kidney cells infected with Semliki Forest virus. J. Cell Biol. 96: 835-850.
- Grifo, J.A., Tahara, S.M., Leis, J.P., Morgan, M.A., Shatkin, A.J. and Merrick, W.C. 1982. Characterization of eukaryotic initiation factor 4A, a protein involved in ATP-dependent binding of globin mRNA. J. Biol. Chem. 10: 5246-5252.
- Grimley, P.M., Berezesky, I.K. and Friedman, R.M. 1968. Cytoplasmic structures associated with an arbovirus infection: loci of viral ribonucleic acid synthesis. J. Virol. 2: 1326-1338.
- Grimley, P.M., Levin, J.G., Berezesky, I.K. and Friedman, R.M. 1972. Specific membranous structures associated with the replication of group A arbovirus. J. Virol. 10: 492-503.
- Habel, K. 1965. Specific complement-fixing antigens in polyoma tumors and transformed cells. Virology 25: 55-61.
- Hall, M.N., Hereford, L. and Herskowitz, I. 1984. Targeting of *Escherichia coli* beta-galactosidase to the nucleus in

- yeast. Cell 36: 1057-1065.
- Hall, W.W. and ter Meulen, V. 1977. The effects of actinomycin D on RNA synthesis in measles virus-infected cells. J. Gen. Virol. 34: 391-396.
- Hamaguchi, M., Maeno, K., Nagai, Y., Iinuma, M., Yoshida, T. and Matsumoto, T. 1980. Analysis of nuclear accumulation of influenza nucleoprotein antigen in the presence of p-fluorophenylalanine. Microbiol. Immunol. 24: 51-63.
- Hamre, D. and Procknow, J.J. 1966. A new virus isolated from the human respiratory tract. Proc. Soc. Exp. Biol. Med. 121: 190-193.
- Hamre, D., Kindig, D.A. and Mana, J. 1967. Growth and intracellular development of a new respiratory virus. J. Virol. 1: 810-816.
- Hardwick, J.M. and Hunter, E. 1981. Rous sarcoma virus mutant LA3382 is defective in virion glycoprotein assembly. J. Virol. 40: 752-761.
- Hasony, H.J. and Macnaughton, M.R. 1981. Antigenicity of mouse hepatitis virus strain 3 subcomponents in C57 strain mice. Arch. Virol. 69: 33-41.
- Hasony, H.J. and Macnaughton, M.R. 1982. Serological relationships of the subcomponents of human coronavirus strain 229E and mouse hepatitis virus strain 3. J. Gen. Virol. 58: 449-452.
- Hawkes, R., Niday, E. and Gordon, J. 1982. A dot-immunobinding assay for monoclonal and other antibodies. Anal. Biochem. 119: 142-147.

- Hay, R.T. 1979. DNA-binding proteins and DNA synthesis in Herpesvirus infected cells. Doctoral dissertation, University of Glasgow, Glasgow, Scotland. p. 88.
- Heggeness, M.H., Scheid, A. and Choppin, P.W. 1980. Conformation of the helical nucleocapsids of paramyxoviruses and vesicular stomatitis virus: Reversible coiling and uncoiling induced by changes in salt concentration. Proc. Natl. Acad. Sci. USA 77: 2631-2635.
- Heggeness, M.H., Smith, P.R., Ulmanen, J., Krug, R.M. and Choppin, P.W. 1982. Studies on the helical nucleocapsid of influenza virus. Virology 118: 466-470.
- Helenius, A., Marsh, M. and White, J. 1980. The entry of viruses into animal cells. Trends Biochem. Sci. 5: 104-106.
- Helenius, A., Marsh, M. and White, J. 1982. Inhibition of Semliki Forest virus penetration by lysosomotropic weak bases. J. Gen. Virol. 58: 47-61.
- Hilwig, I. and Gropp, A. 1972. Staining of constitutive heterochromatin in mammalian chromosomes with a new fluorochrome. Exptl. Cell Res. 75: 122-126.
- Hirano, N., Murakami, T., Fujiwara, K. and Matsumoto, M. 1978. Utility of mouse cell line DBT for propagation and assay of mouse hepatitis virus. J. J. Exp. Med. 48: 71-75.
- Hogue, B. G., King, B. and Brian, D.A. 1984. Antigenic relationships among proteins of bovine coronavirus, human respiratory coronavirus OC43, and mouse hepatitis coronavirus A59. J. Virol. 51: 384-388.
- Holmes, K.V. 1968. Cell fusion induced by the parainfluenza

- virus SV5. Doctoral dissertation, The Rockefeller University, New York. pp. 23-24.
- Holmes, K.V. 1985. Replication of coronaviruses. In: Virology (Fields, B.N., ed.). Raven Press, New York. pp.513-525.
- Holmes, K.V. and Behnke, J.N. 1981. Evolution of a coronavirus during persistent infection in vitro. In Biochemistry and Biology of Coronaviruses (ter Meulen, V., Siddell, S. and Wege, H., eds.). Plenum Press, New York. pp. 287-299.
- Holmes, K.V. and Choppin, P.W. 1966. On the role of the response of the cell membrane in determining virus virulence. Contrasting effects of the parainfluenza virus SV5 in two cell types. J. Exp. Med. 124: 501-520.
- Holmes, K.V., Klenk, H.-D. and Choppin, P.W. 1968. A comparison of immune cytolysis and virus-induced fusion of sensitive and resistant cell types. Proc. Soc. Exp. Biol. Med. 131: 651-657.
- Holmes, K.V., Doller, E.W. and Sturman, L.S. 1981a. Tunicamycin resistant glycosylation of a coronavirus glycoprotein: Demonstration of a novel type of viral glycoprotein. Virology 115: 334-344.
- Holmes, K.V., Doller, E.W. and Behnke, J.N. 1981b. Analysis of the functions of coronavirus glycoproteins by differential inhibition of synthesis with tunicamycin. In: Biochemistry and Biology of Coronaviruses (ter Meulen, V., Siddell, S. and Wege, H.). Plenum Press, New York. pp.133-142.
- Holmes, K.V., Frana, M.F., Robbins, S.G. and Sturman, L.S.

1984. Coronavirus replication. In: Molecular Biology and Pathogenesis in Coronaviruses (Rottier, P.J.M., van der Zeijst, B.A.M., Spaan, W.J.M. and Horzinek, M., eds.). Plenum Press, New York. pp. 37-52.
- Holmes, K.V., Welsh, R.M. and Haspel, M.V. 1986. Natural cytotoxicity against mouse hepatitis virus infected target cells. I. Correlation of cytotoxicity with virus binding to leukocytes. J. Immunol. 136: 1446-1453.
- Holmes, K.V., Boyle, J.F., Williams, R.K., Stephensen, C.B., Robbins, S.G., Bauer, E.C., Duchala, C.S., Frana, M.F., Weismiller, D.G., Compton, S., McGowan, J.J. and Sturman, L.S. 1987. Processing of coronavirus proteins and assembly of virions. In: Positive Strand RNA Viruses (Brinton, M.A. and Rueckert, R.R., eds.). Alan R. Liss, Inc. New York. pp. 339-350.
- Holzworth, J. 1963. Some important disorders of cats. Cornell Vet. 53: 157-160.
- Homma, M. and Ohuchi, M. 1973. Trypsin action on the growth of Sendai virus in tissue culture cells. III. Structural difference of Sendai virus grown in eggs and tissue culture cells. J. Virol. 12: 1457-1465.
- Horzinek, M.C., Lutz, H. and Pedersen, N.C. 1982. Antigenic relationships among homologous structural polypeptides of porcine, feline and canine coronaviruses. Infect. Immun. 37: 1148-1155.
- Horzinek, M.C., Ederveen, J. and Weiss, M. 1985. The nucleocapsid of Berne virus. J. Gen. Virol. 66: 1287-1296.

- Hsu, C.-H. and Kingsbury, D.W. 1982. Topography of phosphate residues in Sendai virus proteins. Virology 120: 225-234.
- Ichihashi, Y., Oie, M. and Tsuruhara, T. 1984. Location of DNA-binding proteins and disulfide-linked proteins in vaccinia virus structural elements. J. Virol. 50: 929-938.
- Ito, Y., Spurr, N. and Dulbecco, R. 1977. Characterization of polyoma virus T antigen. Proc. Natl. Acad. Sci. 74: 1259-1263.
- Jacobs, L., Spaan, W.J.M., Horzinek, M.C. and van der Zeijst, B.A.M. 1981. The synthesis of the subgenomic mRNAs of mouse hepatitis virus is initiated independently: evidence from UV transcription mapping. J. Virol. 39: 401-406.
- Jelinek, W. and Goldstein, L. 1973. Isolation and characterization of some of the proteins that shuttle between cytoplasm and nucleus in Amoeba proteus. J. Cell. Physiol. 81: 181-197.
- Jiang, L.-W. and Schindler, M. 1986. Chemical factors that influence nucleocytoplasmic transport: a fluorescence photobleaching study. J. Cell Biol. 102: 853-858.
- Johnson, D.C. and Schlesinger, M.J. 1980. Vesicular stomatitis virus and Sindbis virus glycoprotein transport to the cell surface is inhibited by ionophores. Virology 103: 407-424.
- Johnson, D.C. and Spear, P.G. 1982. Monensin inhibits the processing of herpes simplex virus glycoproteins, their transport to the cell surface, and the egress of virions from infected cells. J. Virol. 43: 1102-1012.

- Johnson, R.M., Barrett, P. and Sommerville, J. 1984. Distribution and utilization of 5S-RNA-binding proteins during the development of Xenopus oocytes. Eur. J. Biochem. 144: 503-508.
- Kaariainen, L., Hashimoto, K., Saraste, J., Virtanen, I. and Penttinen, K. 1980. J. Cell Biol. 87: 783-791.
- Kalderon, D., Richardson, W.D., Markham, A.F., and Smith, A.E. 1984a. Sequence requirements for nuclear location of Simian virus 40 large T-antigen. Nature (Lond.) 311: 33-38.
- Kalderon, D., Roberts, B.L., Richardson, W.D., and Smith, A.E. 1984b. A short amino acid sequence able to specify nuclear location. Cell 39: 499-509.
- Kamba, K. and Stubbs, G. 1986. Structure of tobacco mosaic virus at 3.6 A resolution: Implications for assembly. Science 231: 1401-1406.
- Kapikian, A.Z., James, H.D., Jr., Kelly, S.J., Dees, H.J., Turner, H.C., McIntosh, K., Kim, H.W., Parrott, R.H., Vincent, M.M. and Chanock, R.M. 1969. Isolation from man of "Avian bronchitis virus-like" viruses (coronaviruses) similar to 229E virus, with some epidemiological observations. J. Infect. Dis. 119: 282-290.
- Kapke, P.A. and Brian, D.A. 1986. Sequence analysis of the porcine transmissible gastroenteritis coronavirus nucleocapsid protein gene. Virology 151: 41-49.
- Kasamatsu, H. and Nehorayan, A. 1979. Intracellular localization of viral polypeptides during simian virus 40 infec-

- tion. J. Virol. 32: 648-660.
- Kauffman, R. and Ginsberg, H.S. 1976. Characterization of a temperature-sensitive hexon transport mutant of type 5 adenovirus. J. Virol. 19: 643-658.
- Kennedy, D.A. and Johnson-Lussenburg, C.M. 1976. Isolation and morphology of the internal component of human coronavirus, strain 229E. Intervirology 6: 197-206.
- Kim, J., Hama, K., Miyake, Y. and Okada, Y. 1979. Transformation of intramembrane particles of HVJ (Sendai virus) envelopes from an invisible to visible form on aging of virions. Virology 95: 523-535.
- Kingsbury, D.W., Jones, I.M. and Murti, K.G. 1987. Assembly of influenza ribonucleoprotein in vitro using recombinant nucleoprotein. Virology 156: 396-403.
- Klenk, H.D. and Rott, R. 1981. Cotranslational and posttranslational processing of viral glycoproteins. Curr. Top. Microbiol. Immunol. 90: 19-48.
- Klenk, H.-D., Rott, R., Orlich, M., Blodorn, J. 1975. Activation of influenza A viruses by trypsin treatment. Virology 68: 426-439.
- Knopf, K.-W. and Kaerner, H.C. 1980. Virus-specific basic phosphoproteins associated with herpes simplex virus type 1 (HSV-1) particles and the chromatin of HSV-1-infected cells. J. Gen. Virol. 46: 405-414.
- Kousoulas, K.G., Bzik, D.J. and Person, S. 1983. Effect of the ionophore monensin on herpes simplex virus type 1-induced cell fusion, glycoprotein synthesis, and virion

- infectivity. Intervirol. 20: 56-60.
- Kraaijeveld, C.A., Madge, M.H. and Macnaughton, M.R. 1980. Enzyme-linked immunosorbant assay for coronaviruses HCV229E and MHV-3. J. Gen. Virol. 49: 83-89.
- Krystyniak, K. and Dupuy, J.M. 1981. Early interaction between mouse hepatitis virus 3 and cells. J. Gen. Virol. 57: 53-61.
- Kyte, J. and Doolittle, R.F. 1982. A simple method for displaying the hydrophobic character of a protein. J. Mol. Biol. 157: 105-132.
- Laemmli, U.K. 1970. Cleavage of structural proteins during the assembly of the head of bacteriophage T4. Nature (Lond.) 227: 680-685.
- Lai, M.M.C. and Stohlman, S.A. 1978. The RNA of mouse hepatitis virus. J. Virol. 26: 236-242.
- Lai, M.M.C. and Stohlman, S.A. 1981. Comparative analysis of RNA genomes of mouse hepatitis viruses. J. Virol. 38: 661-670.
- Lai, M.M.C., Brayton, P.R., Armen, R.C., Patton, C.D., Pugh, C. and Stohlman, S.A. 1981. Mouse hepatitis virus A59 messenger RNA structure and genetic localization of the sequence divergence from the hepatotropic strain MHV3. J. Virol. 39: 823-834.
- Lai, M.M.C., Patton, C.D. and Stohlman, S.A. 1982a. Further characterization of mouse hepatitis virus: Presence of common 5'-end nucleotides. J. Virol. 41: 557-565.
- Lai, M.M.C., Patton, C.D. and Stohlman, S.A. 1982b. Replica-

- tion of mouse hepatitis virus: Negative-stranded RNA and replicative form RNA are of genome length. J. Virol. 44: 487-492.
- Lamb, R.A. 1975. The phosphorylation of Sendai virus proteins by a virus particle-associated protein kinase. J. Gen. Virol. 26: 249-263.
- Lamb, R.A. 1983. The influenza virus RNA segments and their encoded proteins. In: Genetics of Influenza Viruses (Palese, P. and Kingsbury, D.W., eds.). Springer-Verlag, New York. pp. 21-69.
- Lamb, R.A. and Choppin, P.W. 1983. The gene structure and replication of influenza virus. Annu. Rev. Biochem. 52: 467-506.
- Lapps, W., Hogue, B.G. and Brian, D.A. 1987. Sequence analysis of the bovine coronavirus nucleocapsid and matrix protein genes. Virology 157: 47-57.
- Larson, H.E., Reed, S.E. and Tyrrell, D.A.J. 1980. Isolation of rhinoviruses and coronaviruses from 38 colds in adults. J. Med. Virol. 5: 221-229.
- Laskey, R.A., Dingwall, C., Mills, A.D. and Dilworth, S.M. 1985. Transport and assembly of nuclear proteins. In: Nuclear Envelope Structure and RNA Maturation (Smuckler, E.A. and Clawson, G.A., eds.). Alan R. Liss, Inc. New York. pp. 193-205.
- Laude, H. 1981. Thermal inactivation studies on a coronavirus, transmissible gastroenteritis virus. J. Gen. Virol. 56: 235-240.

- Lavi, E., Gilden, D.H., Wroblewska, Z., Rorke, L.B. and Weiss, S.R. 1984. Experimental demyelination produced by the A59 strain of mouse hepatitis virus. Neurology 34: 597-603.
- Lazarowitz, S.G. and Choppin, P.W. 1975. Enhancement of the infectivity of influenza A and B viruses by proteolytic cleavage of the hemagglutinin polypeptide. Virology 68: 440-454.
- Lazarowitz, S.G., Compans, R.W. and Choppin, P.W. 1973a. Proteolytic cleavage of the hemagglutinin polypeptide of influenza virus. Function of the uncleaved polypeptide HA. Virology 52: 199-212.
- Lazarowitz, S.G., Goldberg, A.R. and Choppin, P.W. 1973b. Proteolytic cleavage by plasmin of the HA polypeptide of influenza virus: Host cell activation of serum plasminogen. Virology 56: 172-180.
- Lebeurier, G., Nicolaieff, A. and Richards, K.E. 1977. Inside-out model for self-assembly of tobacco mosaic virus. Proc. Natl. Acad. Sci. USA 74: 149-153.
- Leibowitz, J.L. and Weiss, S.R. 1981. Murine coronavirus RNA. In: Biochemistry and Biology of Coronaviruses (ter Meulen, V., Siddell, S. and Wege, H., eds.). Plenum Press, New York. pp. 227-244.
- Leibowitz, J.L., Wilhelmsen, K.C. and Bond, C.W. 1981. The virus-specific intracellular RNA species of two murine coronaviruses: MHV-A59 and MHV-JHM. Virology 114: 29-51.
- Leibowitz, J.L., Weiss, S.R., Paavola, E. and Bond, C.W.

1982. Cell-free translation of murine coronavirus RNA. J. Virol. 43: 905-913.
- Leis, J. and Johnson, S. 1984. Effects of phosphorylation of avian retrovirus nucleocapsid protein ppl2 on binding of viral RNA. J. Biol. Chem. 259: 7726-7732.
- Lenard, J. and Compans, R.W. 1974. The membrane structure of lipid-containing viruses. Biochim. Biophys. Acta 344: 51-94.
- Levy, G.A., Leibowitz, J.L. and Edgington, T.S. 1982. Lymphocyte-instructed monocyte induction of the coagulation pathways parallels the induction of hepatitis by the murine hepatitis virus. In: Progress in Liver Disease (Popper, H. and Schaffner, F., eds.). Grune and Stratton, New York. Vol. 7, pp. 393-409.
- Lewis, A.M., Jr. and Rowe, W.P. 1971. Studies on nondefective adenovirus-simian virus 40 hybrid viruses. I. A newly characterized simian virus 40 antigen induced by the Ad2+ND 1 virus. J. Virol. 7: 189-197.
- Lin, B.C. and Lai, C.J. 1983. The influenza virus nucleoprotein synthesized from cloned DNA in a simian virus 40 vector is detected in the nucleus. J. Virol. 45: 434-438.
- Liu, C. 1955. Studies on influenza infection in ferrets by means of fluorescein-labelled antibody. 2. The role of soluble antigen in nuclear fluorescence and cross-reactions. J. Exp. Med. 101: 677-686.
- Lok, S. and Abouhaidar, M.G. 1986. The nucleotide sequence of the 5' end of papaya mosaic virus RNA: Site of in vitro

- assembly initiation. Virology 153: 289-296.
- Lomniczi, B. 1977. Biological properties of avian coronavirus RNA. J. Gen. Virol. 36: 531-533.
- Lomniczi, B. and Kennedy, I. 1977. Genome of infectious bronchitis virus. J. Virol. 24: 99-107.
- Lowry, O.H., Rosebrough, N.J., Farr, A.L. and Randall, R.J. 1951. Protein measurement with the Folin phenol reagent. J. Biol. Chem. 193: 265-275.
- Luft, J.H. 1961. Improvements in epoxy resin embedding methods. J. Biophys. Biochem. Cytol. 9: 409-414.
- Luytjes, W., Sturman, L.S., Bredenbeek, P.J., Charite, J., van der Zeijst, B.A.M., Horzinek, M.C. and Spaan, W.J.M. 1987. Primary structure of the glycoprotein E2 of coronavirus MHV-A59 and identification of the trypsin cleavage site. Submitted.
- Macnaughton, M.R. 1981. Structural and antigenic relationships between human, murine and avian coronaviruses. In: Biochemistry and Biology of Coronaviruses (ter Meulen, V., Siddell, S. and Wege, H., eds.). Plenum Press, New York. pp. 19-28.
- Macnaughton, M.R., Davies, H.A. and Nermut, M.V. 1978. Ribonucleoprotein-like structures from coronavirus particles. J. Gen. Virol. 39: 545-549.
- Maeda, T., Kawasaki, K. and Ohnishi, S. 1981. Interaction of influenza virus hemagglutinin with target membranes is a key step in virus-induced hemolysis and fusion at pH 5.2. Proc. Natl. Acad. Sci. 78: 4133-4137.

- Mahy, B.W.J., Siddell, S., Wege, H. and ter Meulen, V. 1983. RNA-dependent RNA polymerase activity in murine coronavirus-infected cells. J. Gen. Virol. 64: 103-111.
- Mallucci, L. 1965. Observations on the growth of mouse hepatitis virus (MHV-3) in mouse macrophages. Virology 25: 30-37.
- Mallucci, L. 1966. Effect of chloroquine on lysosomes and on growth of mouse hepatitis virus (MHV-3). Virology 28: 355-362.
- Mallucci, L. and Edwards, B. 1982. Influence of the cytoskeleton on the expression of a mouse hepatitis virus (MHV-3) in peritoneal macrophages: acute and persistent infection. J. Gen. Virol. 63: 217-221.
- Manaker, R.A., Piczak, C.V., Miller, A.A. and Stanton, M.F. 1961. A hepatitis virus complicating studies with mouse leukemia. J. Natl. Cancer Inst. 27: 29-51.
- Maniatis, T. 1982. Molecular Cloning: A Laboratory Manual (Fritsch, F., ed.). Cold Spring Harbor Laboratory, Cold Spring Harbor, New York. pp. 191-192.
- Mark, G.E. and Kaplan, A.S. 1971. Synthesis of proteins in cells infected with herpesvirus. VII. Lack of migration of structural viral proteins to the nucleus of arginine-deprived cells. Virology 45: 53-60.
- Markwell, M.A. and Fox, C.F. 1980. Protein-protein interactions within paramyxoviruses identified by native disulfide bonding or reversible chemical cross-linking. J. Virol. 33: 152-166.

- Massalski, A., Coulter-Mackie, M. and Dales, S. 1981. Assembly of mouse hepatitis virus strain JHM. In: Biochemistry and Biology of Coronaviruses (ter Meulen, V., Siddell, S. and Wege, H., eds.). Plenum Press, New York. pp. 111-118.
- Massalski, A., Coulter-Mackie, M., Knobler, R.L., Buchmeier, M.J. and Dales, S. 1982. In vivo and in vitro models of demyelinating diseases. V. Comparison of the assembly of mouse hepatitis virus, strain JHM, in two murine cell lines. Intervirology 18: 135-146.
- Maul, G.G. 1982. Aspects of a hypothetical nucleocytoplasmic transport mechanism. In: The Nuclear Envelope and the Nuclear Matrix. (Maul, G.G., ed.). Alan R. Liss, Inc., New York. pp. 1-11.
- Maxam, A.M. and Gilbert, W. 1980. Sequencing end-labeled DNA with base-specific chemical cleavages. In: Methods in Enzymology (Grossman, L. and Moldave, K., eds.). Academic Press, New York. Vol. 65, pp. 499-560.
- McIntosh, K. 1974. Coronaviruses: A comparative review. Curr. Top. Microbiol. Immunol. 63: 84-129.
- McIntosh, K. 1985. Coronaviruses. In: Virology (Fields, B.N., ed.) Raven Press, New York. pp. 1323-1330.
- McIntosh, K., Dees, J.H., Becker, W.B., Kapikian, A.Z. and Chanock, R.M. 1967. Recovery in tracheal organ cultures of novel viruses from patients with respiratory disease. Proc. Natl. Acad. Sci. USA 57: 933-940.
- McIntosh, K., Kapikian, A.Z., Hardison, K.A., Hartley, J.W.

- and Chanock, R.M. 1969. Antigenic relationships among the coronaviruses of man and between human and animal coronaviruses. J. Immunol. 102: 1109-1118.
- McIntosh, K., Kapikian, A.Z., Turner, H.C., Hartley, J.W., Parrot, R.H. and Chanock, R.M. 1970. Seroepidemiologic studies of coronavirus infection in adults and children. Am. J. Epidemiol. 91: 585-592.
- Meric, C., Darlix, J.-L. and Spahr, P.-F. 1984. It is Rous sarcoma virus protein P12 and not P19 that binds tightly to Rous sarcoma virus RNA. J. Mol. Biol. 173: 531-538.
- Monto, A.S. and Rhodes, L.M. 1974. Detection of coronavirus infection of man by immunofluorescence. Proc. Soc. Exp. Biol. Med. 155: 143-148.
- Morgan, E.M., Re, G.G. and Kingsbury, D.W. 1984. Complete sequence of the Sendai virus NP gene from a cloned insert. Virology 135: 279-287.
- Myers, R.M., Rio, D., Robbins, A. and Tijian, R. 1981. SV40 gene expression is modulated by the cooperative binding of T-antigen to DNA. Cell 25: 373-384.
- Nagai, Y. and Klenk, H.-D. 1977. Activation of precursor of both glycoproteins of Newcastle disease virus by proteolytic cleavage. Virology 77: 125-134.
- Nagai, Y., Klenk, H.-D. and Rott, R. 1976. Proteolytic cleavage of the viral glycoproteins and its significance for the virulence of Newcastle disease virus. Virology 72: 494-508.
- Nakai, T., Shand, F.L. and Howatson, A.F. 1969. Development

- of measles virus in vitro. Virology 38: 50-67.
- Namba, K. and Stubbs, G. 1986. Structure of tobacco mosaic virus at 3.6 Å resolution: Implications for assembly. Science 231: 1404-1406.
- Natarajan, A.T. and Gropp, A. 1972. A fluorescence study of heterochromatin and nucleolar organization in the laboratory and tobacco mouse. Exp. Cell Res. 74: 245-250.
- Nelson, J.B. 1952. Acute hepatitis associated with mouse leukemia. I. Pathological features and transmission of the disease. J. Exp. Med. 96: 293-302.
- Niemann, H. and Klenk, H.-D. 1981a. Coronavirus glycoprotein E1, a new type of viral glycoprotein. J. Mol. Biol. 153: 993-1010.
- Niemann, H. and Klenk, H.-D. 1981b. Glycoprotein E1 of coronavirus A59. A new type of viral glycoprotein. In: Biochemistry and Biology of Coronaviruses (ter Meulen, V., Siddell, S. and Wege, H., eds.). Plenum Press, New York. pp. 119-132.
- Niemann, H., Boschek, B., Evans, D., Rosing, M., Tamura, T. and Klenk, H.-D. 1982. Post-translational glycosylation of coronavirus glycoprotein E1: inhibition by monensin. EMBO J. 1: 1499-1504.
- Norrby, E. 1972. Intracellular accumulation of measles virus nucleocapsid and envelope antigens. Microbios. 5: 31-40.
- Norrby, E., Chen, S.-N., Togashi, T., Shesberadaran, H. and Johnson, K.P. 1982. Five measles virus antigens demonstra-

- ted by use of mouse hybridoma antibodies in productively infected tissue culture cells. Arch. Virol. 71: 1-11.
- Ohkuma, S. and Poole, B. 1978. Fluorescence probe measurement of the intralysosomal pH in living cells and the perturbation of pH by various agents. Proc. Natl. Acad. Sci. USA 75: 3327-3331.
- Okuno, T., Yamanishi, K., Shiraki, K. and Takahashi, M. 1983. Synthesis and processing of glycoproteins of varicella-zoster virus (VZV) as studied with monoclonal antibodies to VZV antigens. Virology 129: 357-368.
- Olshevsky, U., Levitt, J. and Becker, Y. 1967. Studies on the synthesis of herpes simplex virions. Virology 33: 323-334.
- Orvell, C. and Grandien, M. 1982. The effects of monoclonal antibodies on biologic activities of structural proteins of Sendai virus. J. Immunol. 129: 2779-2787.
- Oshiro, L.S. 1973. Coronaviruses. In: Ultrastructure of animal viruses and bacteriophages: An Atlas (Dalton, A.J. and Haguenu, F., eds.). Academic Press, New York. pp. 331-343.
- Oshiro, L.S., Schieble, J.H. and Lennette, E.H. 1971. Electron microscopic studies of a coronavirus. J. Gen. Virol. 12: 161-168.
- Otsuki, K. and Tsubokura, M. 1981. Plaque formation by IBV in primary CEF cells in the presence of trypsin. Arch. Virol. 70: 315-320.
- Pabo, C.O. and Sauer, R.T. 1984. Protein-DNA recognition. Ann. Rev. Biochem. 53: 293-321.
- Paine, P.L. 1982. Mechanisms of nuclear protein con-

- centration. In: The Nuclear Envelope and the Nuclear Matrix. (Maul, G.G., ed.). Alan R. Liss, Inc. New York. pp. 75-83.
- Paine, P.L. 1985. Nucleocytoplasmic protein distributions: Roles of the nuclear envelope and the cytomatrix. In: Nuclear Envelope Structure and RNA Maturation. (Smuckler, E.A. and Clawson, G.A., eds.). Alan R. Liss, Inc. New York. pp. 215-231.
- Paine, P.L., Feldherr, C.M. 1972. Nucleocytoplasmic exchanges of macromolecules. Exp. Cell Res. 74: 81-98.
- Paine, P.L., Moore, C. and Horowitz, S.B. 1975. Nuclear envelope permeability. Nature 254: 109-114.
- Palade, G.E. 1952. A study of fixation for electron microscopy. J. Exp. Med. 95: 285-298.
- Partanen, P., Turunen, H.J., Paasivuo, R., Forsblom, E., Suni, J. and Leinikki, P.O. 1983. Identification of antigenic components of Toxoplasma gondii by an immunoblotting technique. FEBS Lett. 158: 252-254.
- Patterson, S. and Bingham, R.W. 1976. Electron microscopic observations on the entry of avian infectious bronchitis virus into susceptible cells. Arch. Virol. 52: 191-200.
- Patton, J.P., Davis, N.L. and Wertz, G.W. 1983. Cell-free synthesis and assembly of vesicular stomatitis virus nucleocapsids. J. Virol. 45: 155-164.
- Pedersen, N.C. 1976. Morphologic and physical characteristics of feline infectious peritonitis virus and its growth in autochthonous peritoneal cells. Amer. J. Vet. Res. 37: 567-

572.

- Pedersen, N.C., Ward, I. and Mengeling, W.L. 1978. Antigenic relationships of the feline infectious peritonitis virus to coronaviruses of other species. Arch. Virol. 58: 45-53.
- Peluso, R.W. and Moyer, S.A. 1983. Initiation and replication of vesicular stomatitis virus genome RNA in a cell-free system. Proc. Natl. Acad. Sci. 80: 3198-3202.
- Pensaert, M.B., Debouck, P. and Reynolds, D.J. 1981. An immunoelectron microscopic and immunofluorescent study on the antigenic relationship between the coronavirus-like agent, CV777, and several coronaviruses. Arch. Virol. 68: 45-52.
- Pesonen, M. and Kaariainen, L. 1982. Incomplete complex oligosaccharides in Semliki Forest virus envelope proteins arrested within the cell in the presence of monensin. J. Mol. Biol. 158: 213-230.
- Petit, M. and Pillot, J. 1985. HBc and HBe antigenicity and DNA-binding activity of major core protein P22 in hepatitis B virus core particles isolated from the cytoplasm of human liver cells. J. Virol. 53: 543-551.
- Piazza, M. 1969. Experimental Viral Hepatitis. Charles C. Thomas, Springfield, Ill. p. 1348.
- Piko, L. 1977. Immunocytochemical detection of a murine leukemia virus-related nuclear antigen in mouse oocytes and early embryos. Cell 12: 697-707.
- Pocock, D.H. and Garwes, D.J. 1975. The influence of pH on the growth and stability of transmissible gastroenteritis

- virus. Arch. Virol. 49: 239-247.
- Pressman, B.C. 1976. Biological applications of ionophores. Ann. Rev. Biochem. 45: 501-530.
- Quinlan, M.P. and Knipe, D.M. 1983. Nuclear localization of herpesvirus proteins: potential role for the cellular framework. Mol. Cell Biol. 3: 315-324.
- Quinlan, M.P., Chen, L.B. and Knipe, D.M. 1984. The intranuclear location of a herpes simplex virus DNA-binding protein is determined by the status of viral DNA replication. Cell 36: 857-868.
- Ray, M.B., Desmet, V.J., Bradburne, A.F., Desmyter, J., Fevery, J. and DeGrootte, J. 1976. Differential distribution of hepatitis B surface antigen and hepatitis B core antigen in the liver of hepatitis B patients. Gastroenterology 71: 462-469.
- Rechsteiner, M. and Kuehl, L. 1979. Microinjection of the nonhistone chromosomal protein HMG 1 into bovine fibroblasts and HeLa cells. Cell 16: 901-908.
- Reedman, B.M. and Klein, G. 1973. Cellular localization of an Epstein-Barr virus (EBV)-associated complement-fixing antigen in producer and non-producer lymphoblastoid cell lines.
- Repp, R., Tamura, T., Boschek, C.B., Wege, H., Schwarz, R.T. and Niemann, H. 1985. The effects of processing inhibitors of N-linked oligosaccharides on the intracellular migration of glycoprotein E2 of mouse hepatitis virus and the maturation of coronavirus particles. J. Biol. Chem. 260:

15873-15879.

- Resta, S., Luby, J.P., Rosenfels, C.R. and Siegel, J.D. 1985. Isolation and propagation of a human enteric coronavirus. Science 229: 978-984.
- Reynolds, D.J., Garwes, D.J. and Lucey, S. 1980. Differentiation of canine coronavirus and porcine transmissible gastroenteritis virus by neutralization with canine, porcine, and feline sera. Vet. Microbiol. 5: 283-290.
- Reynolds, E.S. 1963. The use of lead citrate at high pH as an electron-opaque stain in electron microscopy. J. Cell Biol. 17: 208-212.
- Ricard, C.S. and Sturman, L.S. 1985. Isolation of the subunits of the coronavirus envelope glycoprotein E2 by hydroxyapatite high-performance liquid chromatography. J. Chromatog. 326: 191-197.
- Richardson, C.D. and Vance, D.E. 1978. The effect of colchicine and dibucaine on the morphogenesis of Semliki Forest virus. J. Biol. Chem. 253: 4584-4589.
- Richter, J.M. 1976. The attachment of mouse hepatitis virus to the plasma membrane of L2 cells. Master of Arts Thesis, University of Texas Health Science Center at Dallas. Dallas, Texas.
- Rifkin, D. and Compans, R.W. 1971. Identification of the spike proteins of Rous sarcoma virus. Virology 46: 485-489.
- Riggs, A.D., Suzuki, H. and Bourgeois, S. 1970. lac Repressor-operator interaction. I. Equilibrium studies. J. Mol. Biol. 48: 67-83.

- Robb, J. A. and Bond, C.W. 1979a. Pathogenic murine coronaviruses. I. Characterization of biological behavior in vitro and virus-specific intracellular RNA of strongly neurotropic JHMV and weakly neurotropic A59 viruses. Virology 94: 352-370.
- Robb, J.A. and Bond, C.W. 1979b. Coronaviridae. In: Comprehensive Virology (Fraenkel-Conrat, H. and Wagner, R.R., eds.). Plenum Press, New York. Vol. 14, pp. 193-247.
- Robbins, S.G., Holmes, K.V., McGowan, J.J., Frana, M.F., Boyle, J.F. and Ruyechan, W.T. 1984. RNA-binding proteins of coronavirus MHV. Abstract. Annual Meeting of the American Society for Virology, Madison, Wisconsin. 1984.
- Robbins, S.G., Frana, M.F., McGowan, J.J., Boyle, J.F. and Holmes, K.V. 1986. RNA-binding proteins of coronavirus MHV: Detection of monomeric and multimeric N protein with an RNA overlay-protein blot assay. Virology 150: 402-410.
- Roberts, C.R., Weir, A.C., Hay, J., Straus, S.E. and Ruyechan, W.T. 1985. DNA-binding proteins present in varicella-zoster virus-infected cells. J. Virol. 55: 45-53.
- Rottier, P.J.M., Spaan, W.J.M., Horzinek, M. and van der Zeijst, B.A.M. 1981a. Translation of three mouse hepatitis virus (MHV-A59) subgenomic RNAs in Xenopus laevis oocytes. J. Virol. 38: 20-26.
- Rottier, P.J.M., Horzinek, M.C. and van der Zeijst, B.A.M. 1981b. Viral protein synthesis in mouse hepatitis virus strain A59-infected cells: Effect of tunicamycin. J. Virol. 40: 350-357.

- Rottier, P.J.M., van der Zeijst, B.A.M. and Horzinek, M. (eds.) 1984. Coronaviruses: Molecular Biology and Pathogenesis. Plenum Press, New York.
- Rowe, W.P., Hartley, J.W. and Capps, W.I. 1963. Mouse hepatitis virus infection as a highly contagious, prevalent, enteric infection of mice. Proc. Soc. Exp. Med. Biol. 112: 161-165.
- Rozier, C. and Mache, R. 1984. Binding of 16S rRNA to chloroplast 30S ribosomal proteins blotted on nitrocellulose. Nucl. Acids Res. 12: 7293-7304.
- Russell, P.K., Chiewsilp, D. and Brandt, W.E. 1970. Immunoprecipitation analysis of soluble complement-fixing antigens of Dengue viruses. J. Immunol. 105: 838-845.
- Sabatini, D., Bensch, K.G. and Barnett, R.J. 1962. New means of fixation for electron microscopy and histochemistry. Anat. Rec. 142: 274.
- Sabesin, S.M. 1971. The role of lysosomes in the pathogenesis of experimental viral hepatitis. Am. J. Gastroenterol. 55: 539-563.
- Sanchez, A., Banerjee, A.K., Furuichi, Y. and Richardson, M.A. 1986. Conserved structures among the nucleocapsid proteins of the Paramyxoviridae: Complete nucleotide sequence of human parainfluenza virus type 3 NP mRNA. Virology 152: 171-180.
- Sauer, R.T. and Pabo, C.O. 1983. Protein-DNA recognition: The lambda repressor-operator complex. ASM News 49: 131-135.

- Sauer, R.T., Yocum, R.R., Doolittle, R.F., Lewis, M. and Pabo, C.O. 1982. Homology among DNA-binding proteins suggests use of a conserved super-secondary structure. Nature 29: 447-451.
- Schalk, A.F. and Hawn, M.C. 1931. An apparently new respiratory disease of baby chicks. J. Am. Vet. Med. Assoc. 78: 413-423.
- Scheid, A. and Choppin, P.W. 1974. Identification of biological activities of paramyxovirus glycoproteins. Activation of cell fusion, hemolysis, and infectivity by proteolytic cleavage of an inactive precursor protein of Sendai virus. Virology 57: 475-490.
- Scheid, A., Gravas, M.C., Silver, S.M. and Choppin, P.W. 1978. Studies on the structure and function of paramyxovirus glycoproteins. In: Negative Strand Viruses and the Host Cell (Mahy, B.W.J., Barry, R.D., eds.). Academic Press, New York. pp. 181-193.
- Schindler, M., and Jiang, L.-W. 1986. Nuclear actin and myosin as control elements in nucleocytoplasmic transport. J. Cell Biol. 102: 859-862.
- Schmidt, I., Skinner, M. and Siddell, S. 1987. Nucleotide sequence of the gene encoding the surface projection glycoprotein of coronavirus MHV-JHM. J. Gen. Virol. 68: 47-56.
- Schmidt, O.W. and Kenny, G.E. 1982. Polypeptides and functions of antigens from human coronaviruses 229E and OC43. Infec. Immun. 35: 515-522.

- Schmidt, O.W., Cooney, M.K. and Kenny, G.E. 1979. Plaque assay and improved yield of human coronaviruses in a human rhabdomyosarcoma cell line. J. Clin. Microbiol. 9: 722-728.
- Schochetman, G., Stevens, R.H. and Simpson, R.W. 1977. Presence of infectious polyadenylated RNA in the coronavirus avian infectious bronchitis virus. Virology 77: 772-782.
- Scouten, W.H. 1981. Affinity Chromatography: bioselective adsorption on inert matrices. Wiley and Sons, New York.
- Seto, J.T., Garten, W. and Rott, R. 1981. The site of cleavage in infected cells and polypeptides of representative paramyxoviruses grown in cultured cells of the chorioallantoic membrane. Arch. Virol. 67: 19-30.
- Sharma, S., Brandsma, J., Rodgers, L., Gething, M.-J. and Sambrook, J. 1985. A heterologous signal sequence can divert SV40 T antigen into the exocytic pathway. In: Current Communications in Molecular Biology. Protein Transport and Secretion. (Gething, M.-J., ed.). Cold Spring Harbor Laboratory. pp. 73-78.
- Shatkin, A.J., Darzynkiewicz, E., Furuichi, Y., Kroath, H., Morgan, M.A., Tahara, S.M. and Yamakawa, M. 1982. 5'-Terminal caps, cap-binding proteins and eukaryotic mRNA functions. Biochem. Soc. Symp. 47: 129-143.
- Shif, I. and Bang, F.B. 1970. In vitro interaction of mouse hepatitis virus and macrophages from genetically resistant mice. I. Adsorption of virus and growth curves. J. Exp. Med. 131: 843-850.

- Siddell, S.G., Wege, H., Barthel, A. and ter Meulen, V. 1980. Coronavirus JHM. Cell-free synthesis of structural protein p60. J. Virol. 33: 10-17.
- Siddell, S.G., Barthel, A. and ter Meulen, V. 1981a. Coronavirus JHM. A virion-associated protein kinase. J. Gen. Virol. 52: 235-243.
- Siddell, S.G., Wege, H., Barthel, A. and ter Meulen, V. 1981b. Coronavirus JHM. Intracellular protein synthesis. J. Gen. Virol. 53: 145-155.
- Siddell, S.G., Wege, H., Barthel, A. and ter Meulen, V. 1981c. Intracellular protein synthesis and the in vitro translation of coronavirus JHM mRNA. In: Biochemistry and Biology of Coronaviruses (ter Meulen, V., Siddell, S. and Wege, H., eds.). Plenum Press, New York. pp. 193-208.
- Siddell, S., Wege, H. and ter Meulen, V. 1982. The structure and replication of coronaviruses. Curr. Top. Microbiol. Immunol. 99: 131-163.
- Siddell, S., Wege, H. and ter Meulen, V. 1983. The biology of coronaviruses. J. Gen. Virol. 64: 761-776.
- Silver, P.A., Keegan, L.P. and Ptashne, M. 1984. Amino terminus of the yeast GAL4 gene product is sufficient for nuclear localization. Proc. Natl. Acad. Sci. 81: 5951-5955.
- Skinner, M.A. and Siddell, S.G. 1983. Coronavirus JHM: Nucleotide sequence of the mRNA that encodes nucleocapsid protein. Nucl. Acids Res. 11: 5045-5054.
- Skinner, M.A. and Siddell, S.G. 1984. Nucleotide sequencing of mouse hepatitis virus strain JHM messenger RNA 7. In:

- Coronaviruses: Molecular Biology and Pathogenesis (Rottier, P.J.M., van der Zeijst, B.A.M. and Horzinek, M., eds.). Plenum Press, New York. pp. 163-171.
- Smith, M.M. and Andresson, O.S. 1983. DNA sequences of yeast H3 and H4 histone genes from two non-allelic gene sets encode identical H3 and H4 proteins. J. Mol. Biol. 169: 663-690.
- Smith, J.D. and de Harven, E. 1974. Herpes simplex virus and human cytomegalovirus replication in WI-38 cells. I. Sequence of viral replication. J. Virol. 12: 919-930.
- Sonnenberg, N., Trachsel, H., Hecht, S. and Shatkin, A.J. 1980. Differential stimulation of capped mRNA translation in vitro by cap binding protein. Nature 285: 331-333.
- Sorensen, O., Coulter-Mackei, M., Percy, D. and Dales, S. 1981. In vivo and in vitro models of demyelinating diseases. In: Biochemistry and Biology of Coronaviruses. (ter Meulen, V., Siddell, S. and Wege, H., eds.). Plenum Press, New York. pp. 271-286.
- Spaan, W.J.M., Rottier, P.J.M., Horzinek, M.C. and van der Zeijst, B.A.M. 1981. Isolation and identification of virus-specific mRNAs in cells infected with mouse hepatitis virus (MHV-A59). Virology 108: 424-434.
- Spaan, W.J.M., Rottier, P.J.M., Horzinek, M.C. and van der Zeijst, B.A.M. 1982. Sequence relationships between the genome and the intracellular RNA species 1,3,6, and 7 of mouse hepatitis virus strain A59. J. Virol. 42: 432-439.
- Spaan, W.J.M., Delius, H., Skinner, M., Armstrong, J.,

- Rottier, P., Smeekens, S., van der Zeijst, B.A.M. and Siddell, S.G. 1983. Coronavirus mRNA synthesis involves fusion of non-contiguous sequences. EMBO J. 2: 1839-1844.
- Spear, P.G. and Roizman, B. 1968. The proteins specified by herpes simplex virus. I. Time of synthesis, transfer into nuclei, and properties of proteins made in productively infected cells. Virology 36: 545-555.
- Spelsberg, T.C., Sculley, T.B., Pikler, G.M., Gilbert, J.A. and Pearson, G.R. 1982. Evidence for two classes of chromatin-associated Epstein-Barr virus-determined nuclear antigen. J. Virol. 43: 555-565.
- Srinivas, R.V., Melsen, L.R. and Compans, R.W. 1982. Effects of monensin on morphogenesis and infectivity of Friend murine leukemia virus. J. Virol. 42: 1067-1075.
- Stallcup, K.C., Raine, C.S. and Fields, B.N. 1983. Cytochalasin B inhibits the maturation of measles virus. Virology 124: 59-74.
- Stark, G.R., Brown, R.E. and Kerr, I.M. 1981. In: Methods in Enzymology (Pestka, S., ed.). Academic Press, New York. Vol. 79, pp. 194-199.
- Steckert, J.J. and Schuster, T.M. 1982. Sequence specificity of trinucleoside diphosphate binding to polymerized tobacco mosaic virus protein. Nature 299: 32-36.
- Stern, D.F. and Sefton, B.M. 1982. Coronavirus proteins: Structure and function of the oligosaccharides of the avian infectious bronchitis virus glycoproteins. J. Virol. 44: 804-812.

- Stohlman, S.A. and Frelinger, J.A. 1978. Macrophages and resistance to JHM virus. In: Biochemistry and Biology of Coronaviruses (ter Meulen, V., Siddell, S., and Wege, H., eds.). Plenum Press, New York. pp. 387-398.
- Stohlman, S.A. and Lai, M.M.C. 1979. Phosphoproteins of murine hepatitis viruses. J. Virol. 32: 672-675.
- Stohlman, S.A., Brayton, P.R., Fleming, J.O., Weiner, L.P. and Lai, M.M.C. 1982. Murine coronaviruses: Isolation and characterization of two plaque morphology variants of the JHM neurotropic strain. J. Gen. Virol. 63: 265-275.
- Stohlman, S.A., Fleming, J.O., Patton, C.D. and Lai, M.M.C. 1983. Synthesis and subcellular localization of the murine coronavirus nucleocapsid protein. Virology 130: 527-532.
- Storz, J., Rott, R. and Kaluza, G. 1981. Enhancement of plaque formation and cell fusion of an enteropathogenic coronavirus by trypsin treatment. Infect. Immun. 31: 1214-1222.
- Strauss, E.G. and Strauss, J.H. 1983. Replication strategies of the single stranded RNA viruses of eukaryotes. Curr. Top. Microbiol. Immunol. 105: 1-98.
- Strous, G.J.A.M. and Lodish, H.F. 1980. Intracellular transport of secretory and membrane proteins in hepatoma cells infected by vesicular stomatitis virus. Cell 22: 709-717.
- Stubbs, G., Warren, S. and Holmes, K. 1977. Structure of RNA and RNA binding site in tobacco mosaic virus from 4-A map calculated from X-ray fibre diagrams. Nature 267: 216-221.

- Sturman, L.S. 1977. Characterization of a coronavirus. I. Structural proteins: Effects of preparative conditions on the migration of protein in polyacrylamide gels. Virology 77: 637-649.
- Sturman, L.S. 1981. The structure and behavior of coronavirus A59 glycoproteins. In: Biochemistry and Biology of Coronaviruses (ter Meulen, V., Siddell, S. and Wege, H., eds.). Plenum Press, New York. pp. 1-18.
- Sturman, L.S. and Holmes, K.V. 1977. Characterization of a coronavirus. II. Glycoproteins of the viral envelope: Tryptic peptide analysis. Virology 77: 650-660.
- Sturman, L.S. and Holmes, K.V. 1983. The molecular biology of coronaviruses. Adv. Virus Res. 28: 35-112.
- Sturman, L.S. and Holmes, K.V. 1984. Proteolytic cleavage of peplomeric glycoprotein E2 of MHV yields two 90K subunits and activates cell fusion. In: Coronaviruses: Molecular Biology and Pathogenesis (Rottier, P.J.M., van der Zeijst, B.A.M. and Horzinek, M., eds.). Plenum Press, New York. pp. 25-35.
- Sturman, L.S. and Holmes, K.V. 1985. The novel glycoproteins of coronaviruses. Trends in Biochem. 10: 17-24.
- Sturman, L.S. and Takemoto, K.K. 1972. Enhanced growth of a murine coronavirus in transformed mouse cells. Infect. Immun. 6: 501-507.
- Sturman, L.S., Holmes, K.V. and Behnke, J.N. 1980. Isolation of coronavirus envelope glycoproteins and interaction with the viral nucleocapsid. J. Virol. 33: 449-462.

- Sturman, L.S., Ricard, C.S. and Holmes, K.V. 1985. Proteolytic cleavage of the E2 glycoprotein of murine coronavirus: activation of cell-fusing activity of virions by trypsin and separation of two 90K cleavage fragments. J. Virol. 56: 904-911.
- Sturman, L.S., Eastwood, C., Frana, M.F., Duchala, C., Baker, F., Ricard, C.S., Sawicki, S.G. and Holmes, K.V. 1987. Temperature-sensitive mutants of MHV-A59. Adv. Exp. Med. Biol. In press.
- Swaak, A.J.G., Aarden, L.A., Statius van Eps, L.W. and Feltkamp, T.E.W. 1979. Arthritis Rheum. 22: 226-235.
- Takeuchi, A., Binn, L.N., Jervis, H.R., Keenan, K.P., Hilderbrandt, P.K., Valas, R.B. and Bland, F.F. 1976. Electron microscope study of experimental enteric infection in neonatal dogs with a canine coronavirus. Lab. Invest. 34: 539-549.
- Tanenbaum, S.W. 1978. Cytochalasins. Biochemical and cell biological aspects. In: Frontiers of Biology. North Holland Publishing Co., Amsterdam.
- Tartakoff, A. and Vassalli, P. 1977. Plasma cell immunoglobulin secretion. Arrest is accompanied by alterations in the Golgi complex. J. Exp. Med. 146: 1332-1345.
- Tartakoff, A. and Vassalli, P. 1978. Comparative studies of intracellular transport of secretory proteins. J. Cell Biol. 79: 694-707.
- Tartakoff, A. and Vassalli, P. 1979. Plasma cell immunoglobulin M molecules. Their biosynthesis, assembly, and

- intracellular transport. J. Cell Biol. 83: 284-299.
- Tegtmeyer, P., Robb, J.A., Widmer, C. and Ozer, H.L. 1974. Altered protein metabolism in infection by the late tsB11 mutant of simian virus 40. J. Virol. 14: 997-1007.
- Tegtmeyer, P., Schwartz, M., Collins, J.K. and Rundell, K. 1975. Regulation of tumor antigen synthesis by simian virus 40 gene A. J. Virol. 16: 168-178.
- ter Meulen, V. and Wege, H. 1978. Virus infection in demyelinating diseases. Adv. Exp. Med. Biol. 100: 383-394.
- Thornton, G.B., De, B.P. and Banerjee, A.K. 1984. Interaction of L and NS proteins of vesicular stomatitis virus with its template ribonucleoprotein during RNA synthesis in vitro. J. Gen. Virol. 65: 663-668.
- Tooze, J., Tooze, S. and Warren, G. 1984. Replication of coronavirus MHV-A59 in sac- cells: determination of the first site of budding of progeny virions. Eur. J. Cell Biol. 33: 281-293.
- Toth, T.E. 1982. Trypsin-enhanced replication of neonatal calf diarrhea coronavirus. Am. J. Vet. Res. 43: 967-972.
- Towbin, H., Staehelin, T. and Gordon, J. 1979. Electrophoretic transfer of proteins from polyacrylamide gels to nitrocellulose sheets: Procedure and some applications. Proc. Natl. Acad. Sci. USA 76: 4350-4354.
- Tsu, T.T. and Herzenberg, L.A. 1980. Solid-phase radioimmune assays. In: Selected Methods in Cellular Immunology (Mishell, B.B. and Shiigi, S.M., eds.). Freeman, San Francisco. pp. 373-397.

- Tyrrell, D.A.J. and Bynoe, M.L. 1965. Cultivation of a novel type of common-cold virus in organ culture. Brit. Med. J. 1: 1467-1470.
- Tyrrell, D.A.J., Almeida, J.D., Berry, D.M., Cunningham, C.H., Hamre, D., Hofstad, M.S., Mallucci, L. and McIntosh, K. 1968. Coronaviruses. Nature (Lond.) 220: 650.
- Tyrrell, D.A.J., Almeida, J.D., Cunningham, C.H., Dowdle, W.R., Hofstad, M.S., McIntosh, K., Tajima, M., Zakstelskaya, L. Ya., Easterday, B.C., Kapikian, A. and Bingham, R.W. 1975. Coronaviridae. Intervirol. 5: 76-82.
- Tyrrell, D.A.J., Alexander, D.J., Almeida, J.D., Cunningham, C.H., Easterday, B.C., Garwes, D.J., Hierholzer, J.C., Kapikian, A.Z., Macnaughton, M.R. and McIntosh, K. 1978. Coronaviridae, 2nd report. Intervirology 10: 321-328.
- van der Zeijst, B.A.M., Horzinek, M.C., Jacobs, L., Rottier, P.J.M. and Spaan, W.J.M. 1981. Messenger RNAs of mouse hepatitis virus-A59: isolation and characterization, translation in Xenopus laevis oocytes of RNAs 3, 6 and 7. UV target sizes of the transcription templates. In: Biochemistry and Biology of Coronaviruses (ter Meulen, V., Siddell, S. and Wege, H., eds.). Plenum Press, New York. pp. 209-226.
- van Eekelen, C., Ohlsson, R., Philipson, L., Mariman, E., van Beek, R. and van Vernooij, W. 1982. Sequence dependent interaction of hnRNP proteins with late adenoviral transcripts. Nuc. Acids Res. 25: 7115-7131.
- van Wyke, K.L., Bean, W.J. Jr. and Webster, R.G. 1981.

- Monoclonal antibodies to the influenza virus nucleoprotein affecting RNA transcription. J. Virol. 39: 313-317.
- von Hippel, P.H. 1979. On the molecular basis of the specificity of interaction of transcriptional proteins with genome DNA. In: Biological Regulation and Development (Goldberger, R.F., ed.). Plenum Press, New York. pp. 279-347.
- Wallis, J.W., Hereford, L. and Grunstein, M. 1980. Histone H2B genes of yeast encode two different proteins. Cell 22: 799-805.
- Ward, J.M. 1970. Morphogenesis of a virus in cats with experimental feline infectious peritonitis. Virology 41: 191-194.
- Watanabe, K. 1969. Electron microscopic studies of experimental viral hepatitis in mice. II. J. Electron Microsc. 18: 173-189.
- Watson, B.K. and Coons, A.H. 1954. Studies of influenza virus infection in the chick embryo using fluorescent antibody. J. Exp. Med. 99: 419-428.
- Wege, H., Muller, A. and ter Meulen, V. 1978. Genomic RNA of the murine coronavirus JHM. J. Gen. Virol. 41: 217-227.
- Wege, H., Wege, H., Nagashima, K. and ter Meulen, V. 1979. Structural polypeptides of the murine coronavirus JHM. J. Gen. Virol. 42: 37-47.
- Wege, H., Stephenson, J.R., Koga, M., Wege, H. and ter Meulen, V. 1981a. Genetic variation of neurotropic and non-neurotropic murine coronaviruses. J. Gen. Virol. 54: 67-74.

- Wege, H., Siddell, S., Sturm, M. and ter Meulen, V. 1981b. Coronavirus JHM: Characterization of intracellular viral RNA. J. Gen. Virol. 54: 213-217.
- Wege, H., Koga, M., Wege, H. and ter Meulen, V. 1981c. JHM infection in rats as a model for acute and subacute demyelinating disease. In: Biochemistry and Biology of Coronaviruses (ter Meulen, V., Siddell, S. and Wege, H., eds.). Plenum Press, New York. pp. 327-349.
- Wege, H., Siddell, S. and ter Meulen, V. 1982. The biology and pathogenesis of coronaviruses. Curr. Top. Microbiol. Immunol. 99: 165-200.
- Weiner, L.P. and Stohlman, S.A. 1978. Viral models of demyelination. Neurology 28: 111-114.
- Weiss, S.R. and Leibowitz, J.L. 1981. Comparison of the RNAs of murine and human coronaviruses. In: Biochemistry and Biology of Coronaviruses (ter Meulen, V., Siddell, S. and Wege, H., eds.). Plenum Press, New York. pp. 245-260.
- Weiss, S.R. and Leibowitz, J.L. 1982. Characterization of murine coronavirus RNA by hybridization with virus-specific cDNA probes. J. Gen. Virol. 64: 127-133.
- Welsh, R.M., Haspel, M.V., Parker, D.C. and Holmes, K.V. 1986. Natural cytotoxicity against mouse hepatitis virus-infected cells. II. A cytotoxic effector cell with a B lymphocyte phenotype. J. Immunol. 136: 1454-1460.
- Wengler, G., Boege, U., Wengler, G., Bischoff, H. and Wahn, K. 1982. The core protein of the alphavirus Sindbis virus assembles into core-like nucleoproteins with the viral

- genome RNA and with other single-stranded nucleic acids in vitro. Virology 118: 401-410.
- Westenbrink, F., Brinkhof, J.M. and Gielkins, A.L. 1985. Gel electrophoretic analysis of polypeptides from nucleocapsids of Marek's disease virus strains and herpesvirus of turkey. Arch. Virol. 84: 217-231.
- Wharton, R.P. and Ptashne, M. 1986. An alpha-helix determines the DNA-binding specificity of a repressor. Trends Biochem. Sci. 11: 71-73.
- White, J., Matlin, K. and Helenius, A. 1981. Cell fusion by Semliki Forest, influenza, and vesicular stomatitis viruses. J. Cell Biol. 89: 674-679.
- Wilcox, K.W., Kohn, A., Sklyanskaya, E. and Roizman, B. 1980. Herpes simplex phosphoproteins. I. Phosphate cycles on and off some viral polypeptides and can alter their affinity for DNA. J. Virol. 33: 167-182.
- Wilhelmsen, K.C., Leibowitz, J.L., Bond, C.W. and Robb, J.A. 1981. The replication of murine coronaviruses in enucleated cells. Virology 110: 225-230.
- Willingham, M.C., Spicer, S.S. and Graber, C.D. 1971. Immunocytologic labeling of calf and human lymphocyte surface antigens. Lab. Invest. 25: 211-219.
- Wilson, T.M.A. and Shaw, J.G. 1987. Cotranslational disassembly of filamentous plant virus nucleocapsids in vitro and in vivo. In: Positive Strand RNA Viruses (Brinton, M.A. and Rueckert, R.R., eds.). Alan R. Liss, Inc., New York. pp. 159-181.

- Woyciechowska, J.L., Trapp, B.D., Patrick, D.H., Shekarchi, I.C., Leinikki, P.O., Sever, J.L. and Holmes, K.V. 1984. Acute and subacute demyelination induced by mouse hepatitis virus strain A59 in C3H mice. J. Exp. Pathol. 1: 295-306.
- Wray, W., Boulikas, T., Wray, V.P. and Hancock, R.H. 1981. Silver staining of proteins in polyacrylamide gels. Anal. Biochem. 118: 197-203.
- Yamada, G. and Nakane, P.K. 1977. Hepatitis B core and surface antigens in liver tissue. Light and electron microscopic localization by the peroxidase-labeled antibody method. Lab. Invest. 36: 649-659.
- Yamada, G., Feinberg, L.E. and Nakane, P.K. 1978. Hepatitis B: cytologic localization of virus antigens and the role of the immune response. Hum. Pathol. 9: 93-109.
- Yamaizumi, M., Uchida, T., Okada, Y., Furusawa, M. and Mitsui, H. 1978. Rapid transfer of non-histone chromosomal proteins to the nucleus of living cells. Nature 273: 782-784.
- Yamauchi, M., Nishiyama, Y., Fujioka, H., Isomura, S. and Maeno, K. 1985. On the intracellular transport and the nuclear association of human cytomegalovirus structural proteins. J. Gen. Virol. 66: 675-684.
- Yogo, Y., Hirano, N., Hino, S., Shibuta, H. and Matumoto, M. 1977. Polyadenylate in the virion RNA of mouse hepatitis virus. J. Biochem. (Tokyo) 82: 1103-1108.
- Yoshikura, H. and Tejima, S. 1981. Role of proteins in MHV-induced cell fusion. Virology 113: 503-511.

- Zeevi, M., Nevins, J.R. and Darnell, J.E., Jr. 1981. Nuclear RNA is spliced in the absence of poly (A) addition. Cell 26: 39-46.
- Zimmern, D. 1977. The nucleotide sequence at the origin for assembly on tobacco mosaic virus RNA. Cell 11: 463-482.
- Zimmern, D. and Wilson, T.M.A. 1976. Location of the origin for viral reassembly on tobacco mosaic virus RNA and its relation to stable fragment. FEBS Lett. 71: 294-298.
- Zuidema, D., Cool, R.H. and Jaspars, E.M.J. 1984. Minimum requirements for specific binding of RNA and coat protein of alfalfa mosaic virus. Virology 136: 282-292.
- Zweig, M., Heilman, C.J., Jr. and Hampar, B. 1979. Identification of disulfide-linked protein complexes in the nucleocapsids of herpes simplex virus type 2. Virology 94: 443-450.